Synthetic and Metabolic Studies on Centrally Acting Amines

by

Zhiyang Zhao

Dissertation submitted to the Faculty of the

Virginia Polytechnic Institute and State University

in partial fulfillment of the requirements for the degree of

Doctor of Philosophy

in

Chemistry

APPROVED BY:

Dr. Neal Castagnoli, Jr., Chairman

Dr. Harold M. Bell

Dr. Harry W. Gibson

Dr. Gary L. Long

Dr. Joseph S. Merola

September 1991
Blacksburg, Virginia

Synthetic and Metabolic Studies on Centrally Acting Amines

by
Zhiyang Zhao

Professor Neal, Castagnoli, Jr., Chairman

Abstract

This dissertation is concerned with the metabolic bioactivation of several amines which are either known or suspected to be neurotoxic and with the exploration of bioactivation processes in order to generate metabolites with therapeutic potential. The following three programs were pursued in this work:

(1) Theoretical considerations and recent experimental data have prompted an investigation of the neurotoxicological properties of the 6-hydroxydopamine analog 2-methylamino-1-(2,4,5-trihydroxyphenyl)propane and its possible precursor intermediate 1-(2-hydroxy-4,5-methylenedioxyphenyl)-2-methylaminopropane, potential metabolites of the serotonergic neurotoxin 2-methylamino-1-(4,5-methylenedioxyphenyl)propane, (Methylenedioxymethamphetamine, MDMA). The syntheses and serotonergic neurotoxic properties of the potential metabolites are discussed.

(2) The further biotransformation of the 1-(1-phenylcyclohexyl)-3,4,5,6-tetrahydropyridinium metabolite derived from the psychosis inducing agent phencyclidine [1-(1-phenylcyclohexyl)-piperidine, PCP] has been examined in rat liver and brain subcellular fractions. In the presence of brain mitochondria this tetrahydropyridinium compound was converted to 1-(phenylcyclohexyl)-1,2,3,4-tetrahydropyridine-5-carboxaldehyde. The same product was identified in the corresponding liver mitochondrial and microsomal incubation mixtures and in liver microsomal incubations of phencyclidine. The chemical conversion of the synthetic tetra-

hydropyridinium perchlorate to this product by N^5-formyltetrahydrofolic acid (folinic acid) suggests that the metabolic reaction is mediated by a transformylation process involving this or the corresponding N^{10}-formyltetrahydrofolic acid.

(3) Extensive substrate-activity studies have established that only those 1,2,3,6-tetrahydropyridine derivatives bearing a lipophilic C-4 substituent and an N-methyl group are likely to be good monoamine oxidase B substrates. The design and synthesis of potential prodrugs based on this enzyme-substrate selectivity has been pursued with model compounds.

This dissertation is dedicated to my wonderful wife, Ying.
Her love and understanding have been a great source of inspiration and comfort for me.

I would also like to express my sincerest appreciation to my parents for their unending love and support.

Acknowledgments

The author wishes to express his gratitude and appreciation to Professor Neal Castagnoli, Jr. for his constant enthusiasm and guidance, and for teaching the author not only science but also its place in life.

Grateful acknowledgments are also made to Dr. Harold M. Bell, Dr. Harry W. Gibson, Dr. Gary L. Long and Dr. Joseph S. Merola for their valuable advice and discussions.

The author is grateful to the members of his research group for their discussions, assistance, and friendship, particularly to Mrs. Kay Castagnoli.

This work was partially supported by the Harvey W. Peters Research Center for Parkinson's Disease and Disorders of the Central Nervous System.

Table of Contents

List of Tables

List of Figures

List of Schemes

INTRODUCTION

The effects of drugs on living systems have been studied by generations of pharmacologists but the subject, far from being exhausted, continuously displays new horizons.[1] The reciprocal of such interactions, namely the various influences of an organism upon drug molecules, was given little attention for many years. Progress in several directions was necessary for the maturation of the science of drug metabolism in the fertile soil of medicinal chemistry and also pharmacology. During the past 20 years important advances have been made in the development of new and needed analytical techniques and in the recognition of the importance of metabolism and disposition in terms of the biological activities of drugs and other xenobiotics (compounds foreign to the body). Studies on the metabolism of drugs and other xenobiotics often are pursued in an effort to gain insights into the molecular events associated with the fate and the pharmacological and toxicological properties of biologically active, lipophilic organic chemicals.

Enzyme systems which catalyze metabolic reactions bring about structural modifications of xenobiotics which in general lead to more polar and biologically less active metabolites. This is the classical concept of metabolic detoxification. On the other hand, the enzyme systems which catalyze these transformations do so according to the basic laws of chemistry and physics and often times these transformations lead to pharmacologically active species, which contribute to the overall biological profile of a given xenobiotic, and to chemically reactive (electrophilic) intermediates, which can bioalkylate biomacromolecules to form covalent adducts resulting in irreversible toxicities including cellular neurcosis and mutagenic and carcinogenic effects. In some instances xenobiotics can be metabolized to mitochondrial toxins which can lead to neurodegeneration. Therefore, an understanding of the pharmacokinetic, pharmacodynamic and toxic behavior of xenobiotics requires an appreciation of their metabolic fate and the associated bioorganic reaction mechanisms.

This dissertation is concerned with the metabolic bioactivation of amines which are either known or suspected to be neurotoxic and on the exploration of bioactivation processes to generate metabolites with therapeutic potential. The discussion which follows will review briefly some of the basic features which are known to be associated with the principal drug metabolizing enzymes and will emphasize those enzymes which catalyze oxidative transformations.

Drug metabolism is an immense area of study and this is reflected in the range of chemical reactions that drug substrates undergo during metabolism. These include oxidation, reduction, hydrolysis, hydration, and conjugation pathways. Biotransformation reactions normally are divided into two phases: phase I, or functionalization reactions, and phase II, or conjugation reactions. There is great interest in the inter-relationship of the various metabolic routes in terms of competing reactions of the substrate for phase II enzymes. There is much evidence to suggest that phase I reactions create a reactive functional group which can be derivatized or conjugated by reactions catalyzed by the phase II enzymes. The final effect is to generate highly polar metabolites. Thus, the phase II reactions are the true 'detoxification' pathways and give products that account for the bulk of the inactive drug metabolites that are excreted in the urine.[2]

The metabolism of drug molecules must be considered together with pharmacokinetic and pharmacodynamic aspects of drug behaviors. Drugs are exposed to many enzyme systems involved in the normal maintainance of cellular functions. These systems catalyze transformation leading to structural modifications that increase the polarity of the parent molecules, often in nonspecific ways that are designed to eliminate xenobiotic agents.[3] These metabolic products are not always biologically inactive as will be discussed in greater detail in this dissertation.

An appreciation of drug metabolism contributes to our total understanding of the pharmacological activity of drugs. Recent progress in methodology and instrumentation and the demands of the drug-regulatory agencies have resulted in a greatly increased activity in these fields. In addition, it has been recognized that

rational drug design is not possible without a proper consideration of drug distribution and metabolism.

For many years the metabolism of drugs was equated with detoxification and inactivation. Since the early 1960s, however, it has been increasingly recognized that drugs and environmental chemicals also may be metabolized to toxic and/or pharmacologically active metabolites. One possible mechanism by which otherwise chemically unreactive compounds can exert toxic effects is through the metabolic generation of reactive intermediates which may interact with critical biological macromolecules and thereby modify their structures and functions.

The *in vivo* biotransformation of relatively inert chemicals to highly reactive metabolites, a phenomenon commonly referred to as "metabolic activation", is now recognized or suspected to be an obligatory initial event in several kinds of chemical induced toxicities.[4] Reactive species often times are formed by interaction with drug metabolizing enzymes.[5] In some cases a single enzymatic reaction is involved while in other cases several enzymatic and/or spontaneous chemical reactions are involved in the production of an "ultimate" toxic metabolite. Highly reactive toxic metabolites of xenobiotics may interact with cells in a number of potentially detrimental ways including covalent bond formation with cellular constituents and stimulation of peroxidation leading to decomposition of cellular lipids.[6] Pioneering studies led to the initial formulation and development of the concept of metabolic activation as a mechanism to account for the biological activities of certain types of chemical carcinogens.[4]

Drugs and other xenobiotic chemicals are metabolized by a wide variety of enzymes. Some of these enzymes also catalyze normal reactions of cellular metabolism. Most drugs are metabolized to more polar compounds which can be removed rapidly from the body via the kidneys. Some drugs, termed prodrugs, are transformed to therapeutically active metabolites. The enzymes that catalyze these processes, however, also may catalyze the formation of reactive, toxic metabolites. Whether a metabolic reaction produces a detoxification product or a potentially toxic metabolite is determined

in large part by the structural features of the drug and its metabolites.

Drug metabolism is primarily an hepatic event, although it occurs to some extent in other organs such as the intestine,[7] kidney,[8] lung,[9] placenta,[10] skin,[11] and brain.[12] The enzymes that catalyze the metabolism of nonpolar xenobiotics are most abundant in the liver.[13] Differential centrifugation of a liver homogenate yields several fractions which have been characterized in terms of structures present in the intact cell. The principal fractions obtained include the 10,000 x g sediment, which contains the mitochondria, the 100,000 x g sediment, which contains the microsomal fraction, and the 100,000 x g supernatant fraction which contains the soluble enzymes including the hydrolases, amine oxidases, various dehydrogenases, and aldehyde oxidase. Although mitochondrial monoamine oxidase and the various soluble oxidases can contribute to the fate of selected xenobiotics, the most important fraction for the study of the oxidative metabolism of xenobiotics is the 100,000 x g pellet or microsomal fraction.

The cytochrome P-450 monooxygenases represent a very important class of drug metabolizing enzyme. By far the majority of lipophilic xenobiotics are metabolized in the liver by this family of hemoproteins. The other important family of enzymes which mainly metabolize the nitrogen containing xenobiotics is the flavin containing monooxygenases.[14]

Cytochrome P-450 is found in many tissues including the adrenal cortex,[15] lungs,[16] skin,[11] and kidney,[17] but it is especially highly concentrated in the liver.[13] The cytochromes are a group of hemoproteins which are responsible for certain forms of electron transport.[18] Cytochrome P-450, like most cytochromes, is composed of a polypeptide subunit and an iron porphyrin prosthetic group.[19] Mammalian liver cytochrome P-450 in reality constitutes a family of isozymes with somewhat different substrate specificities and different sensitivities to induction and to inhibition.[20] The mixed function oxygenase activity of hepatocytes is associated primarily with the membranes of the endoplasmic reticulum. Upon mechanical disruption of the cells, the endoplasmic reticulum

fragments forms small vesicles called microsomes. The microsomes can be isolated from whole cell homogenates by differential centrifugation techniques.[21]

The primary source of electrons for the cytochrome P-450 system is NADPH which transfers electrons via a second enzyme, NADPH-cytochrome P-450 reductase (Fig. 1, and Scheme 1, Flavin oxidized form **1**, Half-reduced semiquinone **2**, Fully reduced form **3**). The second of the two electrons involved in the reaction also can be supplied to cytochrome P-450 via the cytochrome b_5 respiratory chain. This minor pathway contributes approximately 10% of the overall rate of steady state reduction of P-450.[22] Microsomal preparations contain the enzymes necessary for cytochrome P-450 metabolism but must be supplemented either with NADPH or an NADPH-generating system such as $NADP^+$, glucose-6-phosphate and glucose-6-phosphate dehydrogenase.

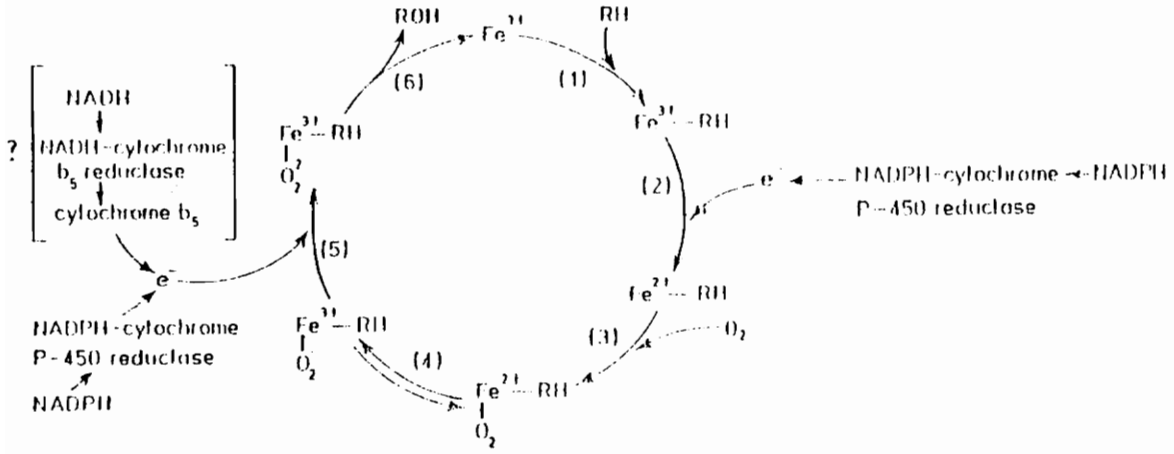

Figure. 1. Catalytic cycle of cytochrome P-450. RH represents the drug substrate, and ROH the corresponding hydroxylated metabolite. [Adapted from White, R., Coon, M. J. (1980) *Ann. Rev. Biochem.* **49,** 315-56.]

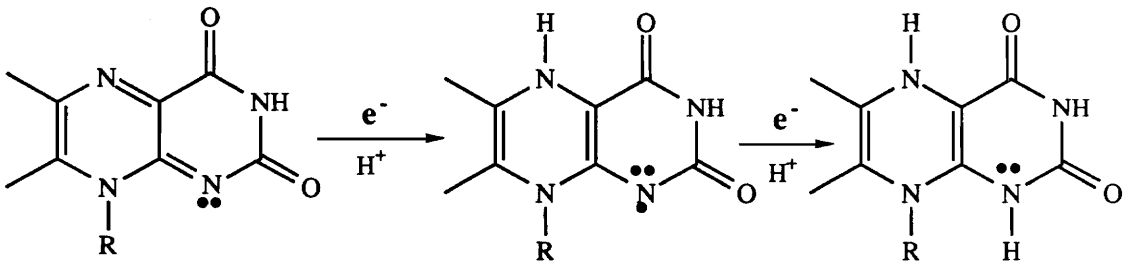

Oxidized form **1** Half-reduced semiquinone **2** Fully reduced form **3**

Scheme 1. Flavin reduction [Adapted from Gibson, G. G., Skett, P. (1986) Introduction to drug metabolism. Chapman and Hall, London, pp 39-81.]

The enzyme monoamine oxidase (MAO), a mitochondrial flavoprotein, is generally thought of as an endobiotic metabolizing enzyme since it catalyses the oxidative deamination of biogenic amines such as the neurotransmitters dopamine (DA, **4**) and 5-hydroxytryptamine (serotonin, 5-HT, **5**).[14] However, the enzyme also is involved in the metabolism of a number of xenobiotics. For example, epinine [N-methyldopamine, (**6**)], the metabolite derived from hydrolysis of Ibopamine [SB-7570, the 3,4-diisobutyryl ester of N-methyldopamine, (**7**)] metabolizing to 3,4-dihydroxyphenylacetic acid (DOPAC, **8**).[23]

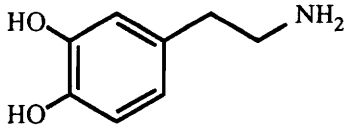

DA (4)

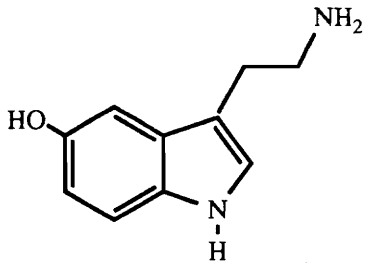

5-HT (5)

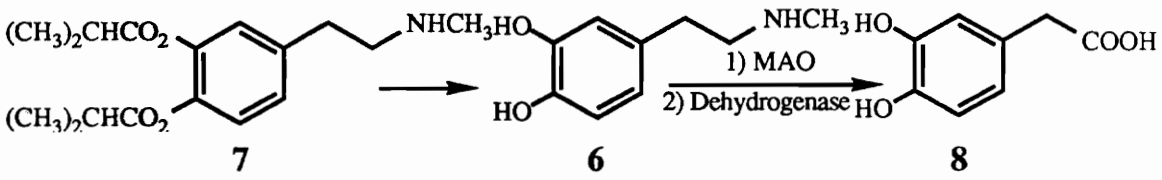

Scheme 2. Metabolism of Ibopamine (**7**) via epinine (**6**) to DOPAC (**8**).

Most MAO substrates are primary or secondary amines such as DA or benzylamine (**9**). An important general structural feature of the substrate specificity of MAO is the requirement for two hydrogen atoms on the α-carbon atom. The immediate product of amine oxidation is believed to be the corresponding imine **10**, formed by removal of an α-hydrogen from the substrate. This intermediate then is hydrolyzed, either on the enzyme surface or after release, to give the corresponding aldehyde **11** plus ammonia. The precise mechanism of hydrogen removal is still unclear.[24]

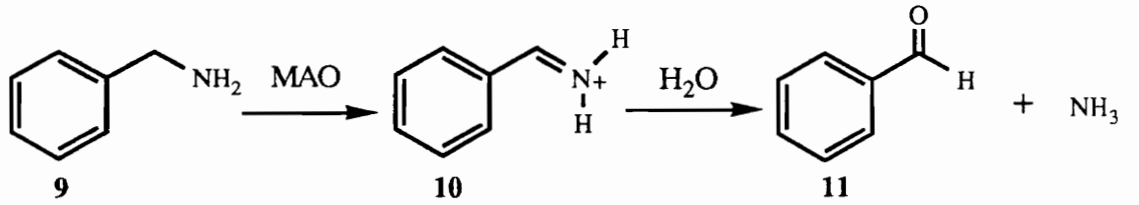

Scheme 3. The oxidative deamination pathway catalyzed by MAO.

Several findings support the view that the unprotonated species are the true substrates for the enzyme. Plausible reaction mechanisms, applicable to primary, secondary and tertiary alkyl- and aryl alkylamines have been advanced by Silverman et al[25]

Two forms (A and B) of MAO, which differ in their substrate specificities and inhibitor sensitivities, are present in mammalian tissues. In the brain MAO-A is localized in catecholamine and noradrenergic neurons while the B form is more concentracted in 5-HT neurons and the surrounding glial cells.[26] MAO-A is inhibited by low (approximately nanomolar) concentrations of clogyline (**12**),

whereas MAO-B is not inhibited until micromolar concentrations of this inhibitor are used. The reverse is true when (s)-1-deprenyl (**13**) is used to inhibit MAO activity. Although substrates of the A and B forms of MAO do not show absolute specificity, 2-phenylethylamine (**14**) may be considered a preferential substrate for MAO-B and 5-HT a preferential substrate for MAO-A.

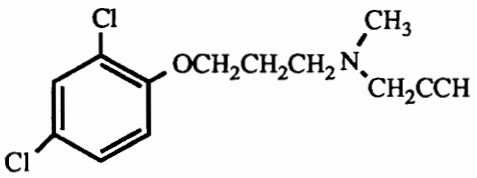

12

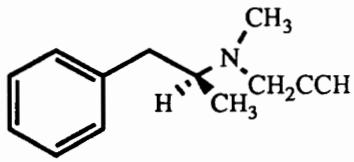

13

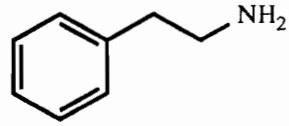

14

MAO is essentially a mitochondrial enzyme which is tightly associated with the outer membrane of that organelle. Some activity has been reported in microsomes.[27]

STUDIES ON 3,4-METHYLENEDIOXYMETHAMPHETAMINE (MDMA)

2.1. Background

The abused substance 2-methylamino-1-(3,4-methylenedioxyphenyl)propane [3,4-methylenedioxymethamphetamine (**15**), MDMA; also known as "Ecstasy"] is a ring-substituted phenylpropylamine that is related to both the amphetamine stimulants and certain hallucinogens. Although patented in 1914, interest in this compound was minimal until the past decade. During this period, MDMA began to be used as an adjunct to psychotherapy by certain therapists due to its purported ability to induce a state of reduced anxiety and lowered defensiveness.[28] In addition, the recreational use of MDMA, particularly on college campuses, appears to have increased significantly in recent years.[29] The human use of this agent is of concern due to the fact that MDMA and some of its congeners are selective serotonergic neurotoxins in laboratory animals.[30]

Partly as a result of the recent concern about human exposure, numerous investigators have begun to explore the neurochemical effects of MDMA. During the past 3 years, over 80 publications on MDMA have appeared in the scientific literature.[30] Administration of MDMA to animals elicits a characteristic biphasic response which can be categorized into acute and long-term effects. Some of the acute effects of MDMA appear to be related more directly to its behavioral and psychological effects, whereas the long-term effects have been correlated with the development of serotonergic neurotoxicity.

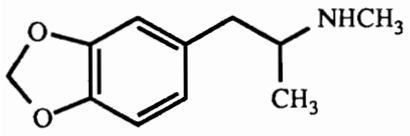

MDMA (15)

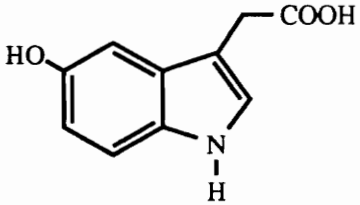

5-HIAA (16)

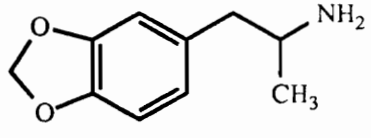

MDA (17)

Long-term reductions in brain levels of 5-hydroxytryptamine (5-HT) and 5-hydroxyindoleacetic acid (5-HIAA, **16**) induced by MDMA can be readily quantified with HPLC and are among the indices of neurotoxicity that have received the most attention. Long-term depletions of 5-HT by MDMA were first reported by Schmidt et al.[31] Ricaurte et al.[32] had noted a similar action of 3,4-methylenedioxyamphetamine (MDA, **17**). Since these initial reports, other investigators have confirmed that MDMA can induce significant, long-term, and regionally specific reductions in 5-HT and 5-HIAA, which in some instances can persist for up to 12 months following repeated administration.[33]

In addition to long-term changes in neurochemical parameters, MDMA also causes pronounced reductions in the density of 5-HT uptake sites and histological changes in the distribution and density of serotonergic nerve fibers. Both of these parameters are indicative of a neurodegenerative process. Battaglia et al.[34] reported a 50-75% reduction in the density of 5-HT uptake sites in the cortex, hippocampus, striatum, hypothalamus, and midbrain at 2 weeks following repeated systemic administration of MDMA and MDA. Schmidt[35] observed that both racemic MDA and MDMA caused acute and long term depletion of cortical 5-HT and loss of 5-HT uptake sites. Schmidt[36] demonstrated that both enantiomers of MDMA caused an acute depletion of cortical 5-HT.

Both the acute and long-term neurochemical deficits produced by MDMA (**15**) or MDA (**17**) can be blocked completely by co-administration of a selective 5-HT uptake blocker.[36] This antagonistic effect of a 5-HT uptake inhibitor on long-term 5-HT depletion, even up to 6 hours post MDMA, suggests that the neurotoxic action of MDMA might involve its extracellular conversion to a toxic metabolite which, unlike MDMA itself, has significant affinity for the 5-HT uptake carrier.[37]

Although the serotonergic neurotoxicity of MDMA is now well established, the underlying mechanisms of action remain unknown. Although various theories have been proposed, two major hypotheses have been advanced to explain MDMA-induced neurotoxicity. (1) Possible formation of a toxic MDMA metabolite.

The finding that MDMA-induced neurotoxicity can be specifically blocked by 5-HT uptake inhibitors illustrates the importance of the 5-HT uptake carrier in mediating the neurotoxic effects of MDMA. However, MDMA itself does not appear to be transported directly into 5-HT nerve terminals.[38] The fact that 5-HT uptake blockers can provide significant protective effects up to 6 hours post MDMA is evidence that the neurotoxic agent may be a metabolite of either MDMA or an endogenous substance. Additional support for the existence of a neurotoxic metabolite is the finding that direct intracerebral injection of MDMA yielded no evidence of a neurotoxic response, whereas systemic administration produces the long-term serotonergic deficits associated with neurotoxicity.[39] (2) Possible formation of a toxic DA metabolite. DA has been implicated as a possible mediator of the neurotoxicity produced by both methamphetamine **18**[40] and MDMA.[41] Interestingly, selective 5-HT uptake blockers block methamphetamine-induced changes in the serotonergic system but do not alter its effects on dopaminergic systems. By contrast, MDMA is selectively neurotoxic to the serotonergic system with relatively little effect on markers for dopaminergic neurotoxicity, such as brain catecholamine levels.

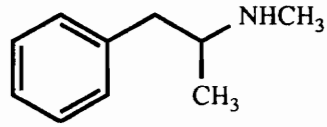

methamphetamine (18)

Inhibition of mixed function oxidases protect against MDMA neurotoxicity while induction of these enzyme increases its neurotoxicity.[42,43]

These considerations have led to a series of metabolic studies designed to evaluate the possible conversion of MDMA to neurotoxic metabolites. The metabolic fate of MDMA has recently been examined in detail by Foltz and colleagues both *in vivo* and in homogenates of rat liver and brain.[44] These studies have established that MDMA undergoes oxidative cleavage of the methylenedioxy moiety to form the corresponding catechol

derivative **19**. This dopamine analog is reported to be oxidized rapidly to the corresponding electrophilic *o*-quinone **20**, a potential neurotoxic alkylating agent (Scheme 4).[45] The enzyme system responsible for this conversion has not been identified.

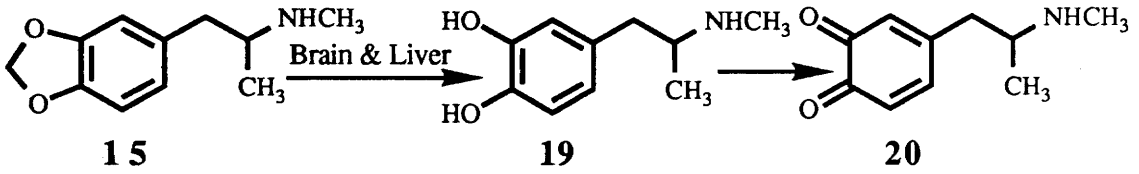

15 **19** **20**

Scheme 4. Oxidative enzymatic cleavage of methylenedioxy group of MDMA.

The ability of 6-hydroxydopamine (6-OHDA, **21**), a potential metabolite of DA, to cause the selective degeneration of dopaminergic and noradenergic neurons in the brain[46] has received considerable attention. It was found both *in vitro* and *in vivo* that autoxidation of dopamine yielded 6-hydroxydopamine.[46] This new biogenic amine was found to deplete norepinephrine from sympathetically innervated tissues. The possibility has been recently considered that in parkinsonism a local disturbance of nigral DA metabolism could result in the formation of analogs similar to (or identical with) 6-OHDA which may lead to the degeneration of the nigrostriatal dopaminergic neurons which characterizes the parkinsonian neuropathology. The selective and irreversible degeneration of sympathetic nerve terminals is due to an irreversible combination of 6-OHDA with tissue constituents. The importance of 6-OHDA as a pharmacological tool for the selective destruction of adrenergic nerve terminals has now been realized. Since 6-OHDA does not cross the blood-brain barrier, no effects on the central nervous system are elicited. However, intraventricular or intracisternal injection of the amine causes the selective destruction of catecholaminergic nerves in the central nervous system but does not affect serotonergic nerves.[47]

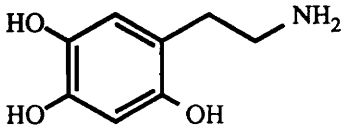

6-OHDA (21)

2.2. Research Proposal

The observation that MDMA is converted to the corresponding catechol by brain enzymes raises the interesting possibility that a combination of biotransformation reactions could result in the generation of the corresponding 2,4,5-trihydroxy metabolites in the brain. The regioselective formation of such a close relative of the neurotoxin 6-OHDA could account for some of the neurotoxic properties of the parent drug. Based on these considerations, we propose to examine the possible metabolic conversion of MDMA to the corresponding α-methylated 6-hydroxydopamine analog **24**. Previous studies have established that amphetamine (**22**) is metabolized to 4-hydroxyamphatamine (**23**) by hepatic monooxygenases (Scheme 5).[48] Consequently aromatic hydroxylation of this system is not unprecedented. The ring hydroxylated derivatives of MDMA could be formed in a similar way. In other words, the proposed biotransformaion pathway of MDMA would involve initial C-2 oxidation of the aromatic ring, a type of biotransformation known to be catalyzed by liver[48] and brain[49] cytochrome P-450 monooxygenases, to yield the corresponding 2-hydroxy-4,5-methylenedioxymethamphetamine species **24**. This hydroxylated metabolite is likely to retain adequate lipophilicity to enter the brain where it may undergo subsequent oxidative cleavage of the methylenedioxy carbon atom to generate the corresponding 2,4,5-trihydroxy compound 2-methylamino-1-(2,4,5-trihydroxy-phenyl)propane (**25**), a close structural analog of the potent neurotoxin 6-OHDA (Scheme 6).

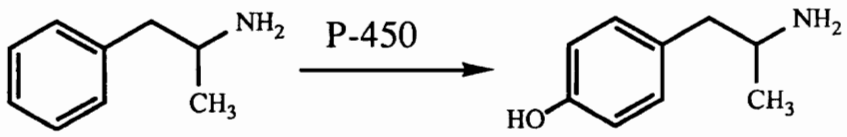

amphetamine (22) **4-hydroxyamphetamine (23)**

Scheme 5. Hydroxylation of amphetamine catalyzed by liver enzyme.

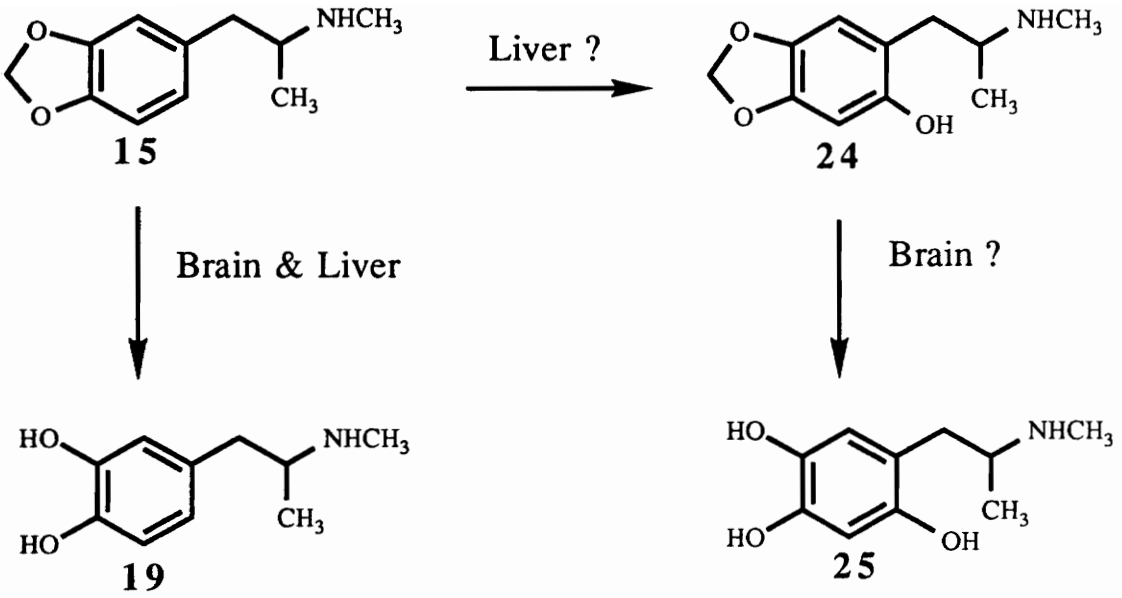

Scheme 6. Proposed metabolic bioactivation of MDMA.

Since the α-methyl analog **26** of 6-OHDA[50] and the structurally related hydroquinone **27**[51] display neurotoxic properties similar to those of 6-OHDA, the α-methyl group present in **21** is unlikely to affect the toxic potential of this system. The neurotoxic properties of the corresponding N-methylated analog of 6-OHDA have not been reported. The proposed studies of MDMA represent an effort to evaluate the possible toxicological significance of this putative metabolic sequence.

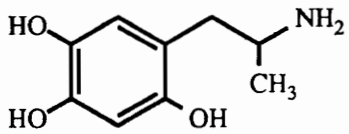

26

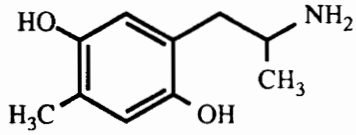

27

2.3. Results and Discussion

2.3.1. Syntheses

The proposed synthetic route which we undertook to obtain the desired products is shown in Scheme 7. Formylation of the commercially available 3,4-methylenedioxyphenol (**28**) should regiosprcifically yield aldehyde **29**.[52] Conversion of phenol **29** as its benzyl ether (**30**)[53] to the corresponding nitrostyrene (**31**) followed by reduction should provide **32**. N-formylation of **32** to yield **33** and reduction of **33** should provide intermediate **34** which upon hydrogenolysis of the benzyl ether group and oxidative cleavage of methylenedioxy group will give the desired 2-hydroxy-MDMA (**24**) and the trihydroxy compound **25**, respectively.

The first intermediate 2-hydroxy-4,5-methylenedioxy-benzaldehyde (**29**) was prepared from commercially available 3,4-methylenedioxyphenol (**28**) via the Vilsmeier reaction with N-methylformanilide and $POCl_3$ in dry methylene chloride. Purification of the product by flash column chromatography yielded a yellow crystalline solid which was identified by GC/MS, IR, ^1H NMR and elemental analysis. The most abundant ion in the EI mass spectrum (m/z 166) is the molecular ion (Fig. 2). The mass spectrum also contains diagnostic fragment ions resulting from loss of H_2O (m/z 148) and a CHO group (m/z 137) from the molecular ion. The IR spectrum showed a strong band at 1660 cm^{-1} which may be assigned to the carbonyl group stretch.

The structure of **29** was confirmed by ^1H NMR analysis (Fig. 3) which also ruled out the possibilities of regioisomers. The singlet proton signals at 6.9 ppm (H-6) and 6.5 ppm (H-3) indicated that the electrophilic substitution on the aromatic ring occured at the 6-position of 3,4-methylenedioxyphenol. The absence of detectable coupling between these two protons is consistent with their *para* relationship as shown in structure **29**. If the substitution had taken place at the 2-position or the 5-position of 3,4-methylenedioxy-phenol, then the remaining two protons would be *ortho* or *meta* to each other and would be expected to appear as doublets due to

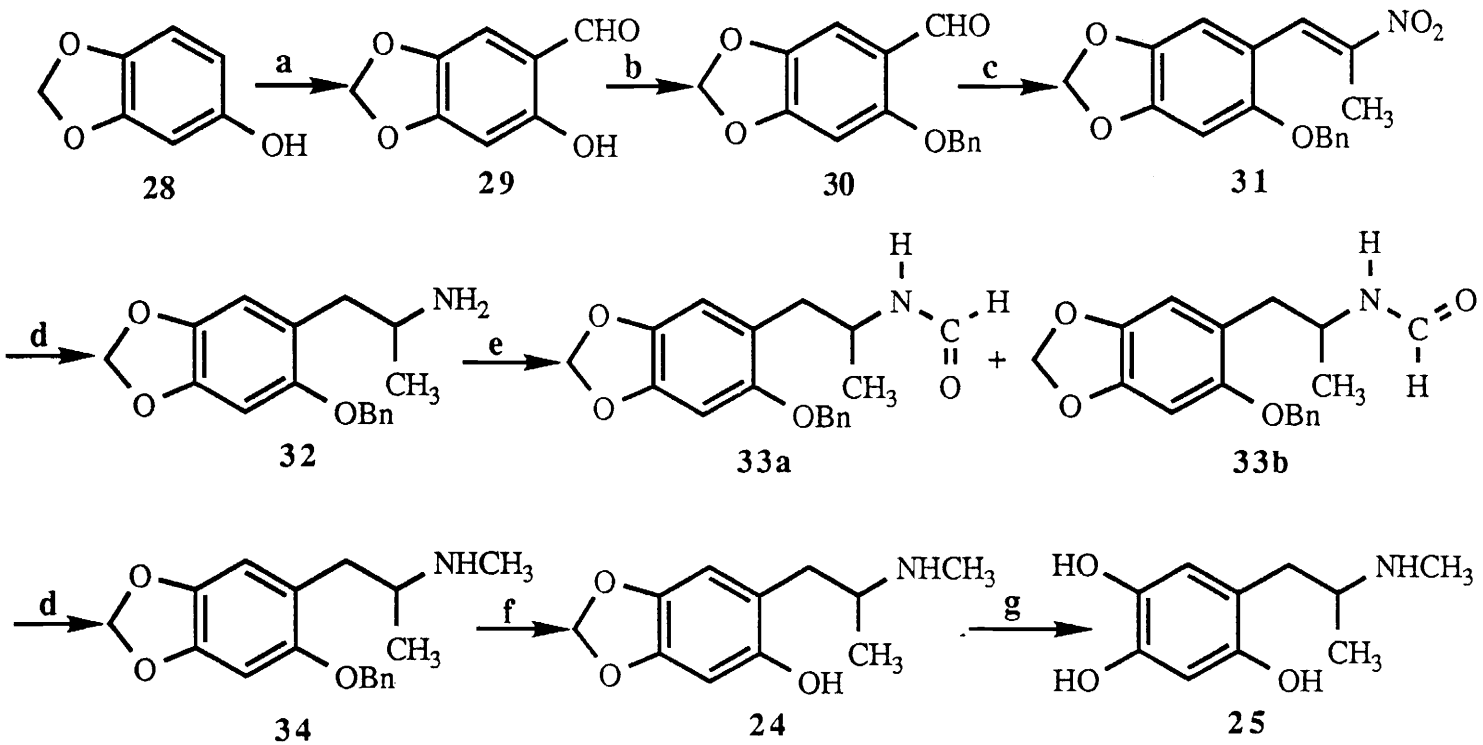

a) $Ph(CH_3)NCHO$, $POCl_3$; b) NaH, $PhCH_2Br$, Bu_4NI; c) $CH_3CH_2NO_2$, $AcONH_4$;
d) $LiAlH_4$; e) CH_3CH_2OCHO; f) Pd(C), H_2; g) BBr_3.

Scheme 7: Synthetic pathway to proposed 2-hydroxylated metabolite of MDMA.

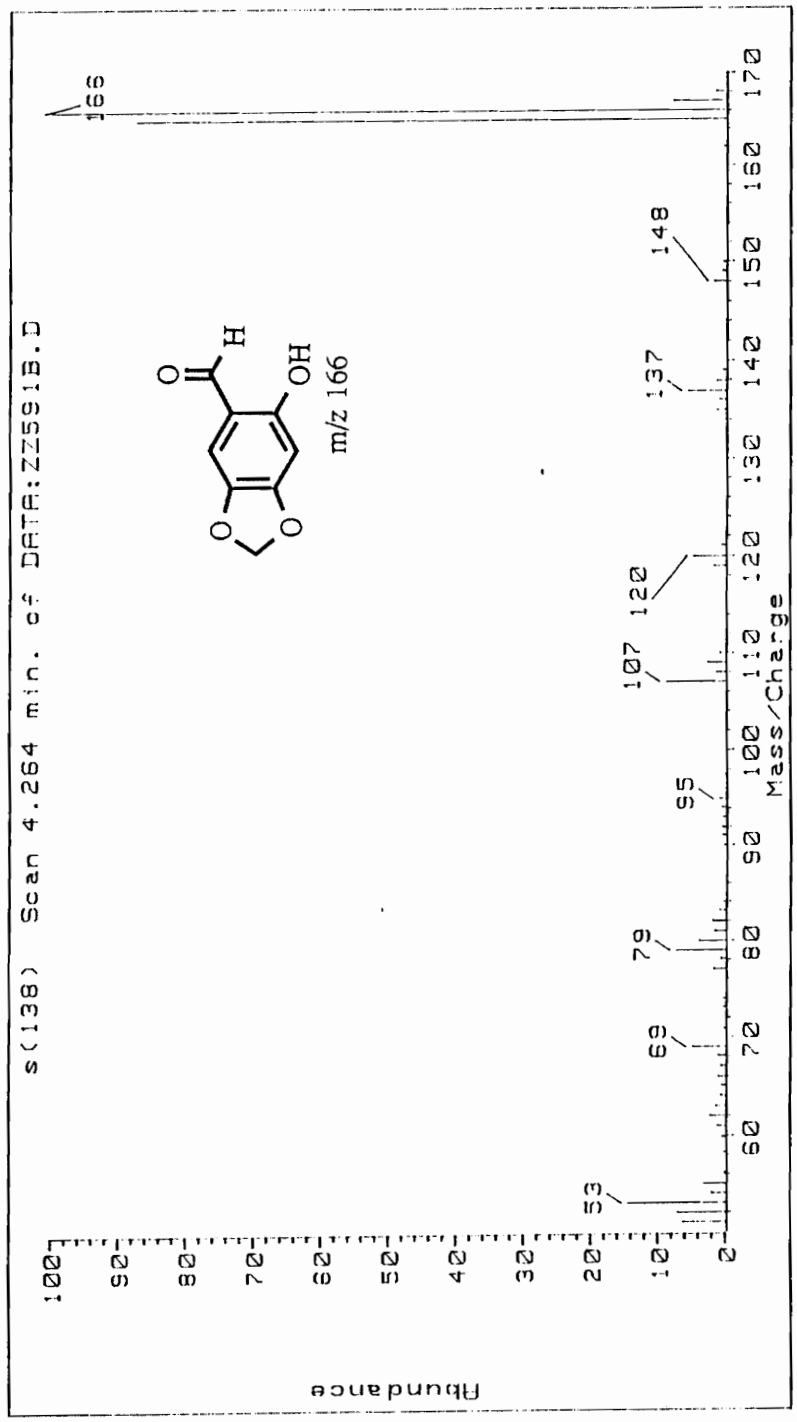

Figure. 2. GC/EIMS of 2-Hydroxy-4,5-methylenedioxybenzaldehyde.

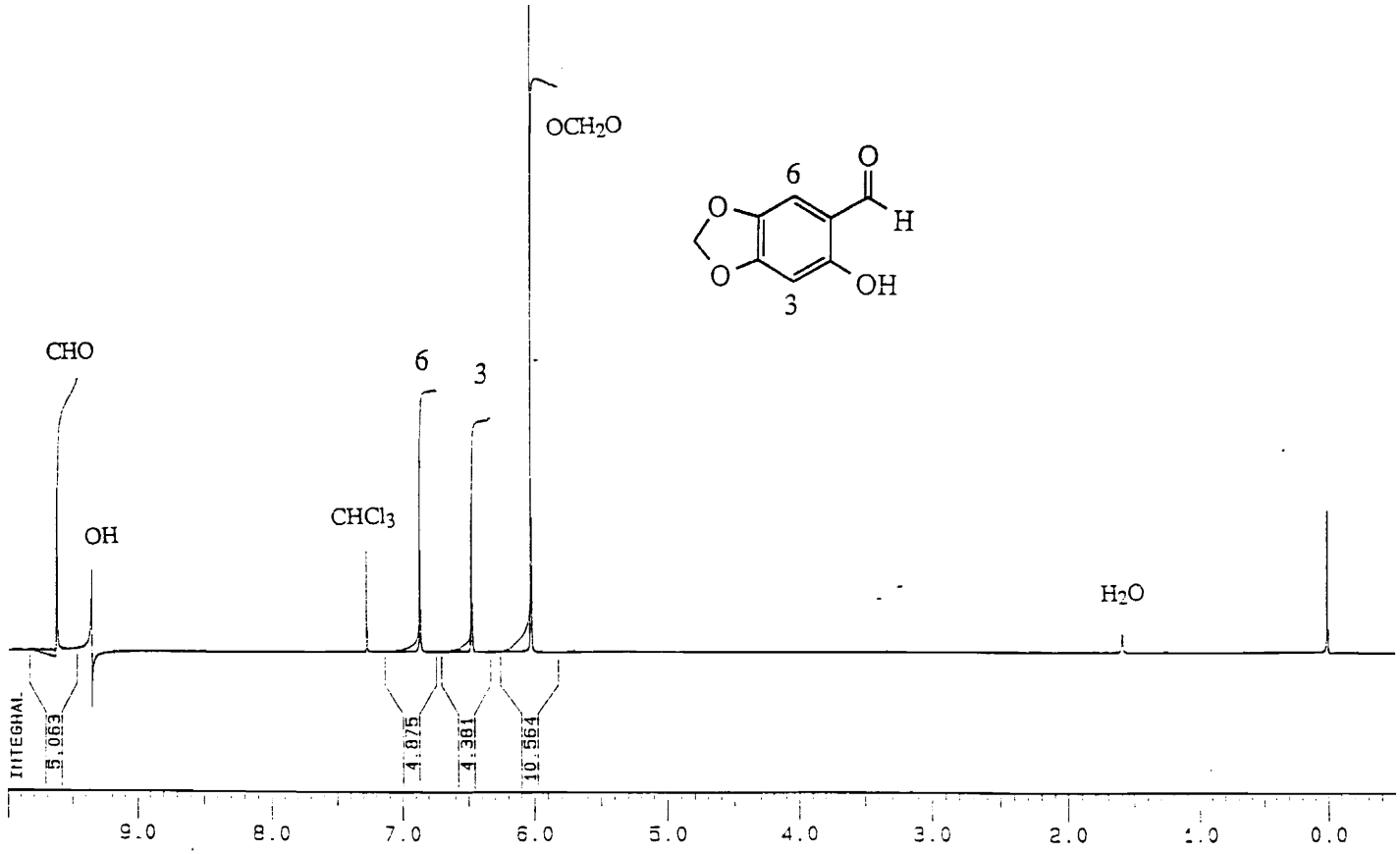

Figure. 3. ^1H NMR Spectrum ($CDCl_3$) of 2-Hydroxy-4,5-methylenedioxybenzaldehyde.

proton-proton coupling. Such *ortho* and *meta* proton-proton coupling was observed clearly in the ^1H NMR spectrum of the starting material, 3,4-methylenedioxyphenol.

The yield of compound **29** was very low. The reason is that a side product (**X**), which was acidic in nature since it dissolved in base but was insoluble in acid and neutral H_2O represented a lager percentage of the starting phenol. This product also had a low solubility in methylene chloride. An estimation of the molecular weight of the compound **X** was attempted by acid-base titration in the methanol with standard NaOH solution. The experiment was not succeseful, however, because no sharp end point was observed.

A consideration of the ^1H NMR spectrum (Fig. 4) of the compound **X** suggests that the phenyl hydrogen atom of **28** that would be replaced by the formyl group in the Vilsmeier reaction has been lost. The initial C-formylation step, therefore, probably had taken place. The possibility of a Cannizzaro condensation reaction was considered at the beginning (Scheme 8). This pathway, however, seems unlikely since no evidence for the formation of the corresponding benzyl alcohol (**36**) was observed and the pure aldehyde product **29** was stable in NaOH solution (pH = 11) for 24 hours.

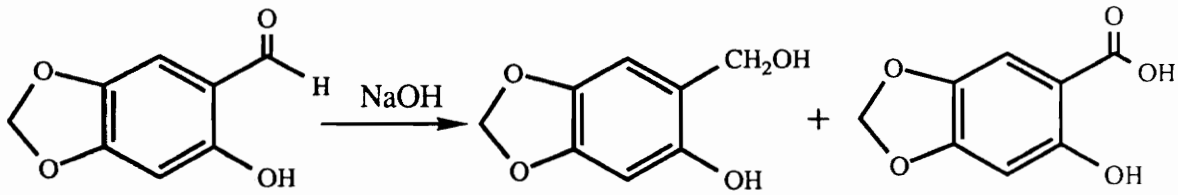

29 **36**

Scheme 8. Possible Cannizzaro condensation reaction.

The ^{13}C NMR spectrum (Fig. 5) of **X** displayed the following signals: low field signals in the region of 140-150 ppm which can be assigned to the aromatic carbon atoms bearing an oxygen atom. These were present in the ^{13}C NMR spectra of the starting material, 3,4-methylenedioxyphenol (**28**) (Fig. 6) and the aldehyde product **29**

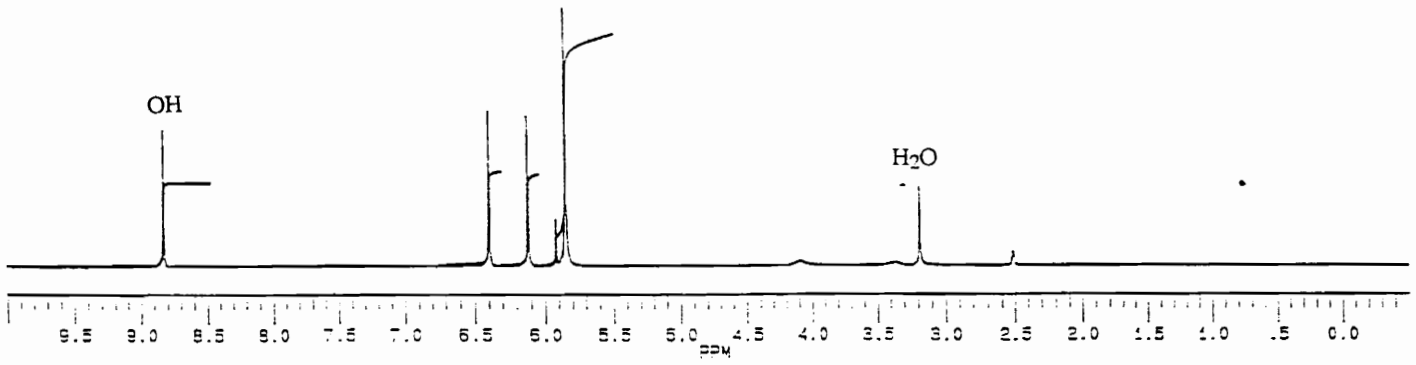

Figure. 4. ^{1}H NMR Spectrum (DMSO-d_6) of Compound X.

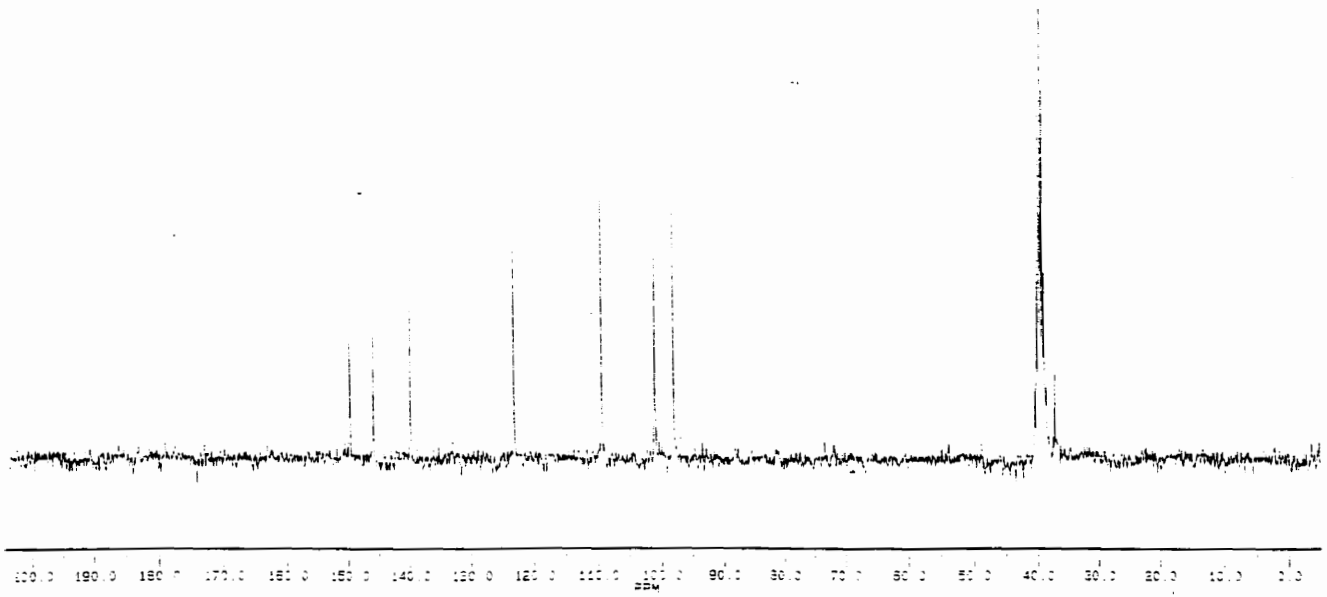

Figure. 5. ^{13}C NMR Spectrum ($CDCl_3$) of Compound X.

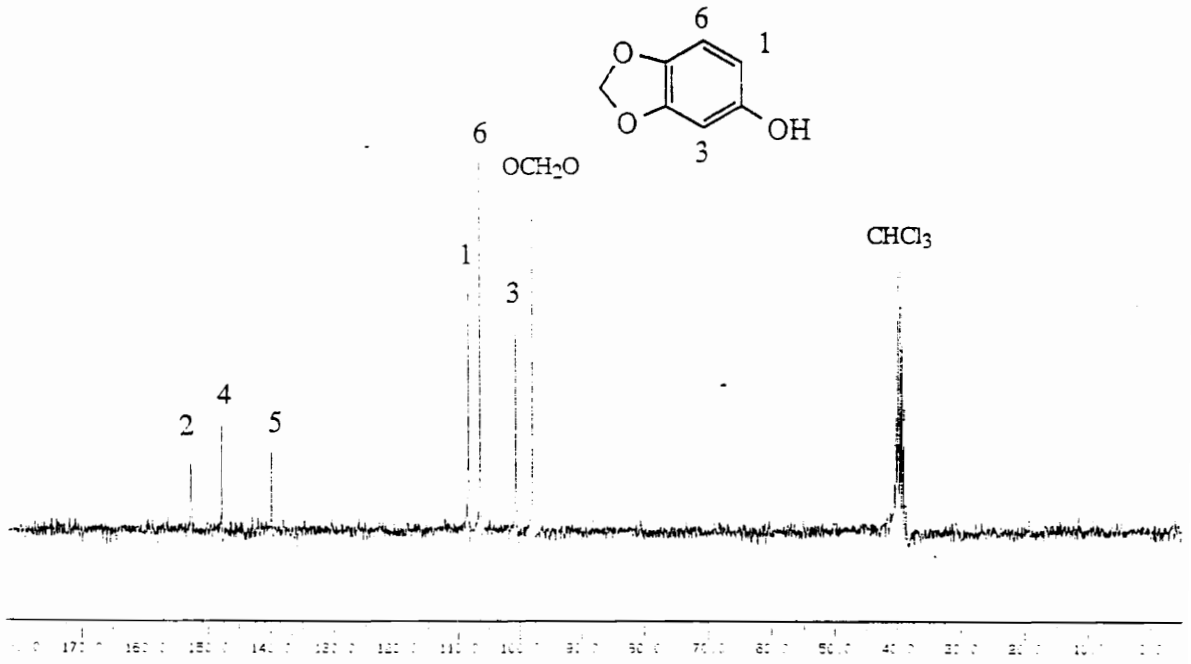

Figure. 6. ^{13}C NMR Spectrum ($CDCl_3$) of 3,4-Methylenedioxyphenol.

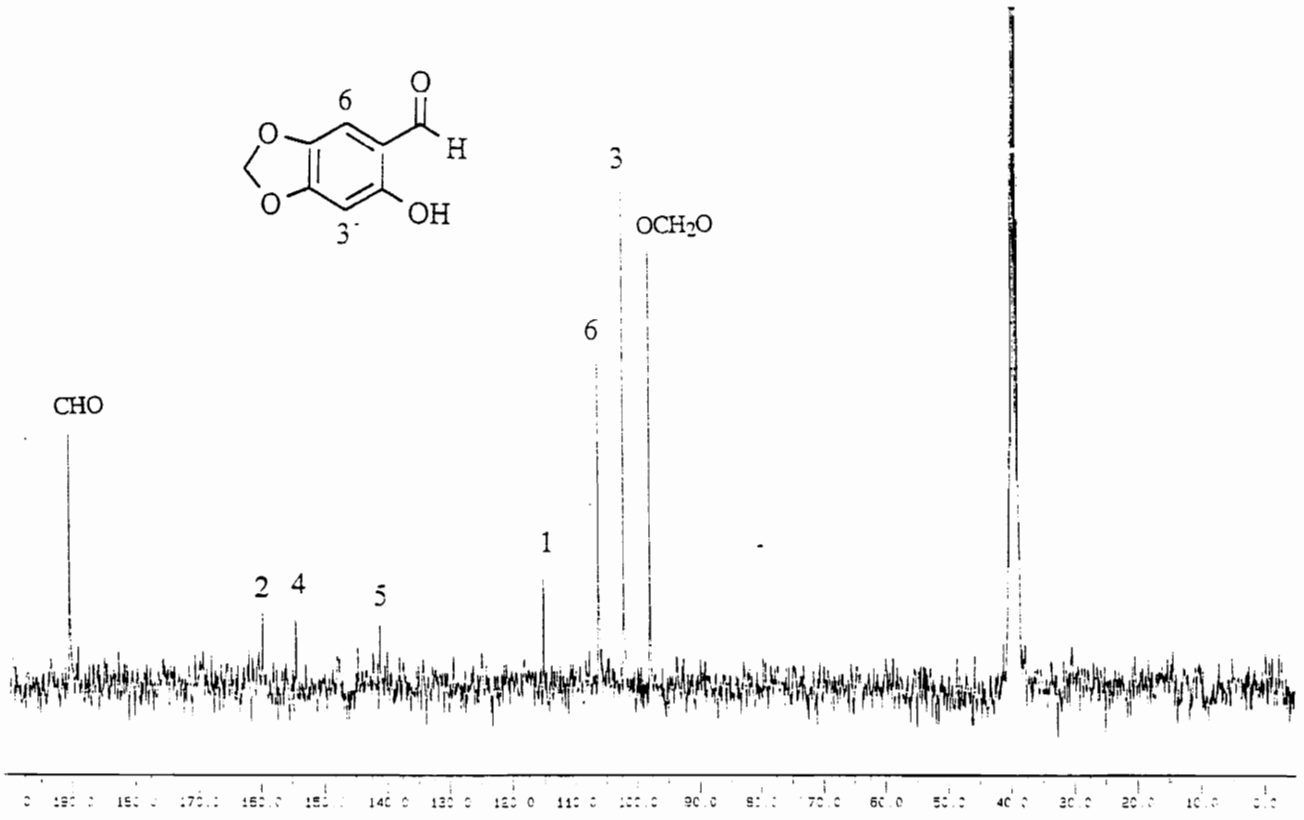

Figure. 7. ^{13}C NMR Spectrum ($CDCl_3$) of 2-Hydroxy-4,5-methylenedioxybenzaldehyde.

(Fig. 7) as well. The carbon atom of the methylenedioxy group can also be unambiguously assigned in all three compounds. The major difference in the ^{13}C NMR spectra between the starting material, the aldehyde **29** and unknown **X** is the appearance of a signal at 123 ppm in the spectrum of **X**. At least tentatively, one would assume that this is due to an aromatic carbon atom bearing a deshielding substituent. What that substituent might be, however, was unclear. The only other carbon signal is the one at 37.5 ppm which, if it were due to a carbon atom attached to C-1, should be deshielding. On the other hand, the high field position of this carbon signal rules out a carbonyl group or a hetero atom substituted carbon atom.

One distant possibility was that the compound **X** is a phosphorus derivative involving reaction with $POCl_3$ at C-1. Elemental (atomic absorption) analysis of this material, however, showed that no phosphorus was present.

The GC/EI mass spectrum of compound **X** showed two peaks on the total ion chromatogram (tic, Fig. 8). We speculated that the presence of two compounds may have represented thermal decomposition since compound **X** had been purified by recrystallizing several times and the ^1H NMR (Fig. 4) was relatively simple. Peak A (retention time of 1.49 minute) displayed a mass spectrum (Fig. 9) with a base peak at m/z 138, the same nominal mass as the starting material 3,4-methylenedioxyphenol (**28**). The second peak (Peak B, retention time 6.37 minute) showed an intense ion at m/z 269 (Fig. 10). This ion, however, is not likely to be the parent ion since the abundance of the ion at m/z 270 is too high to be just an M+1 satellite peak.

The ^1H NMR spectrum (Fig. 4) of compound **X** showed a singlet at 8.90 ppm which was assigned to the hydroxy proton since the signal disappeared after D_2O was added to the sample. The singlets at 6.39 ppm and 6.14 ppm could be assigned to the protons which are *meta* (H-6) and *ortho* (H-3) to the hydroxy group, respectively, based on the proton signal assignments for 2-hydroxy-4,5-methylenedioxybenzaldehyde (**29**, Fig. 7). The signal for the two methylenedioxy protons were recorded at 5.86 ppm as a sharp singlet as observed for aldehyde **29**. A singlet, which was not

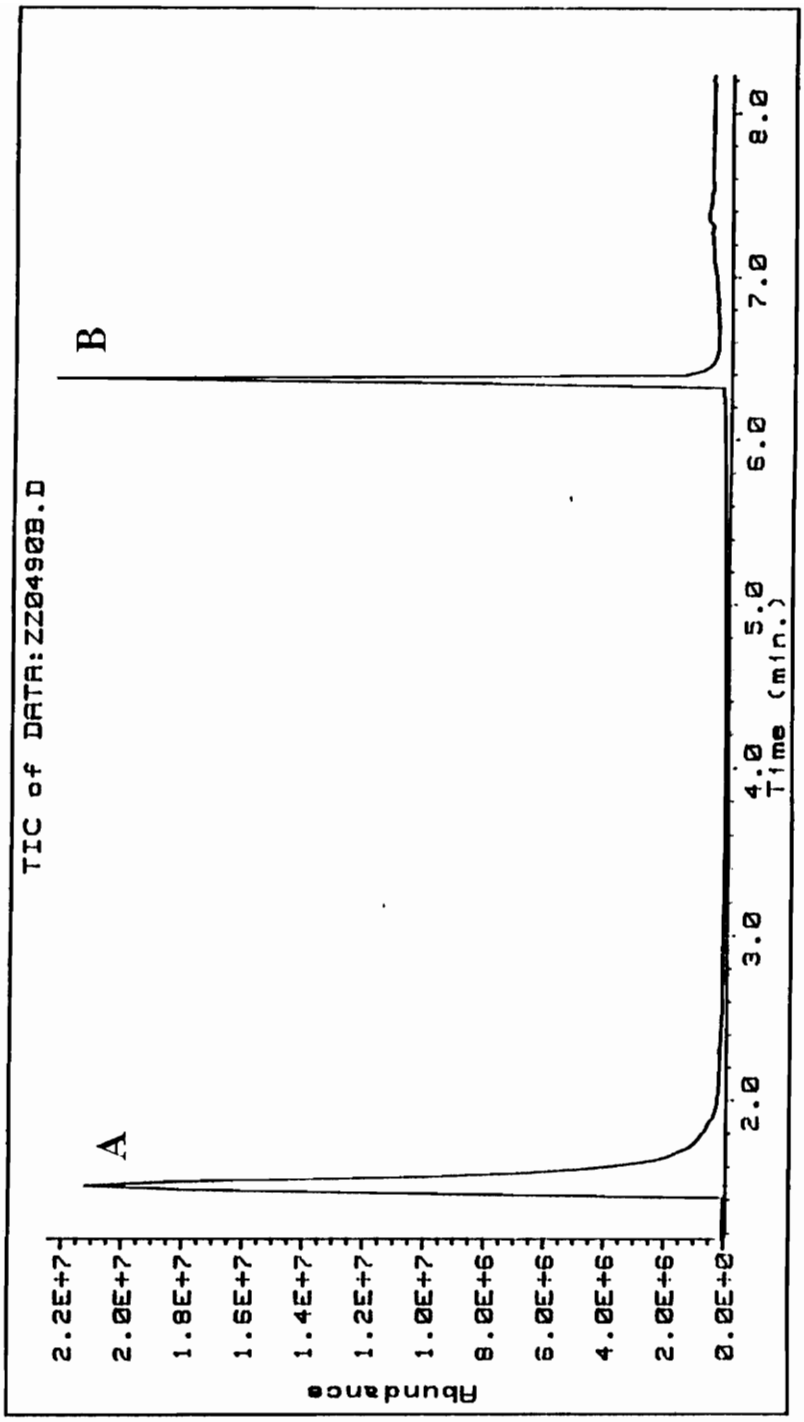

Figure. 8. Total Ion Chromatogram of Compound X.

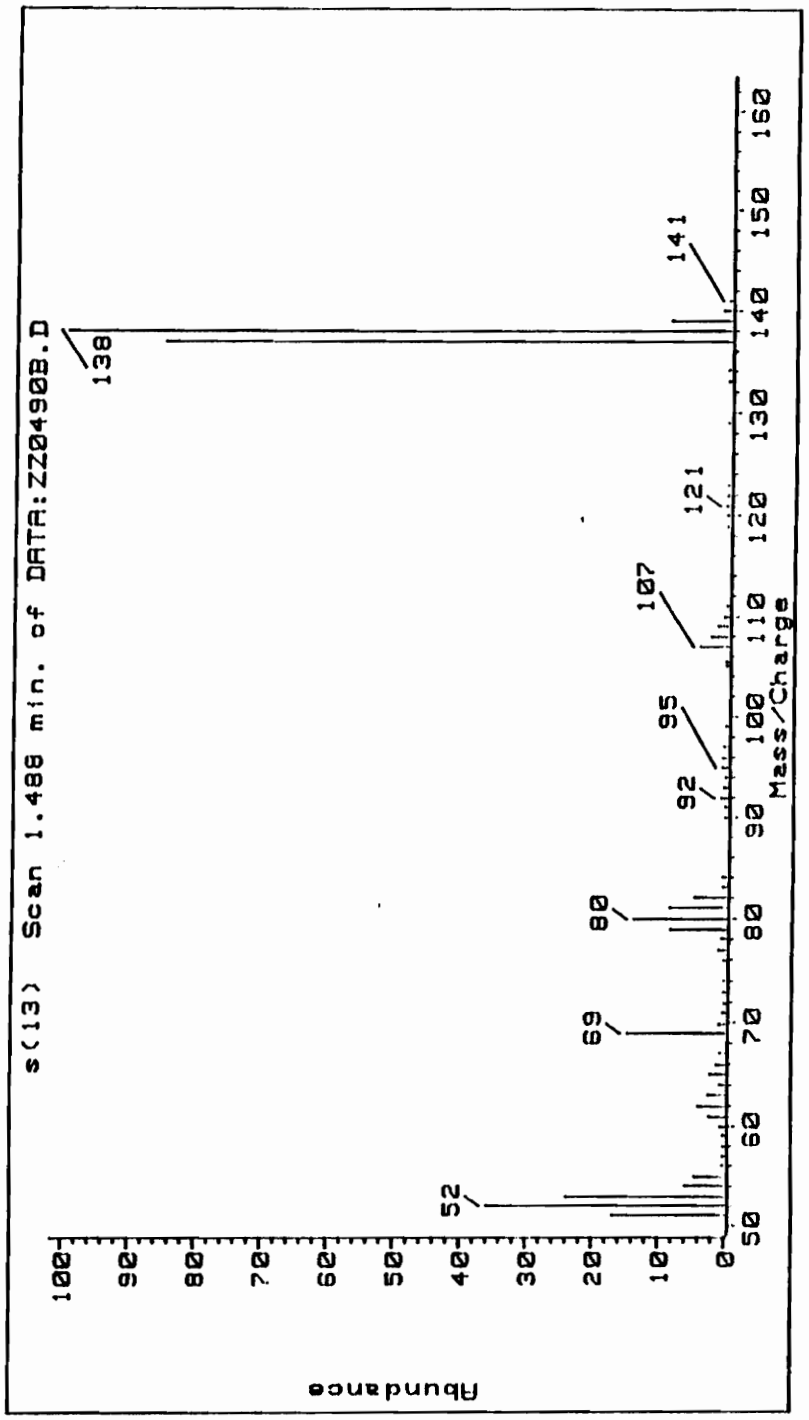

Figure. 9. GC/EIMS of Compound X (A).

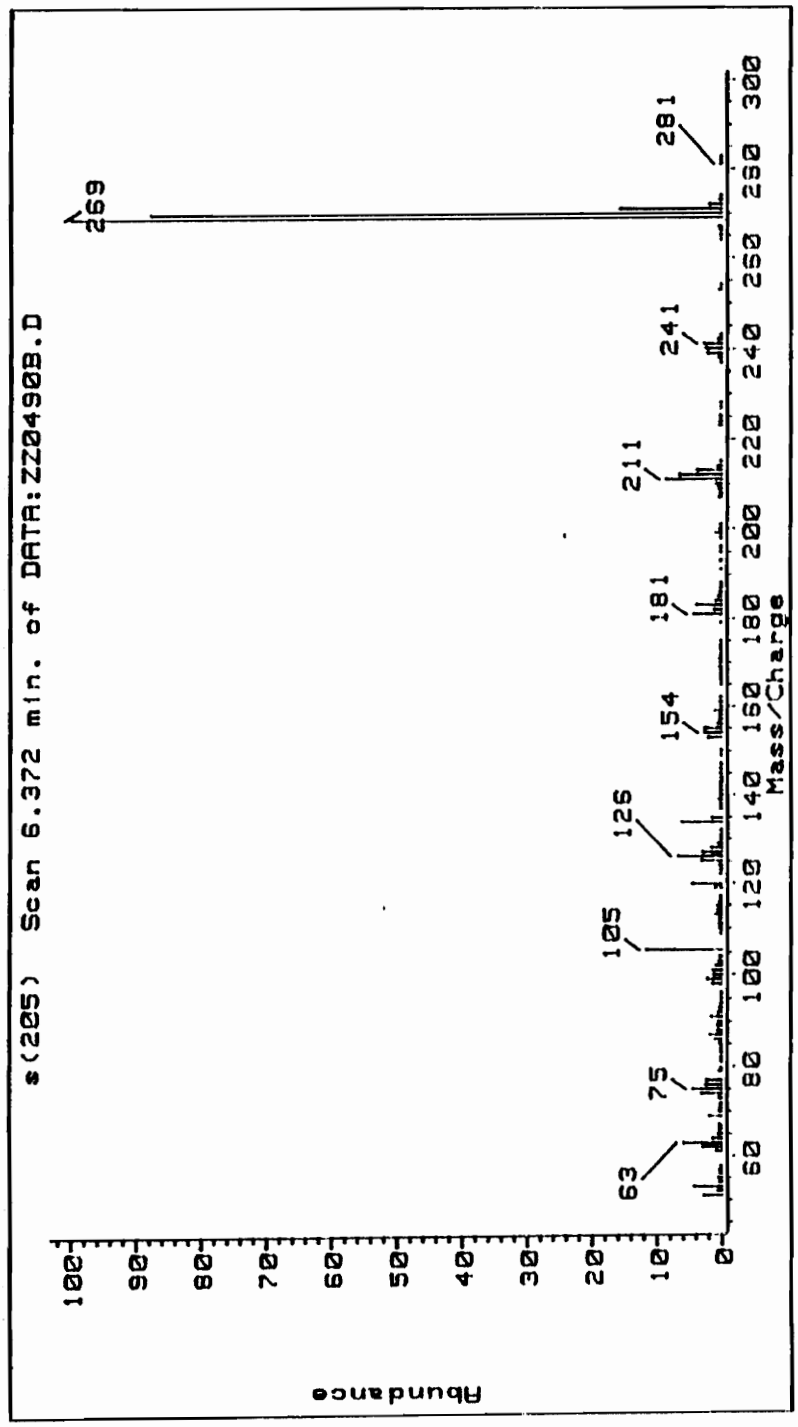

Figure. 10. GC/EIMS of Compound X (B).

observed on the ^1H NMR spectrum of either the starting material **28** or the aldehyde product **29**, was observed at 5.94 ppm. According to the integration, the ratio of these proton signals was either 2:2:2:4:1 or 3:3:3:6:1. A range of values resulted from the fact that the integration for the new signal at 5.94 ppm was too small to be measured accurately.

The direct probe EI mass spectrum of **X** (Fig. 11) showed an ion at m/z 424 but this signal was so weak (0.5%) that it was disregarded at that time. The two strong peaks observed at m/z 269 and m/z 138 were consistent with the results from the GC/EI mass spectrum (Fig. 9 and Fig. 10). The odd mass ion at m/z 269 again could not be the parent if, as we expected, the molecule was composed of C, H and O only.

In summary, the structure of compound **X** must be consistent with the following spectral data: (1) The compound must bear a carbon atom in an environment that will give a ^{13}C NMR signal at about 37 ppm; (2) A proton signal with a ratio of integration relative to the methylenedioxy protons is 1:4 or 1:6 (^1H NMR); (3) A fragmentation pathway leads to an intense ion at m/z 269 (GC/MS and MS). According to these ^1H NMR, ^{13}C NMR and MS spectral data, the symmetric structure **37** was suggested (Scheme 9). The fragment **38** was particularly attractive because of its likely stability.

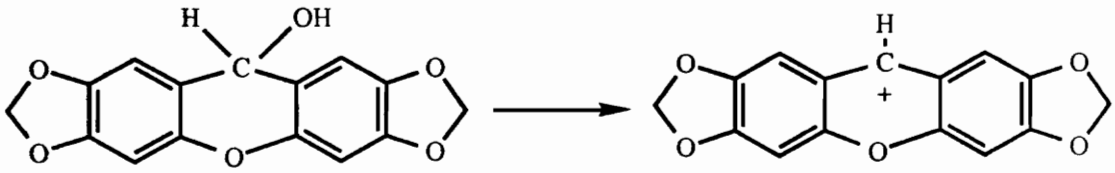

m/z 286 **37** m/z 269 **38**

Scheme 9. Structure **37**, a proposed structure for compound **X** and its fragmentation ion **38**.

This tentative assignment was ruled out after examining the reaction of the compound **X** with chlorotrimethylsilane and triethylamine since on the GC/MS analysis, the resulting derivative

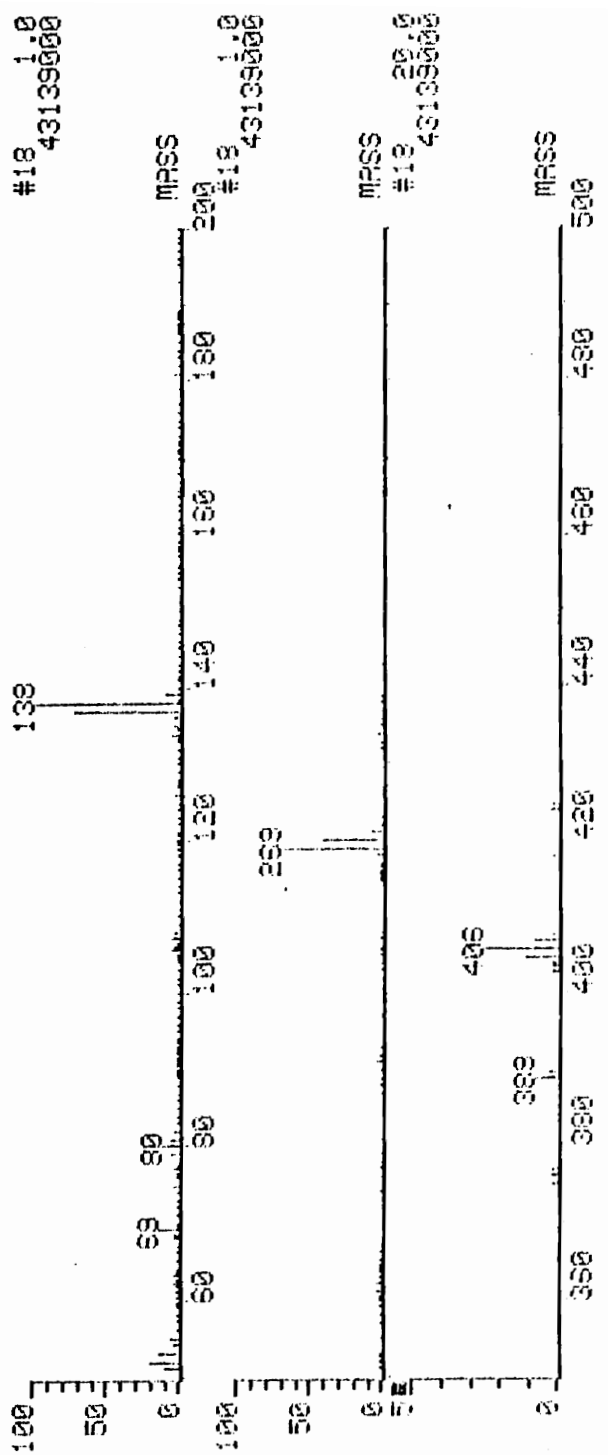

Figure. 11. Mass Spectrum of Compound X.

exhibited an intense molecular ion at m/z 640. This corresponded to the addition of more than one trimethylsilyl groups. The trimer structure, **35**, was then proposed for the compound **X**. The GC/EI mass spectral fragmentation pattern (Fig. 12) of the corresponding *tris*trimethylsilyl derivative supported the tentative structure assignment as evidenced by the m/z 551 ion which resulted from loss of $OSiMe_3$ from the parent ion, m/z 640. The fragment ion at m/z 431 was assigned to the species resulting from loss of methylenedioxytrimethylsilyloxyphenyl moiety (640 - 209 = 431). Similar losses account for fragment ions at m/z 357, 341 and 269.

This tentative assignment for compound **X** was confirmed by preparation of the trimethoxy derivative **40** with diazomethane **41**. The trimethoxy product exhibited the expected molecular ion peak at m/z 466 on the GC/EI mass spectrum (Fig 13). The intense fragment ion at m/z 435 was derived from loss of OCH_3 from the parent ion and the ions at m/z 420 and m/z 405 resulted from further loss of CH_3 groups from the intense ion at m/z 435.

The ^1H NMR spectrum of the trimethoxy derivative **40** showed two singlets at 6.51 ppm (H-6) and 6.33 ppm (H-3) which were assigned to the aromatic proton signals. The singlets at 6.15 ppm and 5.86 ppm were assigned to the signals of the methine proton and methylenedioxy protons, respectively. The singlet for the signals of the methoxy protons were recorded at 3.65 ppm and the ratio of these five sets of proton signals was 3:3:1:6:9, consistent with the trimer structure **40**. The structures **35** and **40** were further confirmed by elemental analysis. A possible mechanism for the formation of the trimer is described in Scheme 10, in which the initial Vilsmeier adduct **42** is attacked by the nucleophilic methylenedioxyphenol **28** to generate the dimeric product **43** that undergoes an additional reaction with **28** to yield the trimer **35**. The proposed fragmentation pathway for the trimer **35** is illustrated in Scheme 11.

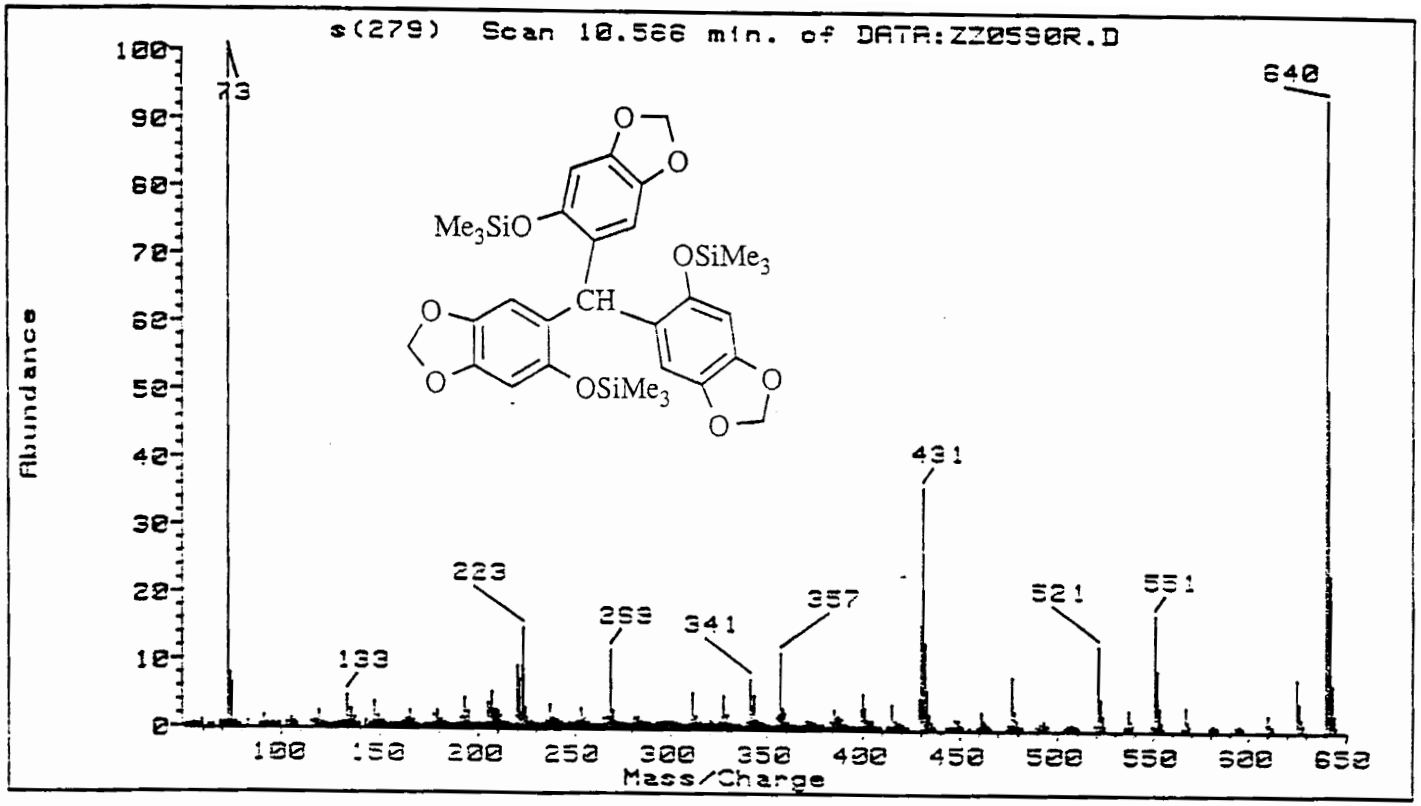

Figure. 12. GC/EIMS of *Tris*(2-trimethylsilyloxy-4,5-methylenedioxyphenyl)methane.

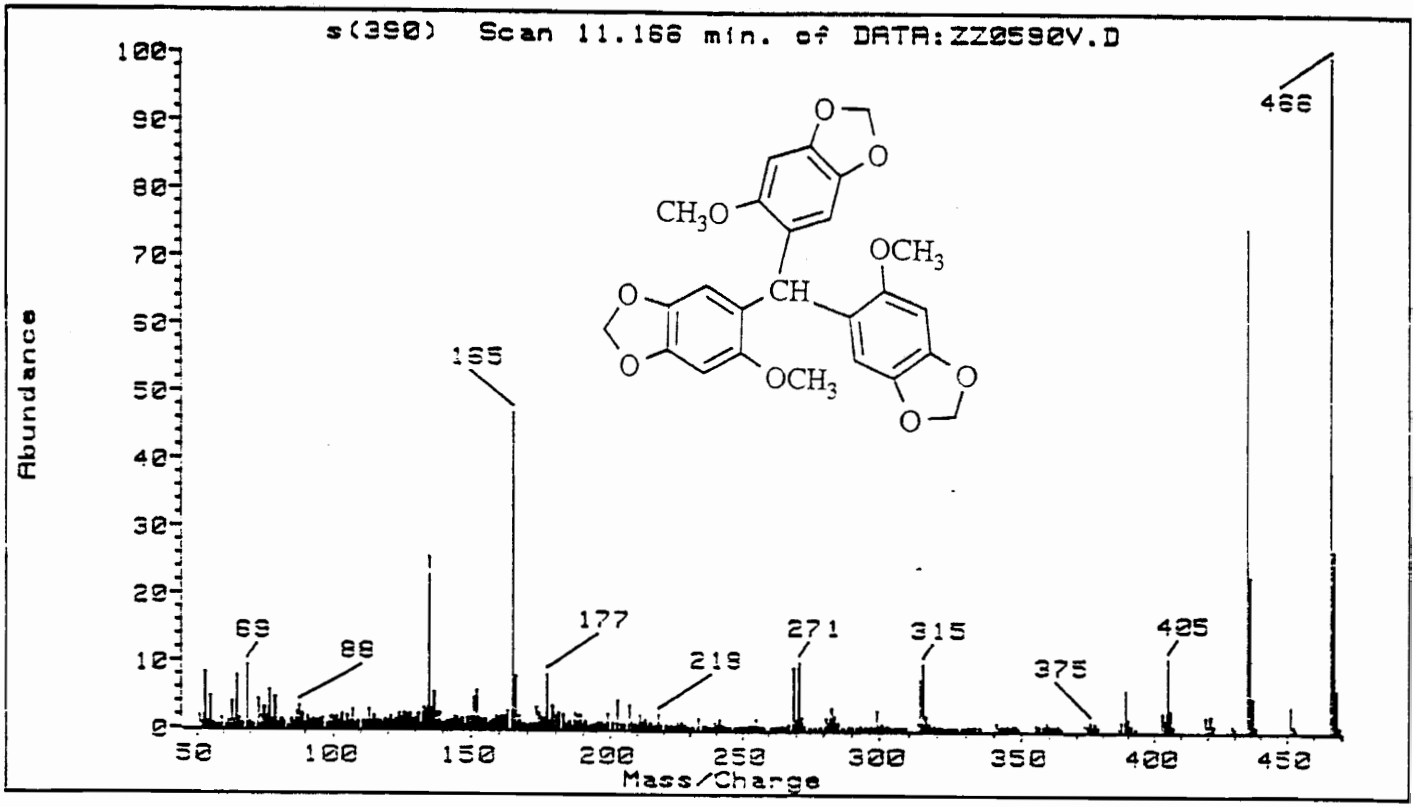

Figure. 13. GC/EIMS of *Tris*(2-methoxy-4,5-methylenedioxyphenyl)methane.

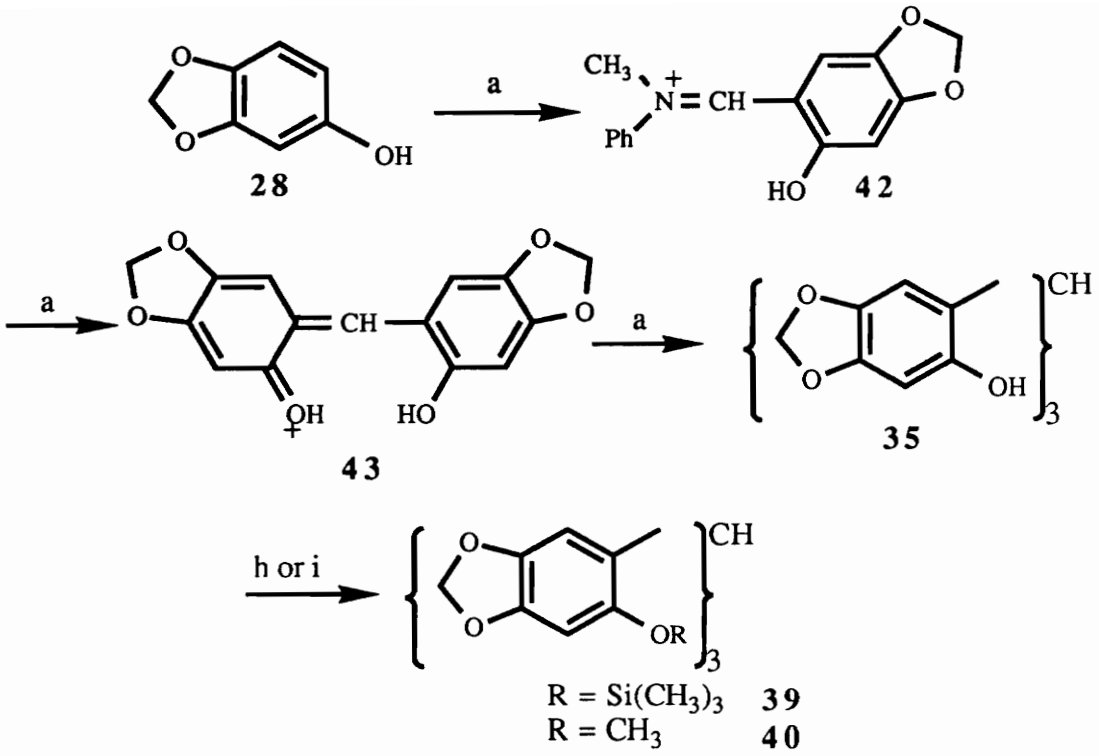

a) $Ph(CH_3)NCHO$, $POCl_3$; h) $(CH_3)_3SiCl$, Et_3N; i) CH_2N_2

Scheme 10. Proposed pathway leading to the trimer **35**.

The original synthetic pathway to obtain **24** involved direct modification of the phenolic aldehyde **29**. Attempts to prepare the corresponding nitrostyrene of this intermediate by reaction of **29** with nitroethane, however, failed. Further transformation directed to the synthesis of **24** involved the conversion of **29** to its benzyl ether **30** with benzyl bromide. The IR and ^1H NMR spectra of **30** were similar to those of **29** except for the additional singlet (5.1 ppm) due to the methylene protons and the multiplet due to the aromatic protons (7.4-7.0 ppm) of the benzyl group (Fig. 14).

The GC/EI mass spectrum (Fig. 15) of **30** showed a strong diagnostic fragment ion at m/z 91 which was assigned to the tropylium species **44**. The molecular ion at m/z 256 is relatively weak compared with the tropylium ion. Another fragment ion resulting from loss of the CHO group from the molecular ion was observed at m/z 227. Treatment of 2-benzyloxy-4,5-

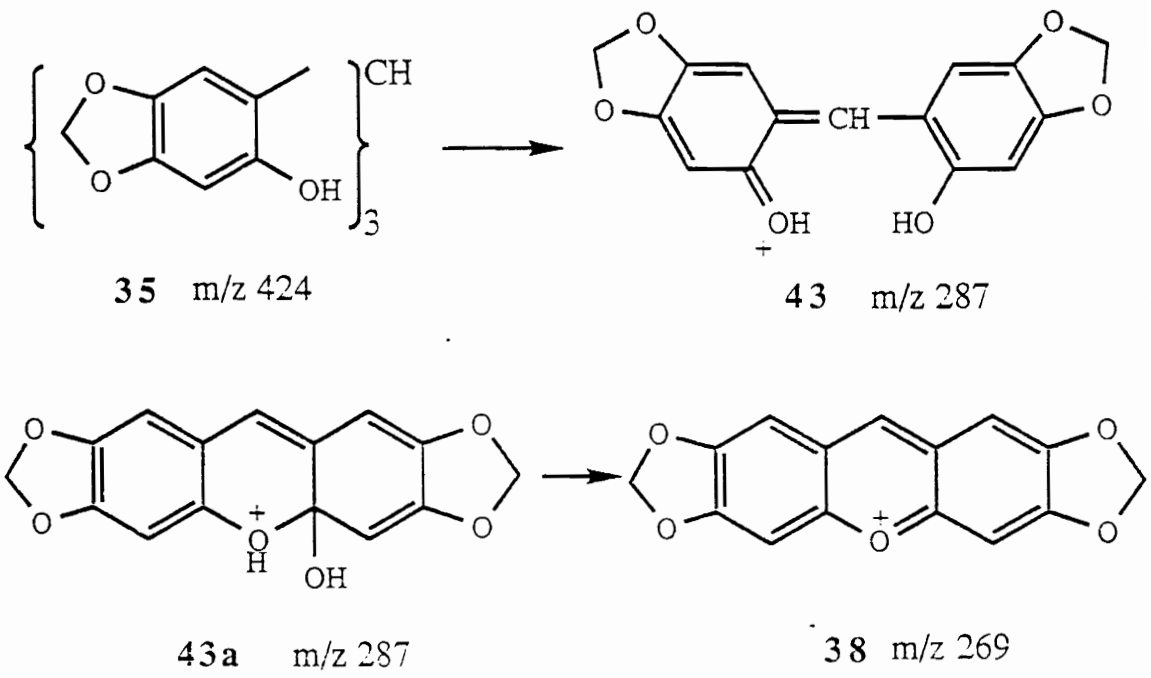

Scheme 11. Proposed fragmentation pattern of the trimer **35**.

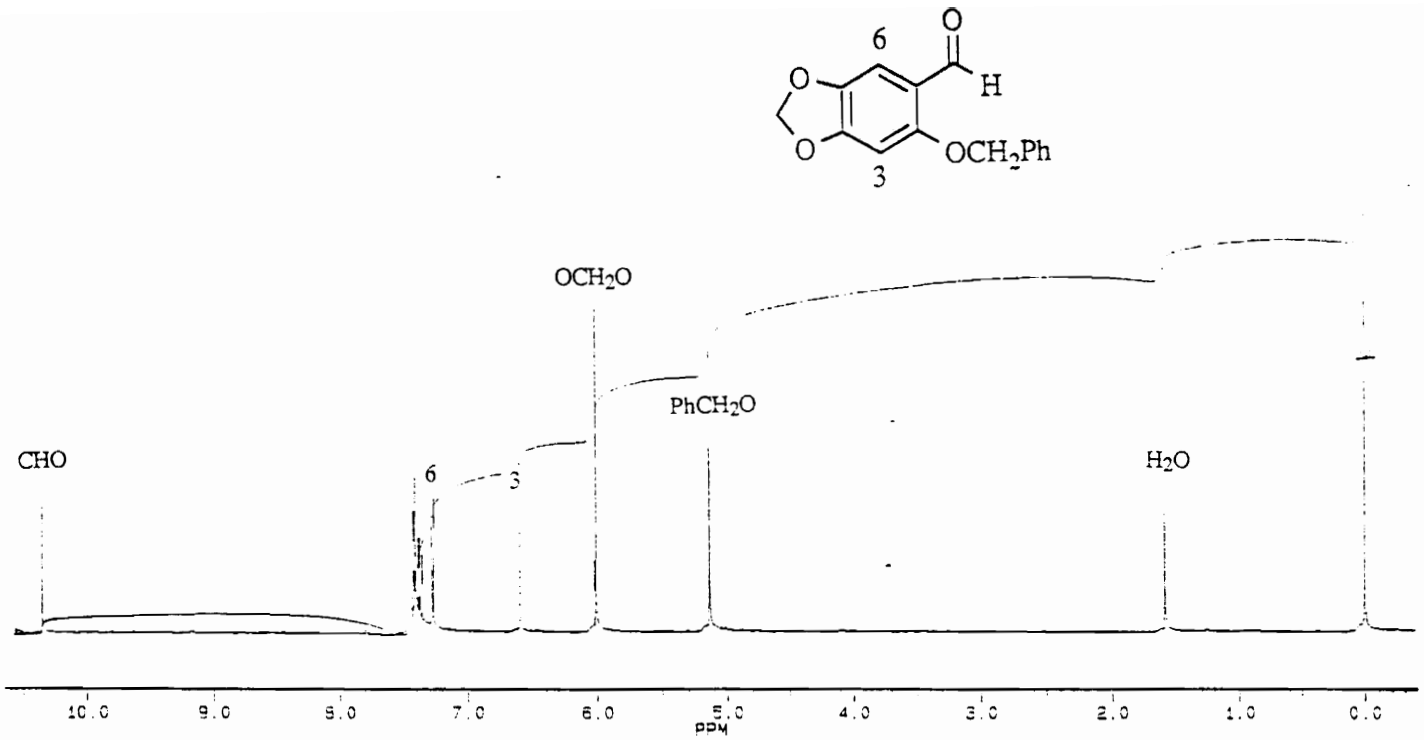

Figure. 14. ^1H NMR Spectrum ($CDCl_3$) of 2-Benzyloxy-4,5-methylenedioxybenzaldehyde.

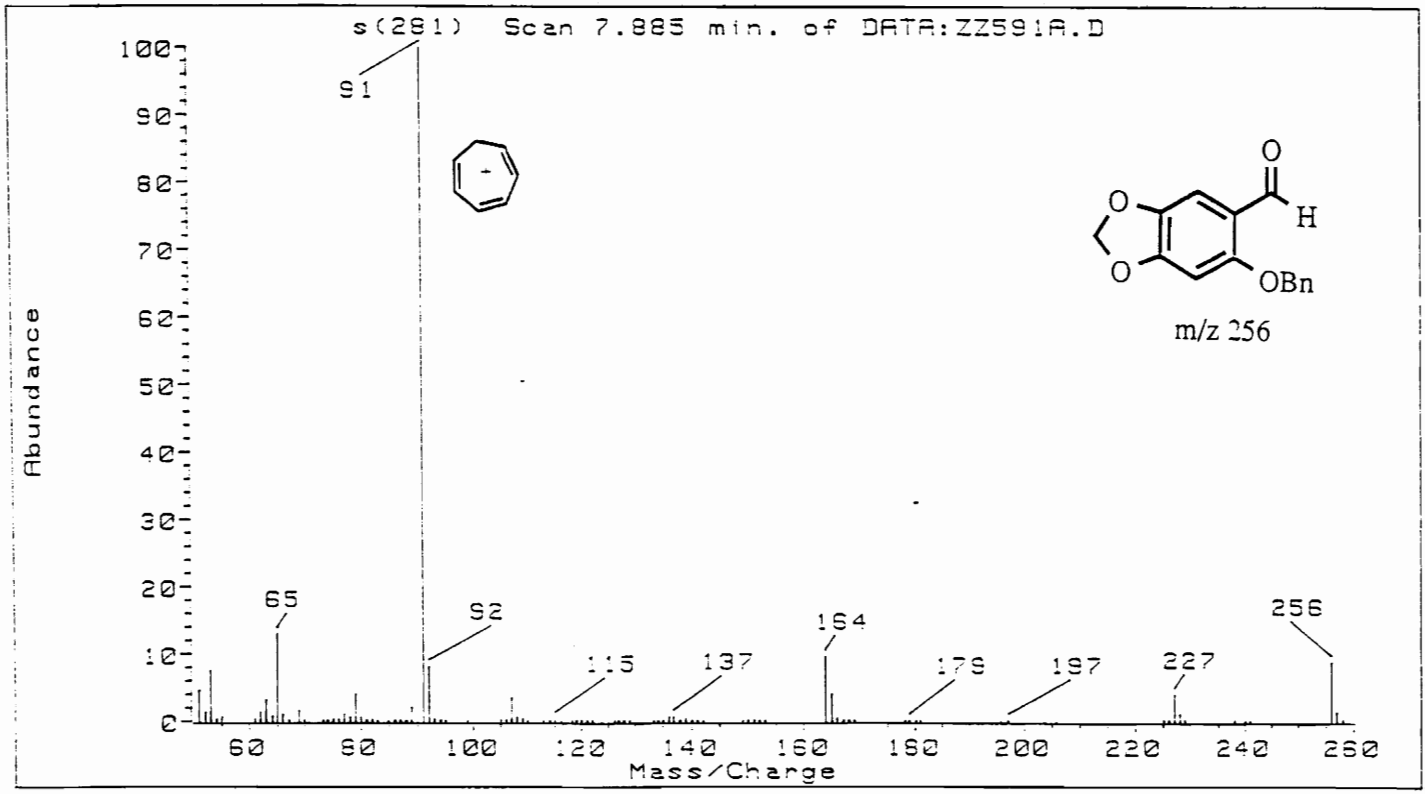

Figure. 15. GC/EIMS of 2-Benzyloxy-4,5-methylenedioxybenzaldehyde.

methylenedioxybenzaldehyde (**30**) with nitroethane yielded the corresponding nitrostyrene **31** as a yellow crystalline solid. This compound was not stable under GC/MS conditions as evidenced by the absence of a molecular ion which was expected at m/z 313. Therefore, its mass spectrum was obtained by the direct probe technique (Fig 16). The molecular ion (m/z 313) was weak but detectable. The two major diagnostic fragment ions were the tropylium ion **44** (m/z 91) and the ion resulting from loss the nitro group and the benzyl group from the molecular ion (m/z 176).

The ^1H NMR spectrum (Fig. 17) of **31** showed a downfield singlet at 8.4 ppm which was assigned to the olefinic proton adjacent to the aromatic ring. The signal for the allylic methyl group protons was recorded as a singlet at 2.4 ppm. The remaining proton signals were similar to those observed in the ^1H NMR spectrum of compound **30**. Only one isomer of the theoretically possible E/Z geometral isomers (**45/46**) was obtained from the reaction according to the ^1H NMR evidence. Since the isomeric features would not effect the subsequent reaction, no effort was made to determine the isomeric structure. The E isomer **45** appears more likely based on steric hindrance considerations.

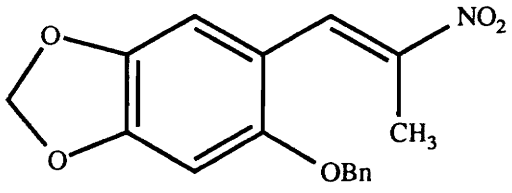

E-isomer **45**

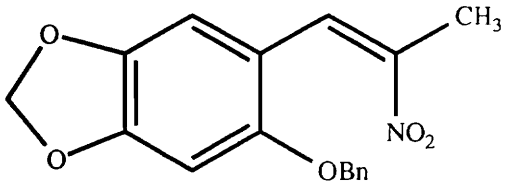

Z-isomer **46**

Lithium aluminum hydride (LAH) reduction of 1-(2-benzyloxy-4,5-methylenedioxyphenyl)-2-nitropropene (**31**) to the corresponding amine **32** followed by treatment of the free base **32** with etheral HCl gave 1-(2-benzyloxy-4,5-methylenedioxyphenyl)-2-aminopropane hydrochloride (**32·HCl**) as a white crystalline solid. The ^1H NMR spectrum (Fig. 18) of **32** showed a doublet for the signal of the methyl group protons at 1.1 ppm. The methine proton signal was observed at 3.2 ppm as a multiplet due to the coupling with two

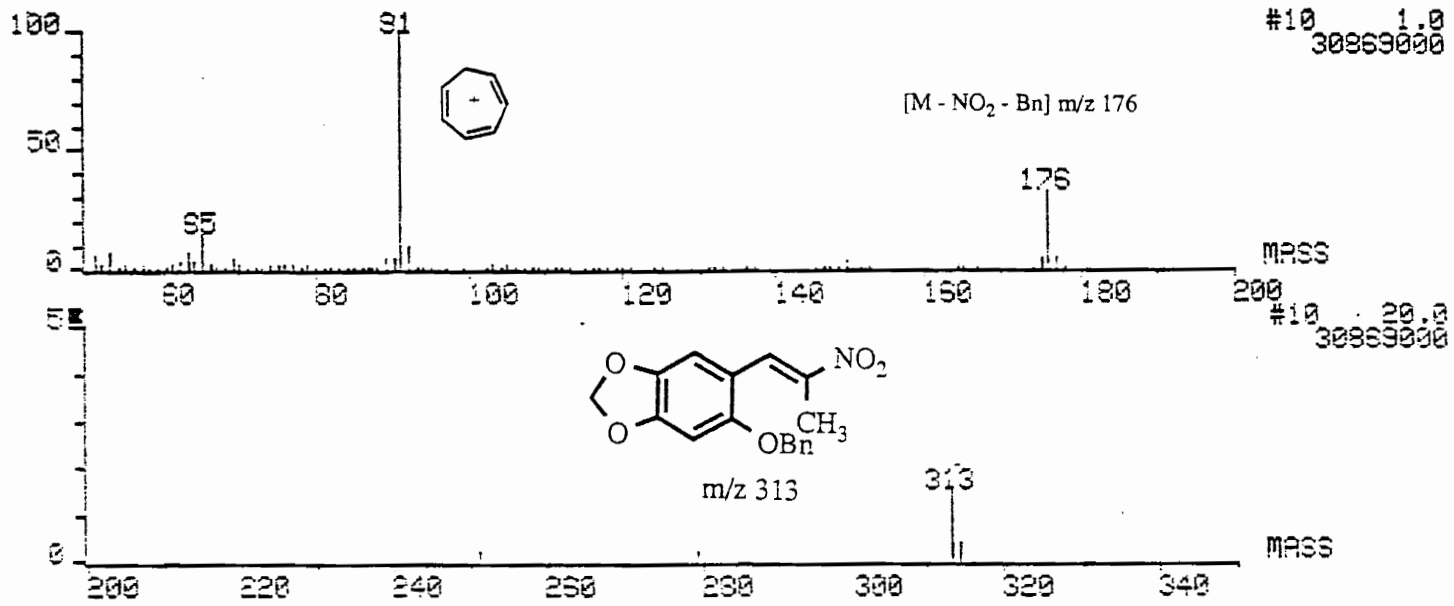

Figure. 16. Mass Spectrum of 1-(2-Benzyloxy-4,5-methylenedioxyphenyl)-2-nitropropene.

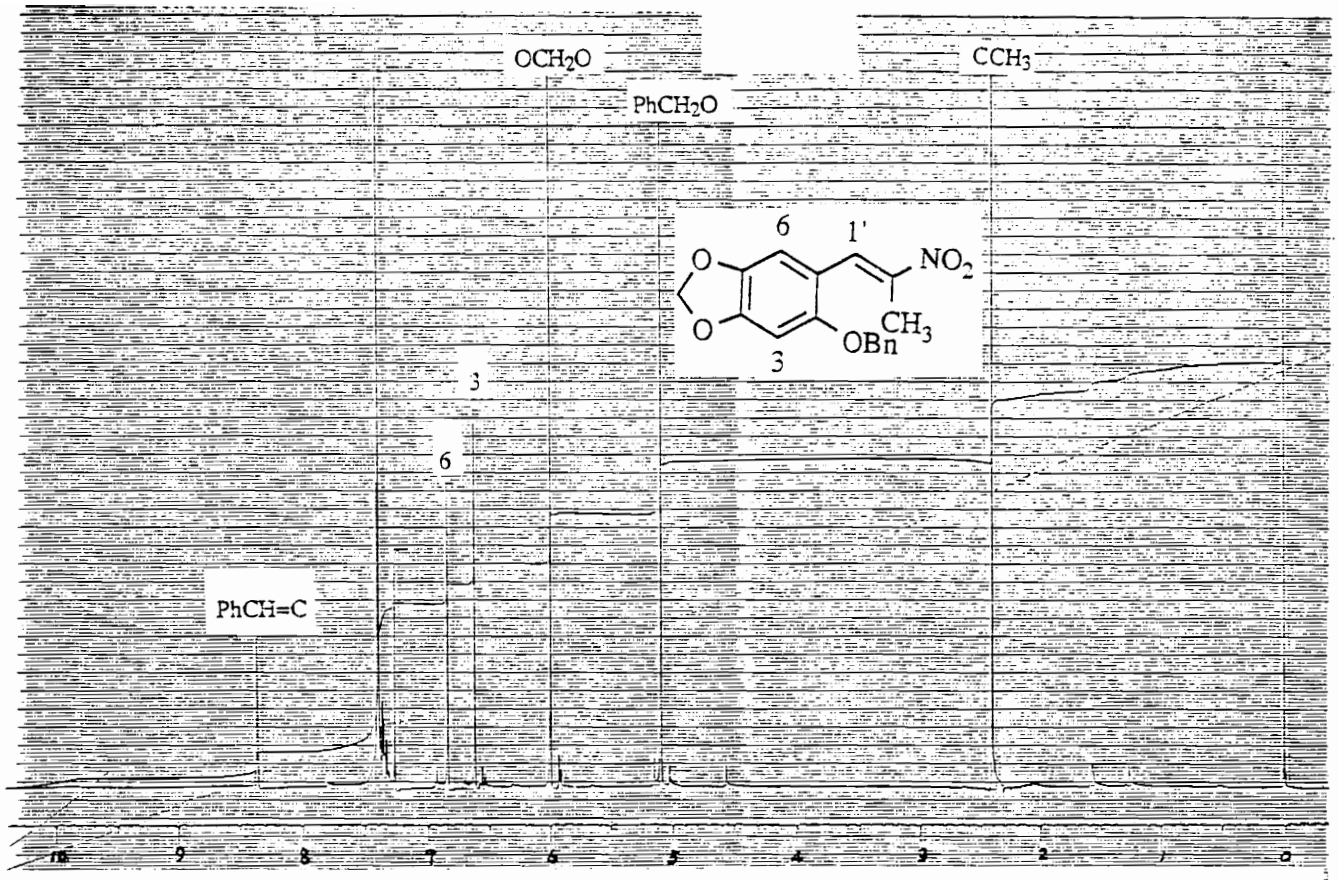

Figure. 17. ^1H NMR Spectrum ($CDCl_3$) of 1-(2-Benzyloxy-4,5-methylenedioxyphenyl)-2-nitropropene.

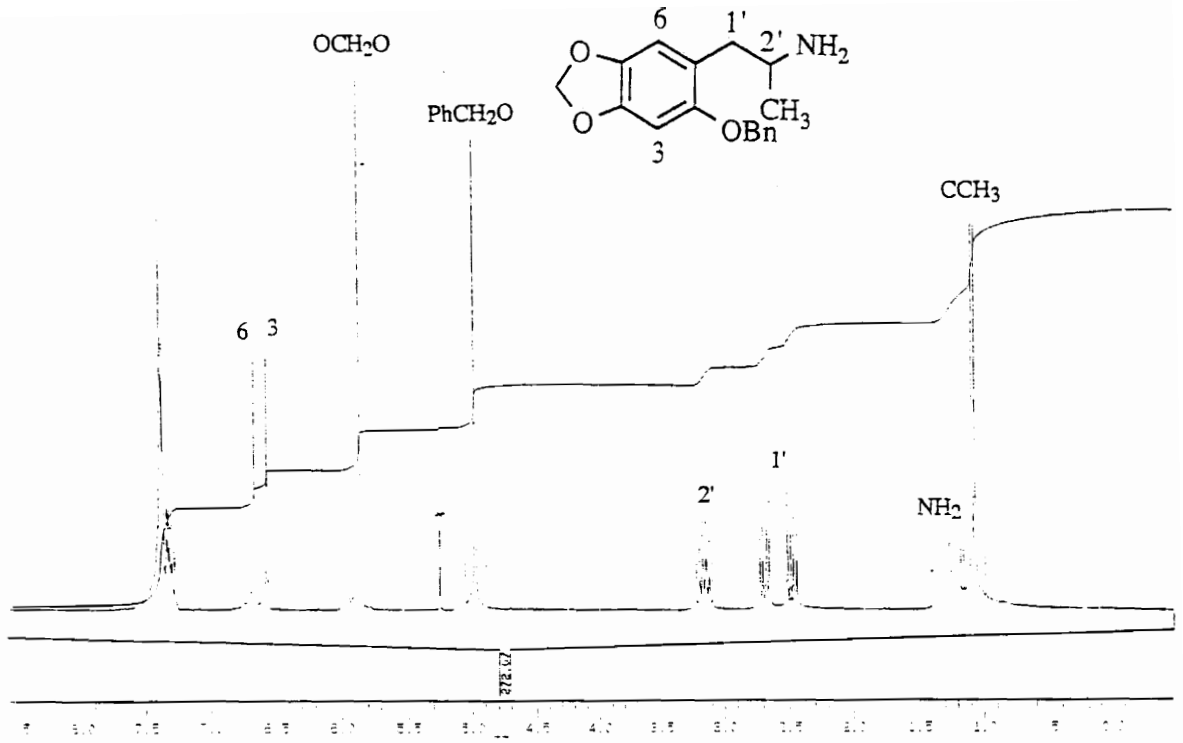

Figure. 18. ^{1}H NMR Spectrum ($CDCl_3$) of 1-(2-Benzyloxy-4,5-methylenedioxyphenyl)-2-aminopropane.

methylene group protons and the three methyl group protons. Two quartets at 2.5 ppm and 2.7 ppm, respectively, were assigned to the two methylene proton signals. Since these two methylene protons are situated next to a chiral center they are not chemically equivalent, and therefore they couple with each other as well as with the methine proton. The methylene protons of compound **32** showed an AB coupling pattern as expected for such diastereotopic protons.

The GC/EI mass spectrum (Fig. 19) of **32** showed a weak molecular ion at m/z 285. As described above for **30**, the most abundant ion in the EI mass spectrum of **32** could be assigned to the tropylium ion **44** at m/z 91. The GC/EI mass spectrum also contained diagnostic fragment ions resulting from cleavage β to the nitrogen atom accompanied by a proton transfer (Scheme 12) (m/z 242, M^+ - $CH_3CH{=}NH$) and from further loss a benzyl group (m/z 151, M^+ - $CH_3CH{=}NH$ - CH_2Ph). This type of proton transfer is similar to the McLafferty rearrangement[54] which involves intramolecular migration of the hydrogen atom on the nitrogen atom to the oxygen atom, probably via a 7-member ring transition state as illustrated below:

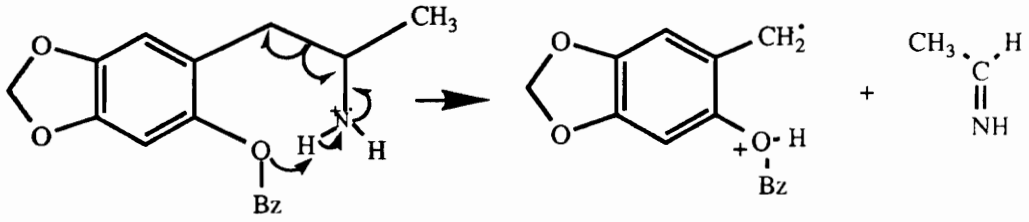

32 (m/z 285) **47** (m/z 242) **48** (m/z 43)

Scheme 12. Proposed GC/MS proton transfer pathway for **32**.

This type of proton transfer also was observed with the model compound 1-(2,4,5-trimethoxyphenyl)-2-aminopropane (**49**) under the same GC/MS conditions used to examine compound **32** (Scheme 13).

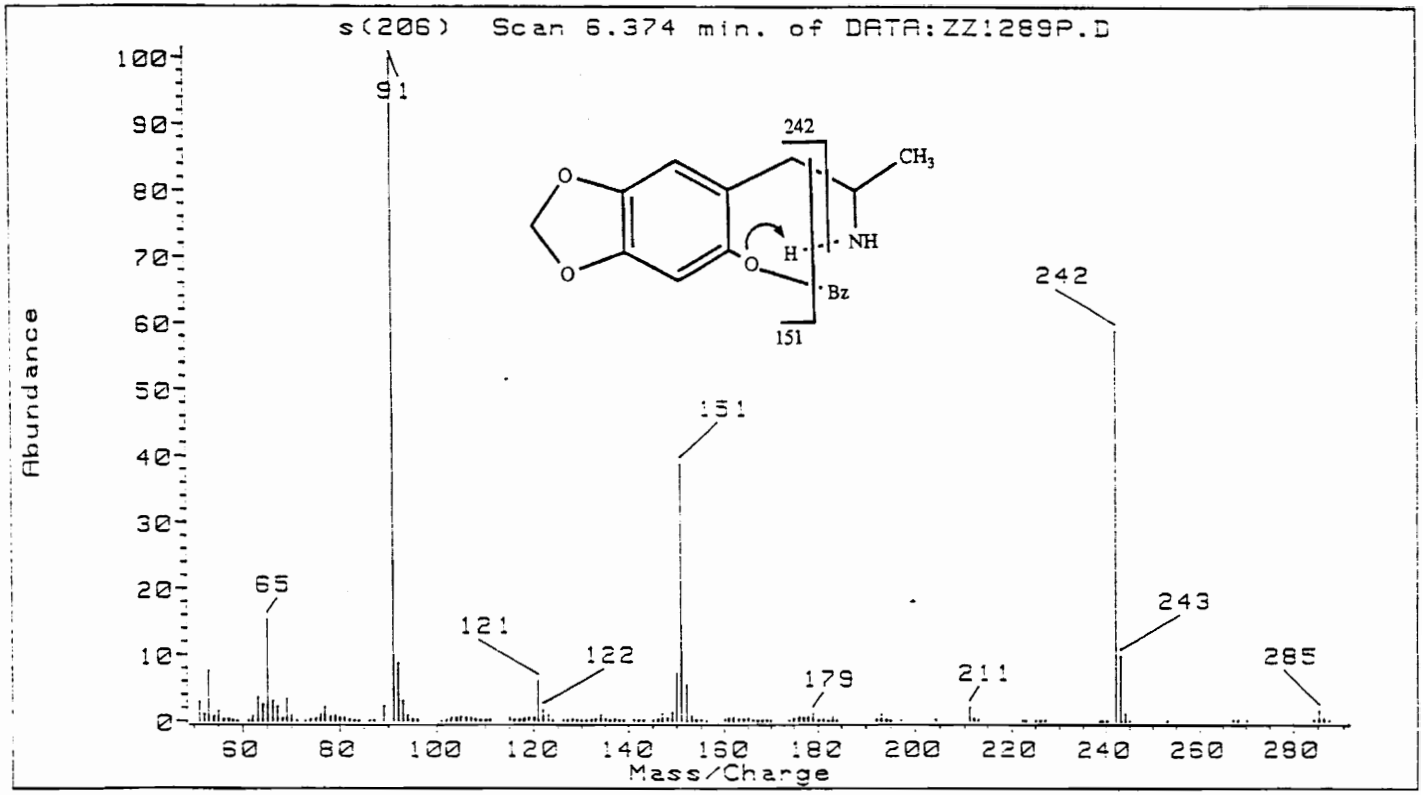

Figure. 19. GC/EIMS of 1-(2-Benzyloxy-4,5-methylenedioxyphenyl)-2-aminopropane.

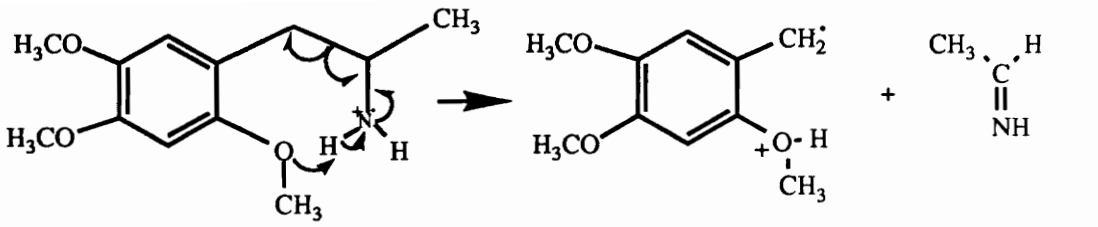

49 (m/z 225) **50** (m/z 182) **48** (m/z 43)

Scheme 13. Example of proton transfer pathway with model compound **49**.

The ^1H NMR spectrum of **32·HCl** was almost identical with that of its free base except that the two methylene proton signals merged at 3.0 ppm and the two benzyl methylene proton signals appeared as a quartet at 5.0 ppm. The coupling between the two benzyl methylene protons in **32·HCl** was probably due to the rigidity of the system which prevented free rotation and caused magnetic nonequivalence between these two protons.

N-Monomethylation of **32** was achieved via formation of the formamide **33** followed by LAH reduction. The formamidation reaction used ethyl formate as the formylation reagent and was straightforward and clean. The formamide was purified by column chromatography and the ^1H NMR, GC/MS, IR spectral data and elemental analysis supported the assigned structure. The IR spectrum showed a strong band at 1658 cm^{-1} and was assigned to the -N-C=O stretch frequency.[54] The most abundant ion (m/z 91) in the GC/MS spectrum (Fig. 20) of **33** was due to the tropylium ion **44**. The molecular ion at m/z 317 was strong. A typical McLafferty-type rearrangement[54] was observed in the EI mass spectrum of compound **33** (m/z 268, Scheme 14). The other diagnostic fragment ions were formed by loss of the combination of $PhCH_2$ and $CH_3CH{=}NCHO$ (m/z 151) and by loss of the another combination of $PhCH_2$ and HN=C(H)OH (m/z 177). The fragment ion observed at m/z 242 resulted from cleavage β to the nitrogen atom with proton transfer, as observed with compound **32**.

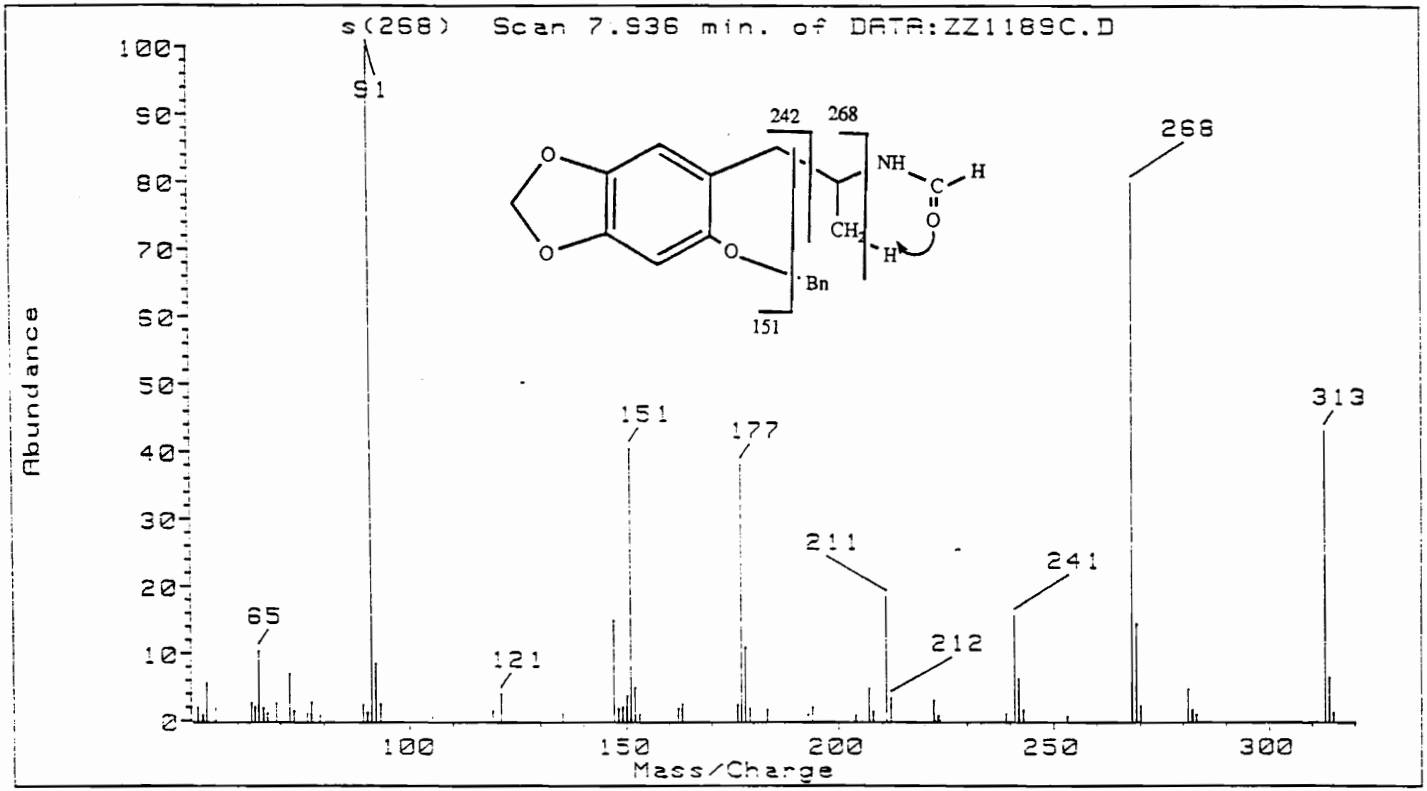

Figure. 20. GC/EIMS of 1-(2-Benzyloxy-4,5-methylenedioxyphenyl)-2-formamidopropane.

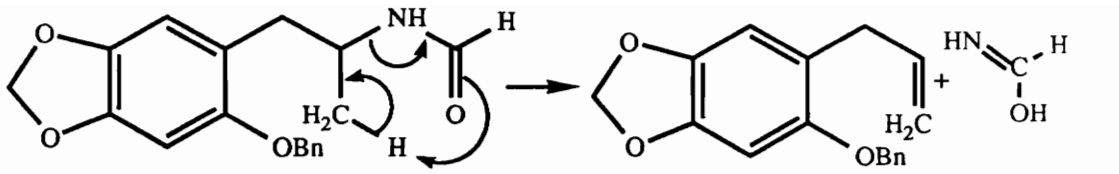

33 (m/z 313) **51** (m/z 268) **52** (m/z 45)

Scheme 14. McLafferty rearrangement of compound **33**.

The ^1H NMR spectrum (Fig. 21) of **33** was quite complicated because almost all the side-chain proton signals were doubled. Signals consistent with the NCHO proton were observed at 7.9 ppm (singlet) and 7.7 ppm (doublet). The signals at 4.2 ppm (multiplet) and 3.7 ppm (multiplet) would be expected for the methine proton of the side-chain. The methylene protons of the side-chain appeared as a broad multiplet centered at 2.7 ppm and the methyl group was monitored as two sets of doublets centered at 1.2 ppm and 1.1 ppm.

The quality of the spectrum and the mass spectral features of this product argued against the presence of impurities. The characteristics of the ^1H NMR spectrum suggested the possibility of the existence of rotomers due to the partial double bond character between the nitrogen and carbonyl carbon atoms. This speculation was not supported at the beginning by a failed attempt to average the rotomers with a high temperature ^1H NMR analysis (at 55 °C). The doubled signals would be expected to simplify at the higher temperature due to the increased rate of rotation. This, however, was not observed.

The ^1H NMR spectrum of 1-(2,4,5-trimethoxyphenyl)-2-formamidopropane (**53**), prepared as a model compound via the same reaction with 1-(2,4,5,-trimethoxyphenyl)-2-aminopropane (**49**) as starting material, showed similar spectral characteristics. This result supported the original speculation concerning rotomers. This assignment was finally confirmed by ^1H NMR analysis in the presence of D_2O (Fig. 22). The aldehyde proton signals in the original spectrum in $CDCl_3$ appeared as a singlet at 7.9 ppm and a doublet centered at 7.7 ppm. Two days after shaking with D_2O, the spectrum showed two singlets at chemical shift values of 7.9 ppm and 7.7 ppm.

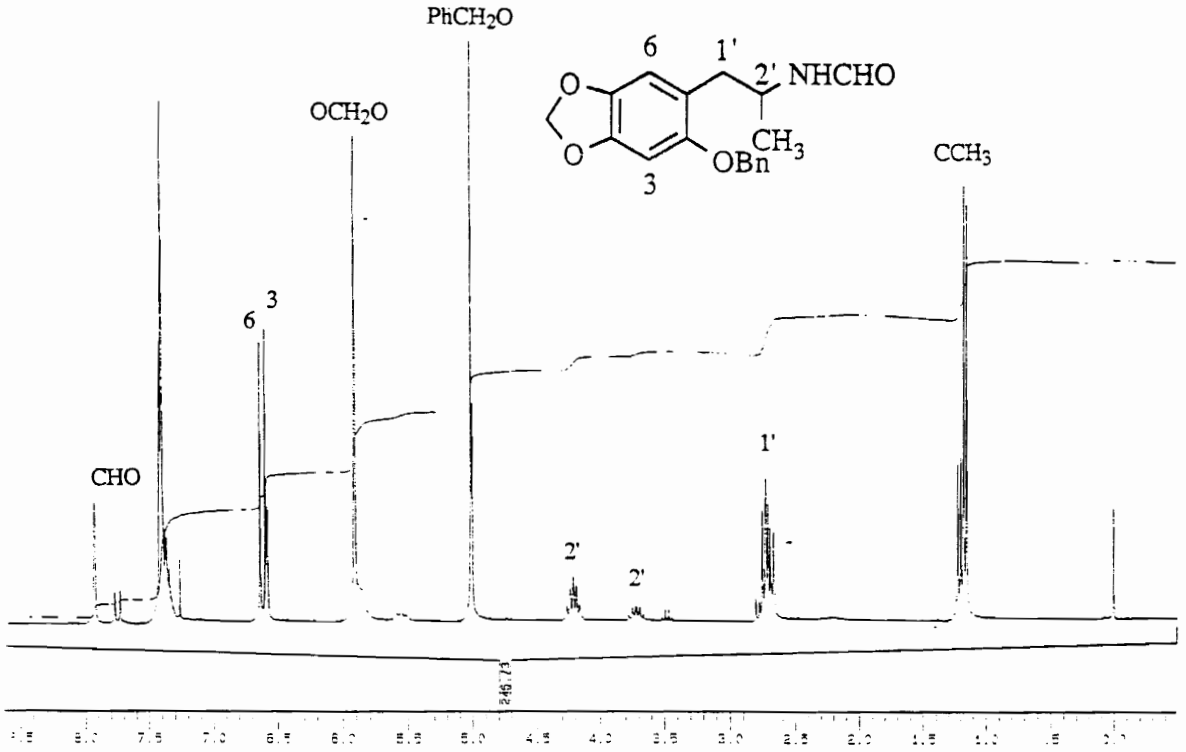

Figure. 21. ^{1}H NMR Spectrum ($CDCl_3$) of 1-(2-Benzyloxy-4,5-methylenedioxyphenyl)-2-formamidopropane.

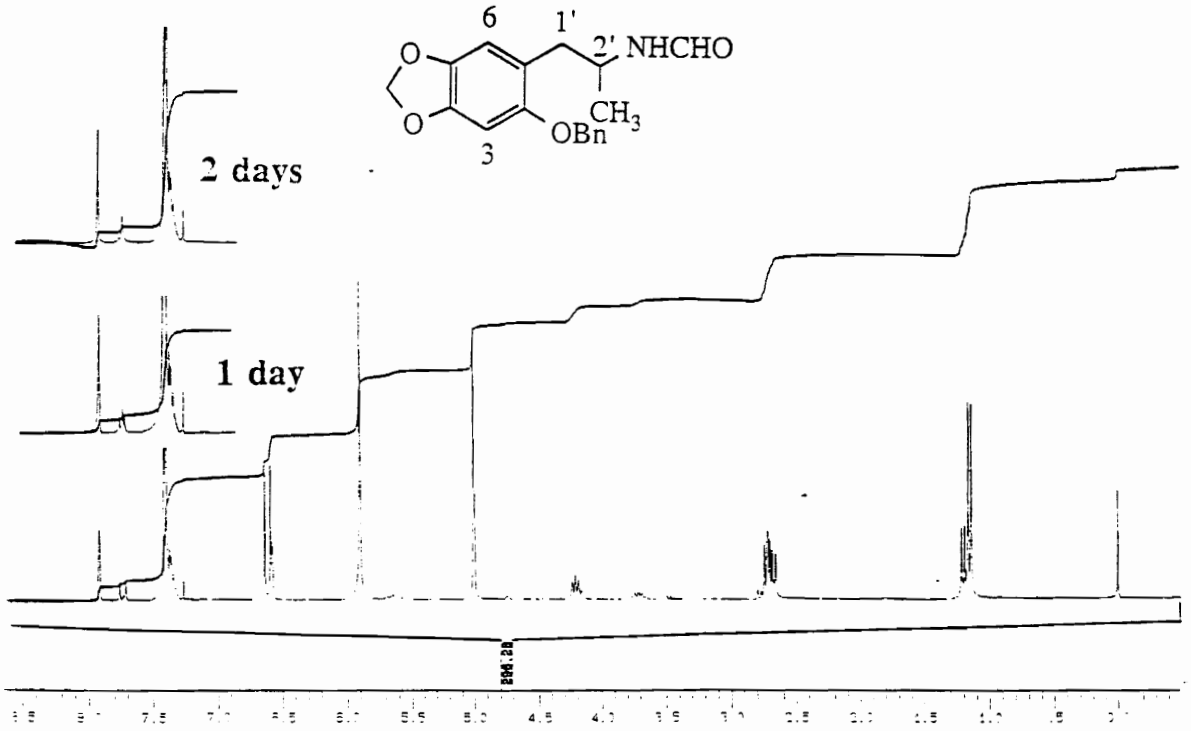

Figure. 22. ^1H NMR Spectrum ($CDCl_3/D_2O$) of 1-(2-Benzyloxy-4,5-methylenedioxyphenyl)-2-formamidopropane.

The original doublet centered at 7.7 ppm had collapsed to form a singlet at 7.7 ppm because no further coupling existed between the CHO proton and NH proton after exchanging the NH proton with deuterium. The other evidence in support of the rotomer assignment was that reduction of **33** led to only one N-methylated compound namely **34**. The explanation for the unsuccessful variable temperature NMR experiment for demonstrating the rotomers was probably due to the fact that the temperature was not high enough. The ^1H NMR spectrum of N,N-dimethylformamide is reported to show two CH_3 peaks at room temperature which merge at about 123 °C.[54]

The reduction of **33** with LAH provided the desired N-methyl derivative **34**. The GC/EI mass spectrum of **34** (Fig. 23) showed a typical fragmentation pattern that included cleavage β to the nitrogen atom with proton transfer to give a fragment ion at m/z 242. This was the same fragment ion observed with compound **32**. The diagnostic tropylium ion **44** at m/z 91 also was present. The most abundant fragment ion, m/z 58, resulted from the normal cleavage β to the nitrogen atom without proton transfer. The molecular ion at m/z 299 was very weak but detectable.

The diagnostic peak in the ^1H NMR spectrum of **34** (Fig. 24) was the singlet signal for the N-methyl group protons at 2.4 ppm. The methine proton signal appeared at 2.8 ppm and overlaped with one of the methylene proton signals. The other methylene proton signal was recorded at 2.6 ppm as a multiplet due to coupling with the methine proton and the germinal proton. The rest of the spectrum was similar to that of **32**.

Compound **34** was converted to **34·HCl** by treatment with ethereal HCl. The methyl group doublet (1.0 ppm) coupled with methine proton in **34** was shifted to 1.3 ppm in the salt. The methine proton signal also was shifted (from 2.8 ppm to 3.3 ppm) as well as the methylene proton signals which shifted to 3.3 ppm and 2.7 ppm. The very interesting point of the ^1H NMR of **34·HCl** was that the N-methyl group protons appeared as a triplet centered at 2.5 ppm. This triplet probably is a consequence of coupling with the $^+NH_2$ group. As expected addition of D_2O caused the triplet to collapse to a sharp singlet at the same chemical shift. A broad peak

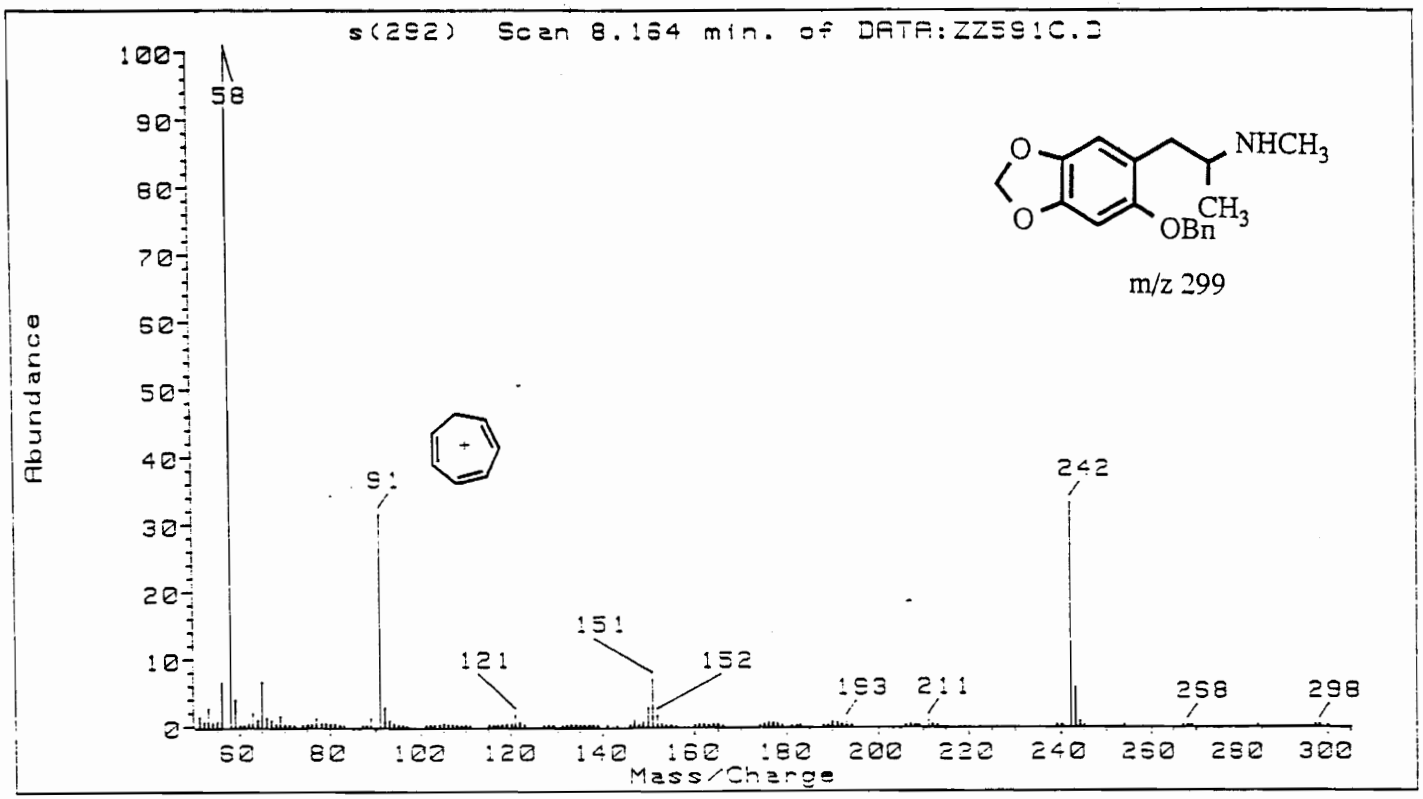

Figure. 23. GC/EIMS of 1-(2-Benzyloxy-4,5-methylenedioxyphenyl)-2-methylaminopropane.

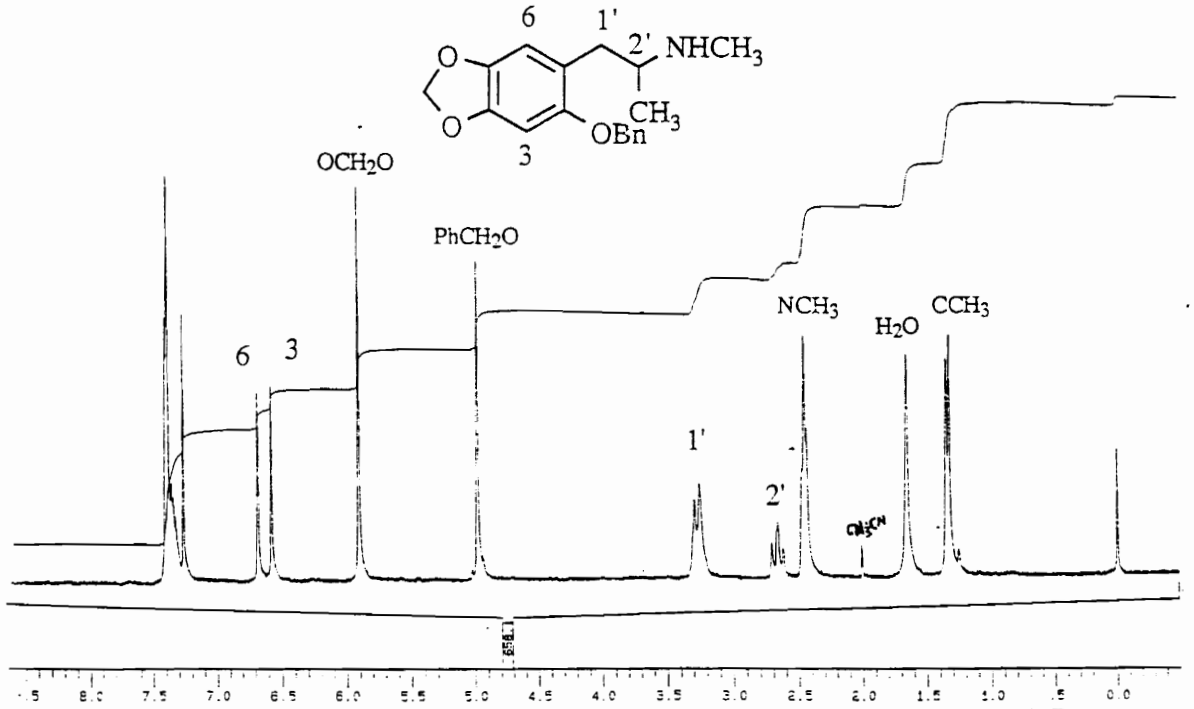

Figure. 24. ^1H NMR Spectrum ($CDCl_3$) of 1-(2-Benzyloxy-4,5-methylenedioxyphenyl)-2-methylaminopropane.

in the ^1H NMR spectrum of **34·HCl** at 9.4 ppm also disappeared after adding the D_2O and therefore this signal was assigned to the $^+NH_2$ protons.

The product **24·HCl** was easily prepared by hydrogenolysis of the **34·HCl** with Pd(C) as a catalyst under one atmosphere of H_2. The product was purified by recrystallization from CH_3CN. The diagnostic ^1H NMR signals (Fig. 25) for the benzyl protons (two benzyl methylene protons at 5.0 ppm and five benzyl aromatic protons at 7.5-7.3 ppm) were not present in the spectrum of **24·HCl**. The methine proton signal was recorded at 3.4 ppm as a multiplet. The side-chain methylene proton signals appeared as quartets centered at 3.1 ppm and 2.7 ppm.

The GC/EI mass spectrum (Fig. 26) showed a molecular ion corresponding to the free base **24** at m/z 209. The most abundant peak (m/z 58) resulted from the cleavage β to the nitrogen atom. The typical diagnostic fragment ion (m/z 152) of this class of compounds was formed by proton transfer with cleavage β to nitrogen atom.

The corresponding trihydroxy compound, 2-methylamino-1-(2,4,5-trihydroxyphenylpropane hydrochloride (**25·HCl**), was obtained from the reaction of **34·HCl** with boron tribromide.[55] The product was purified by ion-exchange chromatography with Dowex AG 50W-X4, a strong acid cation exchange resin. The product eluted with 6 N HCl and the eluent was lyophilyzed to a small volume. It formed an off-white crystalline solid. The ^1H NMR spectrum (Fig. 27) of **25·HCl** supported the assigned structure. The spectrum exhibited two singlets in the aromatic region at 6.49 ppm and 6.33 ppm. The methine proton signal at 3.34 ppm appeared as a multiplet and the two sets of methylene proton signals were observed at 2.83 ppm and 2.63 ppm. The singlet at 2.60 ppm was derived from the N-methyl group protons and the doublet at 1.18 resulted from C-methyl group protons which were coupled to the methine proton. The compound was not analyzed by GC/MS since its free base form is extremely unstable.

The 1-(3,4-dihydroxyphenyl)-2-methylaminopropane (**19**) also was synthesized by oxidative cleavage of the methylenedioxy group

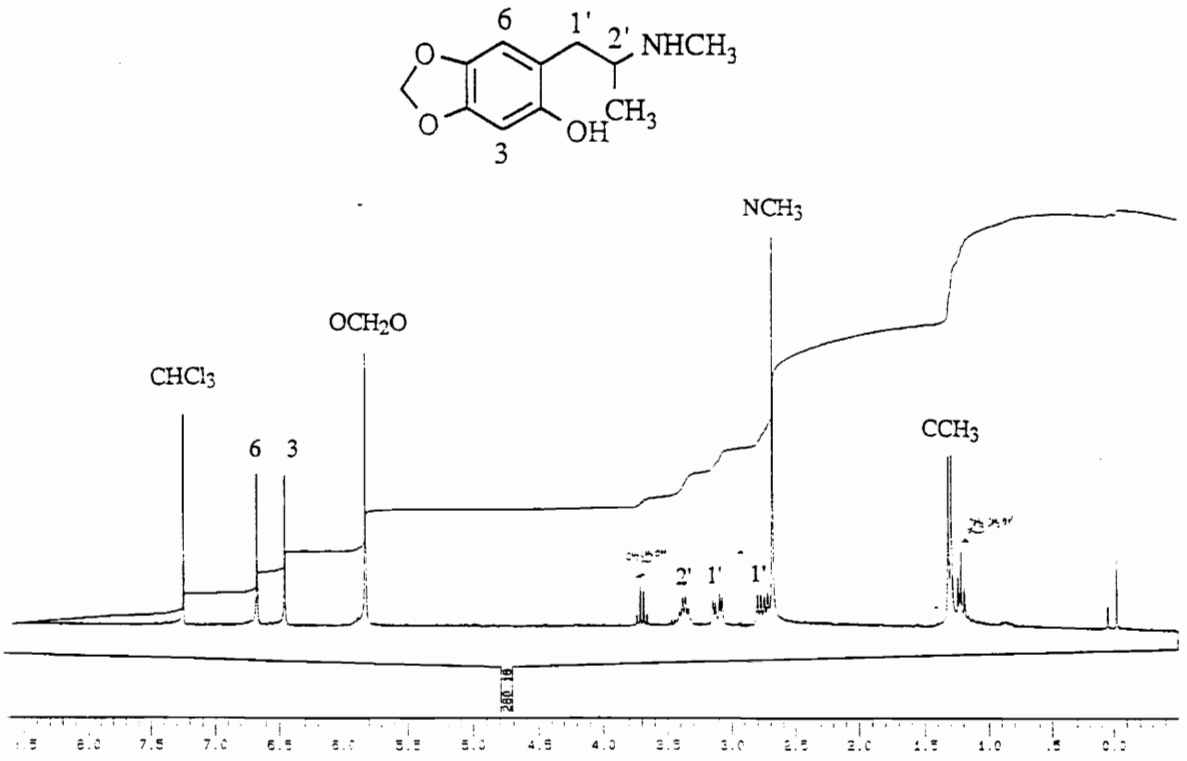

Figure. 25. ^1H NMR Spectrum ($CDCl_3$) of 1-(2-Hydroxy-4,5-methylenedioxyphenyl)-2-methylaminopropane.

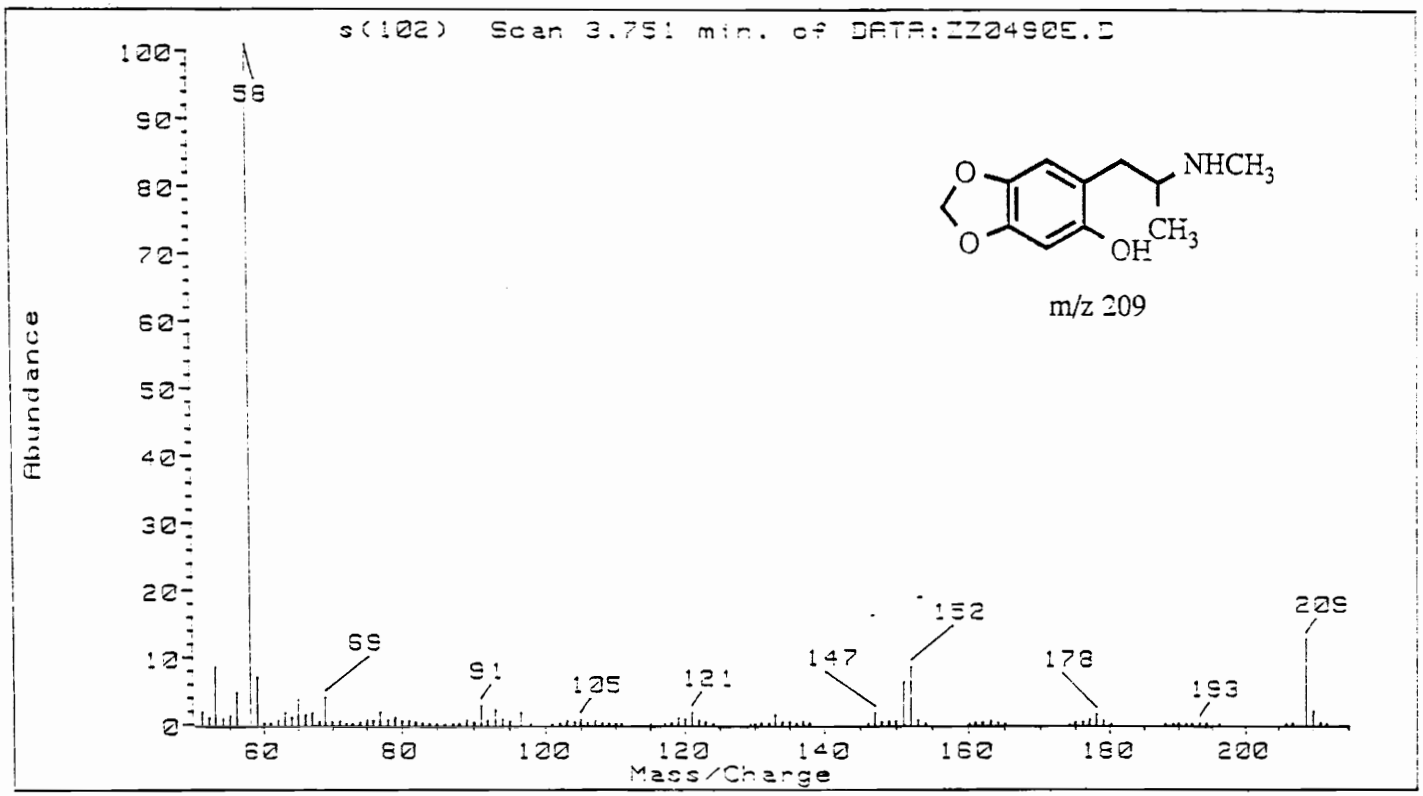

Figure. 26. GC/EIMS of 1-(2-Hydroxy-4,5-methylenedioxyphenyl)-2-methylaminopropane.

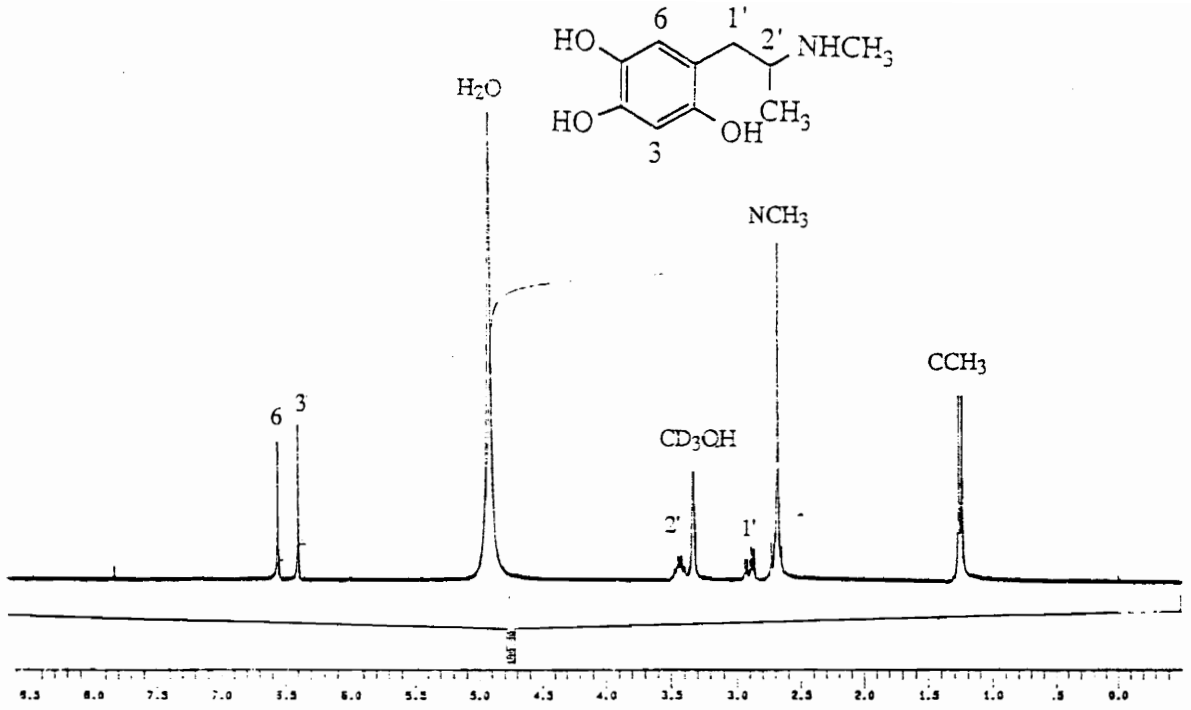

Figure. 27. ^1H NMR Spectrum (CD_3OD) of 2-Methylamino-1-(2,4,5-trihydroxyphenyl)propane.

of MDMA (**15**) with BBr_3 as another potential neurotoxic metabolite derived from MDMA. The ^1H NMR spectrum (Fig. 28) of the product was consistent with the structure assigned as evidenced by the absence of the singlet derived from the methylene protons of the methylenedioxy group present in MDMA. The ^1H NMR spectrum exhibited two doublets in the aromatic region at 6.8 ppm and 6.6 ppm which were assigned to the two *ortho* protons (H-5 and H-6). The other aromatic proton signal due to H-2 was observed at 6.7 ppm as a singlet. The methine proton signal was at 3.4 ppm and appeared as a multiplet while the two sets of methylene proton signals were observed at 2.95 ppm and 2.65 ppm as quartets due to the coupling with the methine proton and geminal proton. The singlet at 2.7 ppm was assigned to the N-methyl group protons and the doublet at 1.2 ppm to the C-methyl group protons which are coupled to the methine proton.

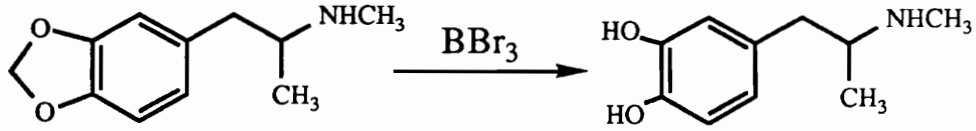

15 **19**

Scheme 15. Synthetic pathway leading to 3,4-dihydroxymethamphetamine.

2.3.2. Toxicology Evaluation

The 2-hydroxy derivative **24** of MDMA and trihydroxy analog **25** were sent to Dr. Ricaurte at Johns Hopkins University for neurotoxicity testing. The results[56] showed that the 2-hydroxy compound **24** failed to deplete 5-HT or DA on a long-term basis in the rat brain regardless of whether it was given systemically (Table 1), intracerebroventricularly (Table 2), or intrastriatally (Table 3). By contrast, established neurotoxins given by identical routes produced marked depletions. For example, MDMA given systemically produced a large depletion of regional brain 5-HT (Table 1). Similarly, 6-OHDA and 5,7-DHT given intracerebroventricularly

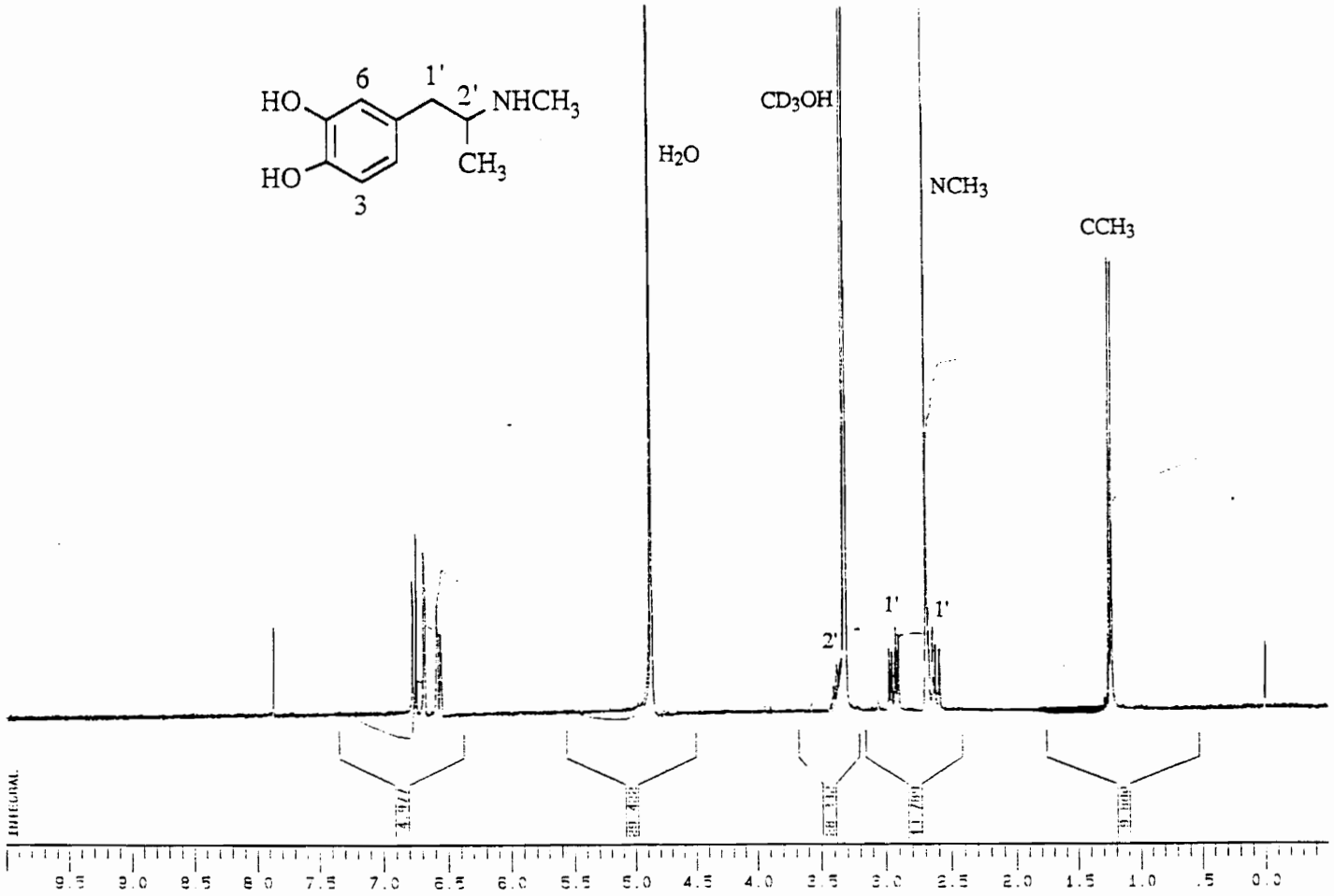

Figure. 28. ^1H NMR Spectrum (CD_3OD) of 1-(3,4-Diydroxyphenyl)-2-methylaminopropane.

Table 1. Regional Brain Levels of 5-HT and DA After IP Drug Administration

treatment	hippocampal 5-HT (μg/g)[a]	% of control	cortical 5-HT (μg/g)[a]	% of control	striatal DA (μg/g)[a]	% of control
saline	0.44 ± 0.02	100	0.41 ± 0.03	100	10.6 ± 0.2	100
24						
10 mg/kg	0.42 ± 0.03	95	0.38 ± 0.03	93	NA	-
40 mg/kg	0.43 ± 0.02	98	0.44 ± 0.08	107	10.7 ± 0.5	101
MDMA						
10 mg/kg	0.17± 0.02[b]	39	0.15 ± 0.02[b]	37	NA	-

[a]Assays were performed one week after ip treament of (n = 6). Drugs or saline were injected 4 times at two hour intervals. [b]Designates significantly different from control ($p < 0.05$; ANOVA followed by Duncan's multiple range test). NA = not assayed.

Table 2. Regional Brain Levels of 5-HT and DA After Intracerebroventriacular Drug Administration

treatment	hippocampal 5-HT (µg/g)[a]	% of control	cortical 5-HT (µg/g)[a]	% of control	striatal DA (µg/g)[a]	% of control
saline	0.34 ± 0.02	100	0.26 ± 0.01	100	10.6 ± 0.2	100
24						
100 µg	0.33 ± 0.01	97	0.28 ± 0.01	108	NA	-
400 µg	0.32 ± 0.02	94	0.27 ± 0.02	104	9.5 ± 0.5	90
5,7-DHT						
100 µg	0.02 ± 0.01*	6	0.05 ± 0.02	19	NA	-
6-OHDA						
100 µg	NA	-	NA	-	3.7 ± 0.5	35

[a]Assays were performed one week after intracerebroventricular treament of (n = 6). The neurotoxins served as positive controls. [b]Designates significantly different from control ($p < 0.05$; ANOVA followed by Duncan's multiple range test). NA = not assayed.

Table 3. Striatal 5-HT and DA Levels After Intrastriatal Drug Administration

treatment	5-HT (μg/g)[a]	% of control	DA (μg/g)[a]	% of control
saline	0.22 ± 0.02	100	7.8 ± 0.5	100
24	0.22 ± 0.02	100	7.9 ± 0.7	101

[a]Assays were performed one week after intrastriatal treament (n = 6).

produced large depletions of DA and 5-HT, respectively (Table 2). The inability of compound **24** to deplete rat brain DA or 5-HT did not appear to be related to administration of an insufficient dosage since lower doses of established neurotoxins had clear depleting effects. For example, the 10 mg/kg regimen of MDMA given systemically produced a 62% depletion of 5-HT, while a four-fold higher dose (40 mg/kg) of compound **24** did not cause significant toxic effects toward dopaminergic or serotonergic neurons. As such compound **24** is unlikely to play a direct role in the neurotoxic action of MDMA.

The long-term effects on brain 5-HT and DA of the 6-OHDA analog **25** were examined following intracerebral administration only since it is unlikely to cross the blood brain barrier. Again, established neurotoxins (6-OHDA and 5,7-DHT) were used as positive controls. Intracerebroventricular adminstration of compound **25** produced a moderate (26%) depletion of striatal DA but had no effect on striatal 5-HT (Table 4). This behavior of compound **25** is similar to that observed with 6-OHDA which, however, was more potent (66% DA depletion). The ability of this preparation to demonstrate a toxic effect on serotonergic neurons was confirmed with 5,7-DHT which caused a profound depletion of striatal 5-HT.

Intrastriatal administration of compound **25** produced a more severe depletion of DA than that produced by an equivalent dose given intracerebroventricularly (89% versus 26%). Notably, when given intrastriatally, compound **25** had greater DA-depleting effects than 6-OHDA (89% versus 66%). The larger DA-depleting effect of compound **25** when given directly into the striatum (rather than the ventricle) did not appear to be related to the method of drug delivery since injections of the vehicle alone were without effect (Table 5). Interestingly, when compound **25** was tested intrastriatally, it also produced a lasting depletion of striatal 5-HT. This depletion, while smaller than the depletion of DA, was still substantial and dose-related (48% depletion after the 100 μg dose). These results highlight the fact that the site of injection is an important determinant of the monoamine depleting action of compound **25**.

Table 4. Striatal 5-HT and DA Levels After Intracerebroventricular Drug Administration

treatment	5-HT (μg/g)[a]	% of control	DA (μg/g)[a]	% of control
saline	0.36 ± 0.02	100	10.5 ± 0.6	100
25				
100 μg	0.33 ± 0.03	92	7.8 ± 0.5[b]	72
saline	NA	100	10.9 ± 0.1	100
6-OHDA				
100 μg	NA		3.7 ± 0.9[b]	
saline	0.34 ± 0.02	100	NA	-
5,7-DHT				
100 μg	0.02 ± 0.01[b]	6	NA	-

[a]Assays were performed one week after intracerabroventricualr treament (n = 6). The neurotoxins served as positive controls. [b]Designates significantly different from control ($p < 0.05$; ANOVA followed by Duncan's multiple range test). NA = not assayed.

Table 5. Striatal 5-HT and DA Levels After Intrastriatal Drug Administration

treatment	n	5-HT (µg/g)[a]	% of control	DA (µg/g)[a]	% of control
saline	9	8.7 ± 0.4	100	0.25 ± 0.01	100
25					
50 µg	5	3.7 ± 0.6	43	0.18 ± 0.01[b]	72
100 µg	4	1.0 ± 0.6	15	0.13 ± 0.01[b]	52
saline	3	10.1 ± 0.3	100	0.24 ± 0.02	100
6-OHDA					
50 µg	3	6.4 ± 0.8	63	0.27 ± 0.04	113

[a]Assays were performed one week after intrastriatal treament. The neurotoxins served as positive controls. [b]Designates significantly different from control ($p < 0.05$; ANOVA followed by Duncan's multiple range test). NA = not assayed.

We also have evaluated the effects of compound **25** in the motor cortex to determine if the 5-HT-depleting properties of **25** are dependent on DA. As before, the effects of compound **25** were compared to those of a documented serotonergic neurotoxin (5,7-DHT). When given intra-cortically, compound **25** again produced a dose-related depletion of brain 5-HT which was approximately one-fourth of that produced by 5,7-DHT (Table 6). These findings, coupled with those in the striatum, indicate that compound **25** possesses significant 5-HT-depleting activity and that the prolonged effects of compound **25** on 5-HT levels are not dependent on dopaminergic innervation.

The ability of compound **25** to cause a long lasting depletion of brain 5-HT is consistent with the view that this potential metabolite of MDMA may mediate the neurotoxic properties of the parent drug. At seeming odds with this view is the fact that MDMA is highly selective for 5-HT neurons[57] whereas compound **25** depletes both brain 5-HT and DA. Although this lack of selectivity of compound **25** argues against its possible role in mediating MDMA neurotoxicity, some factors should be considered which may contribute to this divergence in the neurotoxic profiles of MDMA and compound **25**. First, the intraparenchymal (i.e. more specifically the intrastriatal) route of administration could engender levels of compound **25** within dopaminergic neurons which do not parallel those which develop after systemic administration of MDMA. This specificity may be due to selective transport of MDMA or, more likely, a metabolite by serotonergic neurons. Alternatively, the enzymes responsible for the generation of compound **25** from its precursor may be present exclusively in serotonergic neurons. Finally, it is important to recall that when given at high dosages, MDMA, like compound **25**, depletes both brain DA and 5-HT.[56] Taken together, these considerations suggest that it would be premature to exclude compound **5** from consideration as a mediator of MDMA neurotoxicity.

Table 6. Cortical 5-HT Levels After Intracortical Drug Administration

treatment	5-HT (μg/g)[a]	% of control
saline	0.18 ± 0.02	100
25		
50 μg	0.14 ± 0.01	78
100 μg	0.08 ± 0.02[b]	45
saline	0.15 ± 0.01	100
5,7-DHT		
100 μg	0.08 ± 0.02[c]	53

[a]Assays were performed one week after intracortical treament (n = 6). The neurotoxin served as a positive control. [b]Designates significantly different from control ($p < 0.05$; ANOVA followed Neuman-Keuls test). [c]Designates significantly different from 5m7-DHT vehicle ($P < 0.05$, two-tailed Student's t-test).

2.4. Experimental

Melting points were determined on a Thomas Hoover melting point apparatus and are uncorrected. Reactions requiring anhydrous conditions were carried out under an argon or nitrogen atmosphere. ^{1}H and ^{13}C NMR spectra were taken on a Bruker WP270SY 270 MHz spectrometer. Chemical shifts are recorded in parts per million (ppm) relative to TMS as internal standard. Direct probe insertion mass spectra were obtained by Electron Ionization (EI) method on a VG 7070 HF or MAT-112S mass spectrometer. The gas chromatography/electron ionization mass spectra (GC/EIMS) were analyzed by temperature-programmed capillary column (HP-1) chromatography on an HP 5890 GC linked to an HP 5970B quadripole mass spectrometer. The oven temperature was held at 50 °C or 125 °C for 1 minute after injection and then temperature-programmed to 275 °C at 25 °C/minute. Infrared (IR) spectra were recorded on a Perkin Elmer 710 B infrared spectrophotometer. Ultraviolet (UV) spectra were taken on Beckman DU-50 spectrophotometer. Analytical thin-layer chromatography (TLC) was carried out on silica gel 60 F_{254} (0.2 mm thickness, E. Merck). Preparative TLC was performed on silica gel GF plates, 20 x 20 cm x 1000 um thick (Analtech). Flash chromatography was performed by using silica gel 60, (230-400 mesh) particle size and column sizes were varied based on amount of sample.

2-Hydroxy-4,5-methylenedioxybenzaldehyde (29). A mixture of $POCl_3$ (16.45 g, 10 mL, 0.11 mol) and N-methyl-formanilide (14.24 g, 13 mL, 0.11 mol) was stirred for 90 minutes at room temperature under N_2. A solid was formed and then sesamol **(28)** (10 g, 0.07 mol) in 40 mL of dry CH_2Cl_2 was added dropwise into the solid. Stirring was continued for 2 hours and the reaction was stopped by extracting the reaction mixture with ice-water (3 x 25 mL), then the CH_2Cl_2 layer was extracted with 10% of NaOH (pH = 12). The combined basic aqueous solution was acidified by adding concentrated HCl to pH=2 and extracted with ethyl ether (4 x 40 mL). The ethyl ether layer which contains product was dried over $MgSO_4$,

filtered and concentrated to give a residue (dark yellow). The residue was redissolved in about 30 mL of CH_2Cl_2 and after filtering it gave an unknown off-white solid and a yellow solution which contained the expected product was purified by column chromatography (4 cm x 30 cm, silica gel. 230 mesh) with $CHCl_3$. The pure product 3.19 g (27.4%) was obtained as yellow crystal: mp 121-122 °C; ^1H NMR ($CDCl_3$) 9.70 (s, -COH), 9.39 (s, OH), 6.84 (s, 1H, H-6), 6.44 (s, 1H, H-3), 5.99 (s, 2H, OCH_2O); ^{13}C NMR (DMSO) 192 (carbonyl carbon), 160 (C-2), 155 (C-4), 142 (C-5), 116 (C-1), 107 (C-6), 103 (C-3), 98 (methylene carbon); GC/MS (m/z, %) [GC temperature program: 50 °C for 1 minute, then 25 °C/minute up to 275 °C (retention time of the product is 4.26 minute)] 166 ($M^{+}\cdot$, 100), 165 (96), 148 (6), 137 (12), 120 (10), 107 (10), 53 (15). Anal. Calcd for $C_8H_6O_4$: C 57.84, H 3.64. found: C 57.74, H 3.69.

***Tris*(2-Hydroxy-4,5-methylenedioxyphenyl)methane (35).** The unknown solid (compound **X**) from above reaction was recrystallized from acetone-water to form 3.1 g off-white crystal: mp 195-197°C (dec); ^1H NMR ($CDCl_3$) 8.90 (s, OH), 6.39 (s, 3H, H-6), 6.14 (s, 3H, H-3), 5.94 (s, 1H, methine proton), 5.86 (s, 6H, methylenedioxy protons); The proton signal of OH disappeared after adding D_2O. ^{13}C NMR ($CDCl_3$) 149 (C-2), 146.5 (C-4), 139 (C-5), 123 (C-1), 108.5 (C-6), 101.5 (C-3), 98 (methylene carbon), 37.5 (methine carbon); EIMS (m/z, %) 424 (M^{+}, 1), 406 (M^{+} - 18, 3), 389 (1), 269 (80), 138 (100). Anal. Calcd for $C_{22}H_{16}O_9$: C 62.32, H 3.80. Found: C 61.57, H 3.71.

***Tris*(2-trimethylsilyloxy-4,5-methylenedioxyphenyl-methane (39).** To a solution of compound **X** (20mg, 0.047 mmol) in 15 mL of dry THF was added triethylamine (0.1 mL, 0.74 mmol) and chlorotrimethylsilane (0.11 mL, 0.89 mmol) under nitrogen.[58] The reaction mixture turned cloudy immediately after chlororimethyl-silane was added and the reaction mixture was allowed to stir at room temperature overnight monitored the formation of *Tris*(2-trimethylsilyloxy-4,5-methylenedioxyphenyl)methane by GC/MS. GC/MS (m/z, %) [GC temperature program: 125 °C for 1 minute, then 25 °C/minute up to 275 °C (retention time 10.57 minute)] 640 ($M^{+}\cdot$

95), 625 ($M^{+\cdot}$ - CH_3, 10), 551 ($M^{+\cdot}$ - $OSiMe_3$, 20), 431 ($M^{+\cdot}$ - $OCH_2OPhOSiMe_3$, 40), 357 ($M^{+\cdot}$ - $OCH_2OPhOSiMe_3$ - $SiMe_3$ - H, 15), 341 ($M^{+\cdot}$ - $OCH_2OPhOSiMe_3$ - $OSiMe_3$ - H, 10), 269 ($M^{+\cdot}$ - $OCH_2OPhOSiMe_3$ - $OSiMe_3$ - $SiMe_3$, 15). 223 (15), 73 (100).

Diazomethane (41). Ethanol (95%, 6 mL) was added to a solution of KOH (1.25 g) in H_2O (2 mL) in a 100 mL flask filled with a dropping funnel and condenser for distillation. The condenser was connected to two receiving flasks in series, the second contains about 10 mL ethyl ether. The inlet of the second receiver dips below the surface of the ethyl ether and both receiver were cooled to 0°C. The flask contained the alkali solution was heated in a water bath to 65°C and a solution of diazald (5.35 g) in about 50 mL ethyl ether was added through the dropping funnel at a rate that equals the rate of distillation. When the dropping funnel was empty, another 10 mL of ethyl ether was added slowly and the distillation was continued until the distilling ethyl ether is colorless. The combined ethyl ether distillate contained about 0.8 g of diazomethane in 25 mL.

The distillation should be done in an apparatus that is free from scratches and grounded glass joints.

***Tris*(2-methoxy-4,5-methylenedioxyphenyl)methane (40).** To a solution of compound **X** (40 mg, 0.028 meq.) in 15 mL of methanol was added diazomethane ethyl ether solution (4 mL, 1.52 meq.).[59] The resulting reaction solution was stirred at room temperature overnight. At the end of the reaction, the excess diazomethane was destroyed by adding a few drops of acetic acid, and the solvent was evaporated under vacuum. The residue was dissolved in ethyl ether and washed with $NaHCO_3$ and H_2O, dried over anhydrous $MgSO_4$, and evaporated under reduced pressure. It formed about 30 mg (70%) of off-white solid: mp 202-204°C (dec.); GC/MS (m/z, %) [GC temperature program: 125 °C for 1 minute, then 25 °C/minute up to 275 °C (retention time 11.17 minute)] 466 ($M^{+\cdot}$, 100), 435 ($M^{+\cdot}$ - OCH_3, 85), 405 ($M^{+\cdot}$ - OCH_3 - CH_3 - CH_3, 15), 315 ($M^{+\cdot}$ - methylenedioxymethoxyphenyl, 15), 269 ($M^{+\cdot}$ - methylenedioxymethoxyphenyl - OCH_3 - CH_3, 10), 165 (50), 145 (30);

^1H NMR ($CDCl_3$) 6.51 (s, 3H, H-6), 6.33 (s, 3H, H-3), 6.15 (s, 1H methine H), 5.86 (s, 6H, OCH_2O), 3.65 (s, 9H, OCH_3). Anal. Calcd for $C_{25}H_{22}O_9 \cdot 2H_2O$: C 59.76, H 5.22. Found: C 59.97, H 4.90.

2-Benzyloxy-4,5-methylenedioxybenzaldehyde (30). Compound **29** (2 g, 12.05 mmol) was dissolved in about 25 mL of dry THF and NaH (312 mg, 13 mmol) was added under N_2. Then $Bu_4N^+I^-$ (90 mg, 0.24 mmol) and $PhCH_2Br$ (6.15 g, 4.28 mL, 36 mmol) were added and the reaction mixture was stirred at room temperature for about 20 hrs. The reaction was checked by TLC with $CHCl_3$:MeOH (10:0.1) as the elutent. At the end of the reaction, the THF was evaporated to dryness. The residue was dissolved in about 50 mL of ether and the ether layer was washed with water. After removing the ether, the crude product was subject to the column chromatography (silica gel) with hexane:methylene chloride (1:1) and methylene chloride, it formed 2.67 g (90%) of **30** as light yellow crystal: mp 94-95 °C; NMR ($CDCl_3$) 10.38 (s, COH), 7.45-7.32 (m, 5H, Ph), 7.28 (s, 1H, H-6), 6.60 (s, 1H, H-3), 6.00 (s, OCH_2O), 5.13 (s, OCH_2Ph); GC/MS (m/z, %) [GC temperature program: 50 °C for 1 minute, then 25 °C/minute up to 275 °C (retention time 7.89 minute)] 256 ($M^{+\cdot}$ 20), 227 (10), 164 (15), 91 (100), 65 (15). Anal. Calcd for $C_{15}H_{12}O_4$: C 70.31, H 4.72. found: C 70.05, H 4.76.

1-(2-Benzyloxy-4,5-methylenedioxyphenyl)-2-nitropropene (31). A solution of 2.3 g of **30** (8.98 mmol) and about 690 mg of $AcONH_4$ (wet) (about 8.98 mmol) were dissolved in 20 mL of nitroethane (excess) under N_2 with stirring. The reaction solution was heated under reflex for about 9 hours. The solvent was then removed under vacumm leaving a brown residue, which was subjected to the column chromatography to yield 2.11 g of **31** (80%) as yellow crystal: mp 90-92 °C; ^1H NMR ($CDCl_3$) 8.35 (s, 1H, vinyl H), 7.45-7.32 (m, 5H, Ph), 6.85 (s, 1H, H-6), 6.62 (s, 1H, H-3), 5.98 (s, 2H, OCH_2O), 5.10 (s, 2H, OCH_2Ph), 2.38 (s, 3H, vinyl CH_3), EIMS 313 ($M^{+\cdot}$ 3), 176 (40), 91 (100). Anal. Calcd for $C_{17}H_{15}NO_5$: C 65.17, H 4.83, N 4.47. found: C 65.12, H 4.84, N 4.45.

1-(2-Benzyloxy-4,5-methylenedioxyphenyl)-2-amino-propane hydrochloride (32·HCl). A stirred suspension of lithium aluminum hydride (LAH, 970 mg, 25 mmol) in 30 mL of dry THF was combined with **31** (2 g, 6.39 mmol). The reaction mixture was stirred overnight under N_2 and the excess hydride was decomposed by the addition of some water. Another 30 mL of THF were added to the reaction mixture, which was stirred for another 0.5 hour. The filtration was dried with K_2CO_3, filtered and concentrated to form a yellow oil, **32**. NMR ($CDCl_3$) 7.45-7.32 (m, 5H, Ph), 6.65 (s 1H, H-6), 6.56 (s, 1H, H-3), 5.90 (s, 2H, OCH_2O), 5.02 (s, 2H, OCH_2Ph), 3.20 (m, methine H), 2.62 (2dd, 2H, methylene H), 1.12 (d, CCH_3); GC/MS (m/z, %) [GC temperature program: 125 °C for 1 minute, then 25 °C/minute up to 275 °C (retention time of the product is 6.35 minute)] 285 (M^+· 3), 242 (62), 151 (42), 91 (100), 65 (20). The free base was converted to corresponding HCl salt by dissolving the oil in the dry ether and HCl/ether was added to the solution. After removing the ether, the solid residue was crystallized from MeOH:Et_2O (2:8) to form 1.06 g of light-yellow crystalline (**32·HCl**, 52%): mp 183-185 °C; NMR ($CDCl_3$) 7.45-7.32 (m, 5H, Ph), 6.78 (s, 1H, H-6), 6.58 (s, 1H, H-3), 5.84 (s, 2H, OCH_2O), 5.04 (q, 2H, OCH_2Ph), 3.62 (m, methine H), 2.98 (m, 2H, methylene H), 1.38 (d, 3H, CCH_3). Anal. Calcd for $C_{17}H_{19}NO_3$·HCl: C 63.51, H 6.27, N 4.36. found: C 63.23, H 6.30, N 4.31.

1-(2-Benzyloxy-4,5-methylenedioxyphenyl)-2-form-amidopropane (33). The 2.89 g (8.98 mmol) of **32·HCl** were dissolved in about 25 mL of H_2O and then the solution was adjusted to pH = 11 by adding saturated K_2CO_3 solution. The basic aqueous solution was extracted with CH_2Cl_2 (40 mL x 2). The CH_2Cl_2 layer was dried with K_2CO_3 and after filtering and removing the solvent, it formed a yellow oil, which was dissolved in about 150 mL of ethyl formate under N_2. The reaction solution was heated under reflex for 6 hours, meanwhile, the reaction was monitored by GC/MS. The reaction was stopped by removing the solvent, it left about 3.4 g of yellow oil. The crude product was dissolved in methylene chloride and extracted with saturated $NaHCO_3$ solution and 1 N HCl solution. The neutral methylene chloride layer was dried with $MgSO_4$, and

after filtering, removing the solvent, the product was further purified by a silica gel column with CH_2Cl_2:EtOAc (1:1). The pure product was recrystallized from Et_2O and had the following properties: mp 96-97 °C; IR (KBr) 1658 cm^{-1} (strong, NHCOH); ^1H NMR ($CDCl_3$) 7.90 (s), 7.72 (d), (2 sets, 1H, NCOH), 7.48-7.28 (m, 5H, aromatic), 6.62 (s, 1H, H-6), 6.58 (s, 1H, H-3), 5.90 (s, 2H, OCH_2O), 5.00 (s, 2H, $PhCH_2O$), 3.75 (m), 4.18 (m), (2 sets, 1H, $N\underline{CH}CH_3$), 2.68 (m, 2H, $Ph\underline{CH_2}CH$), 1.14 (d),1.17 (d), (2 sets, 3H, $NCH\underline{CH_3}$); GC/MS (m/z, %) [GC temperature program: 125 °C for 1 minute, then 25 °C/minute up to 275 °C (retention time 7.94 minute)] 313 (M^+· 40), 268 (80), 241 (20), 211 (20), 177 (40), 151 (45), 91 (100). Anal. Calcd for $C_{18}H_{19}NO_4$: C 69.08, H 6.12, N 4.48. Found: C 68.92, H 6.16, N 4.42.

1-(2-Benzyloxy-4,5-methylenedioxyphenyl)-2-methylaminopropane hydrochloride (34·HCl). A stirred suspension of 1.5 g of LAH (38.34 mmol) in about 70 mL of dry THF under N_2 was combined with 2 g of **33** (6.39 mmol). The reaction mixture was heated under reflex for 8 hours with monitored by GC. The reaction was stopped by adding water and after filtering and drying with K_2CO_3, the THF was removed under vacumm. It formed 1.4 g of yellow crystal (73%) which was converted to the HCl salt by adding HCl/Et_2O. The salt was recrystallized from CH_3CN and exhibited following properties: mp 144-146 °C; ^1H NMR ($CDCl_3$) 7.3-7.5 (m, 5H, aromatic), 6.7 (s, 1H, H-6), 6.6 (s, 1H, H-3), 5.95 (s, 2H, OCH_2O), 5.0 (s, 2H, OCH_2Ph), 3.35 (m, 1H, methine H), 3.35 (m), 2.70 (m) (2 sets, 2H methylene H), 2.48 (t, 3H NCH_3), 1.45 (d, 3H, CCH_3); GC/MS (m/z, %) [GC temperature program: 125 °C for 1 minute, then 25 °C/minute up to 275 °C (retention time of the product is 3.16 minute)] 299 (M^+· 2), 268 (2), 242 (40), 151 (10), 91 (40), 58 (100). Anal. Calcd for $C_{18}H_{21}NO_3$·HCl: C 64.34, H 6.61, N 4.18. Found: C 63.92, H 6.62, N 4.29.

1-(2-Hydroxy-4,5-methylenedioxyphenyl)-2-methylaminopropane hydrochloride (24·HCl). The 800 mg (2.39 mmol) of **34·HCl** was dissolved in about 100 mL of EtOH and 40 mg of Pd(C) was added. The reaction mixture was stirred at room

temperature under 1 atm H_2 for 5 hours. After filtering and removing the solvent, it formed 566 mg of off-white solid (96%) which was recrystallized from CH_3CN and had the following properties: mp 133-135 °C; ^1H NMR ($CDCl_3$) 6.68 (s, 1H, H-6), 6.45 (s, 1H, H-3), 5.85 (s, 2H, OCH_2O), 3.38 (m, 1H, methine H), 3.15 (q), 2.75 (q), (2 sets, 2H, methylene H), 2.65 (s, 3H, NCH_3), 1.45 (d, 3H, CCH_3), GC/MS (m/z, %) [GC temperature program: 125 °C for 1 minute, then 25 °C/minute up to 275 °C (retention time of the product is 3.16 minute)] 209 ($M^{+\cdot}$ 15), 178 (4), 152 (10), 147 (5), 121 (4), 105 (2), 91 (4), 69 (5), 58 (100). Anal. Calcd for $C_{11}H_{15}NO_3 \cdot HCl$: C 53.81, H 6.57, N 5.71. Found: C 53.88, H 6.58, N 5.75.

2-Methylamino-1-(2,4,5-trihydroxyphenyl)propane hydrochloride (25·HCl). To a solution of **34·HCl** (700 mg, 2.54 mmol) in 25 mL of $CHCl_3$ cooled to 0 °C was added BBr_3 (12.7 mL, 12.7 mmol, 1 M solution in CH_2Cl_2) dropwise under N_2. The solution was turned to cloudy immediately and the mixture was allowed to stir overnight at room temperature under nitrogen atmosphere. After cooling, the reaction was quenched by dropwise addition of MeOH. The brown, solid residue obtained after evaporation of solvents was dissolved in a small volume of water and chromatographed on a cationic exchange column (15 mL of Dowex AG 50W-X4, 50-100 mesh, washed with 30 mL of 6N HCl, and distilled water until neutral). The column was washed with water until the elutent was free of halide (silver nitrate test). The product was eluted with 6N HCl, and the elutent was lyophilyzed to give 300 mg (50%) of off-white crystalline solid: mp 202-204 °C (dec); ^1H NMR (CD_3OD) 6.49 (s, 1H, H-6), 6.33 (s, 1H, H-3), 3.34 (m, 1H, methine H), 2.83 (m), 2.63 (m), (2 sets, 2H, methylene H), 2.60 (s, 3H, NCH_3), 1.18 (d, 3H, CCH_3). Anal. Calcd for $C_{10}H_{15}NO_3 \cdot HCl$: C 51.43, H 6.91, N 5.99. Found: C 51.29, H 6.90, N 5.97.

1-(3,4-Dihydroxyphenyl)-2-methylaminopropane hydrochloride (19·HCl). To a solution of MDMA·HCl (**12·HCl**) (450 mg, 1.96 mmol) in 20 mL of dry $CHCl_3$ cooled to 0 °C by ice-water bath was added BBr_3 (4.89 mL, 4.89 mmol, 1 M solution in CH_2Cl_2)

dropwise under N_2. The reaction mixture was stirred at 0 °C for 0.5 hour and at room temperature for 15 minutes and cooled back to 0 °C. At the end of the reaction (about one hour), the reaction mixture was quenched by dropwise addition of MeOH (10 mL). The residue obtained after removing the solvents was dissolved in a small amount of water and mixed with 2 mL of cationic ion exchange resin with stirring for 5 minute and chromatographed on a cationic exchange column (5 mL of Dowex AG 50W-X4, 50-100 mesh, washed with 30 mL of 6N HCl, and distilled water until neutral). The column was washed with water until the elutent was free of halide (silver nitrate test). The product was eluted with 4N HCl (about 50 mL), and the elutent was lyophilyzed to give 330 mg (77%) of off-white solid: ^{1}H NMR (CD_3OD) 6.8 (d, 1H, H-5), 6.72 (s, 1H, H-2), 6.58 (d, 1H, H-6), 3.4 (m, 1H, methine H), 2.95 (m), 2.65 (m), (2 sets, 2H, methylene H), 2.72 (s, 3H, NCH_3), 1.22 (d, 3H, CCH_3). Anal. Calcd for $C_{10}H_{15}NO \cdot HCl \cdot H_2O$: C 50.96, H 7.7, N 5.94. Found: C 50.89, H 7.91, N 4.84.

3.1. Background

Phencyclidine [1-(1-phenylcyclohexyl)piperidine, PCP (**54**)] is an arylcyclohexylamine which was developed in the 1950's as an intravenous anesthetic agent. The PCP molecule contains one aromatic and two alicyclic rings commonly encountered in drugs. Due to its 3 ring structure and lack of polar substituents, the drug is very lipid soluble.[60]

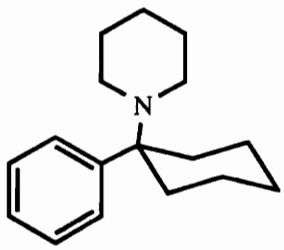

5 4

Depending on species and dosage, PCP actions include tranquilization, excitation, catalepsy, analgesia, anesthesia and convulsions.[61] Small doses of the drug tend to produce a type of 'drunken' state in man while most rodent species display excitation. There are marked species differences in responses to the drug. Primates, especially humans, are most susceptible to its depressant effects.

Because of its undesirable side effects which became apparent during clinical trials, the use of PCP in humans was discontinued. The majority of the toxicological problems associated with PCP use can be attributed to its psychotomimetic properties and the long lasting behavioral disruptions. In recent years these properties have led to its widespread use as a 'recreational' drug of abuse. Next to marijuana, PCP is now the most widely abused 'street drug' in the United States. Its illegal sale on the streets, either alone or in combination with amphetamine, cocaine, mescaline, LSD or

marijuana, has been documented by numerous studies in which street drug samples were analyzed.[62]

Both direct and indirect interactions with the cholinergic, serotonergic, noradrenergic, dopaminergic and GABA (γ-aminobutyric acid, **55**) neurotransmitter systems are known to take place. Recent studies have postulated the existence of specific PCP receptors[63] and neuronal pathways in the CNS.[64] The results from these studies suggest that more than one neurotransmitter system is involved in the complex behavioral and psychiatric pattern of PCP effects.

$H_2NCH_2CH_2CH_2COOH$

55

Possible explanations for the mediation of such long term drug effects include metabolic activation of the parent compound to reactive species which may interact covalently with biological macromolecules and thereby modify their normal function. Interest in the possibility that metabolites may contribute to the pharmacological and toxicological effects of PCP has led to the identification of the ring-hydroxylated metabolites in several species. Oxidative hydroxylation of the piperidine ring is the major known mode of metabolism of PCP. Possible metabolic transformations of the piperiding ring of PCP include hydroxylation to 2-, or 4-substituted hydroxy derivatives or nitrogen oxidation to an N-oxide intermediate.[65, 66] The piperidine ring-opened amino alcohol **56** [67] and amino acid **57** [65] have been characterized as metabolites of PCP. The formation of such ring-opened metabolites presumably proceeds via initial α-C-hydroxylation to yield the carbinolamine **58** which ring opens to the corresponding amino aldehyde **59**, the intermediate leading to the amino alcohol and amino acid (Scheme 16).

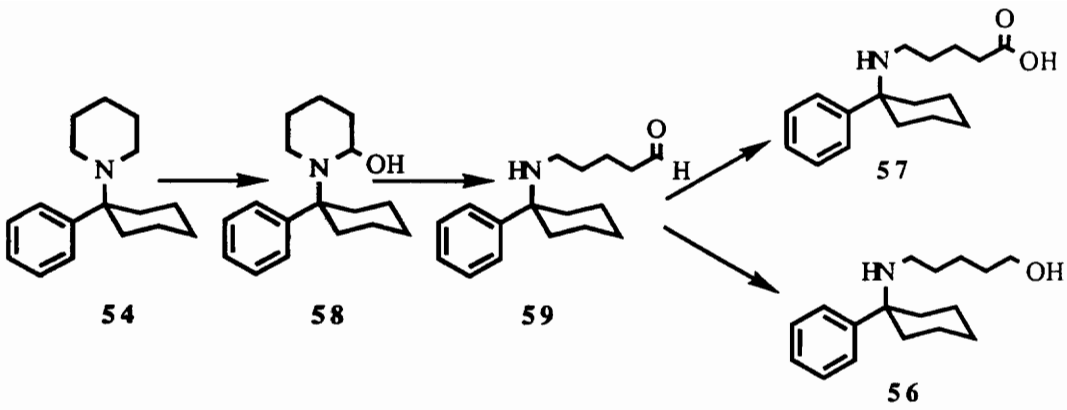

Scheme 16. Pathway of metabolic formation of ring-opened PCP metabolites.

Many drugs are converted in the body to a variety of metabolites which contribute to the pharmacology and toxicology of the parent compound. The role of the microsomal drug-metabolizing enzymes in the formation of toxic, chemically reactive electrophilic metabolic intermediates is well documented.[68] The extent of toxicity will depend on the percent of the administered drug which is converted into reactive metabolite(s) and on the amount covalently bound to the macromolecules vital for cell function, as well as on the efficiency of detoxifying mechanisms that remove reactive intermediates and repair mechanisms of cellular damage.[69]

The metabolism-dependent covalent binding of PCP-derived products to tissue macromolecules *in vitro* in rabbit lung and liver microsomes has been reported.[70, 71] Ward et al[71] and Kalir et al[72] reported that PCP is metabolized *in vitro* by rabbit hepatic microsomes to a reactive, electrophilic iminium ion (**60**) which is capable of binding covalently to microsomal protein. Hydrolysis of the PCP-Im^+ species (**60**) leads to the corresponding aminoaldehyde **59** which has been characterized as its *O*-methyloxime (**61**, Scheme 17).[73] The reactive iminium intermediate was trapped in a metabolic incubation mixture as its cyano addut 1-(1-phenylcyclohexyl)-2-cyanopiperidine (**62**) which was identified by mass spectrometry and by comparison with a synthetic standard. It accounted for over 50% of the PCP metabolized in 30 minute *in vitro*

by liver microsomes. The rate of metabolism-dependent covalent binding was about 3.85 nmol [^{3}H]-PCP/30 minute/mg microsomal protein which constituted about 8% of the total amount of metabolized PCP. Cyanide inhibited the covalent binding in a dose-dependent manner at concentrations not influencing PCP metabolism. This may reflect the competition for the iminium metabolite between cyanide and nucleophile present on the microsomal macromolecules. Glutathione (1 mM) added to the incubation mixture inhibited binding by about 50% indicating a possible physiological detoxifying mechanism. The addition to the microsomal pellet of a cytosolic fraction of the liver homogenate that contains various glutathione-S-transferases should greatly facilitate such a detoxifying reaction. However, there is no evidence for such an extensive retention of PCP-derived material *in vivo* as suggested by these *in vitro* experiments.

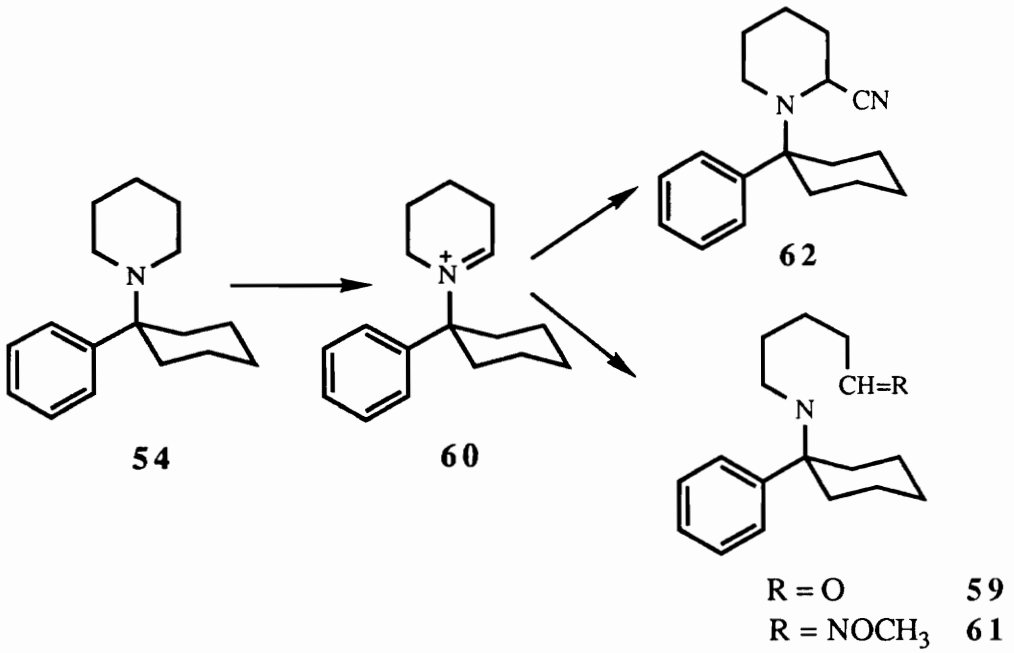

Scheme 17. Oxidative metabolic formation and trapping of the PCP-Im$^+$ species **60**.

PCP also was found to be a mechanism-based inactvating agent for cytochrome P-450 form II. However, PCP-Im$^+$ inactivates both P-450 form II and form IIIb in a metabolism-dependent manner.[74]

Both PCP and its iminium ion give biphasic kinetics of inactivation with similar rate constants. This supports the hypothesis that the iminium ion is an intermediate in the inactivation of P-450 form II by the parent compound. These results are in accord with the suggestion that the α-carbon oxidation of PCP is the principal pathway responsible for the formation of products which are capable of undergoing covalent interactions with macromolecules. The tetrahydropyridinium intermediate **60** itself, however, does not appear to be directly involved in the bioalkylation reactions.[75] The observation that cyanide ion traps the PCP-Im^+ ion as the corresponding α-aminonitrile (**62**) and blocks the metabolism-dependent covalent binding of PCP to microsomal macromolecules and the PCP-mediated inactivation of cytochrome(s) P-450 also supports this conclusion.[75] On the other hand, studies with radiolabled **60** showed that both the bioalkylation reaction and the inhibition of cytochrome P-450 was NADPH dependent.[75] These results argued that although the bioactivation of PCP requires α-carbon oxidation, compound **60** most likely undergoes a further transformation step to yield the ultimate reactive electrophile. Therefore, studies on the fate of the PCP-Im^+ species in liver microsomal homogenates were undertaken in an effort to identify metabolites which are responsible for the binding to macromolecules and inactivation of cytochrome P-450. Hoag et al[76] have reported the characterization of a new PCP derived aminoenone metabolite, 1-(1-phenylcyclohexyl)-2,3-dihydro-4-pyridone (**63**), a 4-electron oxidation product which presumably is formed by initial allylic hydroxylation of tetrahydropyridine intermediate **64** followed by a second 2-electron oxidation of the resulting aminoenol **65** (Scheme 18). This result has led to speculations on the possible involvement of the dihydropyridinium species **66** in the bioalkylation process.

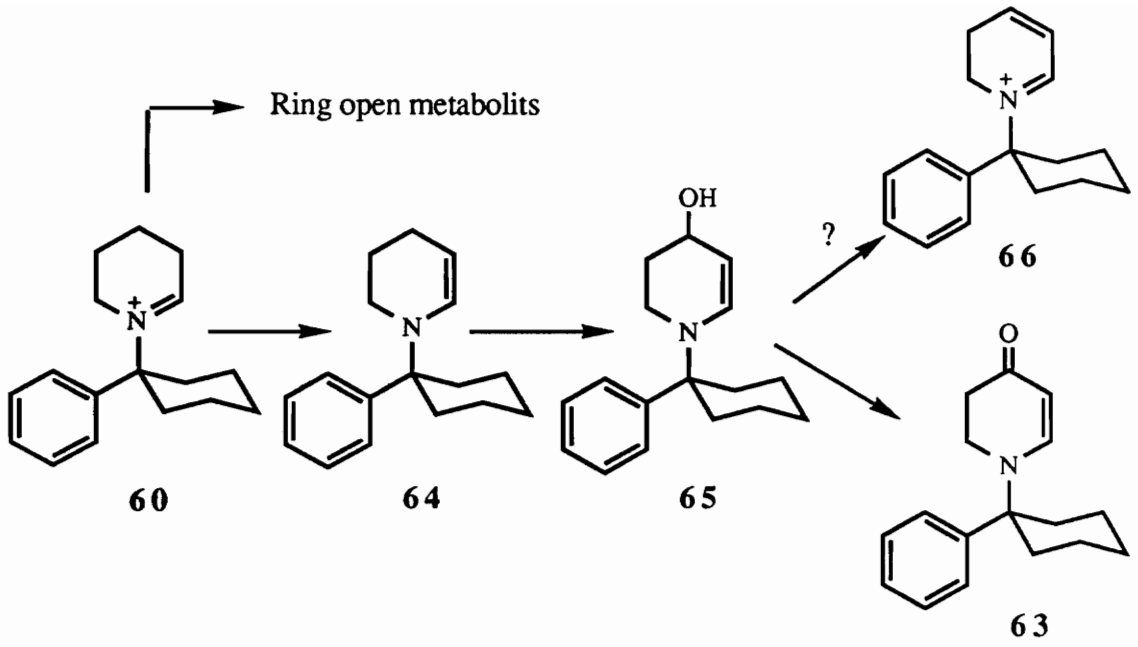

Scheme 18. Pathway of metabolic formation of aminoenone metabolite of PCP.

In summary, PCP is metabolized in the body via a variety of metabolic routes which contribute to the detoxification (inactivation) of the parent drug.[77] In general, PCP metabolites are less active pharmacologically than PCP itself. The primary metabolic route involves cytochrome P-450 mediated hydroxylation of the alicyclic rings. Hydroxylation of the aromatic ring seems to be less likely and has not been conclusively demonstrated. Hydroxylation of PCP at carbon 2 of the piperidine ring to form the unstable carbinolamine leads to the formation of a series of polar, open-ring compounds. Monohydroxylated metabolites are conjugated with glucuronic or sulfuric acid or are further hydroxylated to dihydroxy derivatives that also may be subject to conjugation. Formation of highly reactive electrophilic metabolites of PCP have been demonstrated *in vitro* in microsomal preparations. Covalent modification of tissue macromolecules by reactive intermediates may be responsible for the metabolism-dependent inactivation of cytochrome P-450 and can possibly mediate some long-term toxic effects of PCP.[60]

3.2. Research Proposal

The metabolic formation of reactive intermediates that bioalkylate macromolecules supports the suggestion that the long lasting behavioral disruption caused by PCP might be accounted for by biochemical lesions resulting from covalent interactions of drug metabolites with critical brain macromolecules. Alternatively, metabolites with high affinity for receptors that mediate toxic effects, for example on cellular energenics, may contribute to the observed toxicity. Since PCP is known to undergo extensive hepatic metabolism, one might postulate that PCP metabolites generated in the liver can be discharged into the general circulation from which they might enter the CNS. Once in the brain, the metabolite(s) might exert toxic effects directly or undergo further metabolism to toxic species which could then act locally. In order to explore this concept more thoroughly, we have elected to examine the fate of iminium species **60**, the principal metabolite involved in the bioactivation of PCP, in brain and hepatic tissues.

3.3. Results and Discussion

3.3.1. Metabolism

The further biotransformation of the PCP-Im$^+$ metabolite has been examined in rat liver and brain subcellular fractions. HPLC analysis of the methylene chloride extract obtained from rat brain mitochodrial incubation mixtures containing 0.2 mM tetrahydropyridinum (**60**) perchlorate revealed the time dependent loss of the starting material and the time dependent formation of a new peak which was not observed in the control incubations and the formation of which was not NADPH dependent (Fig 29).[78] This metabolite also was observed in HPLC extracts of rat brain microsomal incubations of the tetrahydropyridinum perchlorate but appeared to be formed more efficiently in the presence of mitochondria. HPLC-diode array analysis of this peak displayed a UV spectrum with λ_{max} 302 nm. Direct insertion probe chemical ionization mass spectral analysis of the material isolated by preparative HPLC displayed a nominal mass at m/z 270 (MH$^+$). The GC/EI mass ion chromatogram monitored at m/z 269 of the incubation extracts showed one major peak with a retention time of 6.34 minutes (Fig. 30). The mass spectrum (Fig. 31) of this peak displayed the expected parent ion at m/z 269 and two intense fragment ions at m/z 159 and 91. These fragment ions, both of which are present in the EI mass spectrum of PCP and PCP-enamine, can be assigned to the phenylcyclohexyl carbocationic species **67** (m/z 159), while the m/z 91 ion is likely to be due to the tropylium species **44**. Therefore the phenylcyclohexyl moiety of the substrate remains intact in the metabolite. Since the molecular weight of the substrate, calculated in terms of the enamine free base **64**, is 241 daltons, the nominal mass of the metabolite (269 daltons) corresponds to the addition of 28 amu to the substrate. Empirical formulas that are consistent with this mass include $C_{17}H_{19}NO_2$ (269.1416, an 8-electron oxidation product equivalent to the introduction of 2 carbonyl groups), $C_{19}H_{27}N$ (269.2143, equivalent to the introduction of C_2H_4), $C_{18}H_{23}NO$ (269.1780, equivalent to the

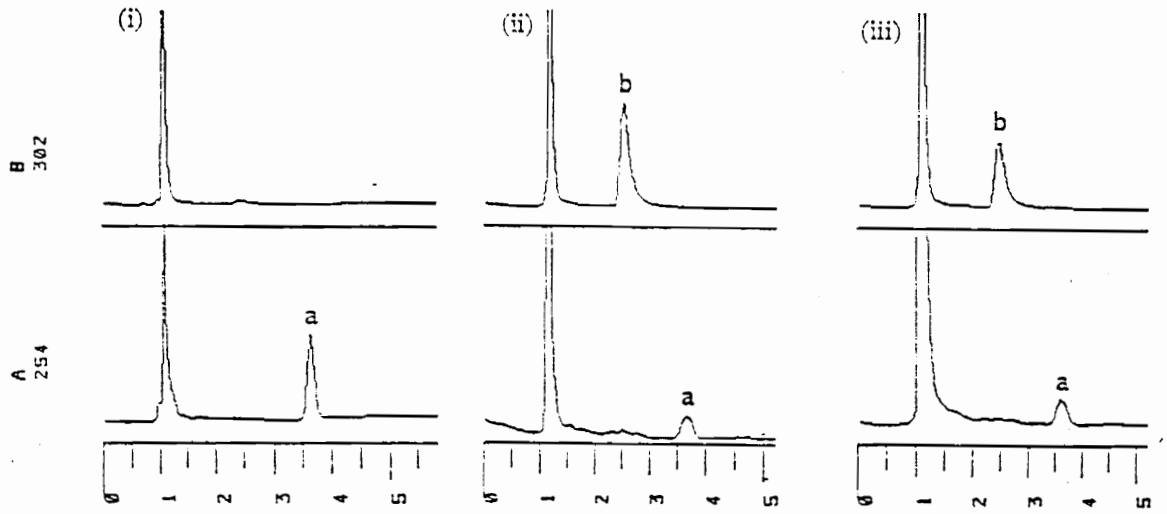

Figure. 29. HPLC Chromatograms of the Formation of Metabolite X (b) from PCP-iminium (a) in Rat Brain Mitochondrial fractions (ii), in the Presence of NADPH (iii) or in the Absence of homogenates (i).

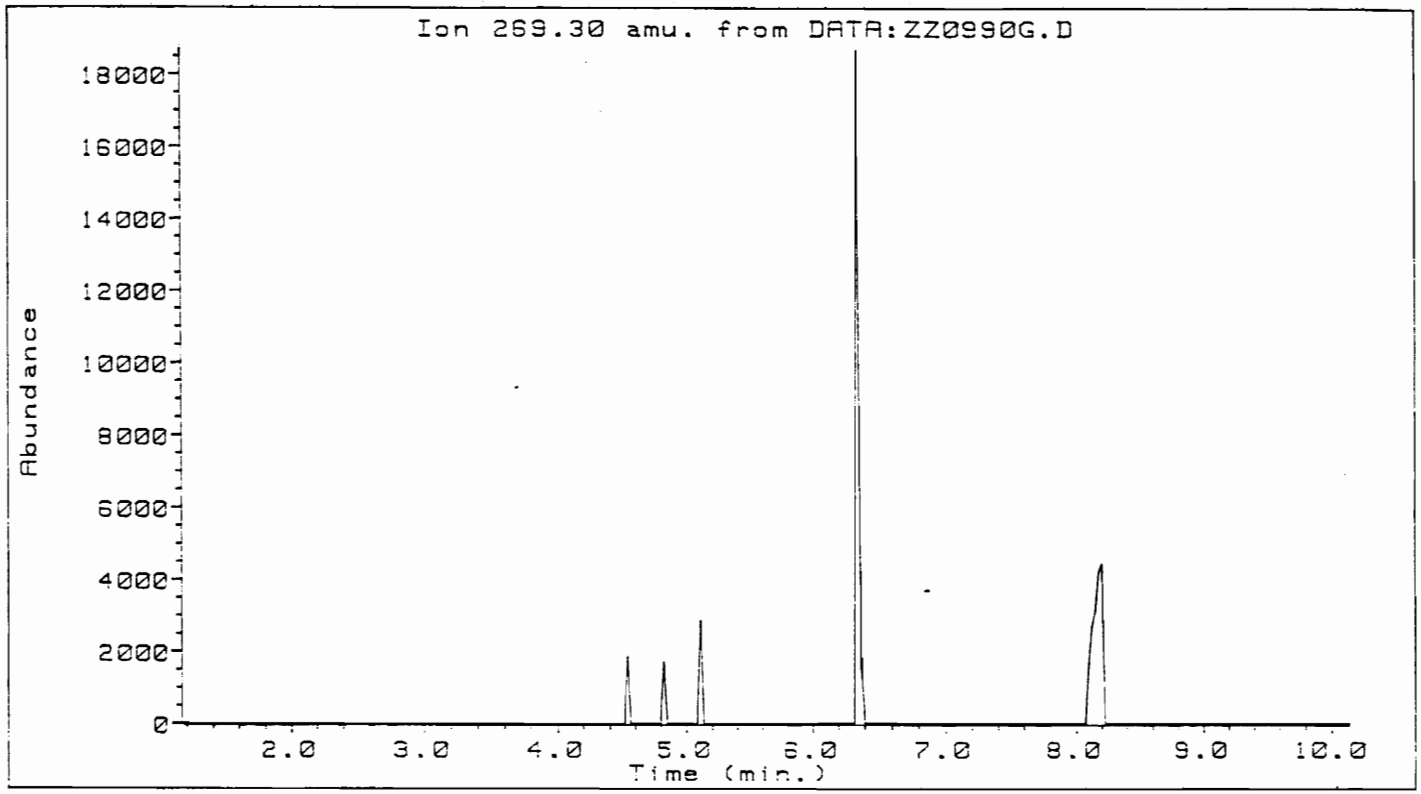

Figure. 30. **Ion Chromatogram (m/z 269) of Phencyclidine Iminium Ion Brain Mitochondrial Incubation Extract**

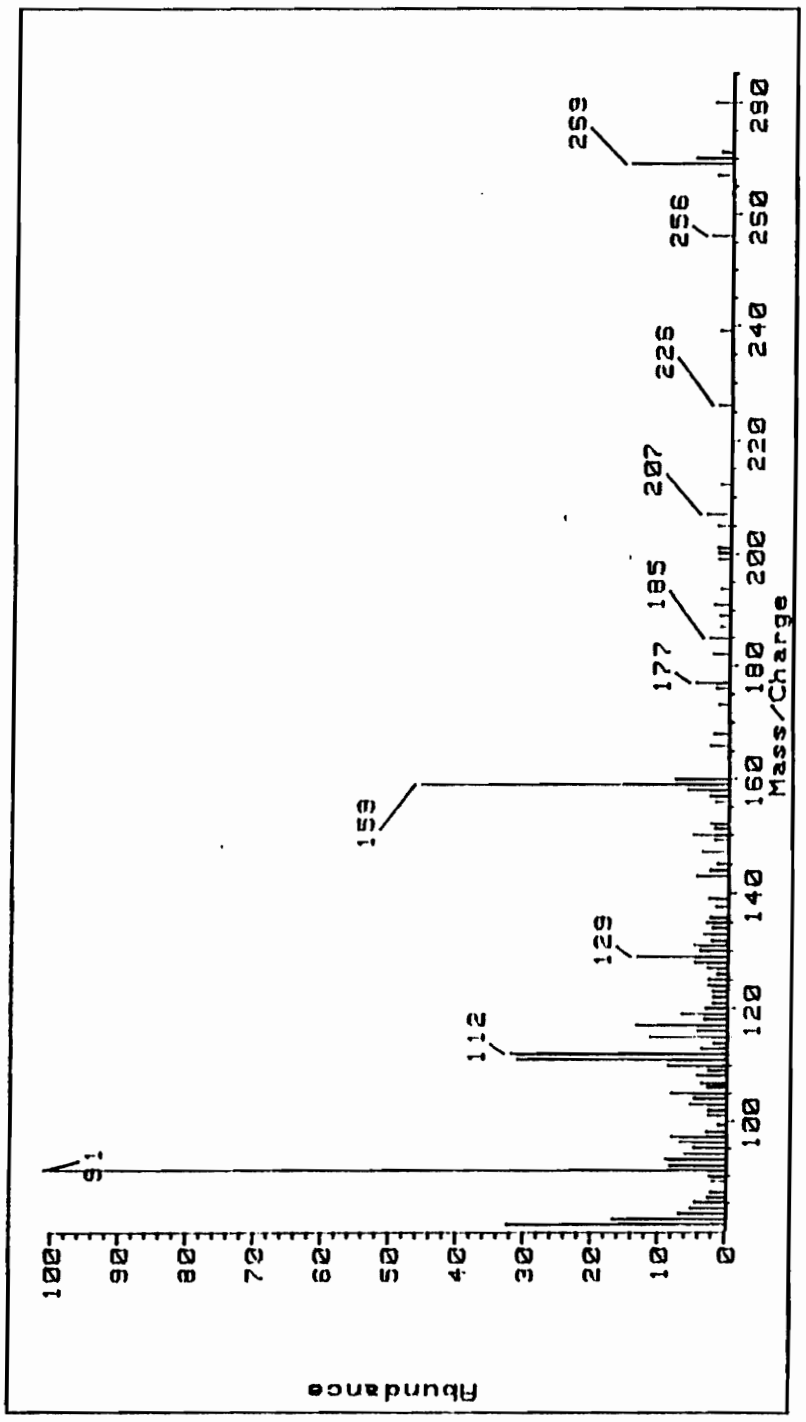

Figure. 31. GC/EIMS of Brain Mitochondrial Metabolite Derived from Phencyclidine Iminium Ion.

introduction of CO) and $C_{17}H_{23}N_3$ (269.1892, equivalent to the introduction of N_2). The high resolution EI mass spectral analysis of the parent ion established its exact mass as 269.1780, consistent with $C_{18}H_{23}NO$, the product resulting from the net introduction of CO into the substrate, that is, in effect, the result of a formylation reaction. The key diagnostic fragmentation at m/z 111, corresponds to a carbonylated tetrahydropyridine **68**, and is postulated to be generated from the cleavage of the phenylcyclohexyl moiety from the parent ion. The ^1H NMR spectrum of the crude metabolite showed a singlet at 8.97 ppm which may be assigned to a shielded formyl proton signal (Fig. 32). These spectral data and in particular the presence of the 302 nm chromophore, which is suggestive of a conjugate system similar to the aminoenone **63** (λ_{max} 314 nm), led to the tentative structure assignment of 1-(1-phenylcyclohexyl)-1,4,5,6-tetrahydropyridine-3-carboxaldehyde **69** for this metabolite. In order to evaluate this possibility we undertook the synthesis of **69**. The fragmentation assignments are demonstrated in Fig. 33.

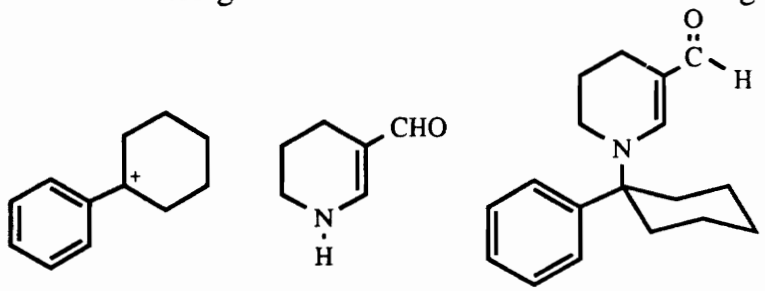

67 **68** **69**

Our approach was modeled on the potential biosynthetic pathway which presumably would involve the enamine free base (**64**) derived from the tetrahydropyridinium substrate molecule, and a biological donor of CHO or its equivalent.

3.3.2. Syntheses

The proposed synthetic pathway leading to **69** involved with condensation of 1-(1-carbonitrilecyclohexyl)piperidine (**70**) with phenylmagnesium bromide to generate the PCP (**54**). Oxidation of

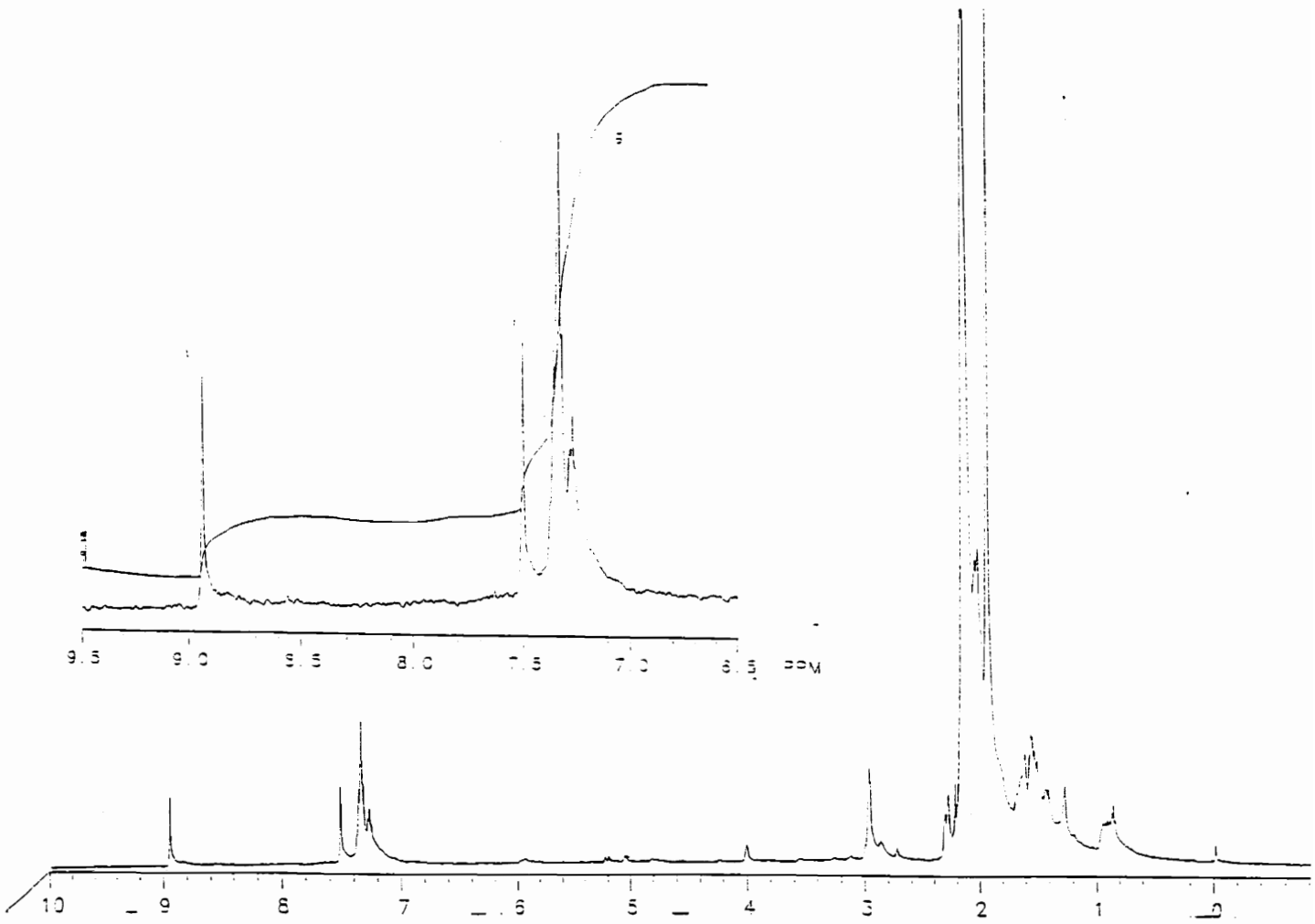

Figure. 32. ^1H NMR Spectrum ($CDCl_3$) of Metabolite from Brain Incubation.

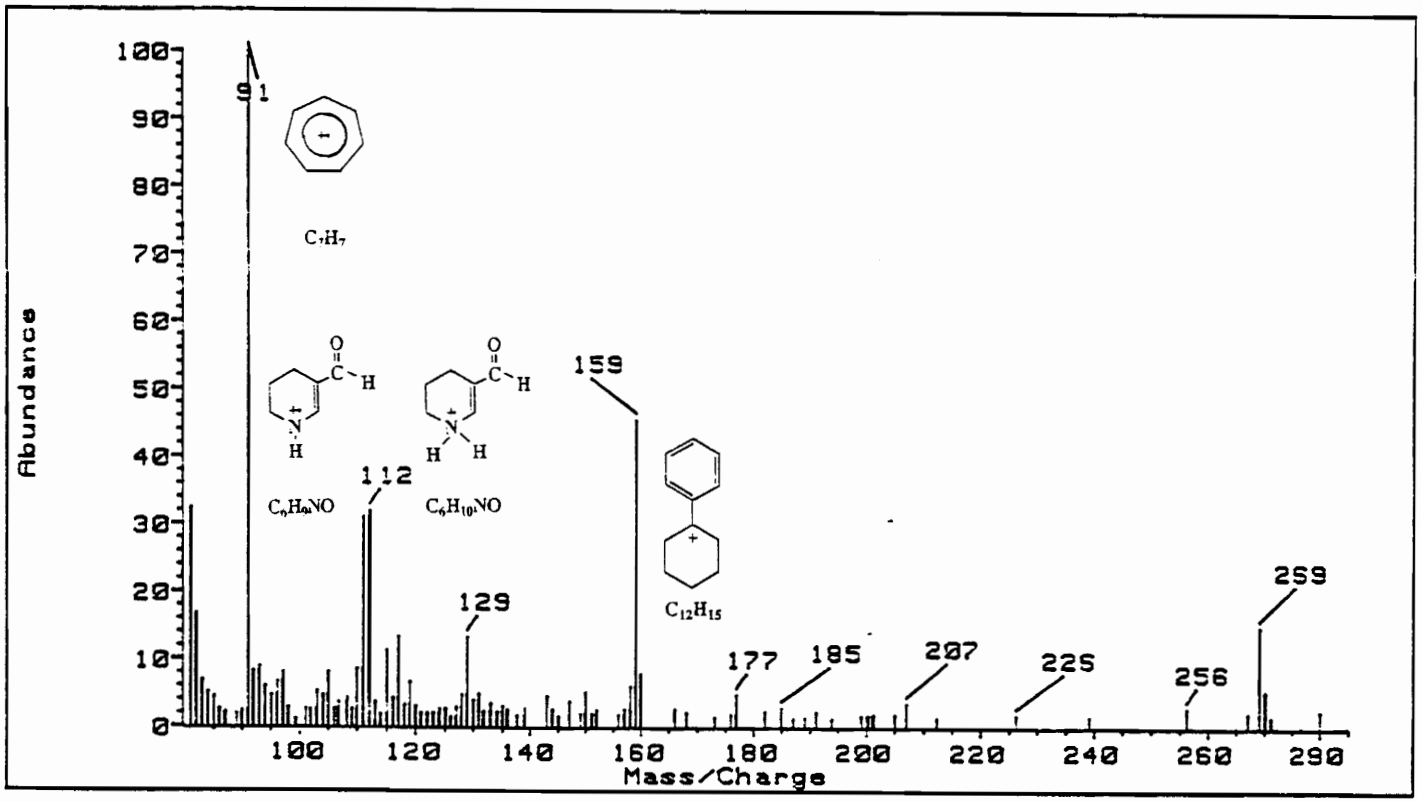

Figure. 33. GC/EIMS Fragmentation of Brain Mitochondrial Metabolite Derived from Phencyclidine Iminium Ion.

PCP should yield PCP-Im$^+$ (**60**) which, as the corresponding enamine **64**, was to be C-formylated with **71** to yield the desired product **69**. Compound **71** was prepared by treatment of carbonyldiimidazole with formic acid.

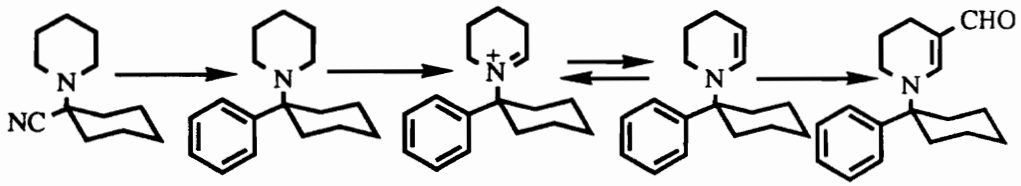

70 **54** **60** **6 4** **69**

Scheme 19. Proposed synthetic pathway to the new metabolite of PCP.

PCP (**54**) was synthesized from 1-(1-carbonitrilecyclohexyl)-piperidine by reaction with phenylmagnesium bromide.[79] After work-up, the product was converted to its HCl salt and was purified by recrystallization from ethanol. The GC/EI mass spectrum of the PCP free base is shown in Fig. 34 together with probable structures for the diagnostically useful fragment ions. All of the assigned ionic compositions are supported by comparison with literature reports.[79] The base peak (m/z 200) in the GC/EI mass spectrum of PCP results from loss of a C_3H_7 fragment from the cyclohexyl ring via a mechanism as follows in Scheme 20.

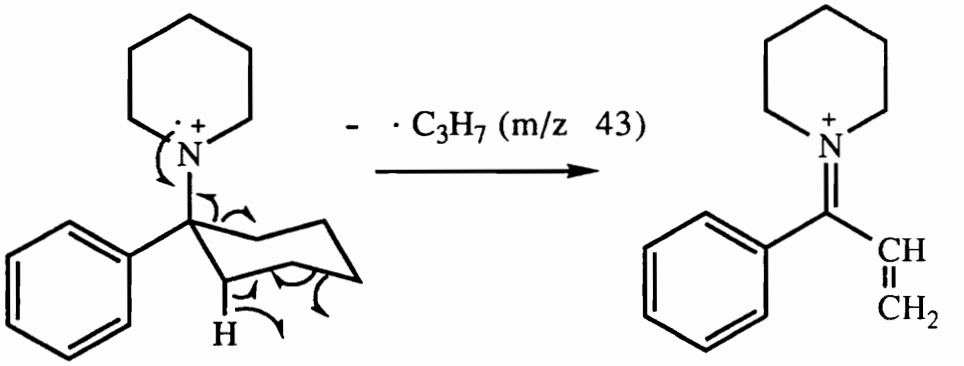

54·$^+$ (m/z 243) **72** (m/z 200)

Scheme 20. Fragmentation pattern of PCP leading to formation of the base peak.

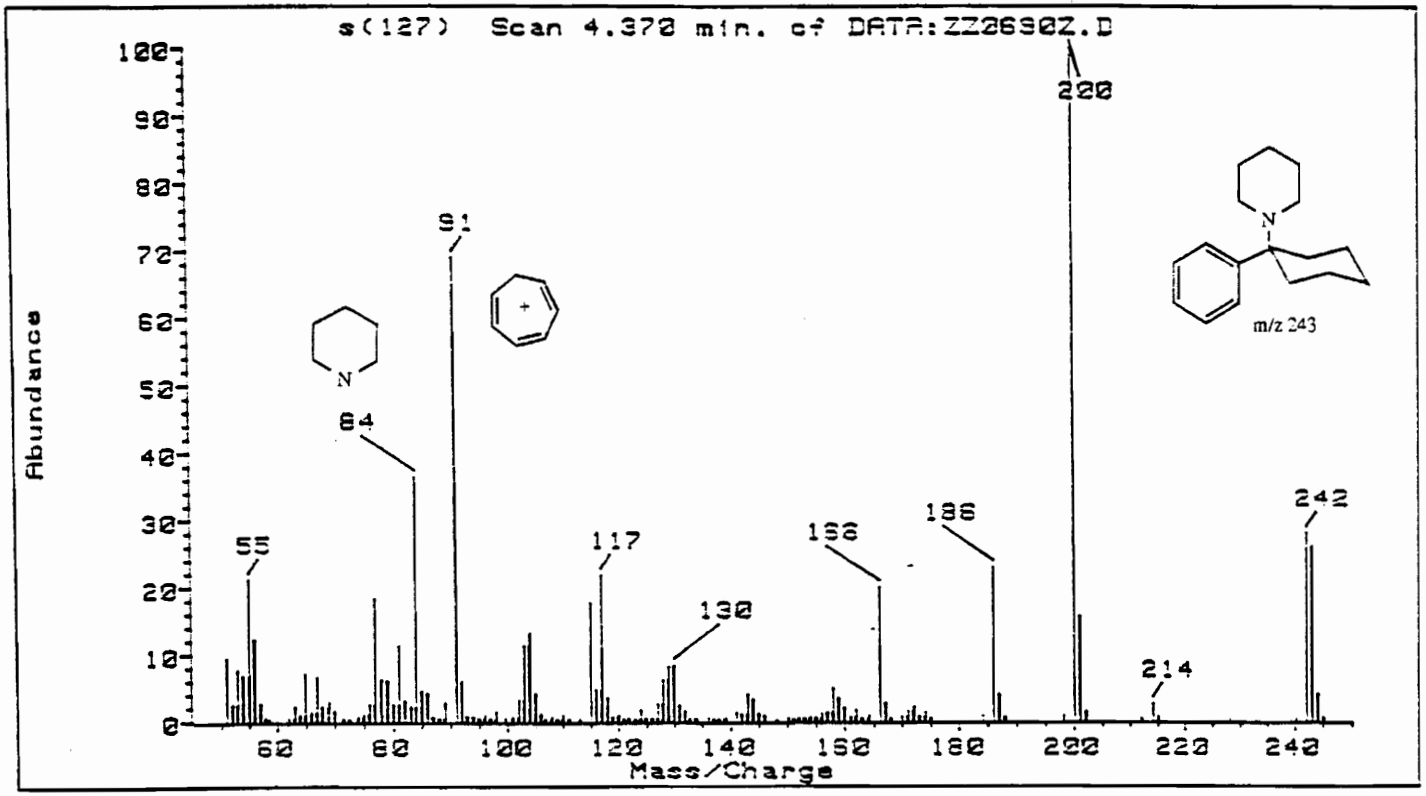

Figure. 34. GC/EIMS of 1-(1-Phenylcyclohexyl)piperidine.

Loss of C_2H_5 and C_4H_9 fragments, also presumably from the cyclohexyl ring, account for the ions at m/z 214 and 186. Expulsion of a phenyl radical from [$M^{+}\cdot$] gives a moderately abundant ion at m/z 166. Expulsion of piperidine gives a weak but detectable ion (**67**) at m/z 159. At the low mass end of the spectrum the tropylium ion (**44**) at m/z 91 and the piperidinyl ion (**73**) at m/z 84 give moderately intense peaks.

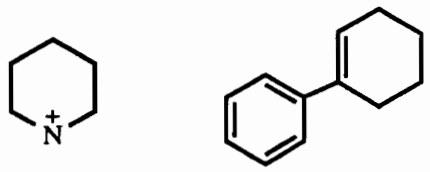

73 **75**

The synthesis of the cyclic iminium species **60** was attempted via treatment of PCP with *m*-chloroperoxybenzoic acid (MCPBA) to generate the PCP N-oxide **74** as the corresponding *m*-chlorobenzoate salt. Reaction of the free base form of the N-oxide, however, did not yield the desired PCP-Im^{+} **60**. The problem with this approach was that the N-oxide decomposed when attempts were made to obtain the free base by basic alumina chromatography. This result suggested a possible intramolecular proton transfer process (Scheme 22) which is supported by the observation that the major component present in the GC/MS spectrum was phenylcyclohexene (**75**) (Fig. 35).

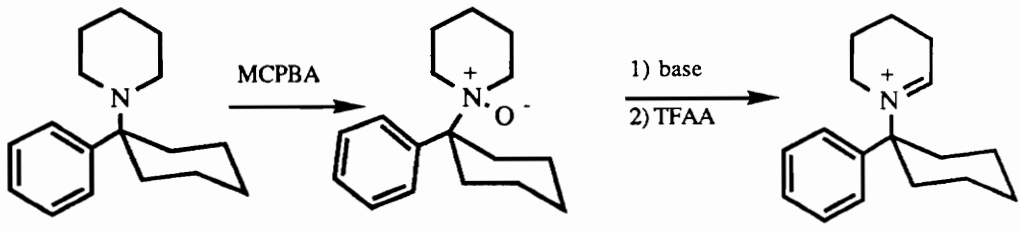

54 **74** **60**

Scheme 21. Proposed reaction pathway leading to PCP-Im^{+} via PCP N-oxide.

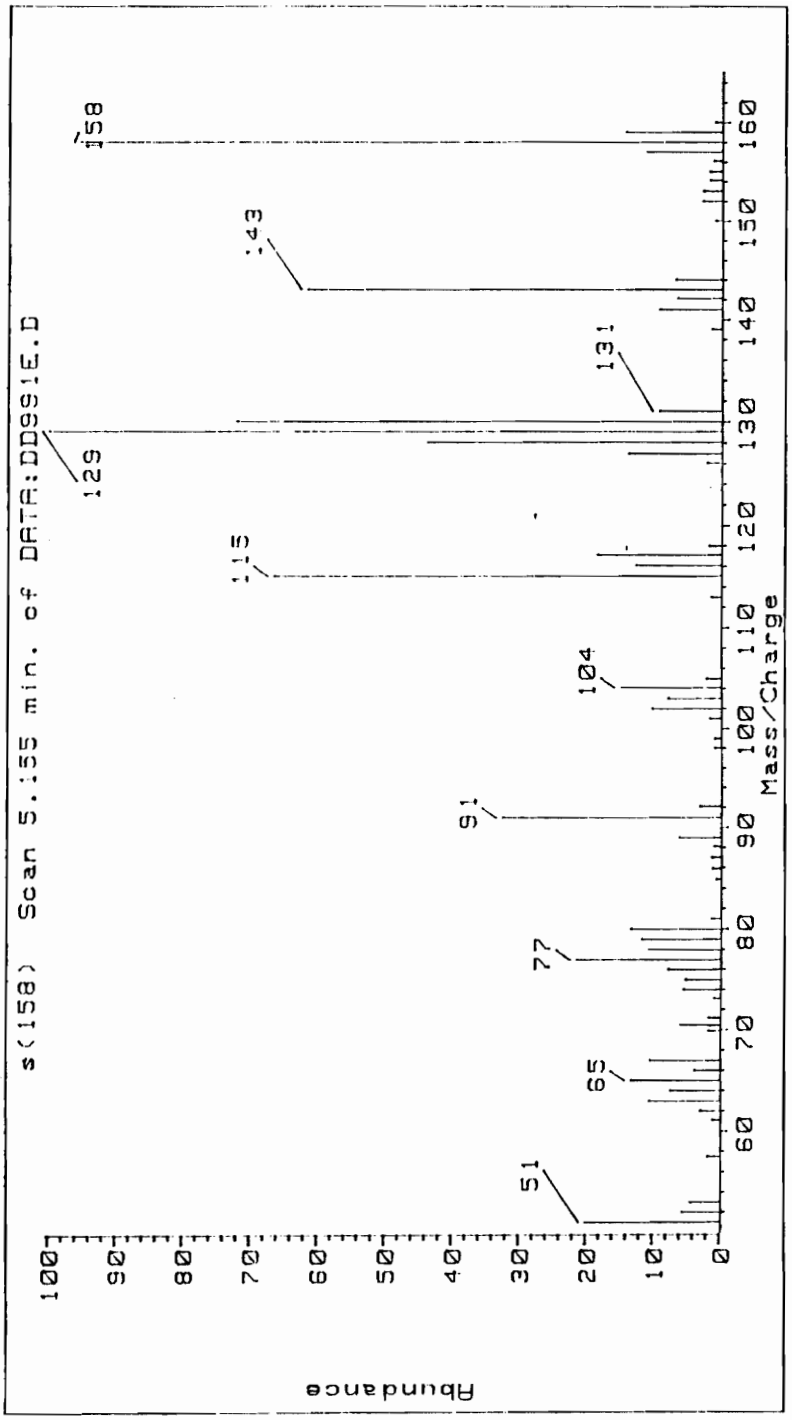

Figure. 35. GC/EIMS of Phenylcyclohexene.

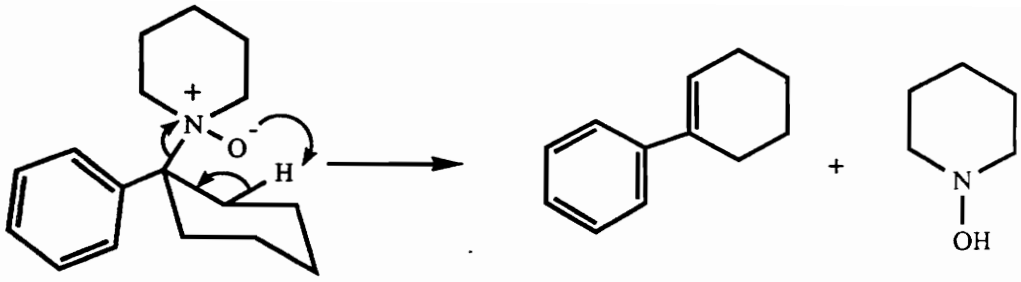

74 **75** **76**

Scheme 22. Proposed proton transfer mechanism for PCP N-oxide cleavage.

An alternative approach to **60** involved oxidation of PCP with mercuric acetate in 5% acetic acid.[75] The PCP-Im^+ species as its perchloric acid salt was obtained by this route as a white crystalline solid. The GC/EI mass spectrum (Fig. 36) of the corresponding enamine **64** exhibited a molecular ion at m/z 241. The base peak at m/z 83 corresponds to the formation of the 1,2,3,4-tetrahydropyridinium cation, **73a**, a analog of **73**. The diagnostic fragment ion at m/z 91 is assigned to the tropylium ion **44** and the ion at m/z 159 to **67**. The latter fragment ion involves the expulsion of 1,2,3,4-tetrahydropyridine moiety.

In order to perform quantitative studies, a deuterated analog of **60** was targeted as a possible internal standard for the GC/MS experiment. Therefore PCP-d_5 (**76**) was synthesized by reaction of 1-(1-carbonitrilecyclohexyl)piperidine (**70**) with phenyl-d_5-magnesium bromide under the same conditions as used for the preparation of PCP. The GC/MS spectrum (Fig. 37) of the deuterated product (**76**) showed a molecular ion at m/z 248 as well as a strong peak at m/z 246. This strong M-2 ion is probably due to migration the one of the *othro*-deuterium on the phenyl ring to the nitrogen atom followed by loss of an adjacent deuterium atom (Scheme 23). The base peak was recorded at m/z 205 which corresponds to **72**-d_5. The other fragment ion at m/z 96 could be assigned to the deuterated tropyrium ion **44**-d_5. The rest of the fragment ions correspond to those present in the spectrum of PCP.

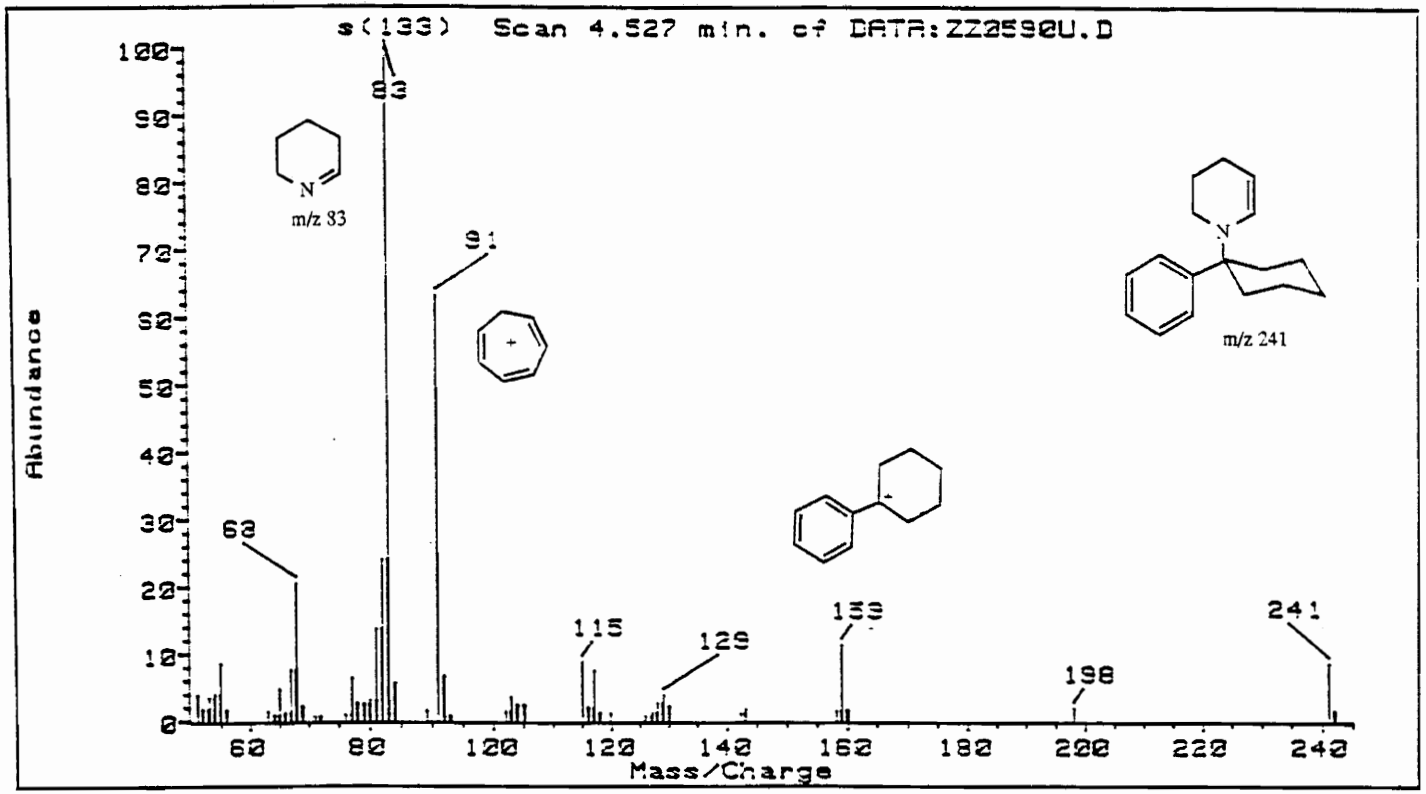

Figure. 36. GC/EIMS of 1-(1-Phenylcyclohexyl)-1,2,3,4-tetrahydropyridine.

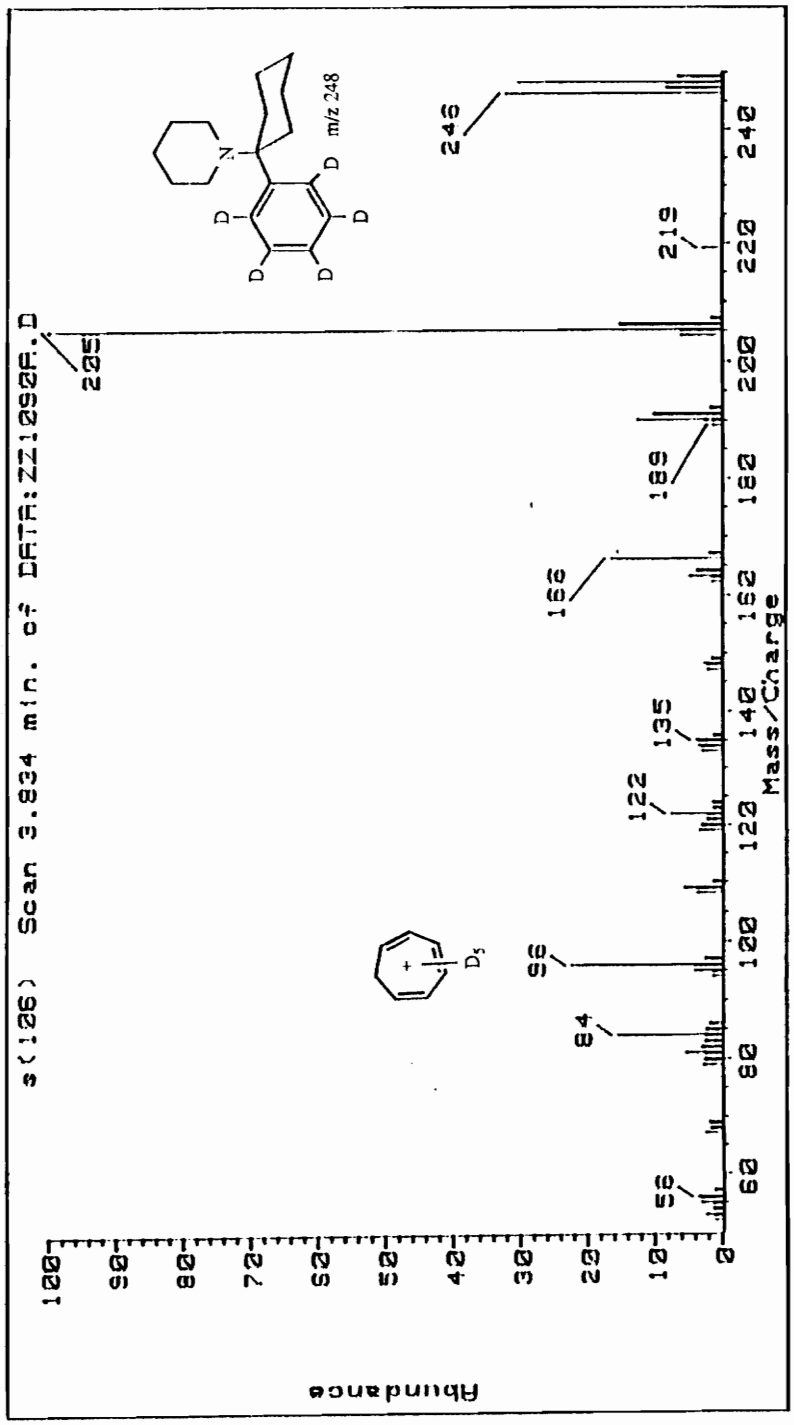

Figure. 37. GC/EIMS of 1-(1-Phenyl-d5-cyclohexyl)piperidine.

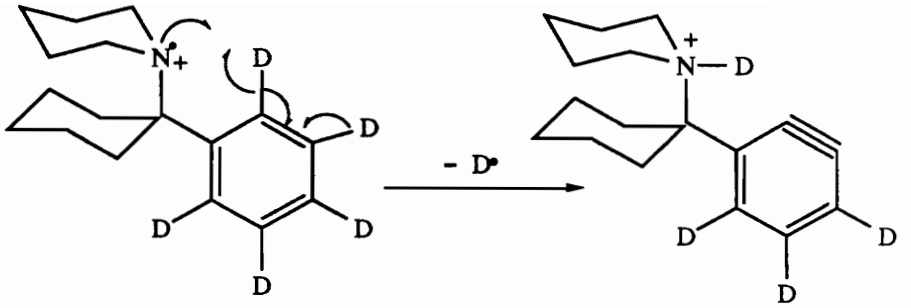

Scheme 23. Proposed fragmentation pathway for PCP-D_5 leading to M-2^+.

The conversion of the PCP-d_5 (**76**) to the corresponding PCP-d_5-Im^+ species **77** was acheived by the same reaction as for PCP-Im^+. The GC/EI mass spectrum (Fig. 38) of the deuterated PCP-enamine **64**-d_5, the corresponding free base form of the PCP-d_5-Im^+ ion, exhibited a molecular ion at m/z 246. Its base peak at m/z 83, which was present in the spectrum of the undeuterated PCP-enamine, corresponded to the formation of the 1,2,3,4-tetrahydropyridinium cation **73a**. The diagnostic fragment ions at m/z 96 and m/z 164 result from the formation of the deuterated tropylium ion **44**-d_5 and expulsion of 1,2,3,4-tetrahydropyridine moiety from the deuterated parent ion to yield species **67**-d_5.

The key step in the proposed synthesis of **69** involved formylation of the enamine **64**. To accomplish this transformation we considered an SN_2' process involving an appropriate formylating reagent. The C-formylation reaction of **64** was first tried with ethyl formate as the formylating reagent. GC/MS analysis of the reaction mixture suggested that no product formation had occured even after heating under reflux overnight. An alternative approach was taken in which the more reactive N-formylimidazole (**71**) served as the potential formylation reagent. This approach was modeled on the potential biosynthetic pathway in which the substrate would react with a biological donor of CHO, such as folinic acid or its equivalent which containing a N-CHO group. The formylimidazole was considered a potentially more effective formylating reagent than

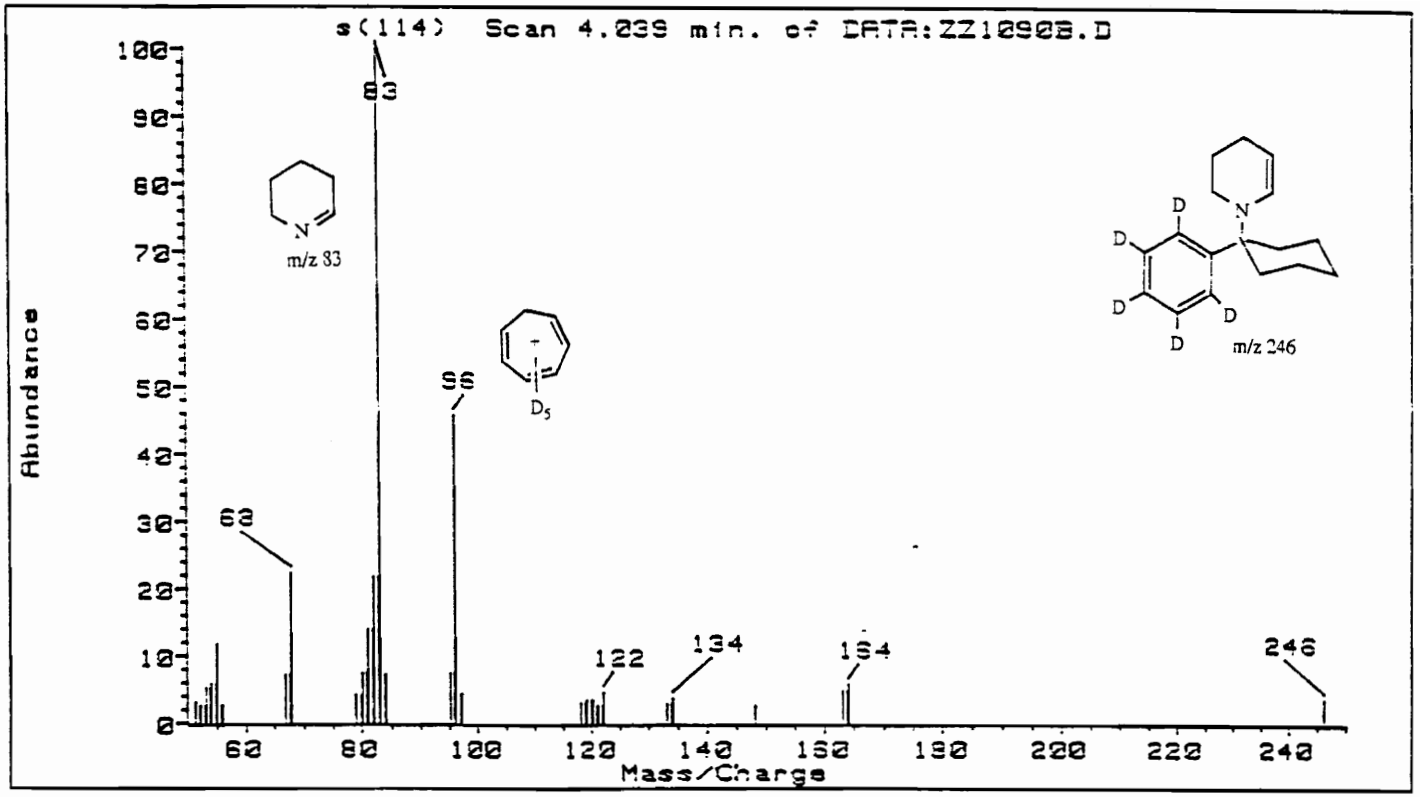

Figure. 38. GC/EIMS of 1-(1-Phenyl-d5-cyclohexyl)-1,2,3,4-tetrahydropyridine.

ethyl formate since the by-product formed in this reaction, imidazole, should be a good leaving group due to its aromaticity. On the other hand, the lone pair of electrons in the *p*-orbital on nitrogen in the formylimidazole molecule is delocalized to the imidazole ring to form a 6-π electron aromatic system which, therefore, makes the carbonyl carbon more electrophilic. The formylimidazole (**71**) was previously reported as a N-formylating reagent but no C-formylation example has been reported in the enamine system. Compound **71** was prepared from commercially available N,N'-carbonyldiimidazole with formic acid in dry THF as the solvent.[80] The crude reagent was used without further purification.

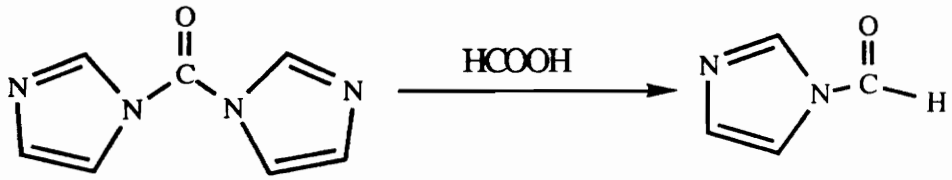

CDI **71**

Scheme 24. Synthetic pathway leading to formylimdazole (**71**).

The enamine free base **64** obtained from **60** was treated with N-formylimidazole in the dry CH_2Cl_2. The crude product was subjected to centrifugal chromatography with ethyl acetate as solvent which provided a yellow crystalline solid that recrystallized from methylene chloride:hexane. The GC/EI mass spectrum (Fig. 39) of **69** was identical to that of the metabolite. It displayed the expected parent ion at m/z 269 and two intense fragment ions at m/z 159 and 91. These fragment ions can be assigned to the phenylcyclohexyl carbocationic species **67** (m/z 159) and the tropylium species **44** (m/z 91). The weak ion at m/z 226 corresponds to loss C_3H_7 from the parent ion via the same fragmentation pattern as PCP described above. The two moderately abundant fragment ions at m/z 111 and m/z 82 probably result from 1,2,3,4-tetrahydropyridine-5-carboxaldehyde (**68**) and 1,2,3,4-tetrahydropyridine, respectively.

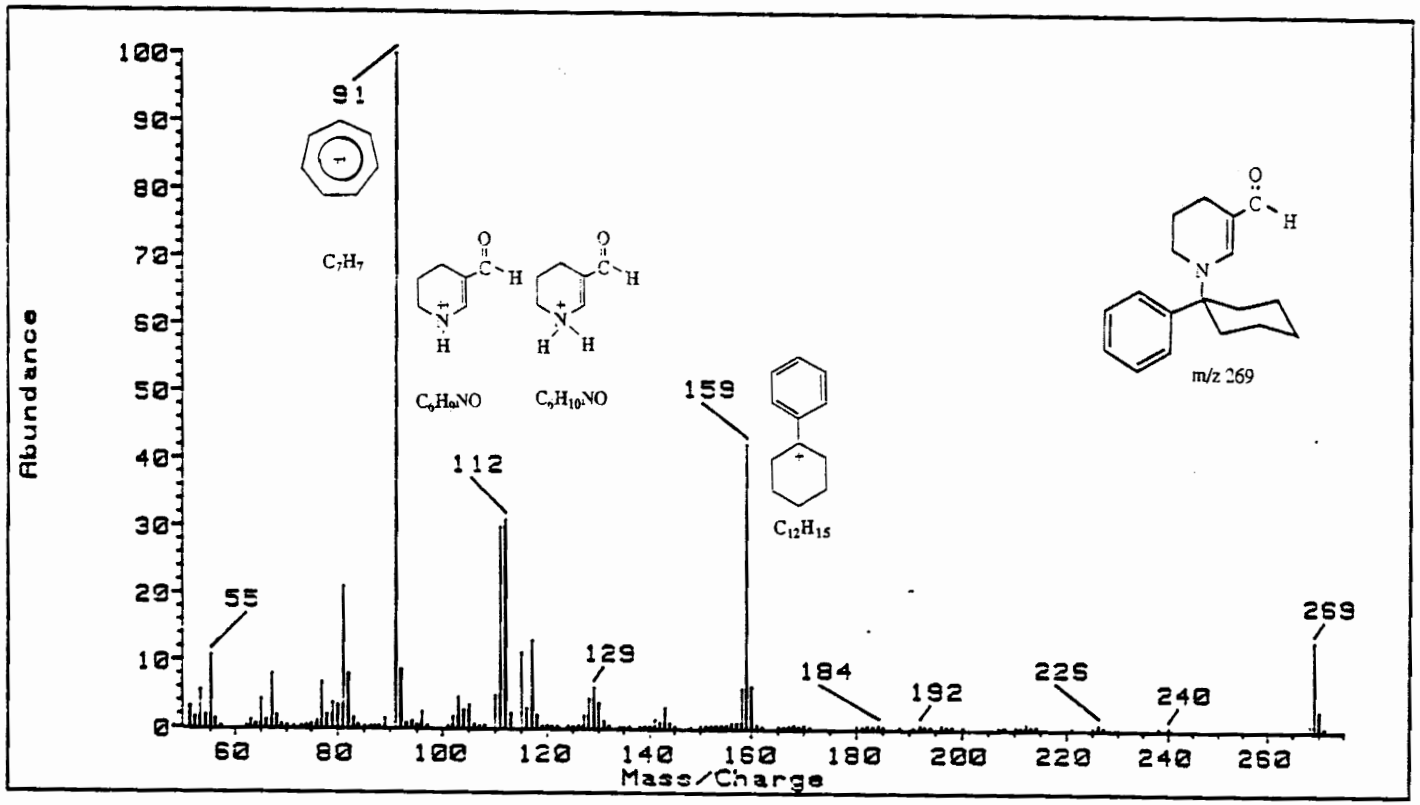

Figure. 39. GC/EIMS of 1-(1-Phenylcyclohexyl)-1,2,3,4-tetrahydropyridine-5-carboxaldehyde.

The ^1H NMR spectrum (Fig. 40) of **69** showed the key diagnostic signals present at 7.43 ppm (uncoupled olefinic proton signal, H_a) and 8.97 ppm (shielded aldehyde proton signal, H_b). The two protons (H_e) on the carbon atom of the tetrahydropyridine ring adjacent to the nitrogen atom appeared as a triplet centered at 2.98 ppm and the two protons (H_c) on the carbon near to the carbonyl group appeared as a partially obscured triplet centered at 2.35 ppm. The two cyclohexyl equatorial protons (H-2' and H-6') of the molecule appeared as a multiplet centered at 2.20 ppm which was separated from the signals at 1.70-1.40 ppm due to the remaining protons of the cyclohexyl group and the two protons (H_d) on the tetrahydropyridine ring. These assignments are based in part on the generally accepted assignments of eq and ax proton signals of the cyclohexyl group in which H_{eq} is usually deshielded relative to H_{ax} by about 0.1-0.7 ppm.[54] The assignments were confirmed by decoupling experiments in which irradiation of the complex centered near 1.6 ppm, which includes the signal for H_d, caused the signals for H_e and H_c to collapse to singlets.

We considered that the N^5-formyltetrahydrofolic acid (folinic acid, **78**) and/or the corresponding N^{10}-formyltetrahydrofolic acid **79**, compounds which are intermediates in the tetrahydrofolic acid complex known to occur in mammalian brain,[81] might be the biological sources for the newly introduced formyl moiety of the metabolite. A possible mechanism to account for these results involves the conjugate addition of **64** across the formamide carbonyl group of **78** and/or **79** to generate the tetrahedral intermediate **80** which, upon subsequent carbon-nitrogen bond cleavage, yields tetrahydrofolic acid (**81**) and the formylated product **69** as summarized in Scheme 25. This biotransformation may be the first example of metabolic C-formylation of a xenobiotic.

The GC/MS ion selected chromatogram at m/z 269 indicated that metabolite **69** was a major peak among those m/z 269 ion containing components (Fig. 30). The results obtained from an incubation run in the absence of substrate (Fig. 41) and in absence of the enzyme (Fig. 42) showed no formation of the corresponding metabolite. Based on a comparison of the peak area integration of

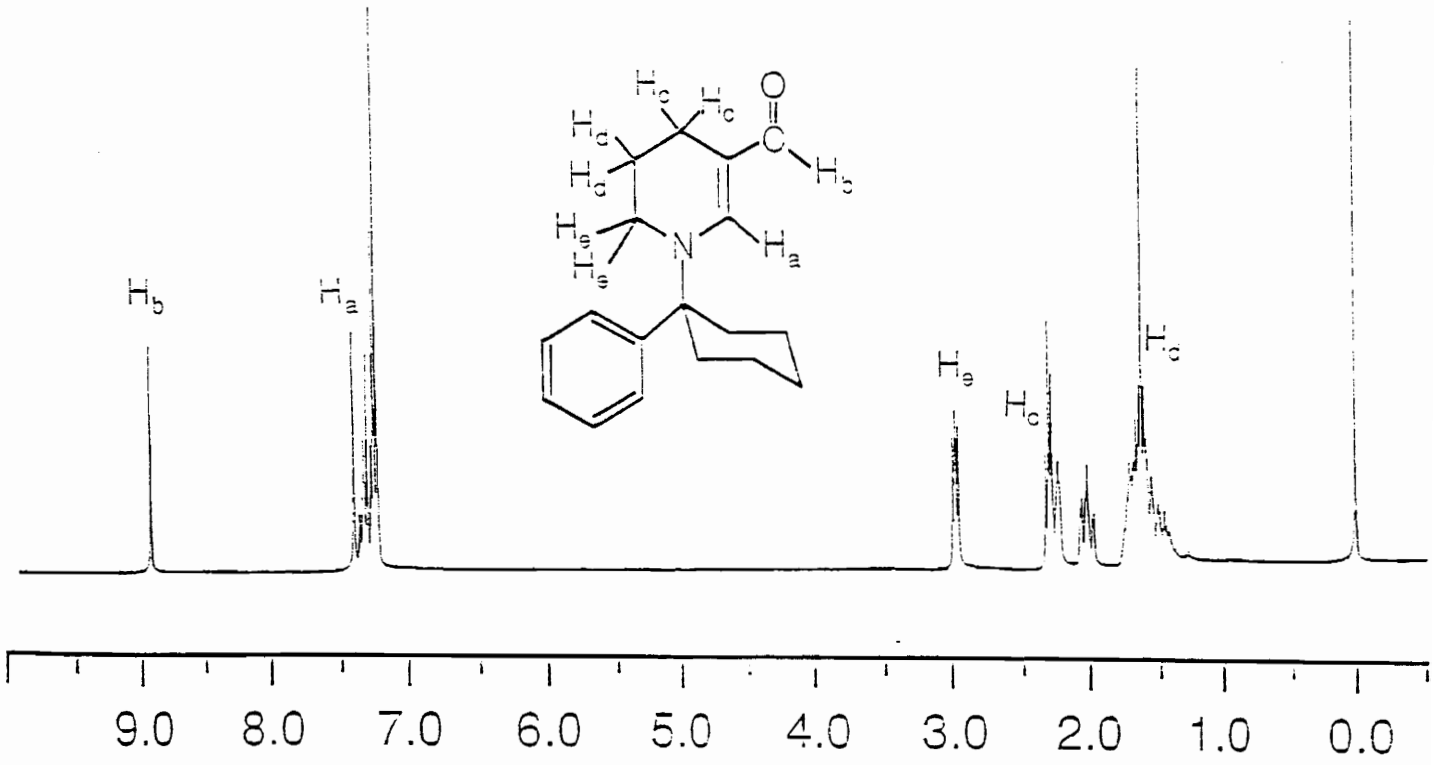

Figure. 40. ^1H NMR Spectrum ($CDCl_3$) of 1-(1-Phenylcyclohexyl)-1,2,3,4-tetrahydropyridine-5-carboxaldehyde.

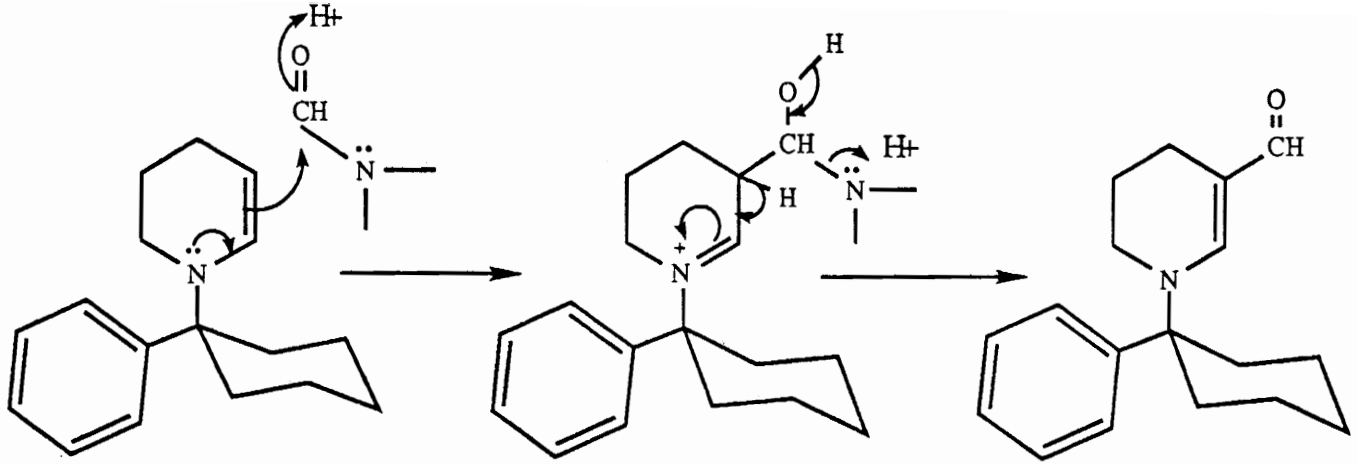

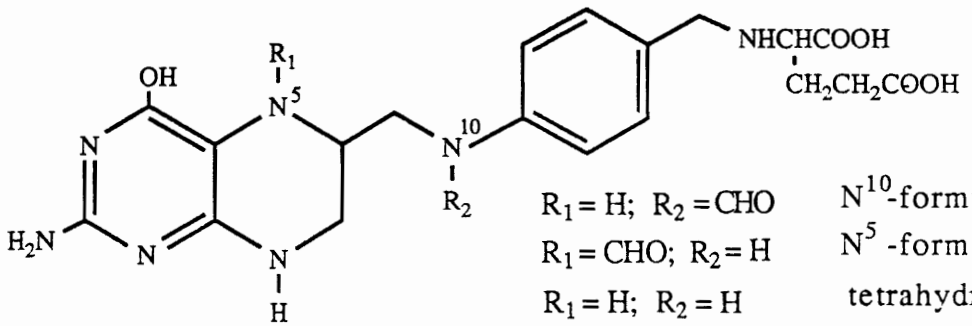

$R_1 = H;\ R_2 = CHO$	N^{10}-formyltetrahydrofolic acid	**79**
$R_1 = CHO;\ R_2 = H$	N^{5}-formyltetrahydrofolic acid	**78**
$R_1 = H;\ R_2 = H$	tetrahydrofolic acid	**81**

Scheme 25. Proposed pathway to the C-formylated metabolite **69**.

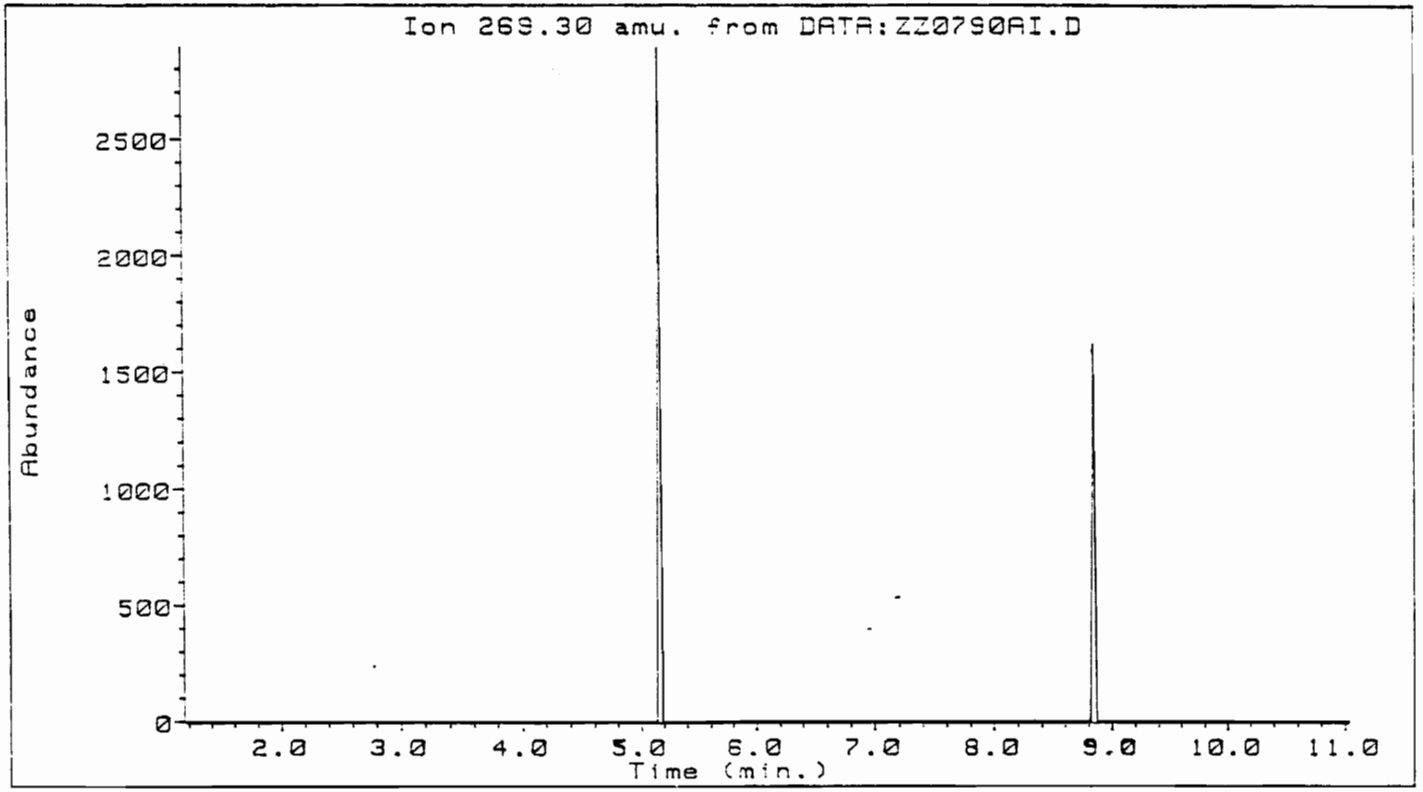

Figure. 41. **Ion Chromatogram (m/z 269) of Control Sample (Absence of Substrate).**

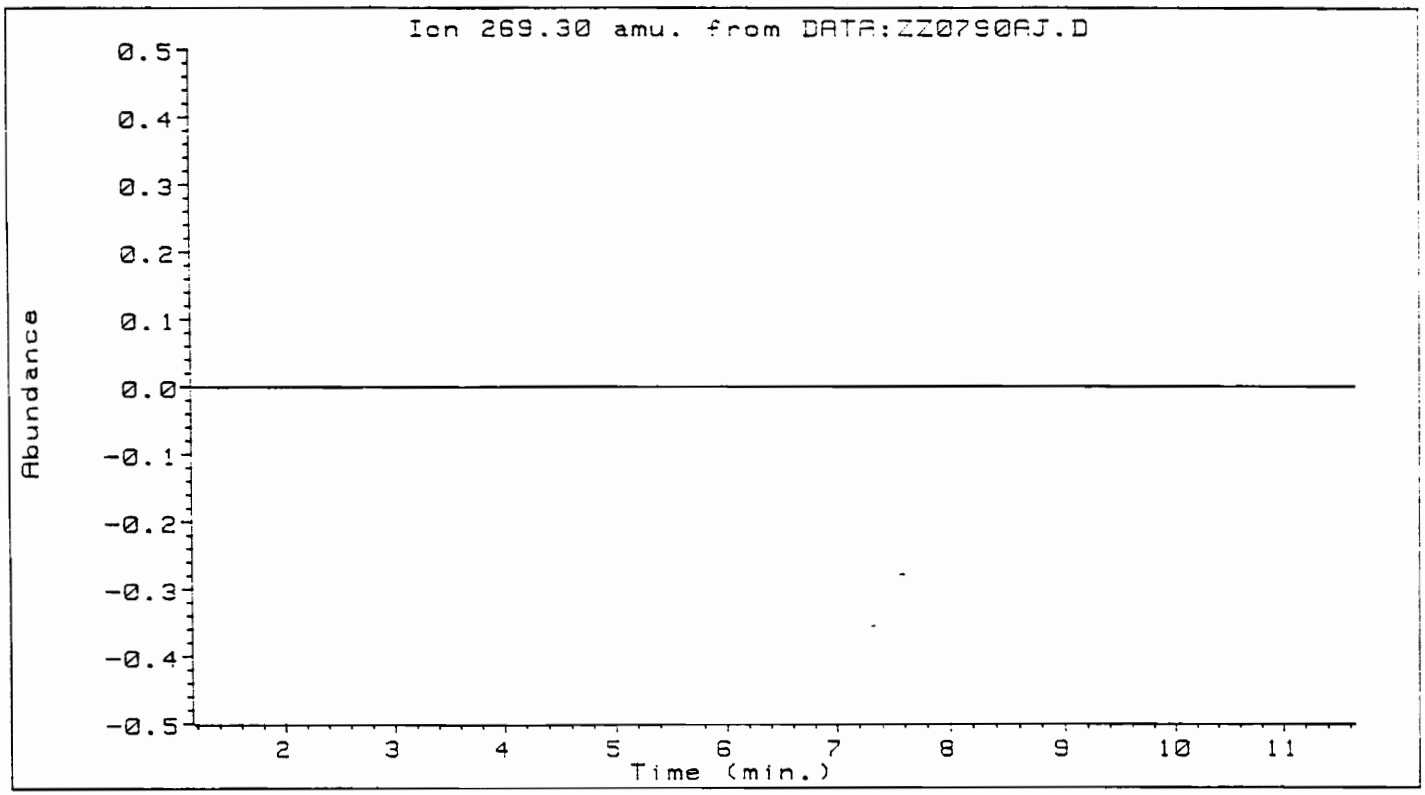

Figure. 42. Ion Chromatogram (m/z 269) of Control Sample (Absence of Enzyme).

the metabolite with that of the control sample, it was roughly estimated that about 45% of the substrate remained intact after a two hours incubation period. The conversion to the metabolite **69** was estimated at about 5% based on total substrate, and about 10%, based on the 55% loss of substrate.

Based on the identification of 1-(1-phenylcyclohexyl)-1,2,3,4,-tetrahyhydropyridine-5-carboxaldehyde (**69**) as a novel metabolite of phencyclidine and consideration of the possibility of conversion of this compound to the corresponding 1-(1-phenylcyclohexyl)-1,2,3,4,-tetrahyhydronicotinic acid (**82**), we have extended these studies to evaluate the neurotoxic potential of this nicotinic acid analog **82** since its structure is similar to that of a known neurotoxin "CI966" (**83**).[82] In order to study the possible metabolic conversion of aldehyde **69** to the corresponding acid **82** and to evaluate the potential neurotoxicity of this acid we undertook the synthesis of this nicotinic acid analog.

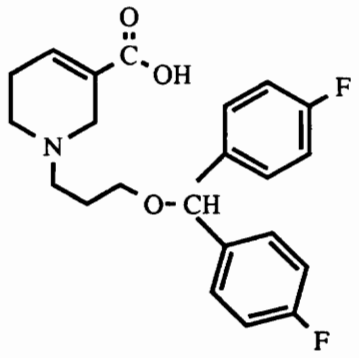

83

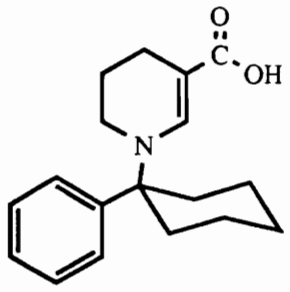

82

The proposed synthetic pathway to the desired nicotinic acid analog **82** involved preparation of potential "precusors", by reactions similar to the C-formylation reaction, followed by hydrolysis. The reaction of the PCP-enamine **64** with benzyl chloroformate or allyl chloroformate was expected to yield the corresponding benzyl 1-(1-phenylcyclohexyl)-1,2,3,4-tetrahydronicotinate (**84**) or allyl 1-(1-phenylcyclohexyl)-1,2,3,4-tetrahydronicotinate (**85**) which upon reaction with chlorotrimethylsilane and sodium iodide should yield 1-(1-phenylcyclohexyl)-1,2,3,4-tetrahydronicotinic acid (**82**).

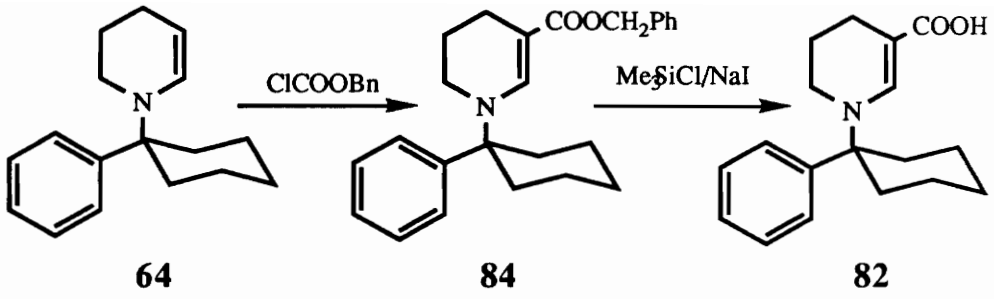

64 **84** **82**

Scheme 26. Proposed synthetic pathway to **82** via **84**.

Benzyl 1-(1-phenylcyclohexyl)-1,2,3,4-tetrahydronicotinate (**84**) was synthesized by reaction of enamine **64** with benzyl chloroformate. The reaction mixture was allowed to stir for 3 days at room temperature at which time GC/MS analysis suggested that the reaction was about 90% complete. After purification by centrifugal chromatography on silica gel with hexane:methylene chloride, a pure colorless oily product was obtained which was characterized by GC/MS and ^{1}H NMR. The GC/EI mass spectrum (Fig. 43) exhibited a moderatly intense molecular ion at m/z 375. The base peak, which appeared at m/z 91, was due to the formation of the tropylium ion **44**. Another intense peak at m/z 217 was derived from expulsion of the phenylcyclohexyl moiety to form benzyl 1,2,3,4-tetrahydronicotinate (**86**). The fragment ions, also observed with PCP, at m/z 332 (loss of C_3H_7) and at m/z 159 (**67**, loss of tetrahydropyridine moiety), were present.

The ^{1}H NMR spectrum (Fig. 44) of **84** showed a key signal at 8.10 ppm (uncoupled olefinic proton signal). This signal is shifted downfield relative to the corresponding olefinic signal of the aldehyde **69**. This shift probably is due to the electronic field repulsion caused by the oxygen atoms in the crowded environment of **84**. Another diagnostic proton signal was observed at 5.25 ppm which is assigned to the uncoupled methylene protons of the benzyl group. The rest of the spectrum is almost identical with that of aldehyde **69**.

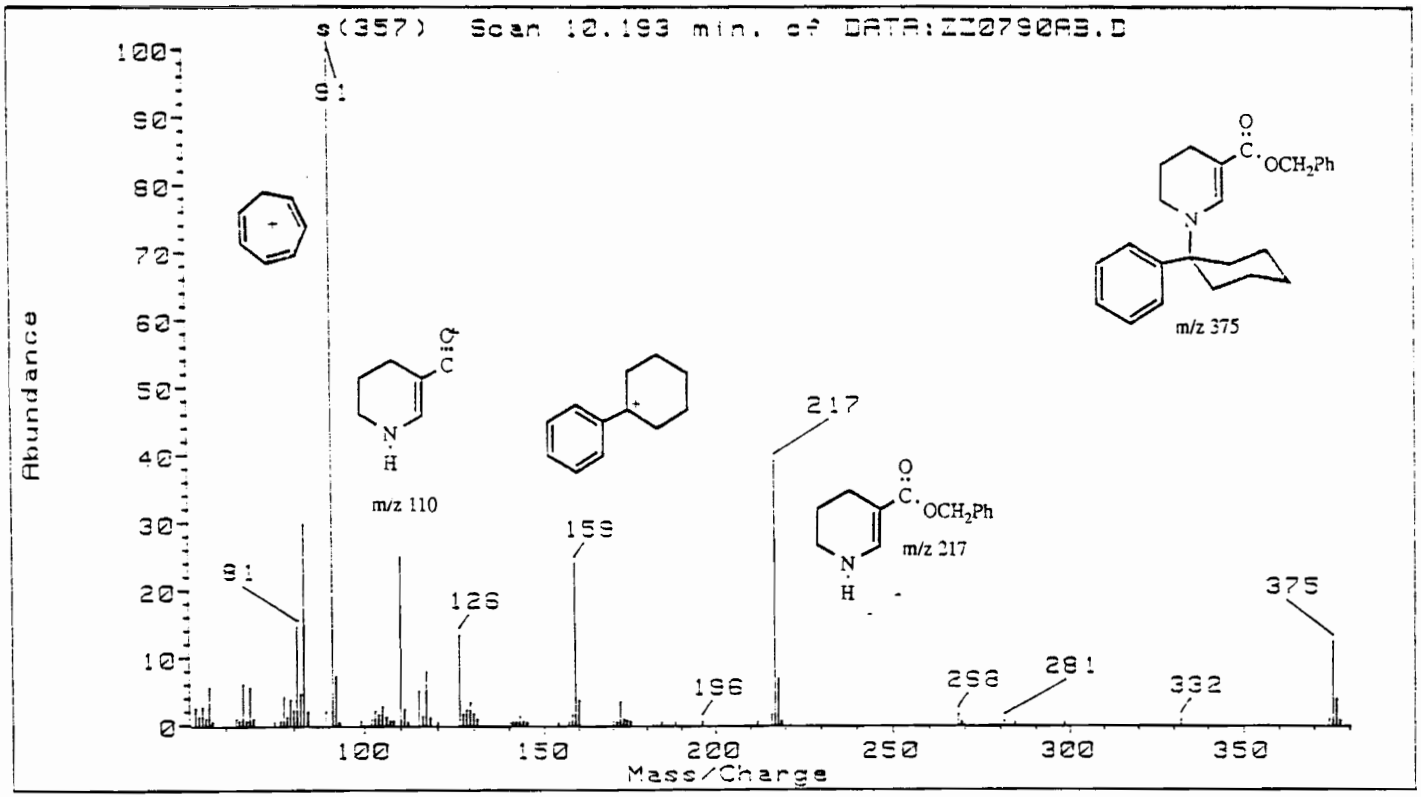

Figure. 43. GC/EIMS of Benzyl 1-(1-Phenylcyclohexyl)-1,2,3,4-tetrahydronicotinate.

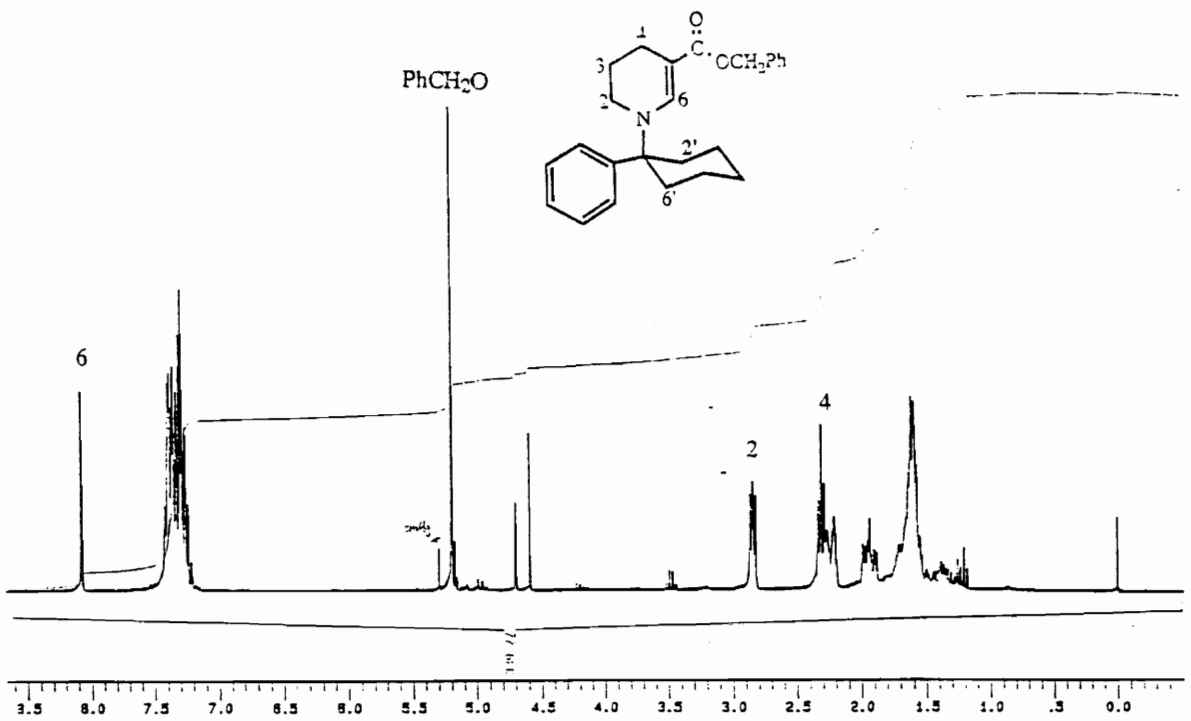

Figure. 44. ^1H NMR Spectrum ($CDCl_3$) of Benzyl 1-(1-Phenylcyclohexyl)-1,2,3,4-tetrahydronicotinate.

The hydrolysis of the benzyl ester **84** to form the designed the 1-(1-phenylcyclohexyl)-1,2,3,4-tetrahydronicotinic acid **82** was first tried by a two-phase reaction with 1N NaOH and methylene chloride at room temperature. No reaction was observed. The hydrolysis then was attempted by treatment of **84** with chlorotrimethylsilane and sodium iodide.[83] The advantage of this method is to provide very mild conditions needed to cleave the ester. This reaction was run at room temperature overnight and monitored by GC/MS. After the starting material had completely disappeared the reaction mixture was extracted with diethyl ether and the product was purified by base/acid partitioning. The product was first extracted into the aqueous solution with $NaHCO_3$ and then extracted back in to the organic layer with ether by adjusting the aqueous solution to pH value of 3-4. Since the expected product is probably not GC detectable due to thermal instability, the diethyl ether layer, which presumably contained the product, was dried and analyzed by ^1H NMR spectroscopy. ^1H NMR analysis showed that the product had not partitioned into the ether layer. The possible reason for loss of the product is that it may be too lipophilic to extract into the $NaHCO_3$ layer and instead remained in the first organic fraction which, unfortunately, was discarded as waste. This reaction, however, was not repeated since a mild Palladium catalyzed deprotection of the allyl ester leading to the corresponding acid was reported in the literature.[84] Therefore the next effort was to synthesize the allyl ester **85**.

Allyl 1-(1-phenylcyclohexyl)-1,2,3,4-tetrahydronicotinate (**85**) was synthesized in a similar way by reacting PCP-enamine **64** with allyl chloroformate. After purification by silica gel chromatography, the product was obtained as a light yellow oil. The ^1H NMR spectrum (Fig. 45) of the allyl ester **85** showed the key diagnostic signal at 8.02 ppm (uncoupled olefinic proton signal). The aromatic proton signals were recorded at 7.08-7.42 ppm. The olefinic proton on carbon (C-2') of the allyl group was observed at 6.02 ppm as a multiplet. The other two terminal olefinic proton signals appeared as two sets of doublets centered at 5.35 ppm and 5.18 ppm. The signal for the methylene protons of the allyl group appeared as a doublet

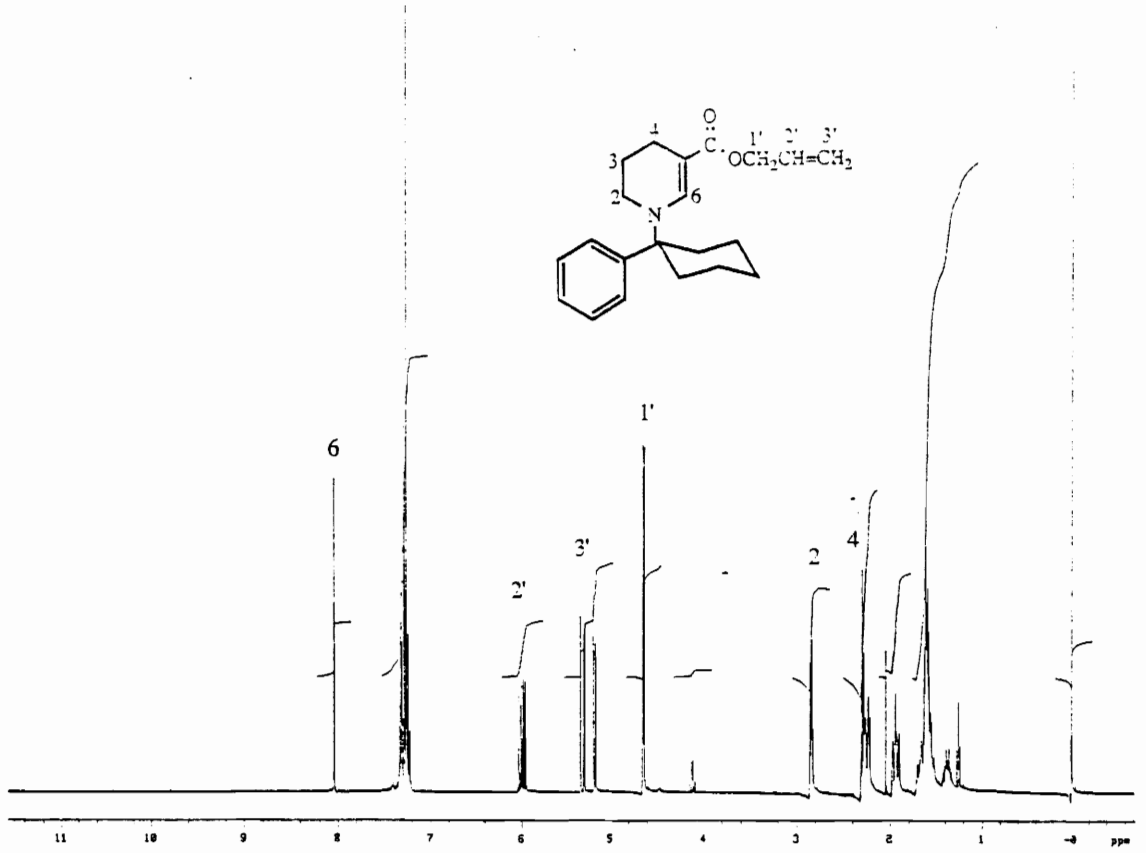

Figure. 45. ^1H NMR of Spectrum ($CDCl_3$) Allyl 1-(1-Phenylcyclohexyl)-1,2,3,4-tetrahydronicotinate.

centered at 4.68 ppm. The protons on the carbon (C-2) adjacent to the nitrogen atom exhibited a triplet centered at 2.90 ppm and the protons on C-4 of the tetrahydropyridine ring near the carbonyl group also gave a triplet centered at 2.32 ppm. The two cyclohexyl equatorial protons on the C-2' and C-6' of the molecule showed as a multiplet at 2.28 ppm which partially overlaped with the signals from the protons on C-4 of the pyridine ring. The signals of the protons on the carbon (C-3) overlaped with the signals of the rest of the protons of the cyclohexyl group at 1.5 ppm - 1.8 ppm.

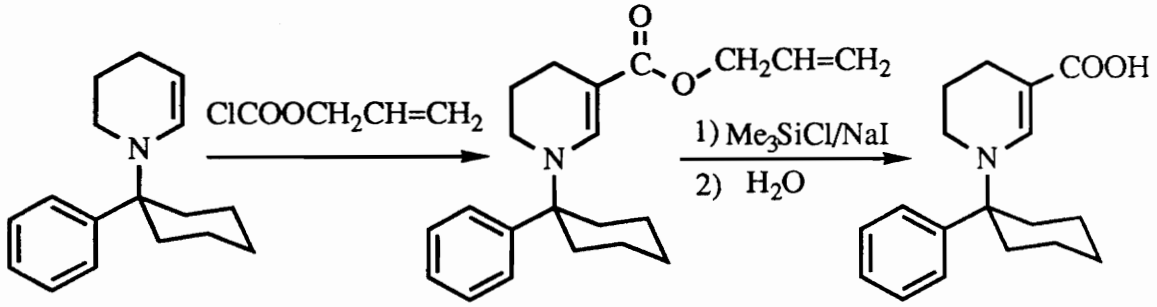

64 85 82

Scheme 27. Proposed synthetic pathway to **82** via **85**.

The GC/MS spectrum (Fig. 46) of the allyl ester displayed the expected parent ion at m/z 325 and two intense fragment ions at m/z 159 and m/z 91. These fragment ions, also present in the EI mass spectrum of PCP and PCP enamine, can be assigned to the phenylcyclohexyl carbocationic species **67** and tropylium species **44**. Another intense fragment ion at m/z 167 resulted from the expulsion of phenylcyclohexyl moiety to form the allyl 1,2,3,4-tetrahydronicotinate species **87**. The fragment ion recorded at m/z 268 was derived from loss of an allyl group from the parent molecular ion.

Attempts to prepare the nicotinic acid analog **82** by deprotecting the allyl ester with $Pd(PPh_3)_4$ and PPh_3 was not successful.[84] The GC/MS spectrum showed no consumption of the starting material even after trying different solvents (including methylene chloride, acetonitrile) and different nucleophiles (such as

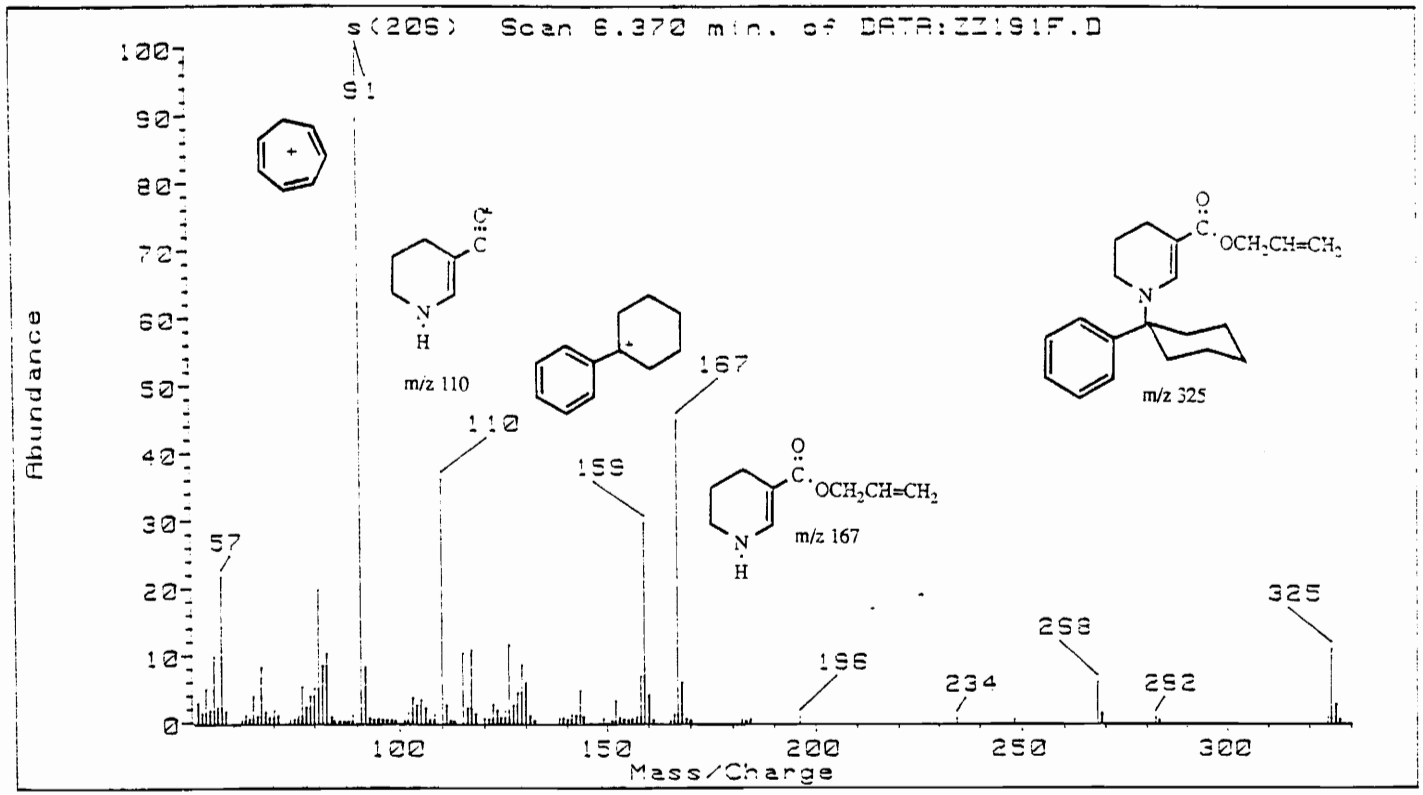

Figure. 46. GC/EIMS of Allyl 1-(1-Phenylcyclohexyl)-1,2,3,4-tetrahydronicotinate.

diethylamine, piperidine). The deprotection reaction then was tried with chlorotrimethylsilane and sodium iodide in acetonitrile.[83] The starting material was consumed according to the GC/MS results but no product peak was observed. This probably was due to the fact that the nicotinic acid analog is thermally unstable. The sample was also sent for LC/MS analysis, but no peak corresponding to the molecular ion of the nicotinic acid analog **82** was observed.

An alterative synthetic pathway to the desired nicotinic acid analog **82** involved synthesis of 5-(1-imidazoylcarbonyl)-1-(1-phenylcyclohexyl)-1,2,3,4-tetrahydropyridine (**88**) as an intermediate followed by an appropriate hydrolysis step. Compound **88** was synthesized by a C-formylation type reaction of PCP enamine with carbonyldiimidazole (CDI).

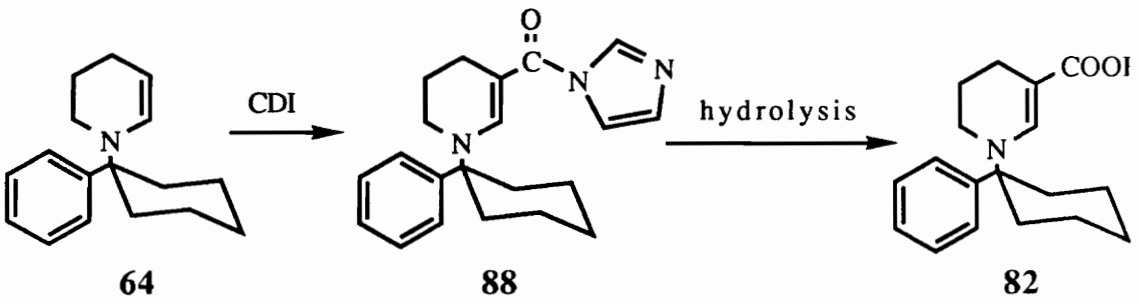

Scheme 28. Proposed synthetic pathway to **82** via **88**.

After general work-up, the product was recrystallized from ethyl ether to form an off-yellow crystalline solid. The ^{1}H NMR spectrum (Fig. 47) of **88** showed the key diagnostic signals present at 7.40 ppm (uncoupled olefinic proton signal of the pyridine ring) and 8.0 ppm, 7.85 ppm and 7.05 ppm, three singlets derived from the three protons of the imidazole ring. The two protons on C-4 of the tetrahydropyridine ring next to the carbonyl group gave a triplet centered at 2.50 ppm. The protons on C-2 adjacent to nitrogen exhibited a triplet centered at 3.05 ppm. The two cyclohexyl equatorial protons on the carbon atoms (C-2' and C-6') of the molecule showed as a multiplet at 2.20 ppm, which was separated from the signals at 1.70-1.40 ppm given by the rest of the protons of

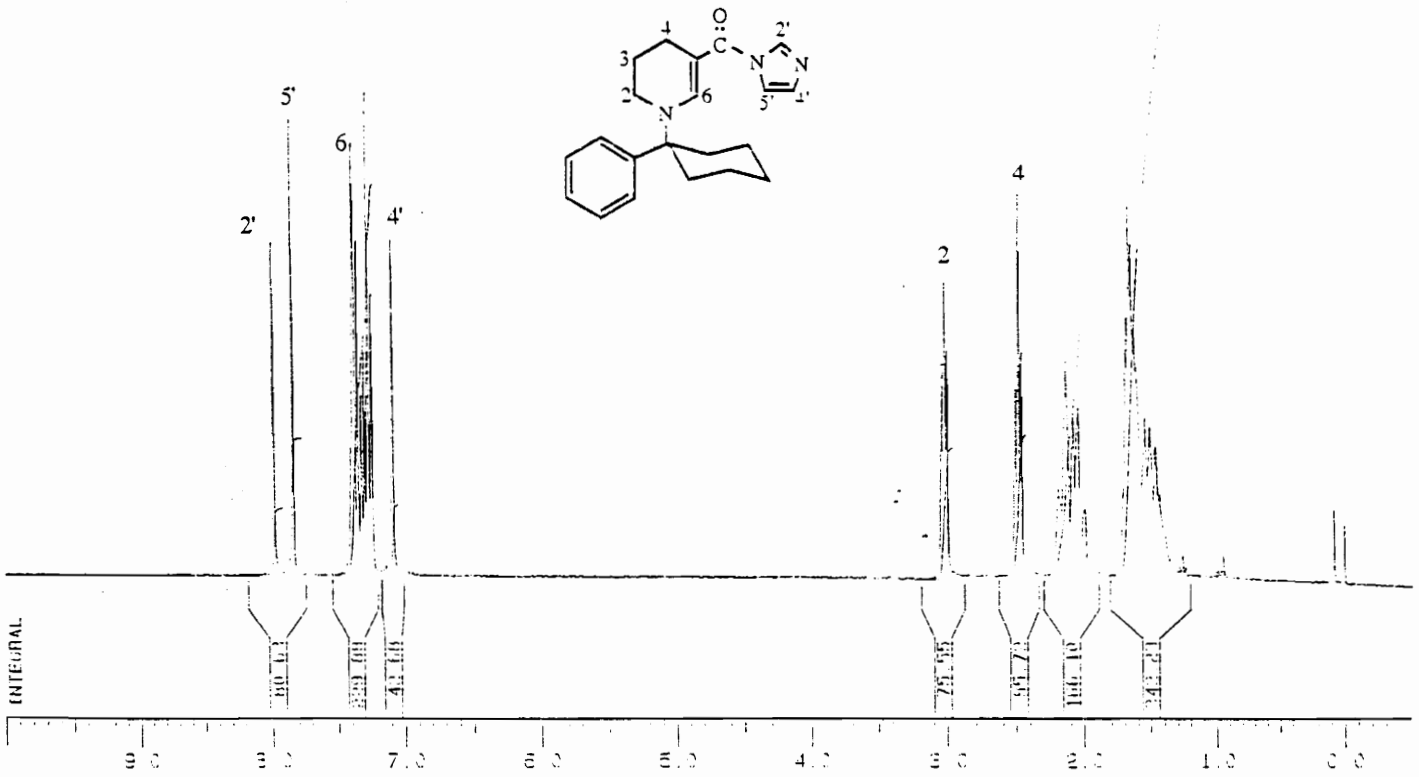

Figure. 47. ^{1}H NMR Spectrum ($CDCl_3$) of 5-(1-Imidazoylcarbonyl)-1-(1-phenylcyclohexyl)-1,2,3,4-tetrahydropyridine.

the cyclohexyl group which were overlaped with the signal for the C-3 proton of the tetrahydropyridine ring. The signal assignments were based on a comparison with those of the fully characterized compound 1-(1-phenylcyclohexyl)-1,2,3,4-tetrahydropyridine-5-carboxaldehyde (**69**, Fig. 41).

The 5-(1-imidazoylcarbonyl)-1-(1-phenylcyclohexyl)-1,2,3,4-tetrahydropyridine (**88**) was thermally unstable. GC/MS of a methanol solution of **88** led to a mass spectrum corresponding to methyl 1-(1-phenylcyclohexyl)-1,2,3,4-tetrahydronicotinate (**89**) which was formed on the GC column by replacement of the imidazoyl group. The GC/EI mass spectrum (Fig. 48) of the methyl ester (**89**) displayed the expected parent ion at m/z 299 and two intense fragment ions at m/z 159 and m/z 91. These characteristic fragment ions can be assigned to the phenylcyclohexyl carbocationic species **67** and tropylium species **44**. Another intense fragment ion at m/z 141 resulted from the expulsion of the phenylcyclohexyl moiety to form methyl 1,2,3,4-tetrahydronicotinate (**90**). Replacement of imidazoyl group by the methoxy group under the GC condition was confirmed by using ethanol instead of methanol which yielded the corresponding ethyl ester (**91**). The GC/MS spectrum (Fig. 49) of **91** showed a molecular ion at m/z 313 and a intense fragmentation ion at m/z 155 which resulted from the formation of ethyl 1,2,3,4-tetrahydronicotinate (**92**). The rest of spectrum is similar to that of the methyl ester **89**.

The synthesis of 1-(1-phenylcyclohexyl)-1,2,3,4-tetrahydronicotinic acid (**82**) was attempted by hydrolyzing the 1-(1-phenylcyclohexyl)-1,2,3,4-tetrahydropyridine-5-carbonylimidazole (**88**) with acid or base as catalyst at different temperatures. Compound **88**, however, decomposed under these conditions to form phenylcyclohexene (**77**) evidenced by GC/MS analysis. No reaction took place at neutral condition.

A future attempt at the synthesis of acid **82** may be approached by hydrogenolysis of the benzyl ester **84** with Pd(C) as catalyst under hydrogen atmosphere. This reaction has not been attempted. Preliminary evidence suggests that **69** may be oxidized with PCC (pyridinium chlorochromate) since ^{1}H NMR analysis of a

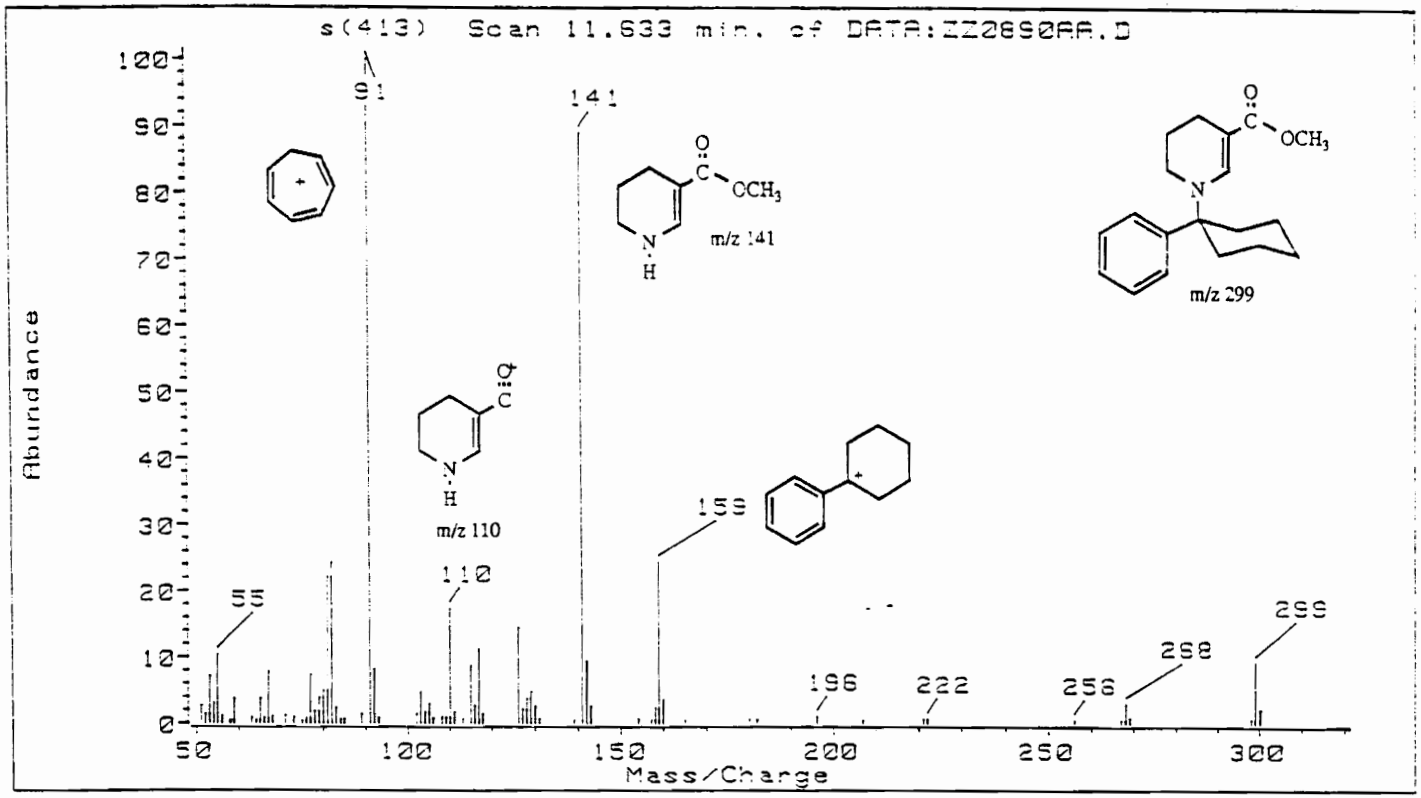

Figure. 48. GC/EIMS of Methyl 1-(1-Phenylcyclohexyl)-1,2,3,4-tetrahydronicotinate.

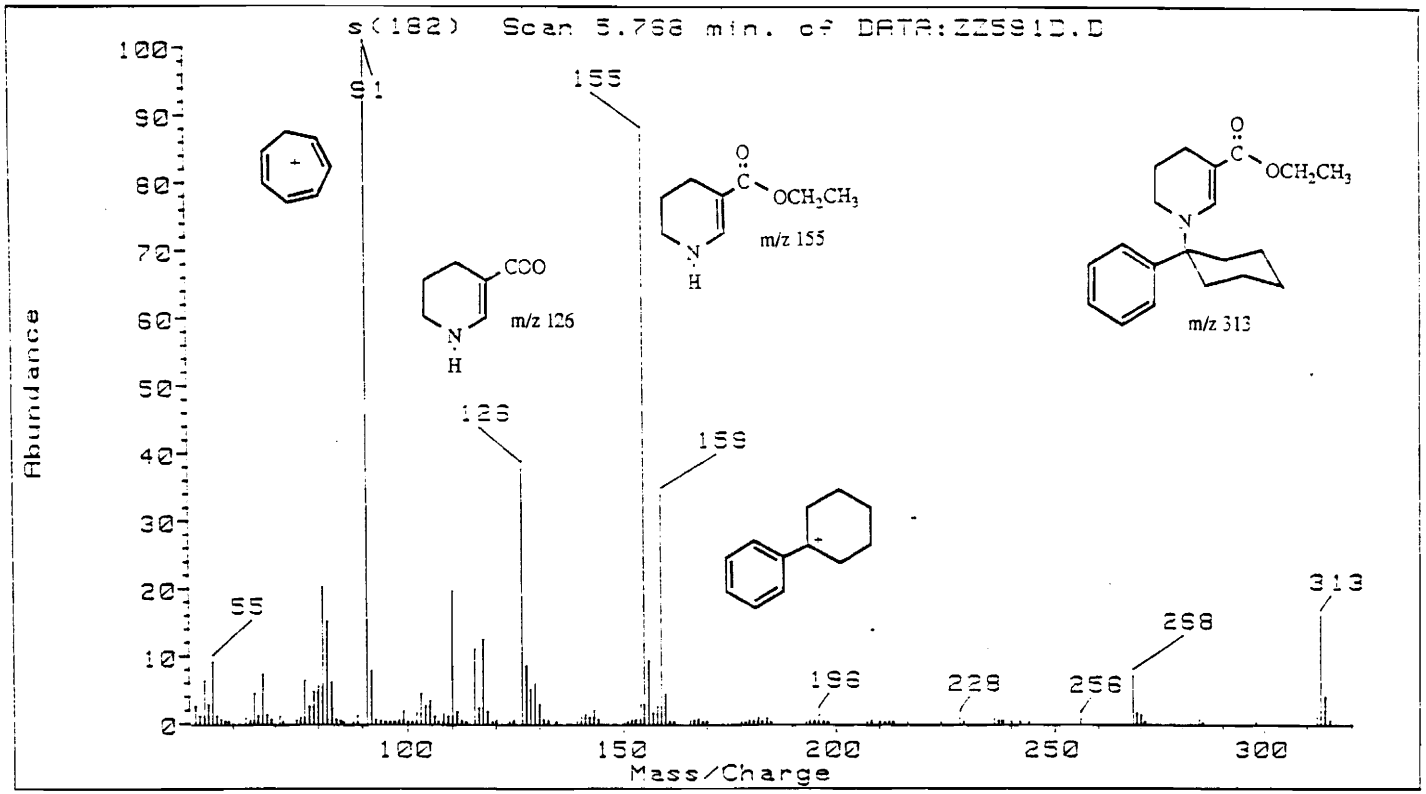

Figure. 49. GC/EIMS of Ethyl 1-(1-Phenylcyclohexyl)-1,2,3,4-tetrahydronicotinate.

small reaction indicated loss of the aldehyde proton signal at 8.97 ppm when **69** was treated with this reagent. That experiment, however, was run in the NMR tube on a very small scale and no product was isolated from the reaction.

3.4 Experimental

All chemicals were reagent grade or, in the case of solvents, HPLC or GC grade. The carbonyldiimidazole was obtained from Aldrich Chemical Co.. Folinic acid, $NADP^+$, NADPH, glucose-6-phosphate and glucose-6-phosphate dehydrogenase were obtained from Sigma Chemical Co., St. Louis, MO.

Analytical HPLC separations were performed on a Beckman Model 330 liquid chromatographic system using an Altex Ultrasphere ODS column (5 m particle size, 4.6 mm x 15 cm) and an HP 1040A on-line diode array detector. The effluent was monitored simultaneously at 254 and 302 nm; full spectra were recorded between 200 and 400 nm. The flow rate of the mobile phase [acetonitrile : acetic acid (85:15 v/v) adjusted to pH 5.6 with triethylamine] was 1.5 mL/minute.

GC/MS analyses were performed on a HP Model 5890 gas chromatograph connected to an HP 5097B EI mass spectrometer with an HP methyl silicone capillary column (12 m x 0.2 mm) and a HP series computer. A temperature program of 125 °C for 1 minute. followed by 25 °C/minute to 275 °C was used. Scanning ion monitored in the ion chromatogram monitoring mode at m/z 269 (M^+ of metabolite). Direct insertion probe CI mass spectra were obtained on an AEI MS 902S instrument using isobutane (*ca.* 0.7 torr) as the reagent gas and high resolution mass spectra on a VG 7070HF double focusing mass spectrometer.

1-(1-Phenylcyclohexyl)piperidine (54). To a solution of the 1-piperidinecyclohexanecarbonitrile (10 g, 52 mmol) in 300 mL of toluene/dry ethyl ether (8:2) was added with vigorous stirring under a nitrogen atmosphere a 3 M ethereal solution of phenylmagnesium bromide (26 mL, 78 mmol). The resulting mixture was heated under reflux for 7 hours. The reaction was monitored by GC/MS and then was cooled in an ice-water bath and treated with 100 mL of NH_4OH and 50 mL of water. The separated aqueous layer was extracted twice with ethyl ether (60 mL x 2) and the combined organic layers were extracted with ice-cold 2N H_2SO_4 (100 mL x 2).

The acidic extracts were poured quickly into a mixture of cold 2N NaOH/ethyl ether (250 mL/100 mL). The separated aqueous layer was extracted with diethyl ether (100 mL x 2) and the combined organic extracts were dried ($MgSO_4$), filtered and the solvent was removed under reduced pressure. It formed 11.5 g (90%) of a light yellow oil. The product was converted to its hydrochloric salt and recrystallized from ethanol to give the pure salt: mp 218-220 °C (lit. 219-220°C[85]); GC/MS (m/z, %) [GC temperature program: 125 °C for 1 minute, then 25 °C/minute up to 275 °C (retention time of the free base is 4.37 minute)] 243 ($M^{+}\cdot$, 30), 242 (30), 214 ($M^{+}\cdot$ -C_2H_5, 6), 200 ($M^{+}\cdot$ - C_3H_7, 100), 186 ($M^{+}\cdot$ -C_4H_9, 25), 166 (20), 159 ($M^{+}\cdot$ - piperidine, 8), 117 (25), 91 (tropylium ion, 55), 84 (40).

1-(1-Phenylcyclohexyl)-2,3,4,5-tetrahydropyridinium Perchlorate (PCP-Im^{+}ClO$_4^{-}$, 60). The PCP hydrochloride salt (**54·HCl**, 800 mg, 2.86 mmol) was converted to the corresponding free base which was treated with mercuric acetate (3.63 g, 11.43 mmol) in 60 mL of 5% acetic acid with vigorous stirring at 100°C overnight. The reaction mixture was cooled in an ice-water bath and the mercurous acetate precipitate was separated by suction filtration. The filtrate was neutralized with 25% NaOH in the cold and then extracted with diethyl ether. The diethyl ether layer was dried ($MgSO_4$) and filtered and the filtrate was treated with 2 mL of an ethanolic perchloric acid solution prepared by mixing equal volumes of 70% $HClO_4$ with 95% EtOH. The crystalline perchlorate salt (490 mg, 50%) melted at 114-116 °C (lit mp 116-117 °C);[75] GC/MS (m/z, %) [GC temperature program: 125 °C for 1 minute followed by 25 °C/minute up to 275 °C (retention time of enamine is 4.53 minute)] 241 ($M^{+}\cdot$, 20), 198 ($M^{+}\cdot$ - C_3H_7, 6), 159 ($M^{+}\cdot$ - tetrahydropyridinium, 20), 115 (15), 91 (tropylium, 80), 83 (tetrahydropyridinuim cation, 100), 68 (25).

N-Formylimidazole (71). A solution of dry formic acid (0.75 mL, 20 mmol) in 15 mL of dry THF was added dropwise to a solution of N,N'-carbonydiimidazole (3.2 g, 20 mmol) in 20 mL of dry THF under nitrogen with stirring. The reaction mixture was allowed to

stir for 1 hour and then the solvent was removed under reduced pressure. The resulting colorless oily residue was analyzed by ^1H NMR spectroscopy and used in the following reaction without further purification: ^1H NMR ($CDCl_3$) 9.15 (s, 1H C<u>H</u>O), 8.70 (s, 1H H-2), 8.15 (br, 1H, H-5), 7.45 (br, 1H, H-4).

1-(1-Phenylcyclohexyl)-1,2,3,4-tetrahydropyridinium-5-carboxaldehyde (69). The PCP-Im$^+$ClO$_4^-$ (**60**, 200 mg, 0.58 mmol) was suspended in 10 mL of water and 2 mL of saturated K_2CO_3 was added. The resulting mixture was extracted with methylene chloride (15 mL x 2) and the methylene chloride layer was dried (K_2CO_3) and filtered. The above crude formylimidazole (**71**, 1.5 mL, 10 mmol) was added to the methylene chloride solution. The reaction mixture was stirred at room temperature and monitored by GC/MS. At the end of the reaction (0.5 hour) the solvent was removed under reduced pressure. The crude product was purified by centrifugal chromatography with ethyl acetate as solvent and to yield 140 mg (89%) of pure product which was recrystallized from hexane:methylene chloride (3:1): mp 125-126°C; GC/MS (m/z, %) [GC temperature program: 125 °C for 1 minute followed by 25 °C/minute up to 275 °C (retention time 6.34 minute)] 269 ($M^{+\cdot}$, 15), 226 ($M^{+\cdot}$ - C_3H_7, 2), 159 (phenylcyclohexyl cation, 40), 111 (tetrahydropyridinium carboxaldehyde cation, 30), 91 (tropylium, 100); ^1H NMR ($CDCl_3$) 8.97 (s, 1H, C<u>H</u>O), 7.43 (s, 1H, olefinic proton), 7.37-7.25 (m, 5H, aromatic protons), 2.98 (t, 2H, H-2, J=5.5 Hz), 2.29 (t, 2H, H-4, J=5.3 Hz), 2.20 (m, 2H, equatorial protons of cyclohexyl, H-2' and H-6'), 2.02 (m, 2H, H_{ax}-2' and H_{ax}-6'), 1.7-1.4 (m, 8H, H-3 and rest of the cyclohexyl protons). Anal. Calcd for $C_{18}H_{23}NO$: C 80.36, H 8.62, N 5.21. Found: C 80.28, H 8.62, N 5.16.

Benzyl 1-(1-Phenylcyclohexyl)-1,2,3,4-tetrahydronicotinate (84). The PCP-Im$^+$ salt **60**·ClO$_4^-$ (200 mg, 0.58 mmol) was converted to its free base **64** which was dissolved in 20 mL of dry methylene chloride (dried by passing through a basic activated alumina column), and then several drops of benzyl chloroformate (excess) was added to the solution. The reaction mixture was

allowed to stir at room temperature for 3 days and was monitored by GC/MS and TLC. The reaction was stopped by removing the solvent under reduced pressure. The crude product was purified by centrifugal chromatography with hexane:methylene chloride (1:1) to yield 100 mg (49%) of an oil: GC/MS (m/z, %) [GC temperature program: 125 °C for 1 minute, then 25 °C/minute up to 275 °C (retention time 10.19 minute)] 375 ($M^{+}\cdot$, 30), 332 ($M^{+}\cdot$ - C_3H_7, 2), 268 (5), 217 (benzyl tetrahydronicotinate cation, 50), 159 (phenylcyclohexyl cation, 35), 126 (15), 110 (25), 91 (tropylium, 100), 83 (tetrahydropyridinium cation, 35); ^1H NMR ($CDCl_3$) 8.06 (s, 1H, deshield olefinic proton), 7.39-7.17 (m, 10H, aromatic protons), 5.20 (s, 2H, $OC\underline{H}_2Ph$), 2.84 (t, 2H, H-2), 2.31 (t, 2H, H-4), 2.26-2.21 (m, 2H, equatorial protons of cyclohexyl, H-2' and H-6'), 1.9-1.4 (m, 10H, H-3 and rest of the cyclohexyl protons).

Allyl 1-(1-phenylcyclohexyl)-1,2,3,4,-tetrahydronicotinate (85). The PCP iminium perchlorate (1.5 g, 4.39 mmol) was converted in methylene chloride to the corresponding PCP enamine **64** and then was treated with allyl chloroformate (530 mg, 0.47 mL, 4.39 mmol) by a syringe. The reaction mixture was stirred at room temperature overnight until no PCP enamine was observed on GC/MS. The solvent was removed under reduced pressure and the residue was subjected to chromatography (silica gel) with methylene chloride, methylene chloride:ethyl acetate (8:2) as the solvent systems. The first light yellow band which contained the product was collected as a light yellow oil (600 mg, 42%): ^1H NMR ($CDCl_3$) 8.02(s, 1H, H-6), 7.42-7.08 (m, 5H, aromatic protons), 6.02 (m, 1H, H-2') 5.35, 5.18 (d, two sets, 2H, H-3'), 4.68 (d, 2H, H-1'), 2.90 (t, 2H, H-2), 2.32 (t, 2H, H-4), 2.28 (m, 2H, two equatorial protons of cyclohexyl,), 1.8-1.5 (m, 10H, H-3 and rest of the cyclohexyl protons); GC/MS (m/z, %) [GC temperature program: 125 °C for 1 minute, then 25 °C/minute up to 275 °C (retention time 6.37 minute)] 325 ($M^{+}\cdot$, 20), 268 ($M^{+}\cdot$ - $OCH_2CH{=}CH_2$, 10), 167 (allyl tetrahydronicotinate cation, 50), 159 (phenylcyclohexyl cation, 30), 110 ($M^{+}\cdot$ - $OCH_2CH{=}CH_2$ - phenylcyclohexyl, 40), 91 (tropylium, 100).

Anal. Calcd for $C_{21}H_{27}NO_2 \cdot 2/3H_2O$: C 75.3, H 8.58, N 4.18. Found: C 75.88, H 8.32, N 4.20.

5-(1-Imidazoylcarbonyl)-1-(1-phenylcyclohexyl)-1,2,3,4-tetrahydropyridine (88). The PCP free base (3.45 g, 14.2 mmol) was dissolved in 60 mL of 5% HOAc and $Hg(OAc)_2$ (18.06 g, 56.8 mmol) was added. The resulting mixture was stirred under reflux overnight. The reaction mixture was cooled in an ice-water bath and the mercurous acetate precipitate was separated by suction filtration. With continued cooling, the filtrate was saturated with hydrogen sulfide and the resulting black mercuric sulfide was filtered and washed with 5% HOAc. The combined filtrates were stirred vigorously in a 1-liter Erlemmeryer flask with 50 mL of methylene chloride, while an excess 25% aqueous NaOH was added carefully in the cold. The methylene chloride layer was promptly separated, the aqueous solution was extracted with methylene chloride (25 mL) and the combined extracts were dried over $MgSO_4$. After filtering, the filtrate was transfer to another 250 mL round-bottom flask and carbonyldiimidazole (6.9 g, 42.6 mmol) was added to the solution. The reaction mixture was stirred at room temperature overnight and monitored by GC/MS until all of the starting material was consumed. The reaction mixture then was washed with water (100 mL x 2) to remove the by-product imidazole and the methylene chloride layer was dried with $MgSO_4$. After filtering and removing the solvent, the resulting solid was crystallized from ethyl ether to yield 2.15 g (45%) of off-yellow crystals: mp 145-146 °C; UV(MeOH) λ_{max} 317.5 (2300); ^1H NMR ($CDCl_3$) 8.0 (s, 1H, H-2'), 7.85 (s, 1H, H-5') 7.40 (s, 1H, olefinic proton of pyridine ring), 7.37-7.20 (m, 5H, aromatic protons), 7.05 (s, 1H, H-4') 3.05 (t, 2H, H-2, J=5.5 Hz), 2.50 (t, 2H, H-4, J=5.3 Hz), 2.25-2.00 (m, 4H, two equatorial protons of cyclohexyl, and two protons of H-3 on pyridine ring), 1.7-1.4 (m, 8H, rest of the cyclohexyl protons); GC/MS (m/z, %) [GC temperature program: 125 °C for 1 minute, then 25 °C/minute up to 275 °C (retention time of the corresponding methyl ester **89** is 11.63 minute)] 299 ($M^{+}\cdot$, 15), 268 ($M^{+}\cdot$ - OCH_3, 7), 159 (phenylcyclohexyl cation, 30), 141 (methyl tetrahydronicotinate

cation, 90), 126 (15), 110 (20), 91 (tropylium, 100). Anal. Calcd for $C_{21}H_{25}N_3O$: C 75.19, H 7.51, N 12.53. Found: C 75.10, H 7.55, N 12.45.

1-(1-Phenylcyclohexyl)-1,2,3,4,-tetrahydronicotinic acid (82). The allyl 1-(1-phenylcyclohexyl)-1,2,3,4,-tetrahydronicotinate (140 mg, 0.43 mmol) was dissolved in dry acetonitrile (15 mL) and then sodium iodide (129 mg, 0.86 mmol) was added. To the above solution was added chlorotrimethylsilane (93 mg, 0.11 mL, 0.86 mmol) and the reaction mixture was allowed to stir at room temperature overnight until no starting material was observed by GC/MS. The solvent was removed under reduced pressure to yield a dark brown residue which was redissolved in 25 mL of methylene chloride. The methylene chloride layer was washed with 5% acetic acid, dried over $MgSO_4$ and the residue obtained after removing the solvent was purified by silica gel PTLC with methylene chloride/ethyl acetate/methanol (10/50/5) as a the solvent. No desired product was obtained.

Preparation of Rat Brain and Liver Subcellular Fractions. The livers and brains of male Sprague-Dawley rats (150-200 g) were used for the preparation of tissue fractions. All buffers were bubbled with N_2 just prior to use. Animals were euthanized by exposure to CO_2. The rat whole brains were removed, chilled on ice, weighed and perfused in situ with 15 mL of 0.25 M sucrose-0.05 M Tris.buffer (pH 7.4). The tissues were minced and homogenized in 3 volumes of this buffer with a Teflon-glass homogenizer, and the resulting homogenates were subjected to centrifugation at 700 g for 10 minutes. The resulting supernatant (S_1) fractions were centrifuged further at 10,000 g for 20 minutes. The 10,000 g (P_2) pellet was resuspended in 3 volumes of the sucrose-Tris buffer and recentrifuged at 10,000 g for 20 minutes. The P_2 was then resuspended in 3 volumes of 0.1 M phosphate buffer (pH 7.4) to yield the mitochondrial fraction. Rat liver fractions were prepared similarly.

Protein Assay. Protein concentrations were measured according to Lowry et al.[86] The protein concentrations of the homogenates are 5.4 mg/mL (Brain) and 6.9 mg/mL (Liver), respectively.

Incubations of Phencyclidine Iminium Perchlorate 60. Phencyclidine iminium perchlorate (0.2 mM, total volume 3 mL) was incubated in the presence of rat brain and liver mitochondrial fractions (about 5 mg protein/mL) at 37 °C for up to 2 hours in potassium phosphate buffer (0.1 M, pH 7.35). Control incubations were run in the absence of the tissue homogenate fraction and absence of the substrate as well as with denatured homogenate preparation. At designated time points, 0.1 mL of NaOH (0.1 N) was added to convert the remaining phencyclidine iminium species to the corresponding phencyclidine enamine. After a brief centrifugation to remove precipitated protein, the mixtures were extracted with 2 x 10 mL methylene chloride. The combined extracts were dried (Na_2SO_4), evaporated to near dryness, and the residues reconstituted in methanol (200 μL) for GC/MS analysis.

STUDIES ON PRODRUGS

4.1. Background

The effective design of prodrugs through a consideration of enzyme-substrate specifities requires considerable knowledge of the target enzyme or enzyme system. In addition to substrate selectivity, the type of reaction catalyzed, the enzyme distribution and level, and the functional role of the enzyme in the cellular biochemistry should be known. The necessary conversion or activation of prodrugs to potential pharmacologically active drug molecules in the body can take place by a variety of reactions. The most common prodrugs are those requiring a hydrolytic cleavage mediated by esterases and amidases. Active drug species containing carboxyl groups can often be converted to ester prodrug from which the active forms are regenerated by esterase within the body. In other cases, active drug substances are regenerated from their prodrugs by biochemical reductive or oxidative process.[87] Given that a drug has a free carboxyl, amino or hydroxyl group, the corresponding ester, carbamate or carbonate can be made so as to alter the physical properties in a desired direction from that of the parent drug.

The design of site-specific and sustained amine releasing prodrugs for delivery to the brain has been developed recently by Bodor and coworkers.[88] Several amines of pharmacological interest are not sufficiently lipophilic to be able to pass the blood-brain barrier in their protonated form. By linking such drugs to a lipophilic dihydropyridine carrier through an amide linkage the derivative obtained, **94**, is distributed quickly throughout the body, including the brain, following its administration. The dihydro derivative **94** is then rapidly oxidized in the brain to the quarternary salt **95** which, because of its ionic character, is eliminated rapidly from the body except from the brain. Slow enzymatic cleavage in the brain of the amide linkage to form **96** and **97** then result in a sustained delivery of the drug species **97** in the brain.

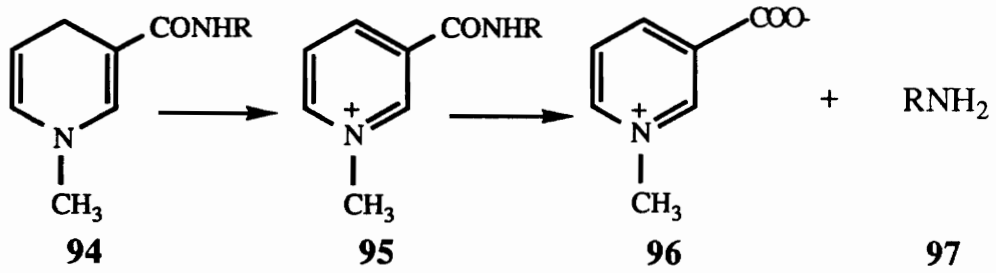

94 **95** **96** **97**

Scheme 29. An example of a prodrug system targeted to brain tissues.

This idea leads to the possibility of targeting polar amine drugs to the brain. This approach, however is not enzyme specific nor does it target specific cells. The studies summarized below explore the possibility of prodrug design which targets monoamine oxidase as the bioactivating enzyme. Since specific cell types are especially rich in monoamine oxidase A or B, this approach to prodrug design has the attractive feature of a high degree of regioselectivity with respect to the mammalian central nervous system.

Recently, the cyclic tertiary allylamine 1-methyl-4-phenyl-1,2,3,6-tetrahydropyridine (MPTP, **98**) has been characterized as a selective neurotoxin that is responsible for a Parkinsonism-like syndrome in humans.[89] This compound also causes a movement disorder similar to Parkinson's disease in nonhuman primates which is accompanied by selective destruction of dopaminergic neurons in the substantia nigra and a loss of dopamine terminals from the striatum.

Studies by various researchers have since shown that MPTP is not the actual cause of cell death and that MPTP must be activated before it exerts its neurotoxic actions. Langston et al[90] hypothesized that MPTP might be converted to the 1-methyl-4-phenylpyridinium species MPP^+ (**99**) *in vivo* since a similar conversion for dihydropyridines had been reported by Bodor et al[88] To test this hypothesis, squirrel monkeys were injected with MPTP and sacrificed several days later. The brain homogenates were then examined for MPTP. None was found initially but after sodium

borohydride reduction, which reduces MPP^+ to MPTP, large amounts were found. This finding supported their proposal. Later a study using dopaminergic neuron culture also proved that MPTP does not destroy the cells but that MPP^+ does.[91] It became apparent as the investigation of MPTP continued that MPTP is converted to MPP^+ in a two-step reaction via the intermediate dihydropyridinium derivative **100**.[92] It was confirmed that MPTP is first oxidized to the 1-methyl-4-phenyl-2,3-dihydropyridinium species $MPDP^+$ (**100**) in a reaction catalyzed by MAO-B. This intermediate **100** was first isolated as the 6-cyano adduct **101** by Castagnoli's group.[93] MPP^+, being a positively charged molecule, is unable to cross the blood-brain barrier (BBB) and must therefore be formed within the brain. It was demonstrated that monoamine oxidase B (MAO-B) and to a lesser extent MAO-A as well as P-450IIB1 and P-450IA1[94] catalyze the oxidation of MPTP to $MPDP^+$, which then undergose further oxidation to form MPP^+.[95] $MPDP^+$ is not stable; standing in buffer at pH = 7.4 it will chemically disproportionate to give MPTP and MPP^+.

As stated in the introduction section, MAO is localized in the outer mitochondrial membrance and exists in two forms: A and B. Although they are similar, certain selectivities for substrates and inhibitors are known. In the brain MAO-A is localized in catecholamine neurons and the B form is more concentrated in serotonergic neurons and the surrounding glial cells.[26] MPTP behaves as a time-dependent irreversible inhibitor as well as a substrate for MAO-B, which will limit the production of MPP^+.[96]

Although there will be competing microsomal and mitochondrial systems for the metabolism of MPTP in the liver, it appears that in brain only the MAO is involved in the bioactivation of MPTP.[97] The dominant role of MAO-B in this process was established by the observations that selective inhibitors of that form of the enzyme, but not inhibitors of MAO-A, protect against the toxic effects of MPTP.[98] MAO can also catalyze the conversion of the dihydropyridine intermediate $MPDP^+$ to MPP^+ although this reaction can also occur non-enzymatically.[99, 100] Additional requirements for toxicity include the active transport of the corresponding

pyridinium metabolite first into the striatal nerve terminals via the DA uptake system[101] and then into the inner mitochondrial membrane[102] where it must inhibit mitochondrial respiration.[103] As might be expected, many compounds related to MPTP are not neurotoxic because they are (a) not substrates for MAO-B, (b) the resulting dihydropyridinium species is not converted to the corresponding pyridinium species, (c) the pyridinium species is not a substrate for the dopamine transporter, or (d) the pyridinium species is not an inhibitor of mitochondrial respiration.

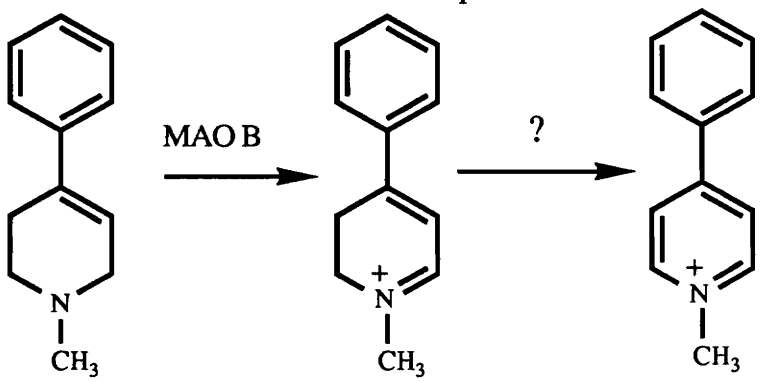

98 **100** **99**

Scheme 30. Metabolic pathway of MPTP to MPP^+.

In the central nervous system the selectivity of MPTP towards dopaminergic nerves presumably is due to the absence of an active uptake of MPP^+ into other types of nerve endings since MPP^+ is unselective as an inhibitor of mitochondrial respiration.[102] The existence of alternative metabolic pathways for MPTP in liver presumably also contributes to the insensitivity of peripheral tissues to potential cytotoxic effects of MPP^+.

A number of MPTP analogs has been prepared in order to evaluate their neurotoxicity. Extensive structure-MAO substrate activity studies have established that only those 1,2,3,6-tetrahydropyridine derivatives bearing a lipophilic C-4 substituent and an N-methyl group are likely to be good MAO substrates.[104] Some structural features are recognized as essential for MAO substrates:[105]

A) The 4,5 double bond is essential for compounds to be MAO substrates.[106]

B) The substitution of alkyl groups in the tetrahydropyridine ring diminishes reactivity towards MAO.[107]

C) The N-methyl group is essential for activity; compound with larger N-substitutents are not substrates.[104]

D) The phenyl ring is not necessary for a compound to be an MAO substrate; for example, replacement of the phenyl ring by a benzyl group enhances MAO activity.[108]

E) Substitution of a methyl, ethyl, fluoro, or trifluoromethyl group in position 2 of the phenyl ring enhances reactivity towards MAO.[109]

Youngster et al[104] have reported that the 4-benzyl analog BMTP [4-benzyl-1-methyl-1,2,3,6-tetrahydropyridine, (**102**)] of MPTP is oxidized in the presence of MAO-B, presumably to yield the corresponding dihydropyridinium species $BMDP^+$ (**103**). Thus, BMTP's biological activity was of great interest to researchers. Administration of BMTP to C57 black mice at 10 times MPTP's toxic dose, however, failed to cause symptoms and neurotoxicity associated with MPTP.[110] Subsequent studies have shown that the suspected pyridinium metabolite BMP^+ (**104**) like the MPP^+ (**99**) inhibits mitochondrial respiration and therefore might be expected to display MPP^+-type neurotoxic properties. The I_{50} values for MPP^+ and BMP^+ with the submitochondrial particles were approximately the same while the concentration for BMP^+ was approximately three times higher for the intact mitochondria.[111] Also, intracerebral microdialysis showed BMP^+ to be neurotoxic although not as toxic as MPP^+. The MPP^+ challenge following initial MPP^+ exposure caused a 150% dopamine release over basal values while the BMP^+ exposure led to a 390% increase.[112] So if BMTP is a substrate for MAO-B and BMP^+ is neurotoxic, why doesn't administration of BMTP cause a parkinsonian syndrome?

The answer to this question was addressed recently by Naiman et al[113] in which mitochondrial preparations and purified MAO-B were used to catalyze the oxidation of BMTP and the incubation mixtures were examined for the amounts of pyridinium product

formed. The conclusion drawn from ^1H NMR spectra was that once the dihydropyridinium metabolite **103** forms, a benzylic proton may be lost to give the exocyclic dienamine **105**. The exocyclic dienamine can protonate to yield $BMDP^+$ or the iminium species **106**. Therefore, on the basis of proton exchange behavior observed in the ^1H NMR spectra, it seems likely that $BMDP^+$ is in equilibrium with the exocyclic dienamine and isomeric iminium species **106** (Scheme 31). The conversion to **104** is, therefore, minimized.

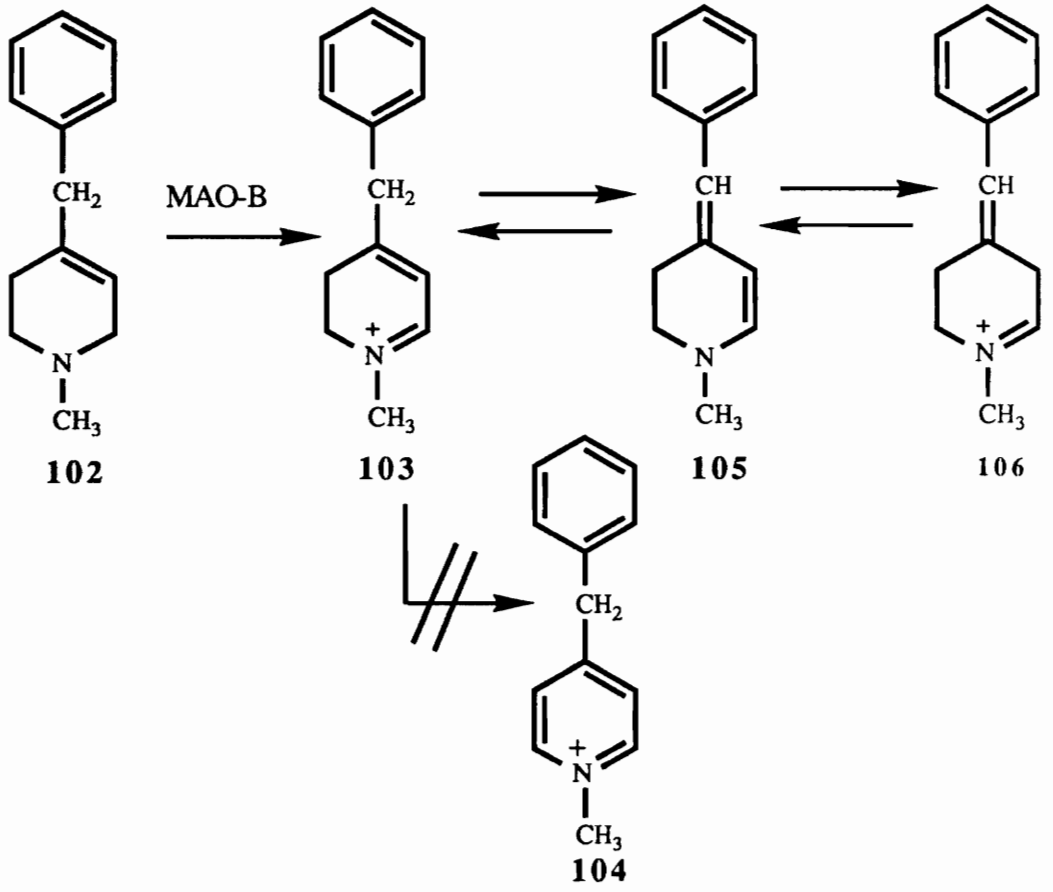

Scheme 31. Proposed equilibria of $BMDP^+$.

The excellent substrate properties of the 4-benzyl analog of MPTP plus the variability of substituents at C-4 which is tolerated by the enzyme suggested that novel MPTP analogs might be designed in which the CH_2 group of BMTP is replaced with a heteroatom such as N, O, or S. For example, the phenoxy compound **107** has similar special features to those of the benzyl analog but with no acidic

benzylic hydrogen atoms. If it were a substrate for MAO-B, such a compound would yield the phenoxydihydropyridinium metabolite **108** that would not suffer from the difficulties of the corresponding benzyl compound **102**.

Studies on the 4-phenoxy analog **107** (1-methyl-4-phenoxy-1,2,3,6-tetrahydropyridine, MPOTP) of MPTP showed that it displayed properties similar to those of BMTP in term of its excellent MAO-B substrate characteristics. This analog was converted rapidly to the corresponding dihydropyridinium product, the 1-methyl-4-phenyloxy-2,3-dihydropyridinium species **108**. *In vivo*, however, **107** proved to be not neurotoxic.[114]

The reason why **107** showed no toxicity is that although it is a very good substrate for MAO-B and is converted to the phenoxy-dihydropyridinium metabolite **108**, this product is not metabolyzed further to the neurotoxic pyridinium metabolite **109** but rather is rapidly hydrolyzed via intermediate **110** (Scheme 32) to form phenol **112** and the 2,3-dihydro-1-methylpyrid-4-one (**113**). These observations have led to the development of a prodrug concept based on the design of tetrahydropyridine derivatives bearing an appropriate leaving group at C-4 that will be hydrolytically 'released' following MAO catalyzed oxidation to give the corresponding dihydropyridinium metabolite.

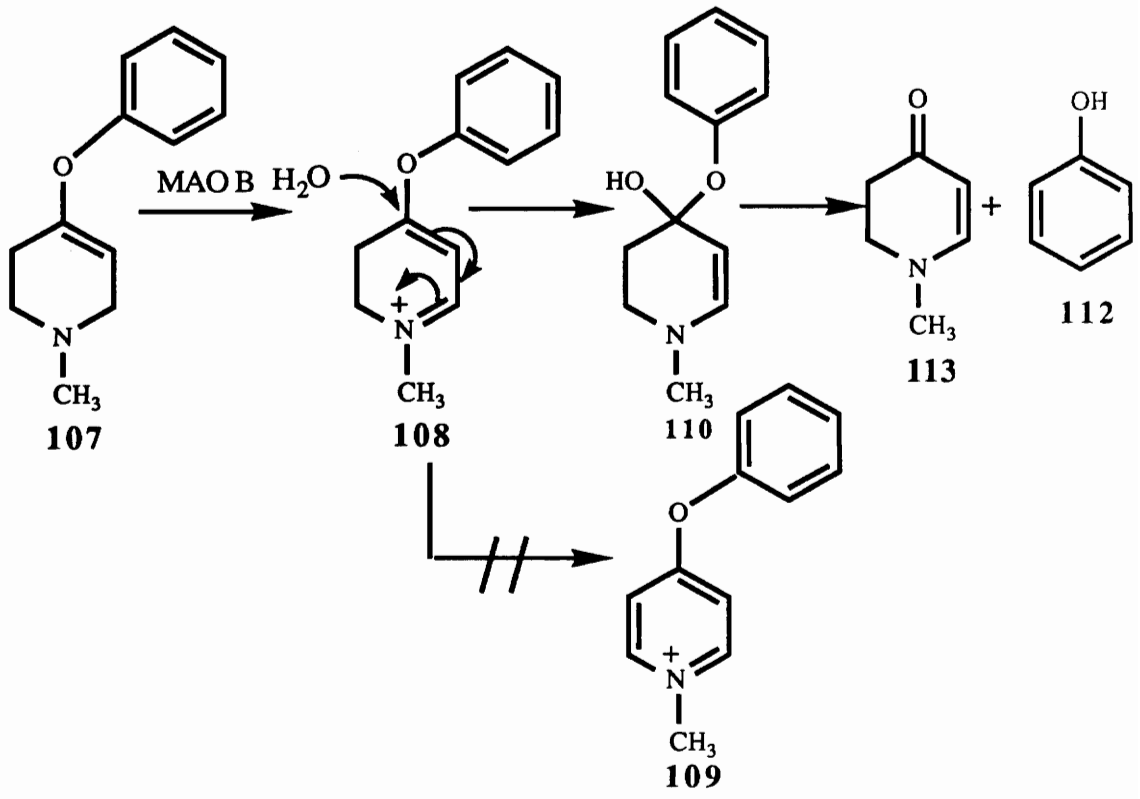

Scheme 32. Proposed mechanism for hydrolysis of MPODP+.

4.2. Research Proposal

If the substituents at the C-4 position of the tetrahydropyridine ring are good leaving groups, the resulting compounds will be of interest since they will give us the opportunity to investigate further the structural requirements for MAO substrates with appropriate substituents. This metabolic scheme may be exploited to develop 'prodrugs'. Pharmacologically active species could be selectively delivered to MAO-B containing cells (where following conversion to the dihydropyridinium intermediate, the drug would be released by hydrolytic cleavage) thereby targeting the action of the drug. In view of these considerations, we have undertaken a study to synthesize potential MAO-B substrate analogs which might serve as model compounds to evaluate this concept. The proposed pathway is generalized in Scheme 33. A wide variety (amines, alcohols, thiols, and acids) of functional groups conceivably could be accommodated by this system. Key issuers concern whether or not C-4 carbonyloxy substituted tetrahydropyridines (**A**) will be substrates for MAO-A and/or MAO-B and whether or not the corresponding dihydropyridinium metabolites **B** will undergo hydrolysis via **C** to yield the aminoenone (**112**) and desired drug **D**.

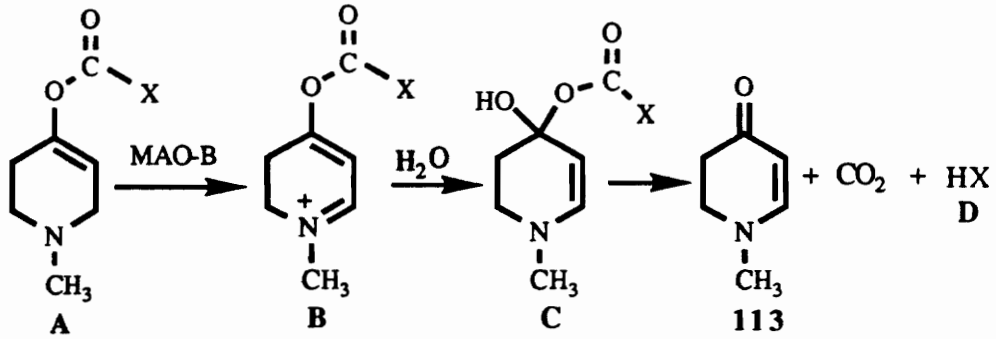

Scheme 33. Proposed pathway for releasing of the tetrahydropyridine prodrugs.

4.3. Results and Discussion

4.3.1. Syntheses

The studies summarized below address these issuers using simple 4-benzoyloxy derivatives of 1-methyl-1,2,3,6-tetrahydropyridine (BOMTP, **114**) as simple model compounds. The proposed initial approach involved reaction of the enolate **117** derived from 1-methyl-4-piperidone (**115**) with an appropriate benzoylating regent. A variety of reagents were used in our attempts to generate **117** (n-BuLi, t-BuLi, PhLi, and LDA), but we failed to detect any of the corresponding products.

The second effort was to synthesize the known compound 1-methyl-1,2,3,6-tetrahydro-4-(trimethylsilyloxy)pyridine (**116**),[115] which was reported to react directly with electrophiles to form *C*-alkylation products. Previous studies also have established[115a] that treatment of compound **116** with methyllithium would subsequently form the corresponding enolate anion **117** which is required for the following reaction. We expected that treatment of the resulting enolate anion with benzoic anhydride and other electrophiles would hopefully form a variety of the desired *O*-alkylation products (Scheme 34). 1-methyl-4-piperidone (**115**) was first distilled over P_2O_5 and then was treated with chlorotrimethylsilane and triethylamine in 1,4-dioxane under reflux for 3 days. After purification by extraction and distillation under vacuum, the expected product **116** was obtained as a light yellow oil. The GC/MS (Fig. 50) of the product showed an intense molecular ion at m/z 185 and an even more intense fragment ion at m/z 184 (100) which probably resulted from loss of a proton on the carbon atom adjacent to the nitrogen atom to form the dihydropyridinium cation **120**. The fragment ion at m/z 170 was derived from loss of a methyl group from the molecular ion and the key diagnostic fragment ion at m/z 96 resulted from the formation of 1-methyl-1,2,3,6-tetrahydropyridinium cation **121**.

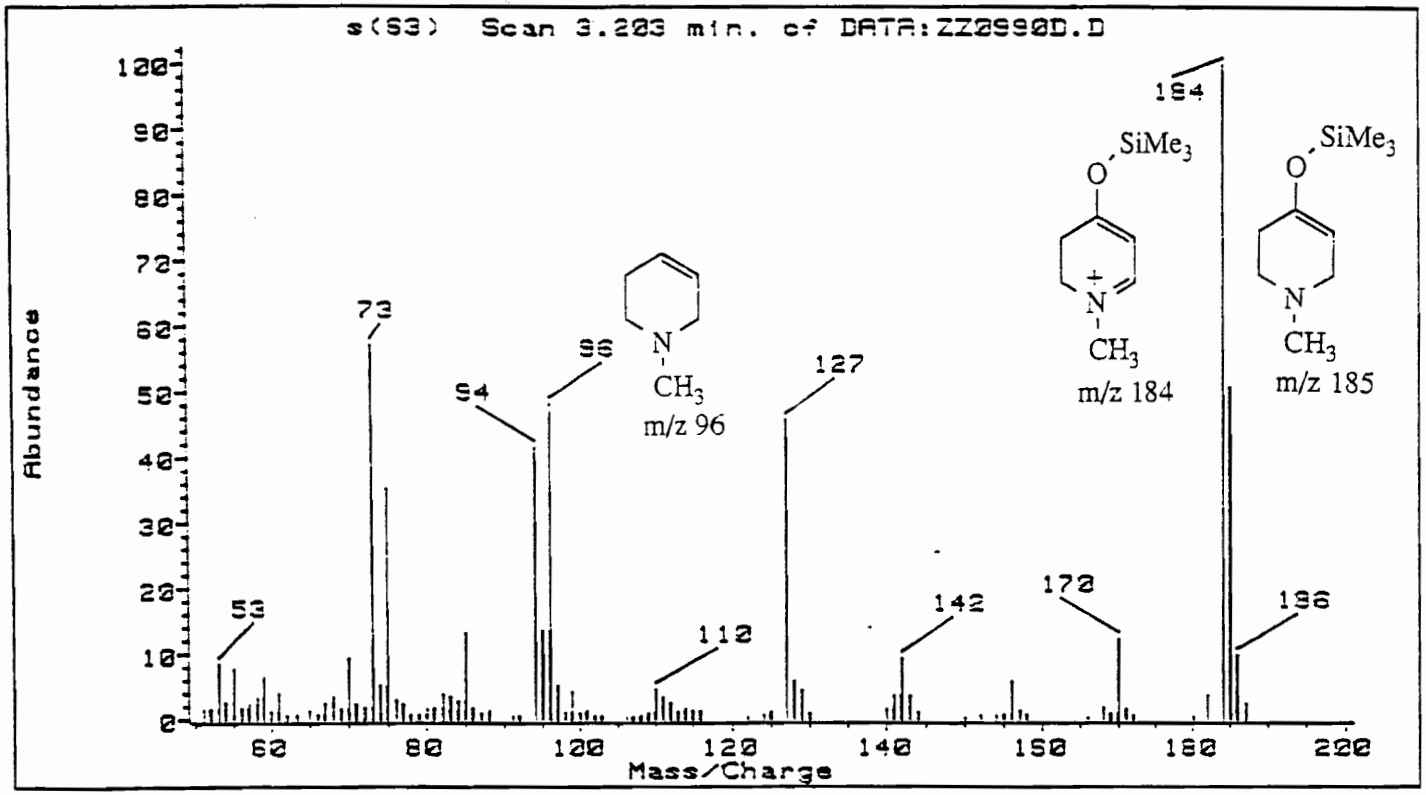

Figure. 50. GC/EIMS of 1-Methyl-4-trimethylsilyloxy-1,2,3,6-tetrahydropyridine.

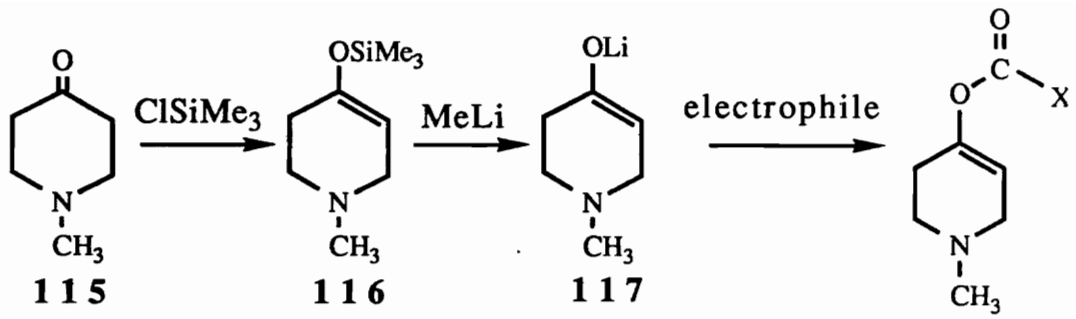

Scheme 34. Proposed synthetic pathway to potential model prodrugs.

The ^1H NMR spectrum of the product showed a triplet centered at 4.75 ppm (C-5 olefinic proton signal). The doublet at 2.85 ppm was assigned to the two protons on C-6 and the triplet centered at 2.48 ppm was assigned to the two C-2 protons. The N-methyl protons appeared as a sharp singlet at 2.26 while the signal of two C-3 protons was observed at 2.12 ppm. Finally, the trimethylsilane protons, as expected, recorded at 0.1 ppm. All signal assignments are consistent with the literature report.[115]

The 1-methyl-1,2,3,6-tetrahydro-4-(trimethylsilyloxy)pyridine was then converted to the corresponding enolate anion **117** with methyllithium in dry THF solution. Treatment of this enolate with benzylisocyanate, however, gave the cyclic trimer of benzylisocyanate as the only isolable product. The structure of the trimer was confirmed by ^1H NMR spectroscopy and GC/MS. The GC/EI mass spectrum showed an intense molecular ion at m/z 399. It seems likely that trimer formation was probably due to that the reactivity of benzylisocyanate in the presence of a strong base e.g. methyl anion.

The reaction of benzylisothiocyanate with the enolate anion **117** led to the formation of a yellow solid. The GC/MS (Fig. 51) of the solid showed a molecular ion at m/z 262, which was expected for the desired product. Also present are intense fragment ions at m/z 261 and m/z 260, which probably resulted from subsequent loss of protons. The ^1H NMR spectrum, however, indicated that the solid was not the expected product **122** because there was no proton

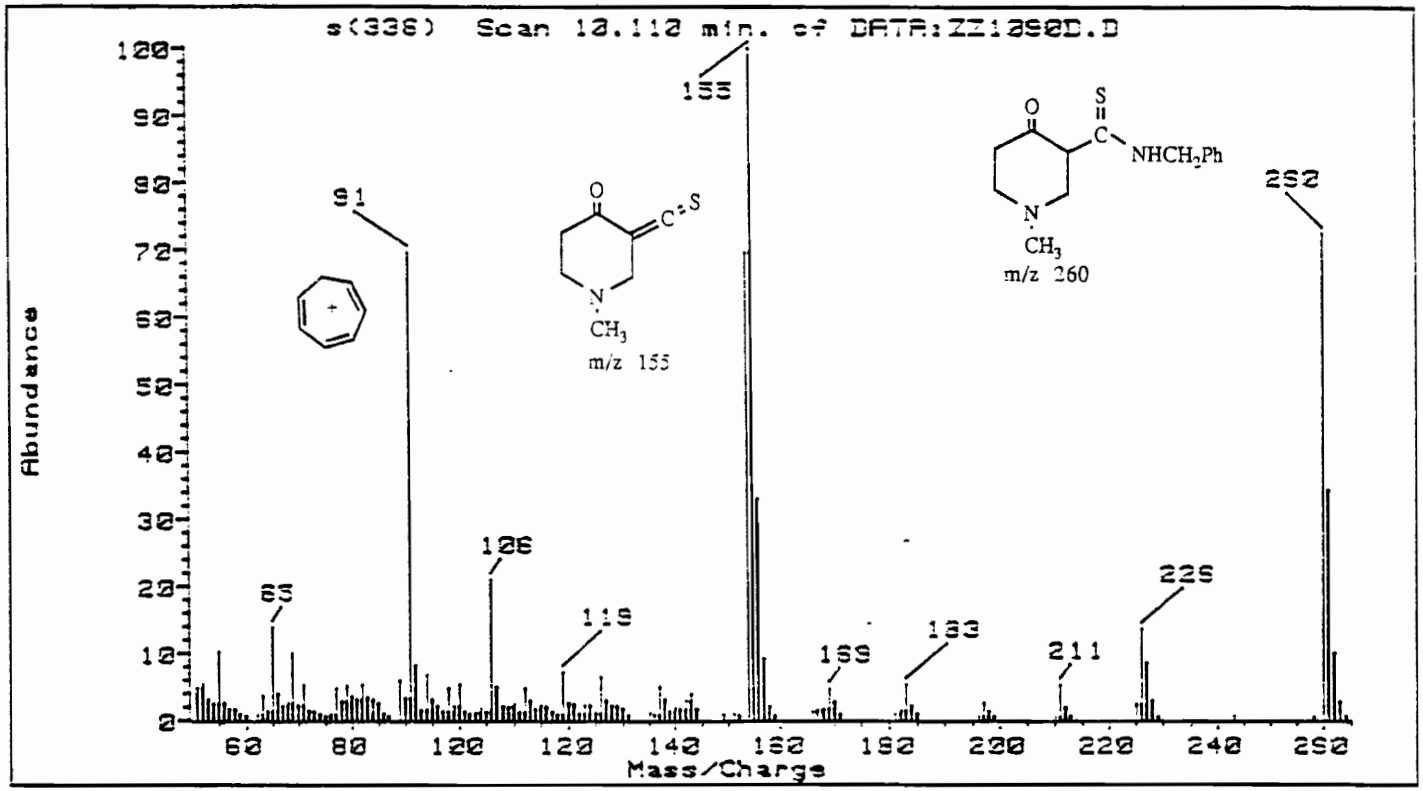

Figure. 51. GC/EIMS of 3-Benzylaminocarbonyl-1-methyl-4-piperidone.

signal in the region between 4-5.5 ppm which was expected for the olefinic proton. The tentative structure **123** was proposed. *C*-alkylation instated of *O*-alkylation would generate **123**.

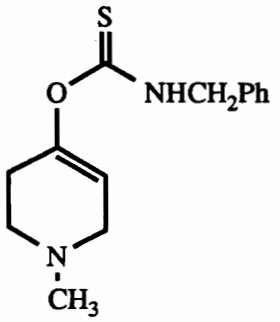

122

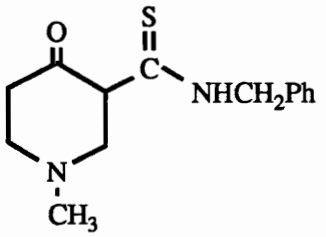

123

Full characterization of this C-alkylation product was not achieved since it decomposed when heated in the drying pistol.

Reaction of the enolate **117** with the carbonyldiimidazole formed a yellow solid. GC/MS analysis (Fig. 52) of a methanol solution of the solid showed a molecular ion at m/z 171, which was expected for the corresponding methyl ester. The fragment ion **126** at m/z 156 was derived from loss of a methyl group from the molecular ion. The two intense fragment ions present at m/z 138 and m/z 112 were assigned to the ions resulting from expulsion a methoxy group and to a piperidone analog, respectively (Fig. 52).
This type replacement of imidazole by methoxy group was confirmed by using ethanol as the solvent to prepare the GC/MS sample instead of methanol. On GC/EI mass spectrum (Fig. 53) of the corresponding ethyl ester **127** gave a molecular ion at m/z 185 and a fragment ion **126** at m/z 156 which was derived by loss of an ethyl group. The rest of the fragmentation of the ethyl carbonate on GC/EI mass spectrum were identical with that of the methyl ester **125**. As was the case with benzylisothiocyanate, there was no olefinic proton signal at 4.0-5.5 ppm on the ^{1}H NMR spectrum. Therefore, the solid **124** formed in this reaction probably was also a *C*-alkylation by-product with a tentative structure as follows. Full characterization of this by-product was not achieved because no pure product was isolated.

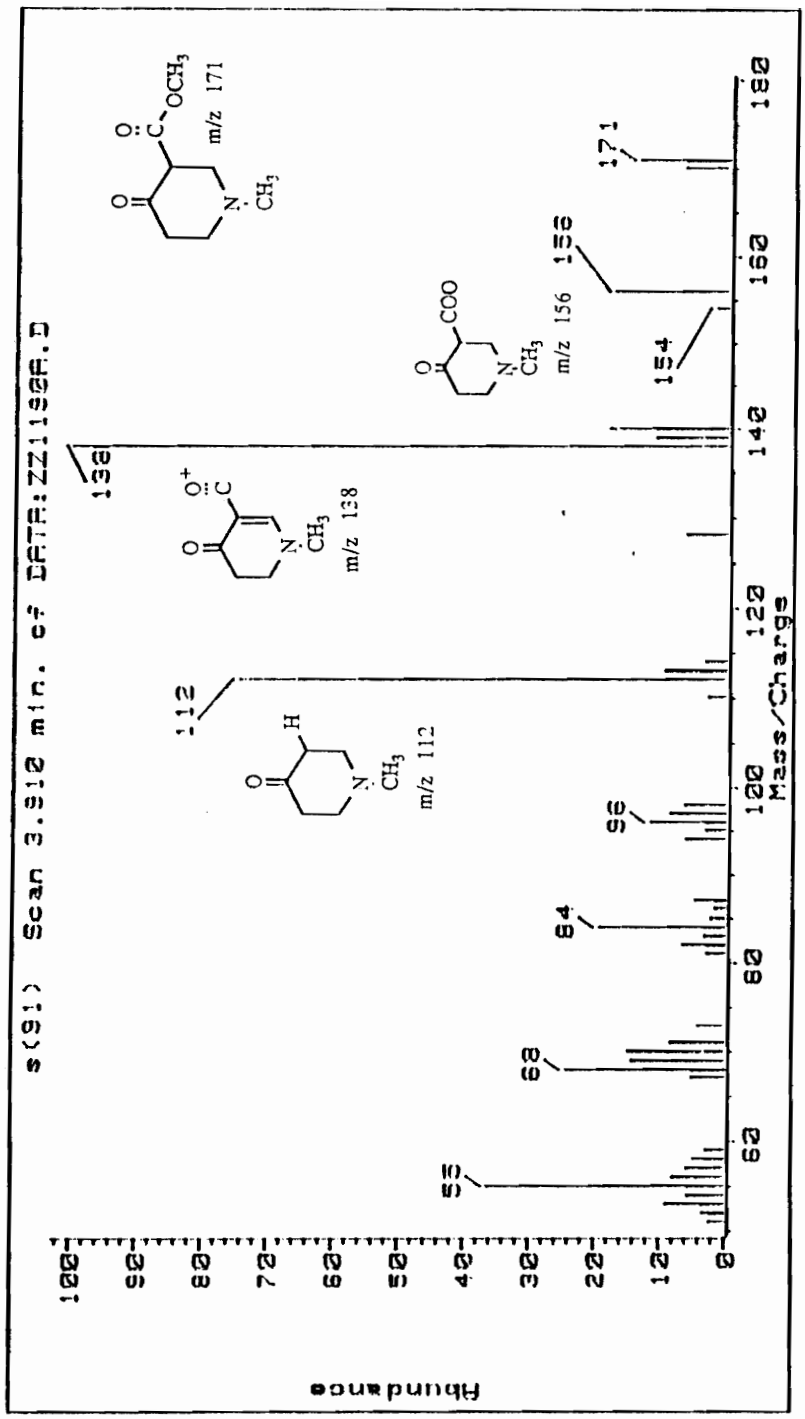

Figure. 52. GC/EIMS of 3-Methoxycarbonyl-1-methyl-4-piperidone.

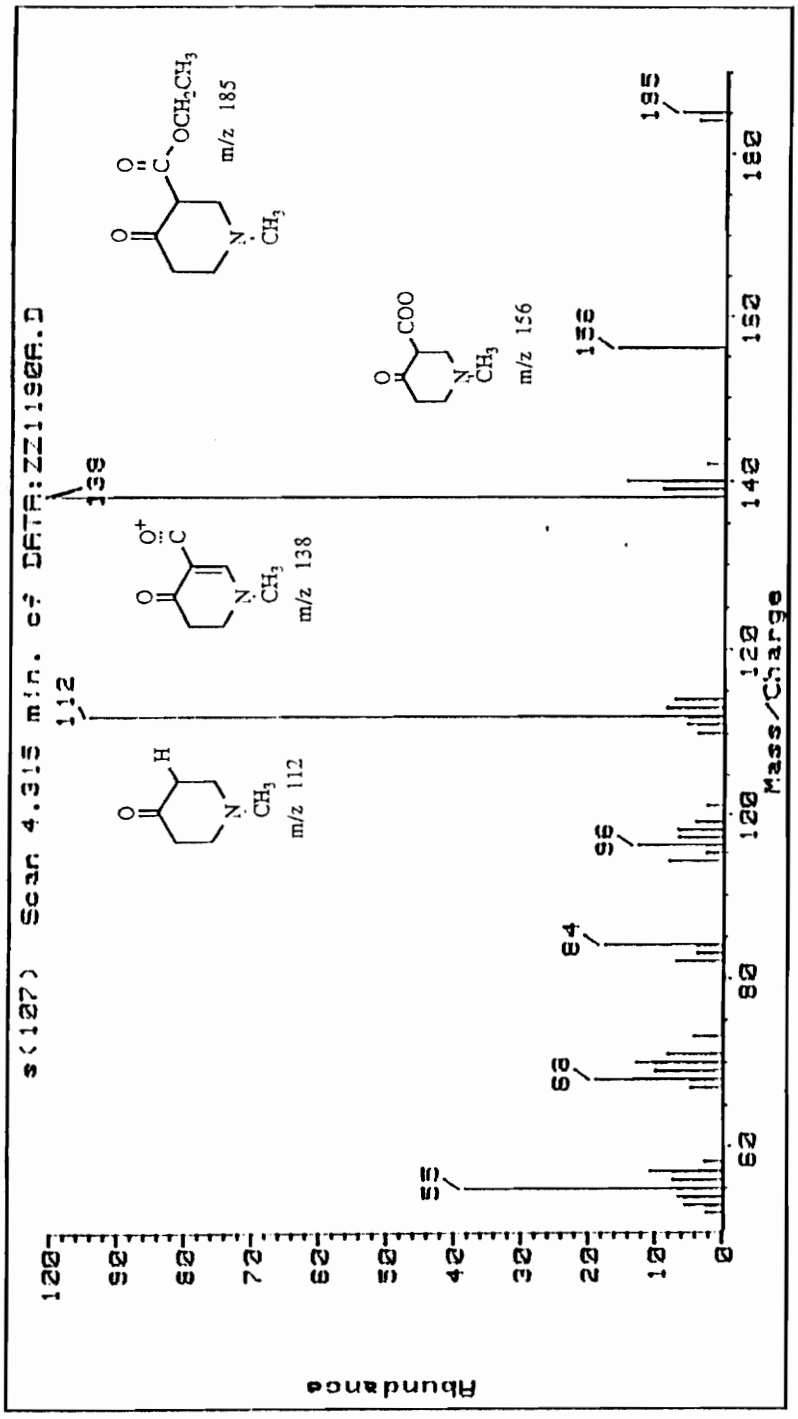

Figure. 53. GC/EIMS of 3-Ethoxycarbonyl-1-methyl-4-piperidone.

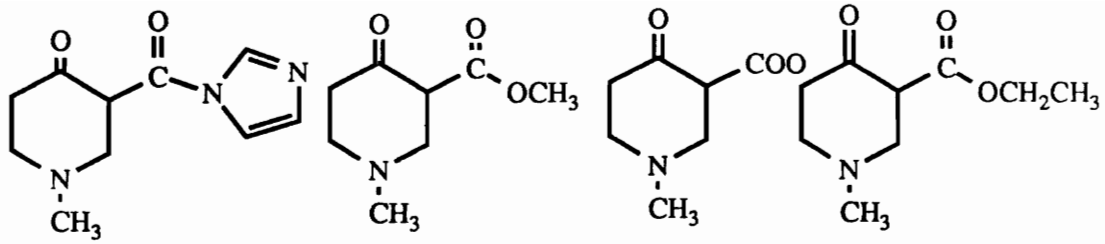

124 **125** **126** **127**

Based on the results of the above reactions, we were faced with the problem of an ambident anion undergoing selective *C*-attack instead of the desired *O*-attack. In many cases solvent is known to influence such reactions.[116] The freer the nucleophile, the more likely it is to attack with its more electronegative atom. Tight ion pairs tend to favor attack by the less electronegative atom. In polar, aprotic solvents the nucleophile is not greatly solvated but these solvents are very effective in solvating cations. Thus in a polar aprotic solvent the more electronegative end of ambident nucleophile is less encumbered. Thus a change to a polar, aprotic solvent often increases the extent of attack by the more electronegative atom.[116]

In an attempt to explore the potential effects of such a polar, aprotic solvent, a solution of the enolate **117** prepared as usual in dry THF solution was further diluted with hexamethyl-phosphoramide (HMPA) and the resulting solution was treated with benzoic anhydride.[117] After purification by centrifugal chromatography on silica gel, a light yellow crystalline solid which proved to be desired 4-benzoyloxy-1-methyl-1,2,3,6-tetrahydro-pyridine product (**114**), was obtained.

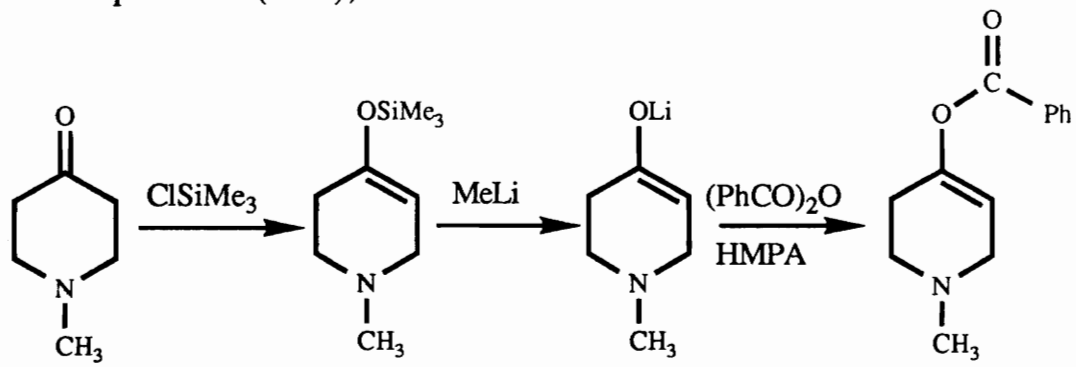

115 **116** **117** **114**

Scheme 35. Synthetic pathway (A) leading to BOMTP (**114**).

The GC/MS (Fig. 54) of the product showed a parent molecular ion at m/z 217 and a base peak at m/z 105 (100) which resulted from the formation of a benzoyl cation **128** by loss of a 1-methyl-4-oxy-1,2,3,6-tetrahydropyridinium unit from the parent ion. The fragment ion of 1-methyl-4-oxy-1,2,3,6-tetrahydropyridinium cation **129** was observed at m/z 112 as well as the fragmentation **130** at m/z 96 which is derived from loss of the benzoyloxy moiety **131** from the molecular ion **114**. The key diagnostic fragment ion **130** appeared at m/z 96. Only the *O*-alkylation product could form this fragment ion which distinguished this product from the isomeric *C*-alkylation product.

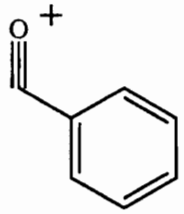

128

The ^1H NMR spectrum (Fig. 55) of compound **114** showed a triplet centered at 5.52 ppm which is assigned to the olefinic proton on C-5 of the tetrahydropyridine ring. The doublet at 3.12 ppm is assigned to the two protons on C-6 and the triplet centered at 2.72 ppm to the two C-2 protons. The signal for the N-methyl protons was recorded as a sharp singlet at 2.42 ppm while the signal of the two C-3 protons overlapped with the N-methyl signal at 2.42 ppm. Finally, the aromatic protons, as expected, appeared at 8.15-8.05 ppm and 7.65-7.42 ppm.

The overall yields in the above pathway were only moderate and hence an alternative route to the **114** was sought. The alternative synthetic pathway starts with commercially available 4-hydroxypyridine (**132**) which upon reaction with benzoic anhydride forms the corresponding 4-benzoyloxypyridine (**133**), a known compound.[118] Treatment of **133** with iodomethane would give the corresponding novel compound 4-benzoyloxypyridinium iodide (**134**) which upon treatment by $NaBH_4$ would be expected to form

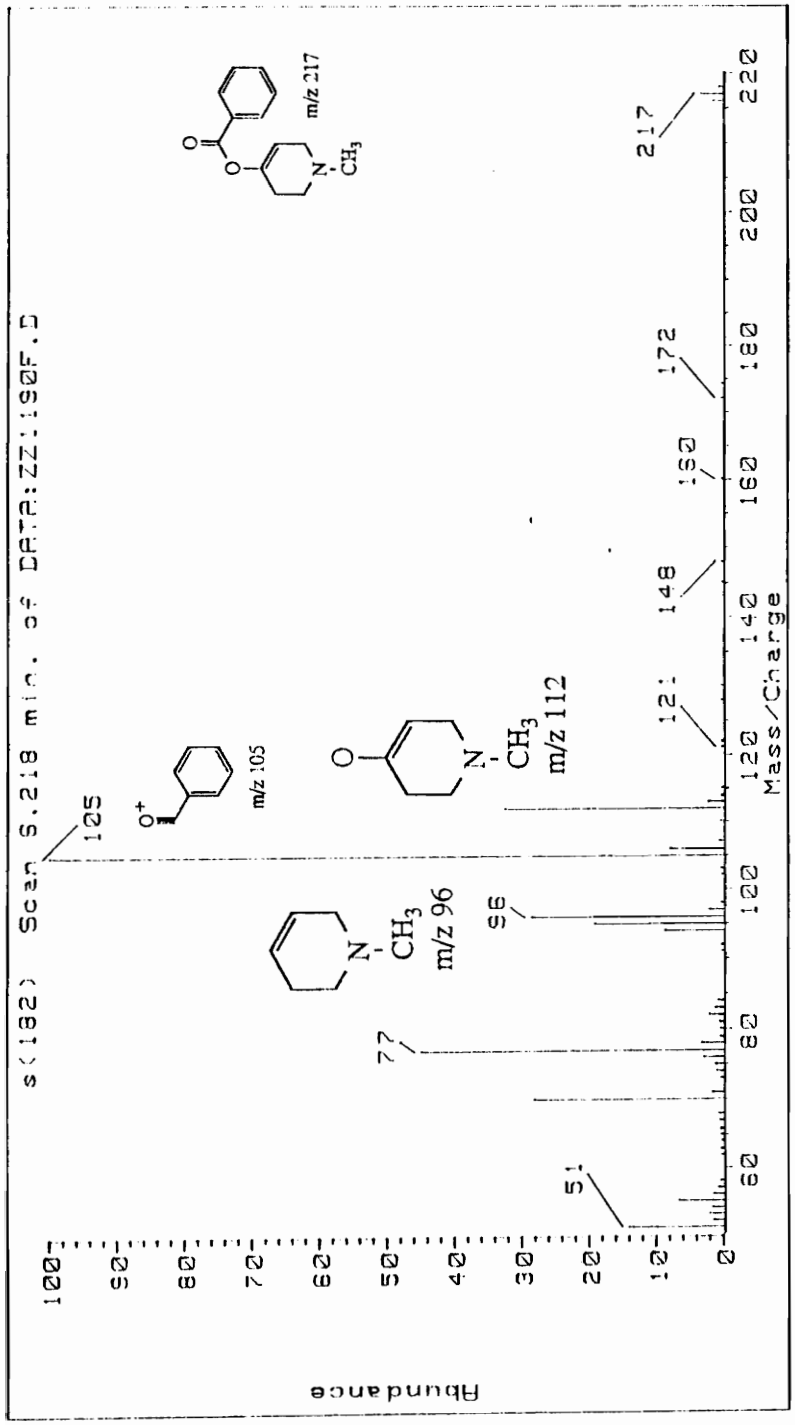

Figure. 54. GC/EIMS of 4-Benzoyloxy-1-methyl-1,2,3,6-tetrahydropyridine.

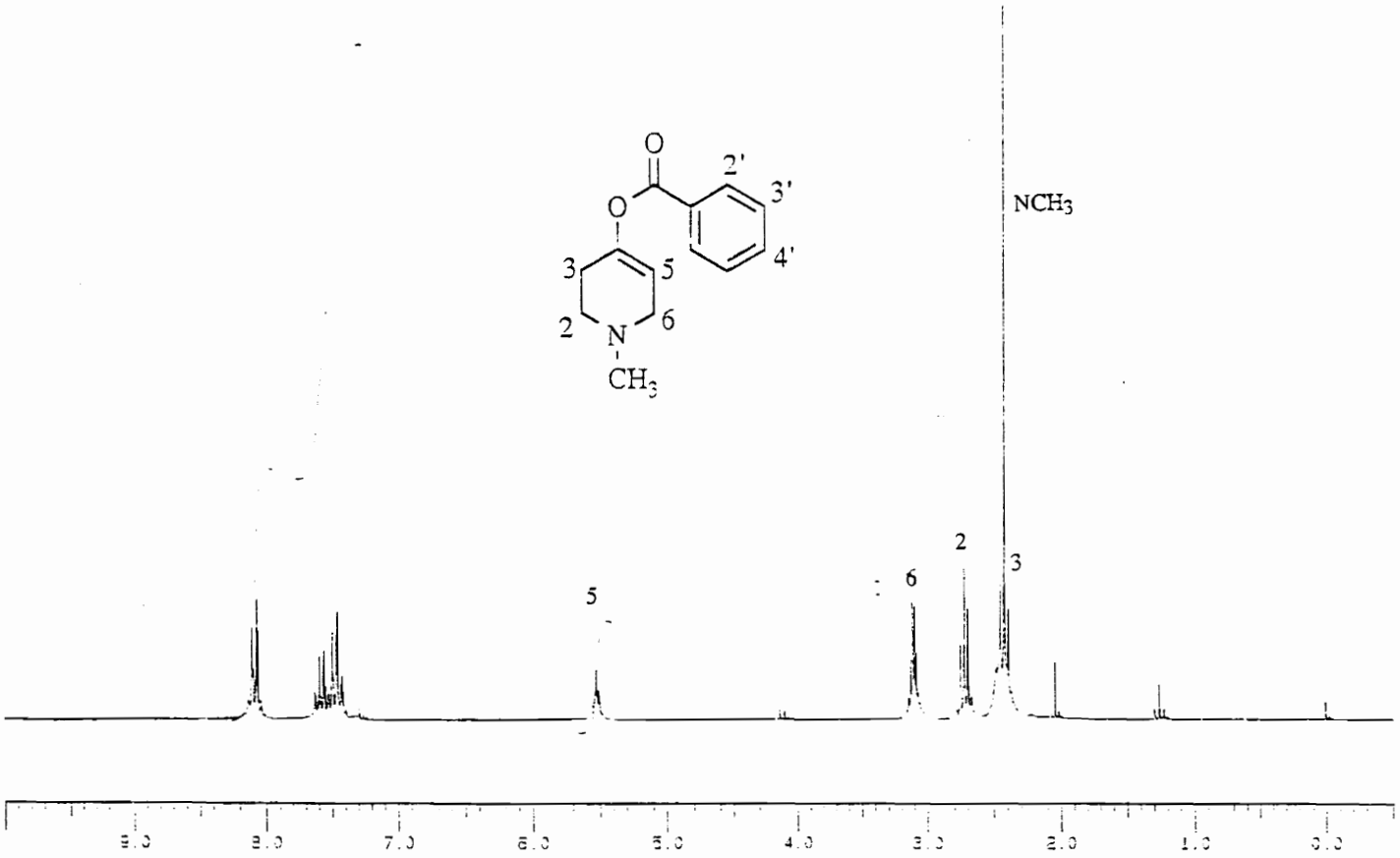

Figure. 55. ^1H NMR Spectrum ($CDCl_3$) of 4-Benzoyloxy-1-methyl-1,2,3,6-tetrahydropyridine.

the desired product 4-benzoyloxy-1-methyl-1,2,3,6-tetrahydro-pyridine (**114**).

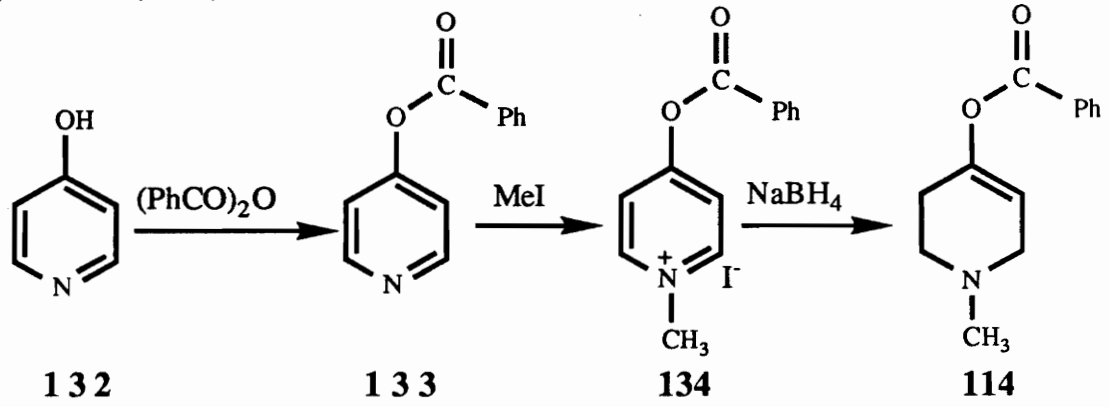

132 **133** **134** **114**

Scheme 36. Synthetic pathway (B) leading to BOMTP.

When compound **132** was heated under reflux with benzoic anhydride in freshly distilled chloroform, a product formed which could be isolated as a white solid of the free base **133** by simply washing the reaction mixture with aqueous potassium carbonate and removing the solvent. The GC/EI mass spectrum (Fig. 56) showed the expected molecular ion at m/z 199. The two intensive fragment peaks at m/z 105 and m/z 77 could be easily assigned to the benzoyl cation **128** and phenyl cation species **135**. The ^{1}H NMR spectrum (Fig. 57) of 4-benzoyloxypyridine showed two sets of doublets at 8.78 and 7.30 ppm which are assigned to protons H-2 and H-6 and to protons H-3 and H-5. The five phenyl proton signals were located between 8.25 and 7.45 ppm.

The crude 4-benzoyloxypyridine was then treated with iodomethane which gave the corresponding 4-benzoyloxypyridinium iodide (**134**). The ^{1}H NMR spectrum (Fig. 58) of **134** showed a diagnostic sharp signal due to the N-methyl group protons at 4.50 ppm expected for a pyridinium N-methyl group. The signals for protons H-2 and H-6 appeared at 9.0 as a doublet and the signals for the two other protons (H-3 and H-5) on the pyridinium ring were observed as a doublet at 8.18 ppm. Protons H-2' and H-6' on the *ortho*-position of the benzoyl ring were observed as a doublet centered at 8.34 ppm and protons H-3' and H-5' at 7.62 ppm. Finally

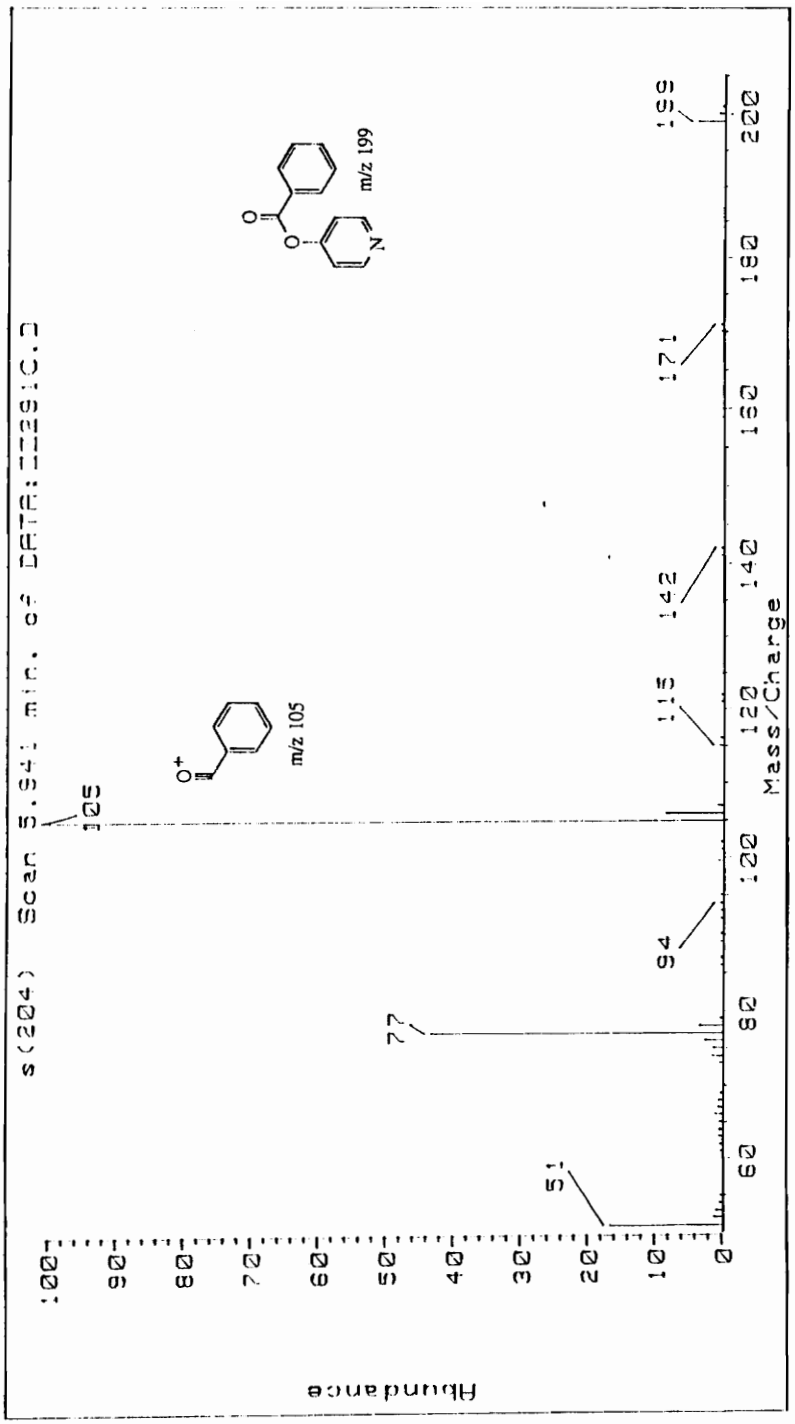

Figure. 56. GC/EIMS of 4-Benzoyloxypyridine.

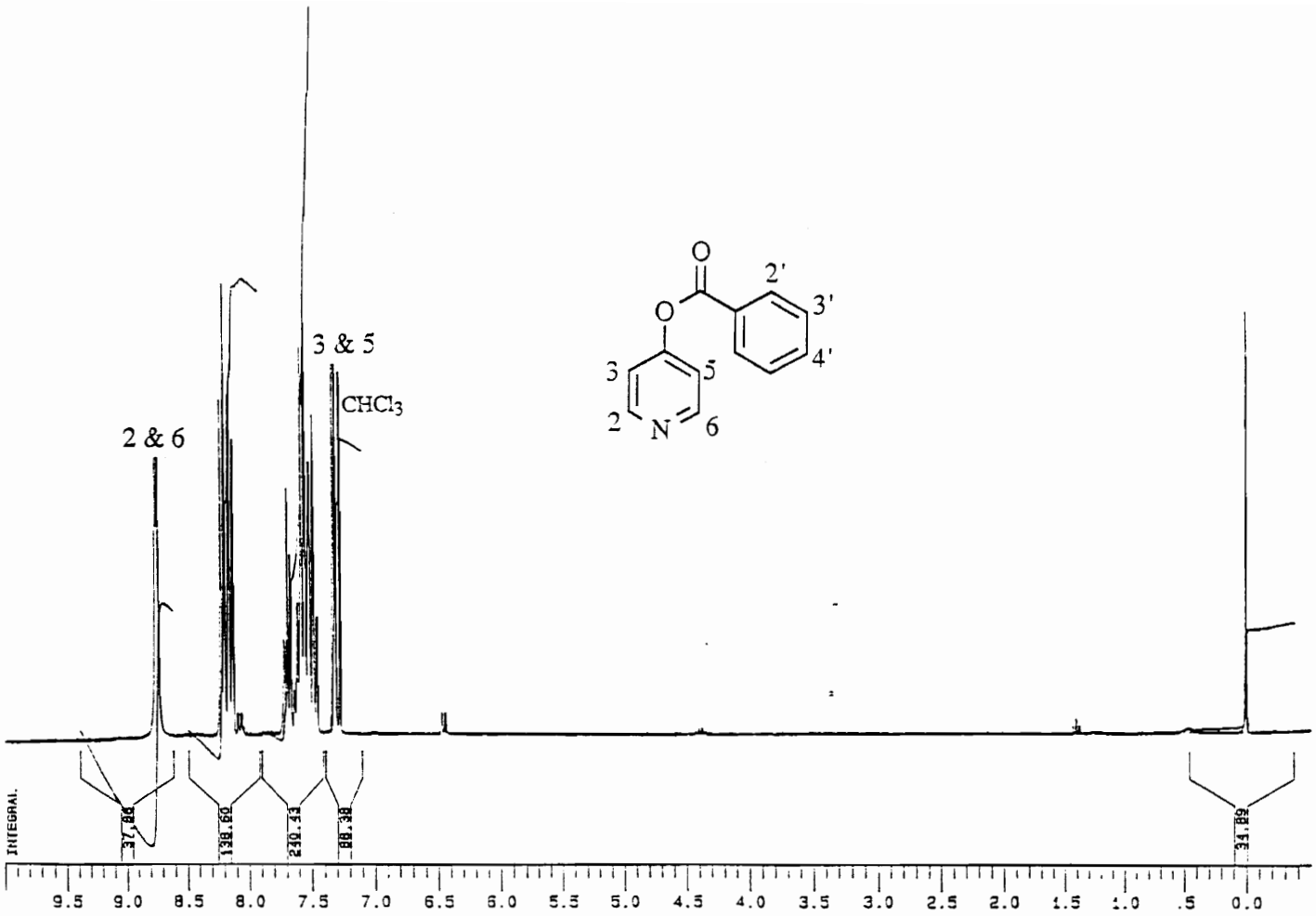

Figure. 57. ^{1}H NMR Spectrum ($CDCl_3$) of 4-Benzoyloxypyridine.

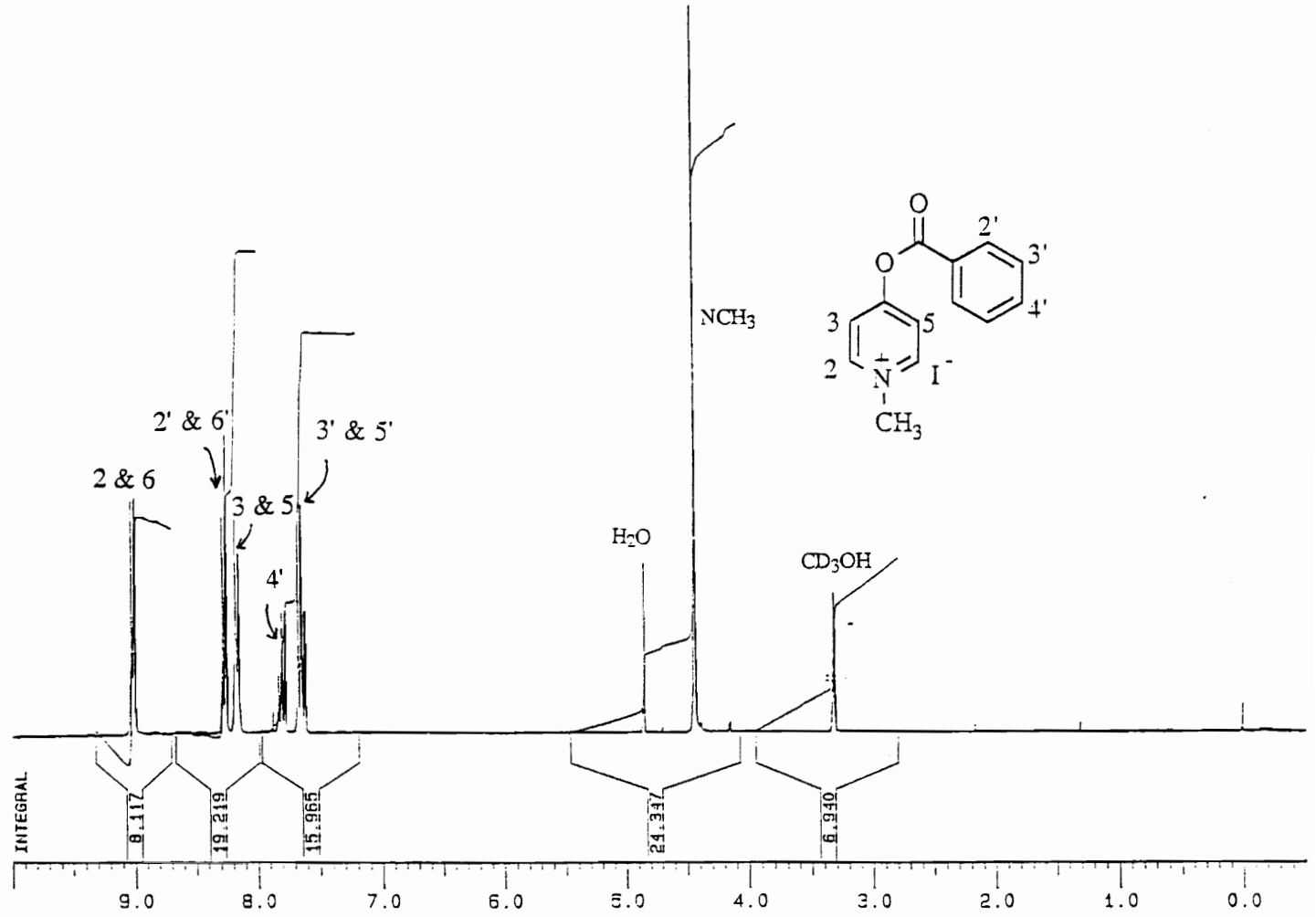

Figure. 58. ^{1}H NMR Spectrum (CD_3OD) of 4-Benzoyloxy-1-methylpyridinium iodide.

the H-4' proton at the *para*-position of the phenyl ring was present as a multiplet centered at 7.82 ppm.

The final product was obtained by reduction of the pyridinium iodide with $NaBH_4$ in methanol. The spectroscopic data of the product obtained from this reaction were identical with those of the compound synthesized following the original pathway which had been fully characterized by GC/MS, ^1H NMR and elemental analysis.

A second model prodrug, 4-(2-acetylsalicyloyl)-1-methyl-1,2,3,6-tetrahydropyridine (ASMTP, **136**), also was synthesized from 4-hydroxypyridine in a manner analogous to that described above for **114** and using acetylsalicyloyl chloride (Scheme 37).

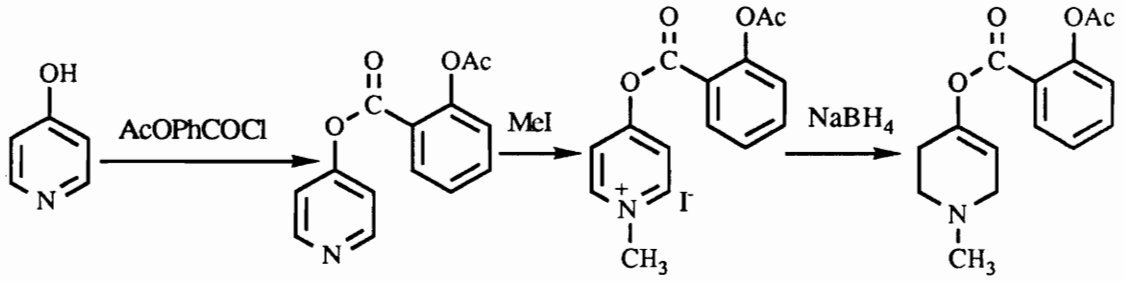

132 **137** **140** **136**

Scheme 37. Synthetic pathway leading to **136**.

The GC/EI mass spectrum (Fig. 59) of 4-(2-acetylsalicyloyl)-pyridine (**137**) showed a weak molecular ion at m/z 257 and a base fragment ion at m/z 121 (100) which probably resulted from the formation of 2-hydroxybenzoyl cation species **138**. The another strong fragment ion at m/z 163 was derived from the formation of 2-acetylsalicyloyl ion **139** by loss of a 4-oxypyridine group from the parent ion.

The ^1H NMR spectrum (Fig. 60) of **137** showed two sets of doublets at 8.78 and 7.28 ppm which were assigned to protons H-2 and H-6 and protons H-3 and H-5. The signal for phenyl proton H-6' on the carbon next to carbonyl carbon of the acetylsalicyloyl ring was recorded as a doublet at 8.24 ppm. The other doublet at 7.98 ppm

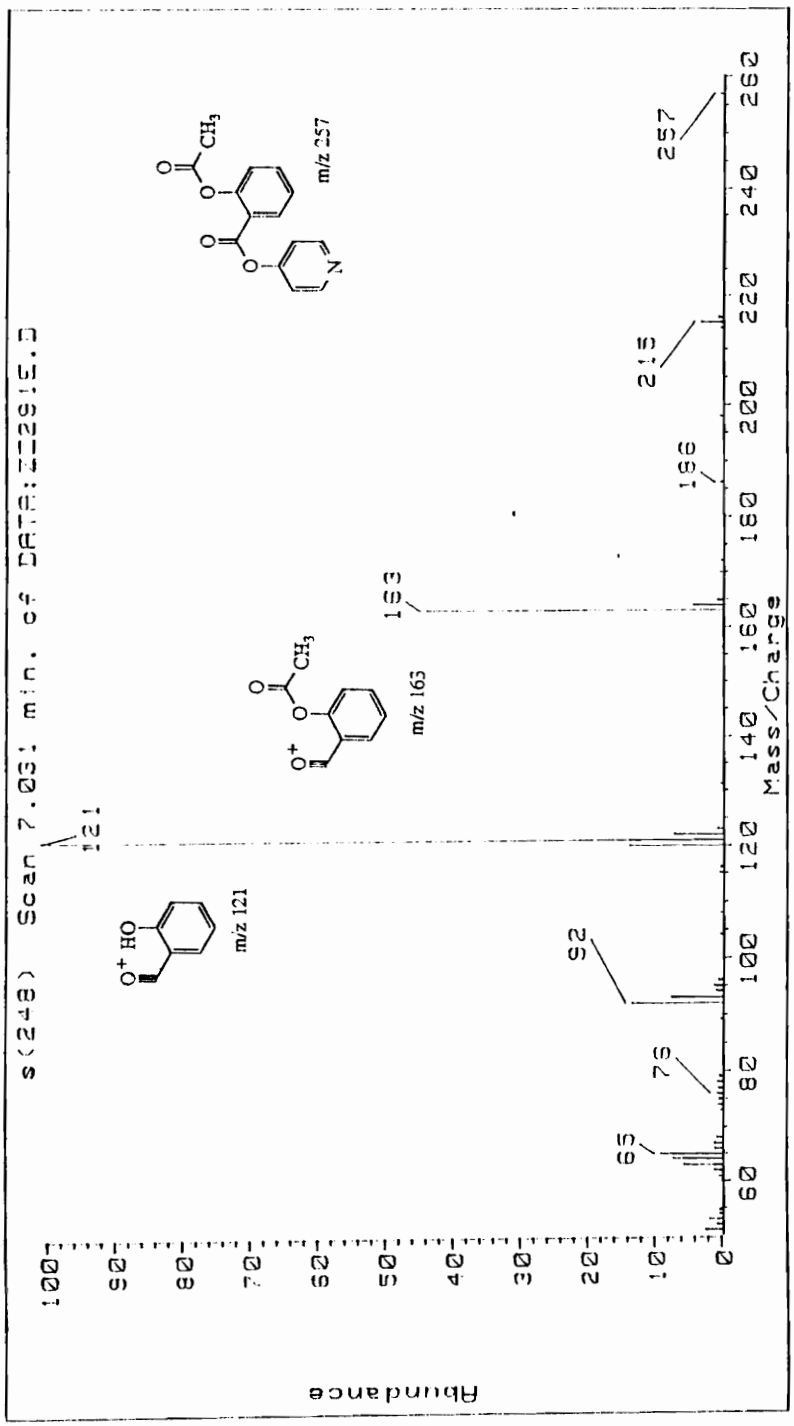

Figure. 59. GC/EIMS of 4-(2-Acetylsalicyloyl)pyridine.

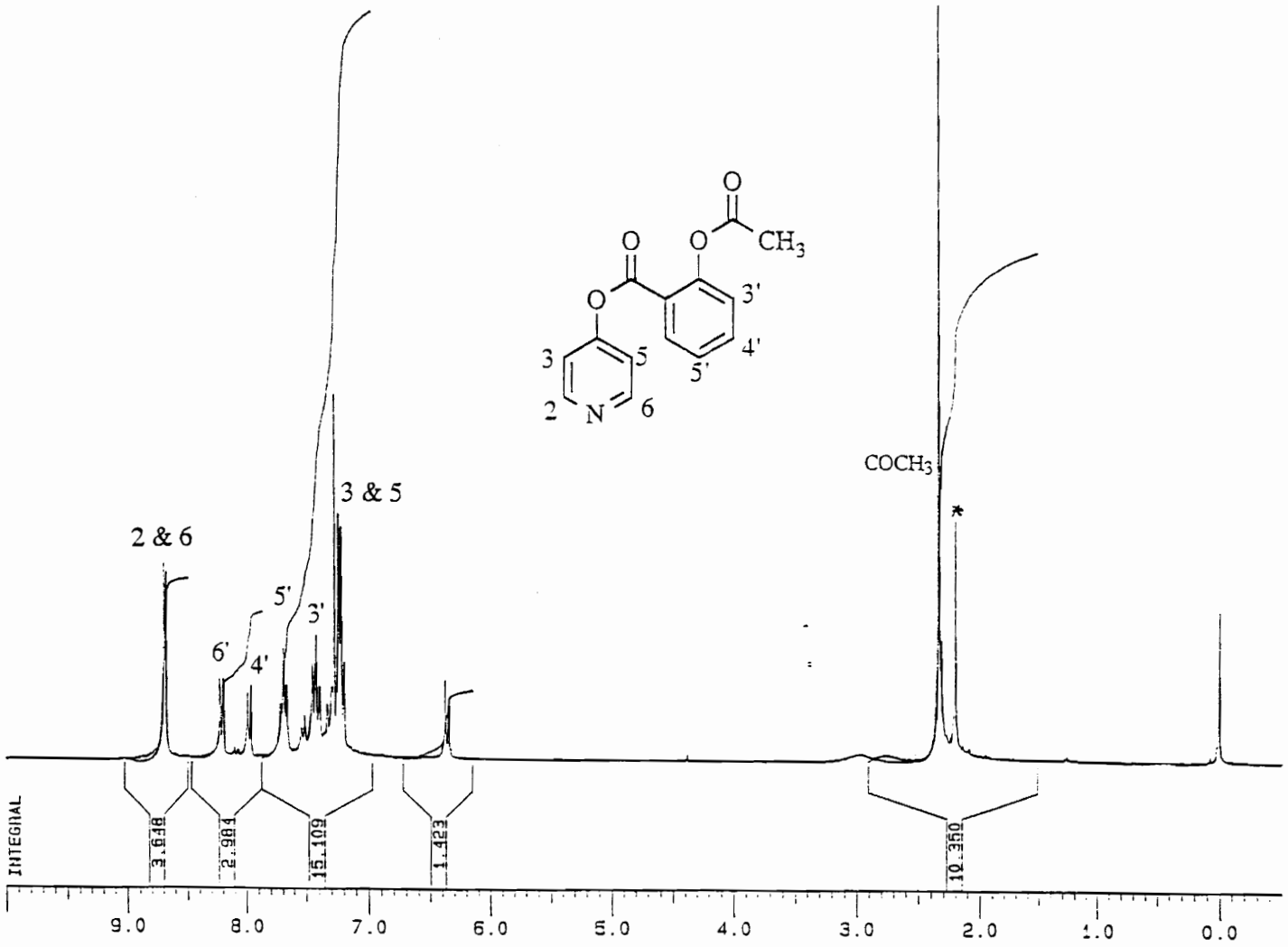

Figure. 60. ^{1}H NMR Spectrum ($CDCl_3$) of 4-(2-Acetylsalicyloyl)pyridine.

was assigned to the proton (H-3') next to acetyloxy group. The remaining two aromatic protons were observed at 7.75-7.35 ppm.

The 4-(2-acetylsalicyloyl)pyridine **137** was methylated with iodomethane in acetone and the product **140** was isolated as a yellow crystalline solid. The ^1H NMR spectrum (Fig. 61) of the N-methylpyridinium salt **140** showed two sets of doublets at 9.05 and 8.12 ppm which were assigned to protons H-2 and H-6 and protons H-3 and H-5. The aromatic protons on the 2-acetylsalicyloyl ring were recorded at 8.40 (H-6'), 7.82 (H-4'), 7.55 (H-5') and 7.35 (H-3') ppm. The N-methyl group signal was observed at 4.52 ppm as a sharp singlet. The methyl group signal from the acetyloxy group was also observed at 2.38 ppm as a sharp singlet. The signal assignments were based in part on decoupling experiments.

The 4-(2-acetylsalicyloyl)-1-methyl-1,2,3,6-tetrahydropyridine (**136**) was obtained as its oxalate salt by reduction of corresponding pyridinium derivative **140** with $NaBH_4$ in methanol followed by treatment with oxalic acid. The GC/EI mass spectrum (Fig. 62) of 4-(2-acetylsalicyloyl)-1-methyl-1,2,3,6-tetrahydropyridine (**136**) showed a weak but detectable parent molecular ion at m/z 275. The base fragment ion appeared at m/z 121 (100) and resulted from the formation of 2-hydroxybenzoyl cation species **138**. The other strong fragment ion at m/z 163 was derived from the formation of 2-acetylsalicyloyl ion **139** by loss of a 4-oxy-1-methylpyridine group from the molecular ion. The two important diagnostic fragment ions at m/z 112 and m/z 96 derived from methyltetrahydropyridyloxy cation **129** and methyltetrahydropyridyl cation **130** also were present.

The ^1H NMR spectrum (Fig. 63) of the final tetrahydro compound **136** as its oxalate salt showed a broad signal at 5.68 ppm (olefinic proton on C-5 of the tetrahydropyridine ring). The other broad signal at 3.98 ppm was assigned to the two protons on C-6 and the triplet present at 3.58 ppm was assigned to the two C-2 proton signals. The N-methyl protons were recorded at 3.05 as a sharp singlet while the other sharp singlet at 2.35 was assigned to the three protons of the acetyl group. The remaining signals were similar to those found for compound **114**.

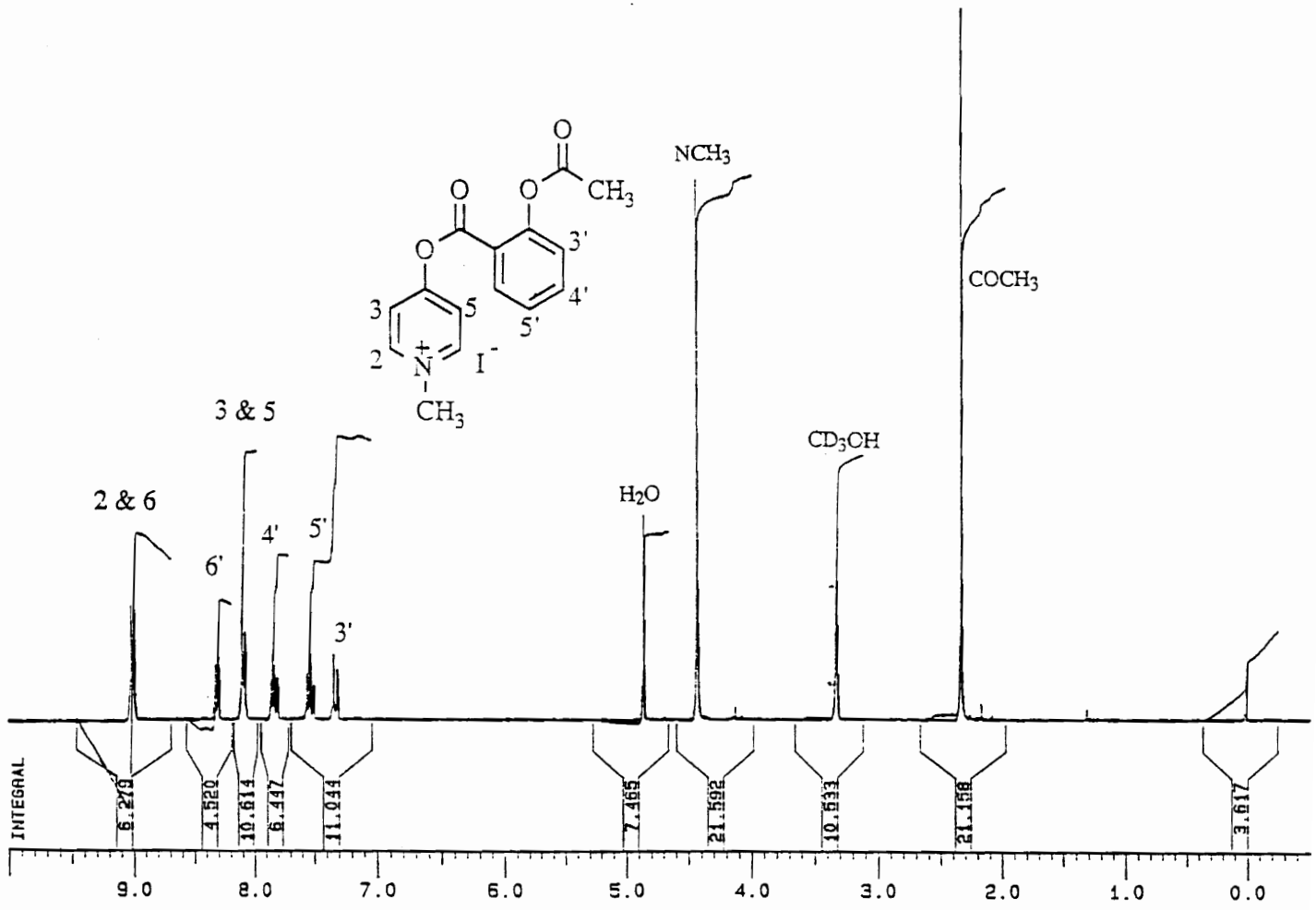

Figure. 61. ^1H NMR Spectrum (CD_3OD) of 4-(2-Acetylsalicyloyl)-1-methylpyridinium iodide.

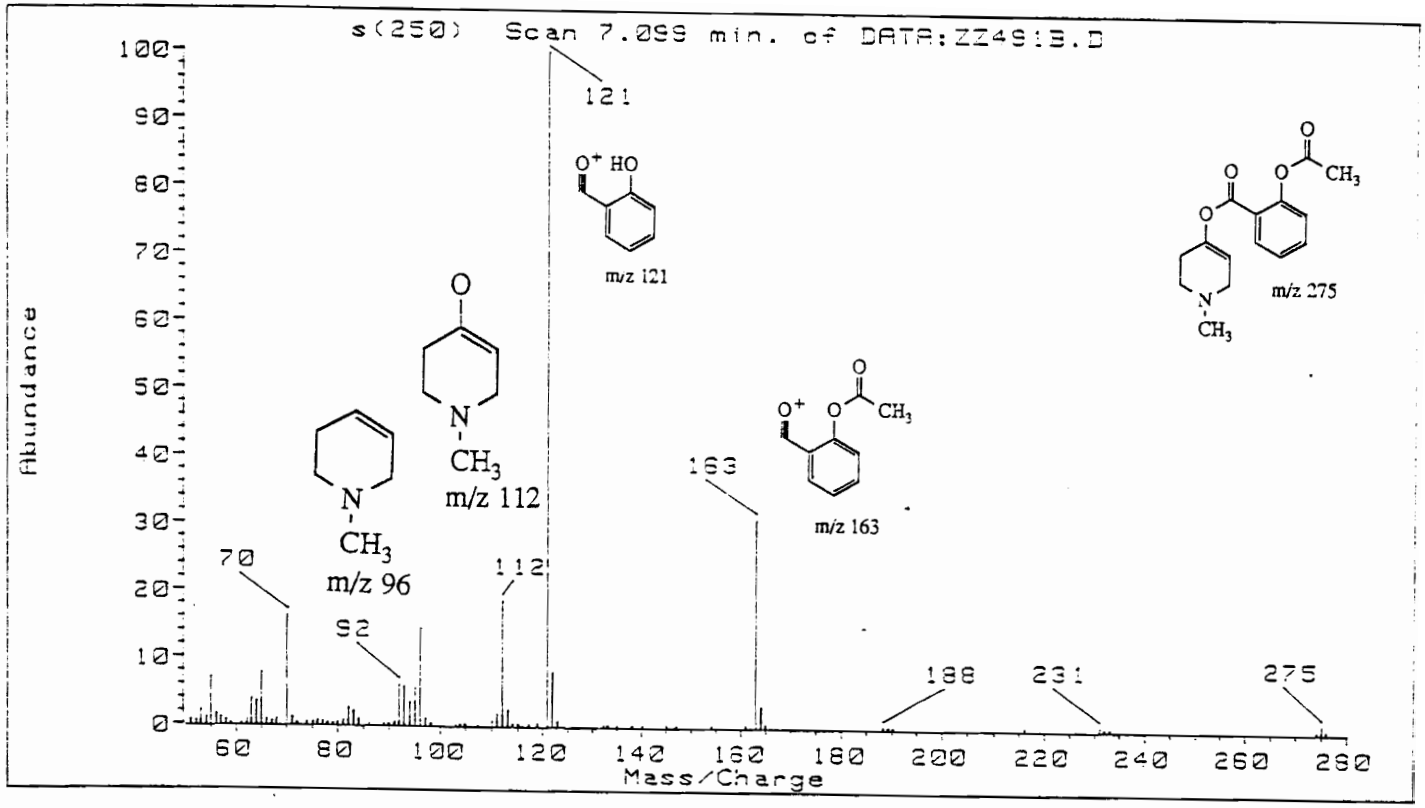

Figure. 62. GC/EIMS of 4-(2-Acetylsalicyloyl)-1-methyl-1,2,3,6-tetrahydropyridine.

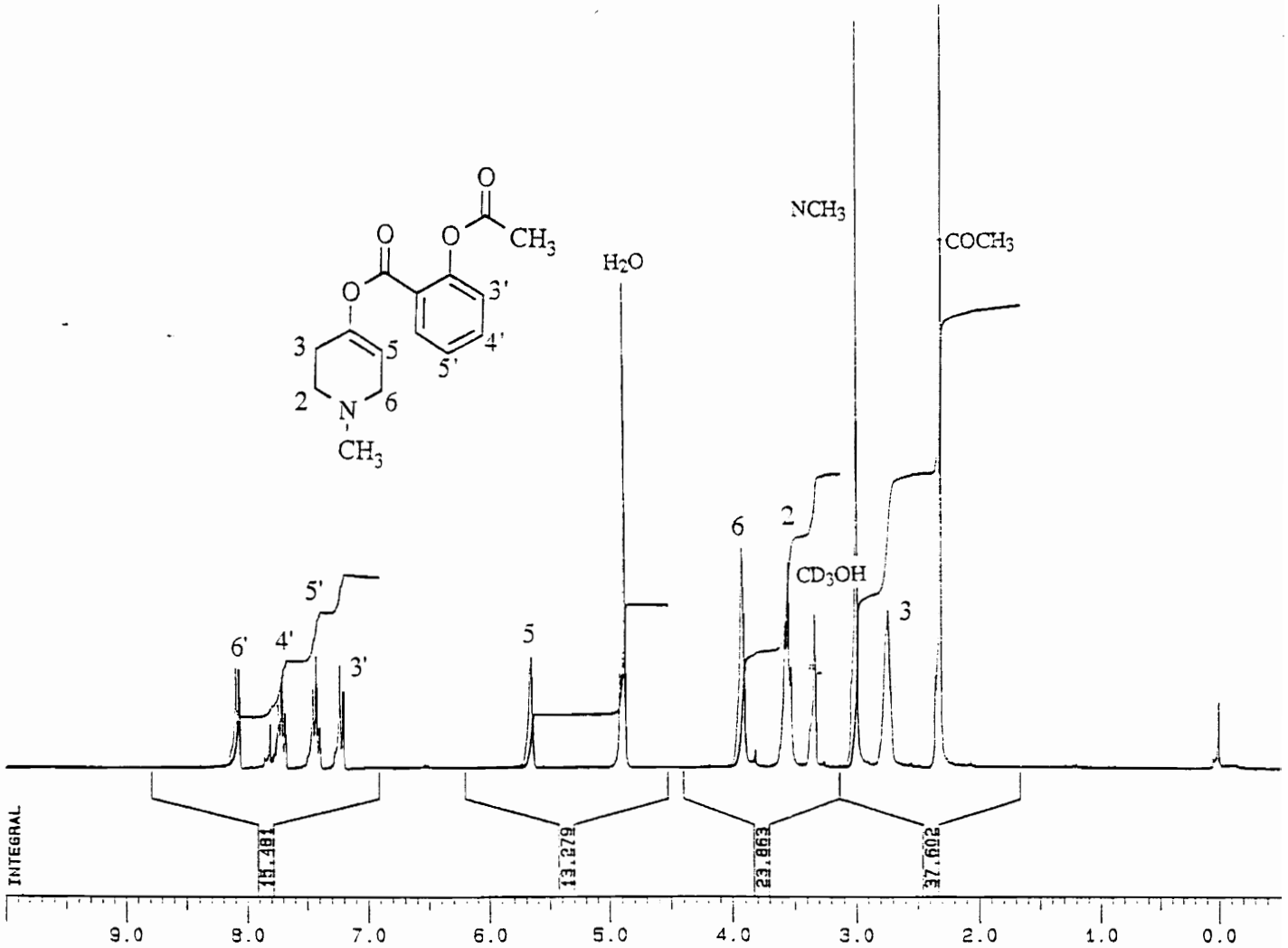

Figure. 63. ^1H NMR Spectrum (CD3OD) of 4-(2-Acetylsalicyloyl)-1-methyl-1,2,3,6-tetrahydropyridine.

For future synthetic efforts in this general field we were interested in preparing a reagent with general synthetic potential that would be readily convert to a variety of 4-carbonyloxy-tetrahydropyridines. One such synthone is the symmetric *bis*1-methyl-1,2,3,6-tetrahydro-4-pyridyloxy carbonate (**141**). Our approach to **141** is summarized in Scheme 38 in which triphosgen and 4-hydroxypyridine would give the *bis*pyridyl carbonate **142**. Methylation of **142** followed by reduction of the resulting *bis*pyridinium intermediate **143** would yield the desired carbonate **141**.

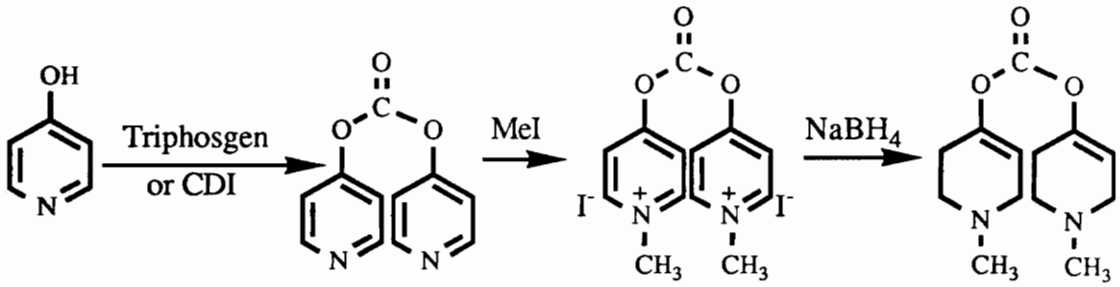

132 **142** **143** **141**

Scheme 38. Proposed synthetic pathway leading to **141**.

Unfortunately, all efforts to obtain the intermediate *bis*pyridyl carbonate failed. The reaction 4-hydroxypyridine with triphosgen at room temperature gave 4-chloropyridine (**144**), as the only isolable product. This result indicated that the initial reaction may have occured as expected and that the by-product, chloride ion, reacted with the intermediate **142**. The same outcome was realized even at 0 °C.

A second attempt to prepare **142** involved reaction of 1,1'-carbonyldiimidazole (CDI) with 4-hydroxypyridine at room temperature. The only product observed on GC/MS analysis was the 1-(4-pyridyloxy)carbonylimidazole (**145**). More vigorous condition (reflux overnight) did not change this outcome. Treatment of **145** with methanol gave, according to GC/MS analysis, 1-methoxycarbonylimidazole (**146**). No evidence of the carbonate **147** was observed in the GC mass spectrum. These results suggest that 4-

hydroxypyridine is a better leaving group than imidazole. In order to overcome this problem, a more reactive formylating reagent, such as a carbonylditriazole, should be used in any future attempts at this synthesis.

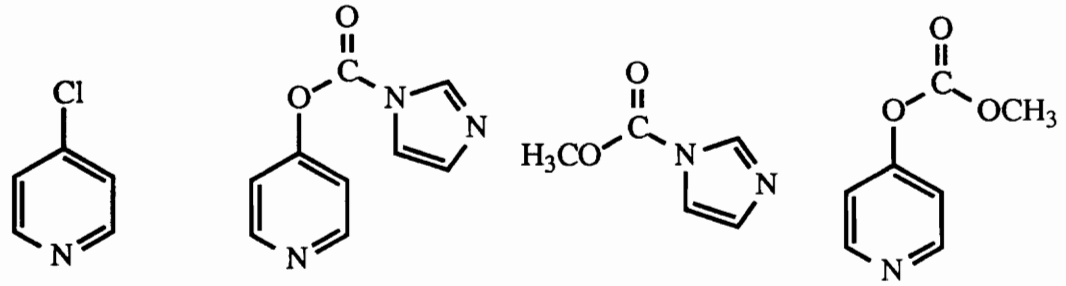

144 **145** **146** **147**

Since the 4-benzoyloxy-1-methyl-2,3-dihydropyridinium species **150** (BOMDP+) was the expected MAO-B catalyzed oxidative product of the tetrahydropyridine **114**, we also undertook this synthesis as summarized in Scheme 39. Following a literature procedure, compound **114** first was converted to the corresponding N-oxide (**151**) by treatment with *m*-chloroperoxybenzoic acid (MCPBA).

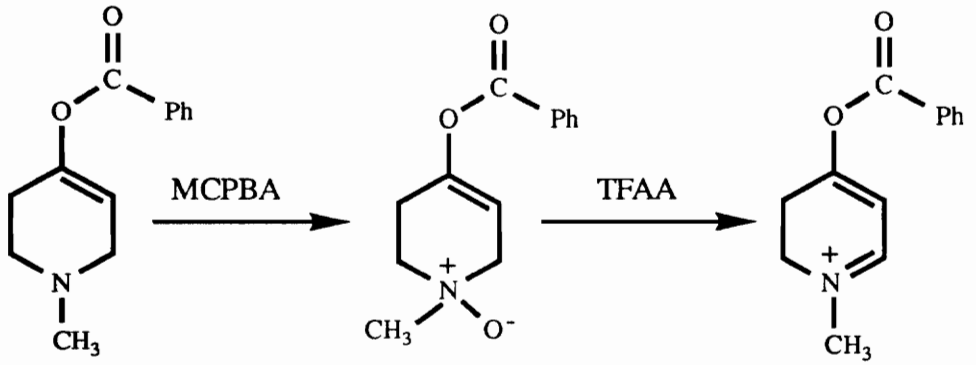

114 **151** **150**

Scheme 39. Synthetic pathway of BOMDP+ **150**.

The ^{1}H NMR spectrum (Fig. 64) of N-oxide **151** showed a doublet centered at 8.18 ppm which we assigned to the signals for phenyl protons H-2' and H-6'. The signal for proton H-4' was

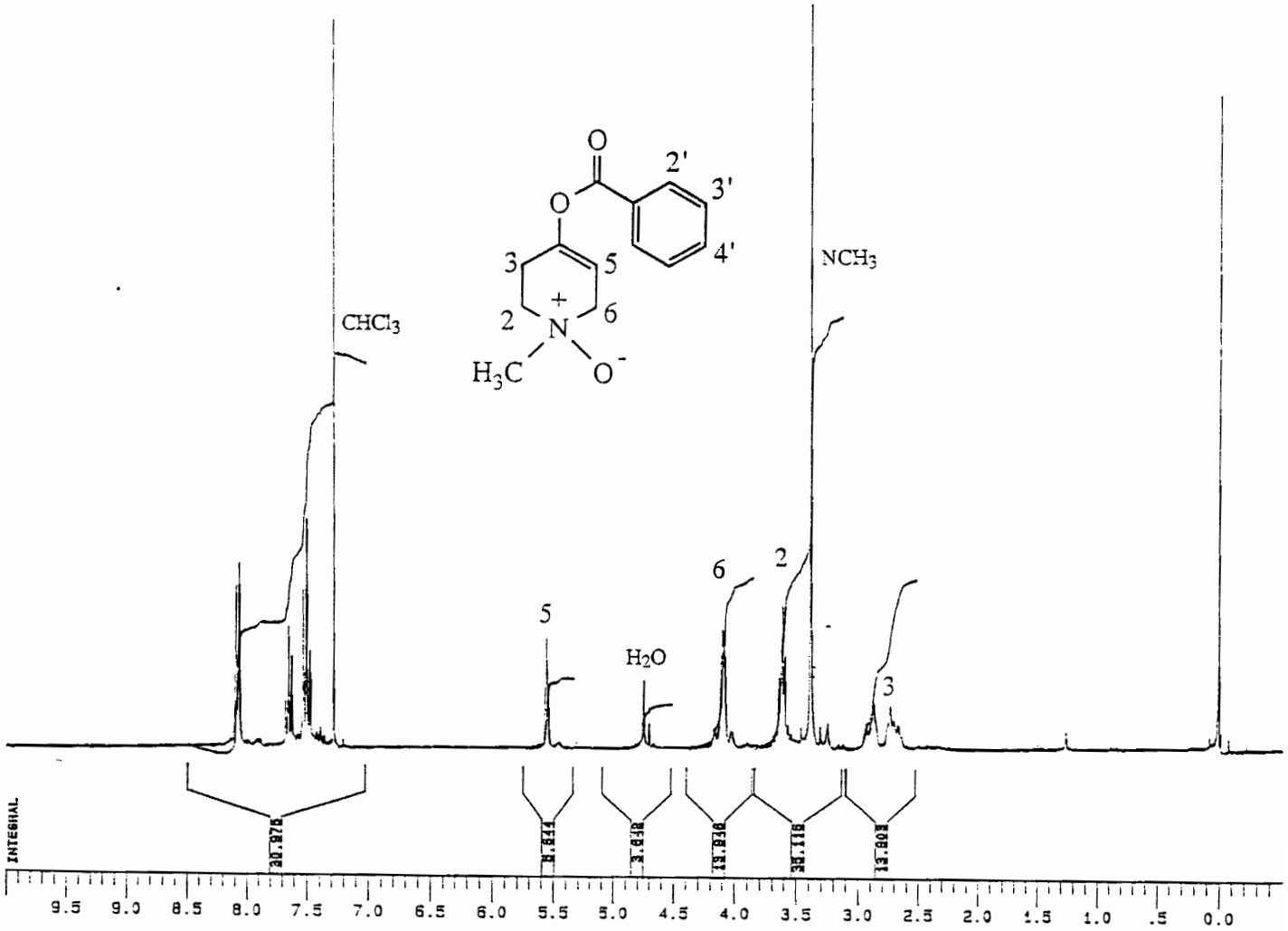

Figure. 64. ^{1}H NMR Spectrum ($CDCl_3$) of 4-Benzoyloxy-1-methy-1,2,3,6-tetrahydropyridine N-oxide.

observed as a triplet centered at 7.65 ppm and the signals for H-3' and H-5' were observed at 7.55 ppm as a triplet. The broad triplet at 5.55 ppm was assigned to the signal for the C-5 olefinic proton. The two protons on the carbon atom C-6 adjacent to nitrogen atom exhibited a doublet centered at 4.1 ppm. The triplet centered at 3.65 ppm was assigned to the protons on C-2. The signal for the three protons of the N-methyl group was recorded at 3.4 ppm as a sharp singlet and the two protons (H-3) are found as a multiplet centered at 2.8 ppm.

Treatment of N-oxide **151** with trifluoroacetic anhydride (TFAA) in cold methylene chloride yielded the expected dihydropyridinium species **150**. The ^1H NMR spectrum (Fig. 65) of BMDP$^+$ (**150**) showed a doublet at 8.52 ppm which is due to the azomethine proton signal on C-6. The signal due to the proton on C-5 was observed at 6.78 ppm also as a doublet. The two protons on the carbon (C-2) adjacent to nitrogen atom appeared as a triplet centered at 3.68 ppm. The triplet centered at 2.78 ppm was assigned to the protons on C-3. The three N-methyl protons appeared as a sharp singlet recorded at 3.74 ppm. All of these assignments were confirmed by decoupling experiments.

The dihydropyridinium compound adsorbed in the UV with λ_{max} 280 nm. Upon standing in the trifluoroacetic acid containing $CDCl_3$ solvent, this chromophore rapidly was replaced by a spectrum which exhibited a chromophore with λ_{max} at 321 nm and 241 nm. These values corresponds to those reported for aminoenone **113**[119] and benzoic acid **152**, respectively. The aminoenone **113** and benzoic acid also were identified by ^1H NMR and GC/MS. The chemical shift values of the aminoenone ^1H NMR spectrum was offset by about 0.3 ppm - 0.5 ppm compared with the literature values,[119] probably because of the presence of the trifluoroacetic acid. This assumption was confirmed by obtaining the identical spectral data as reported in the literature by passing the crude **113** through a short alumina column to free it from the trifluoroacetic acid. The GC/MS of benzoic acid (**152**) showed a molecular ion at m/z 122 and a base peak of benzoyl cation at m/z 105. The BOMDP$^+$ then was synthesized again in a more controled condition.

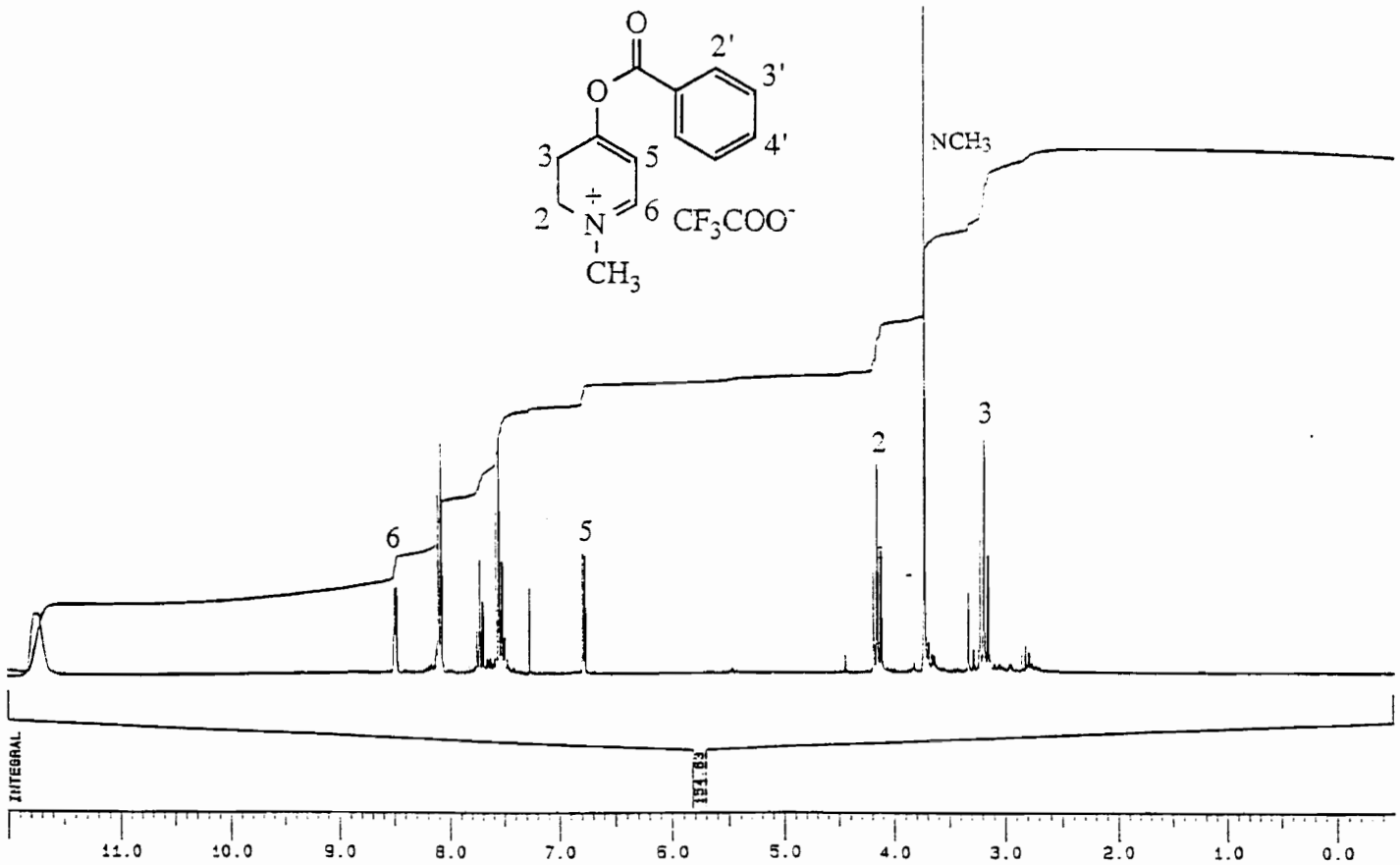

Figure. 65. ^1H NMR Spectrum ($CDCl_3$) of 4-Benzoyloxy-1-methyl-2,3-dihydropyridinium salt.

In view of the likely formation of aminoenone **113**, a synthetic standard of this compound was required. The literature method[119] for the synthesis of **113** involved several steps as follows (Scheme 40):

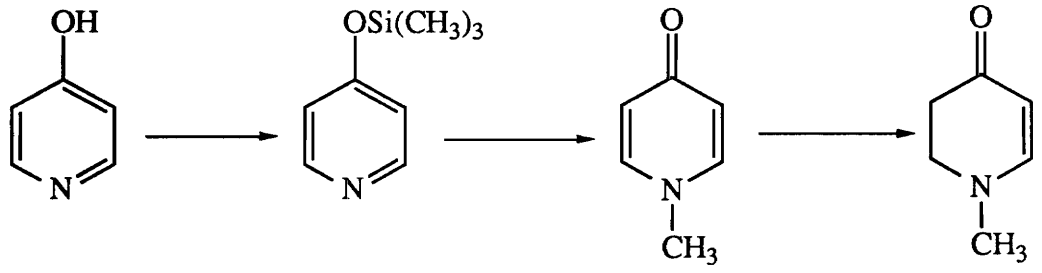

132 **153** **154** **113**

Scheme 40. Literature method for the synthesis of **113**.

In order to develop a more direct route to **113** methods that oxidize commercially available 1-methyl-4-piperidone (**115**) were considered. Our first attempt employed MCPBA to form the corresponding intermediate N-oxide **155.** After passing through a short basic alumina column, the free base was treated with TFAA to generate **113**. Although the GC/MS spectrum did show the presence of the desired product, the mixture was quite complex and therefore this approach was abandoned.

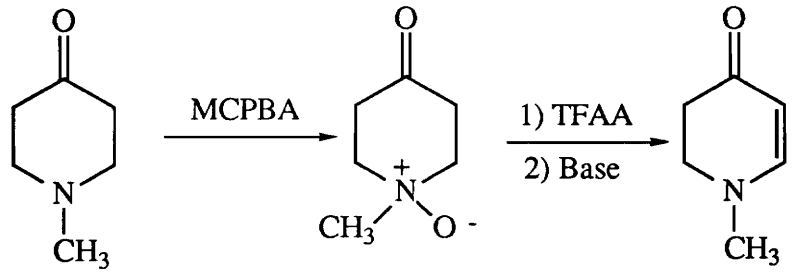

115 **155** **113**

Scheme 41. Proposed synthetic pathway for **113** via N-oxide **155.**

Treatment of **115** with mercuric acetate led to a mixture of the desired product **113** and starting material but **113** could be isolated in pure form by alumina followed by silica gel chromatography. The GC/EI mass spectrum (Fig. 66) of the product showed the molecular ion at m/z 111 as the base peak. The other two intensive fragment ions at m/z 82 and m/z 55 may be derived from loss of an NCH_3 group from the parent ion followed by further loss of a C=O group.

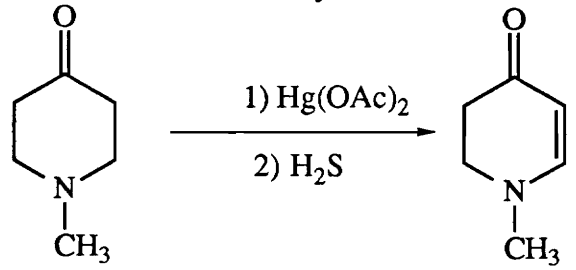

115 **113**

Scheme 42. Synthetic pathway leading to **113**.

The ^1H NMR spectrum (Fig. 67) of **113** showed a doublet at 6.98 ppm which we assigned to the olefinic proton (H-6) signal on the carbon atom adjacent to the nitrogen atom and a second doublet at 4.94 ppm which we assigned to the olefinic proton (H-5) on the carbon atom attached to the carbonyl carbon. Two sets of triplets were recorded at 3.44 ppm corresponding to the methylene proton signals (H-2) next to the nitrogen atom and 2.50 ppm corresponding to the methylene proton signal (H-3) α to the carbonyl group. The N-methyl proton signal was observed as a sharp singlet at 3.04 ppm. The chemical shifts and assignments of these signals were consistent with the literature report.[119]

When the ^1H NMR spectrum of **113** was taken in D_2O with DCl at low pH (pH = 2), the proton (H-5) signal observed in the original spectrum as a doublet at 4.95 disappeared and the H-6 proton doublet at 7.25 ppm was replaced by a sharp singlet at 7.05 ppm (Fig. 68). The explanation for these changes is that at low pH compound **113** exists as its 1,2,3,4-tetrahydropyridinium form **113a** and leading to exchange of the proton (H-5) with deuterium.

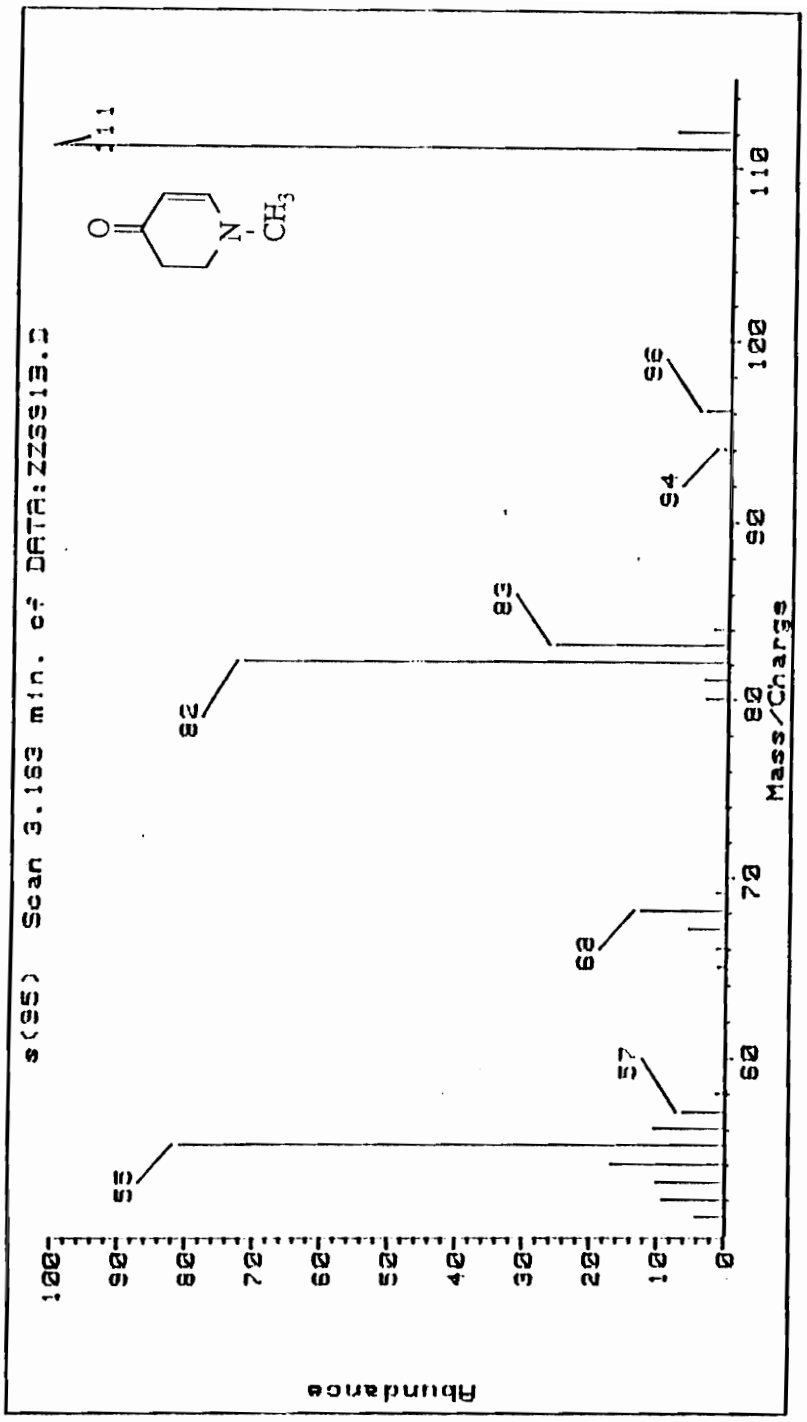

Figure. 66. GC/EIMS of 2,3-Dihydro-1-methyl-4-pyridone.

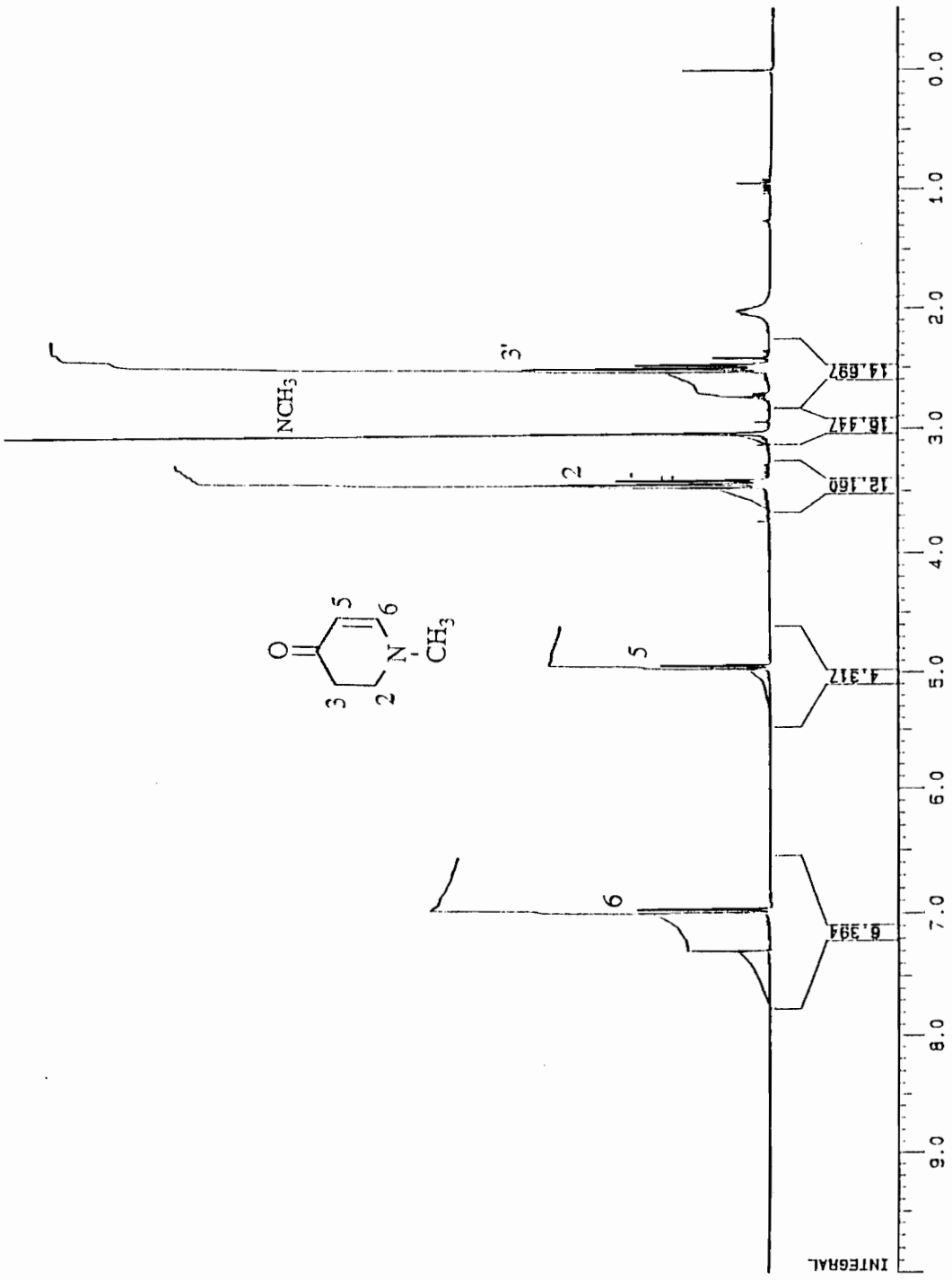

Figure. 67. 1H NMR Spectrum ($CDCl_3$) of 2,3-Dihydro-1-methyl-4-pyridone.

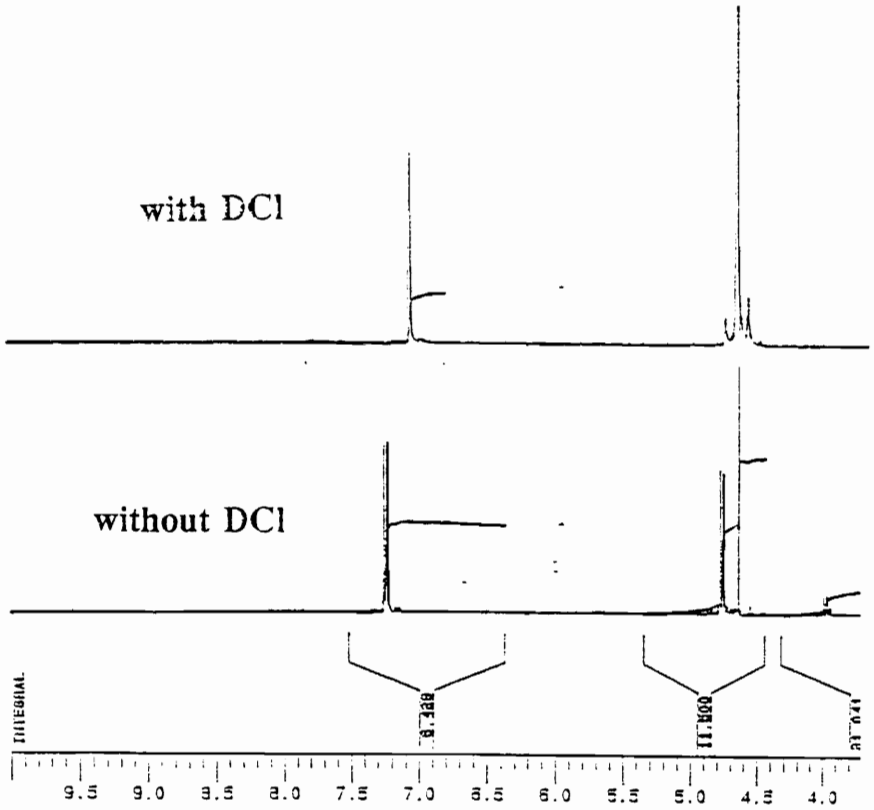

Figure. 68. ^{1}H NMR Spectrum (D_2O) of 2,3-Dihydro-1-methyl-4-pyridone.

Therefore the signal for H-5 is lost and the signal for H-6 becomes a singlet due to loss of coupling with the deuterium at C-5.

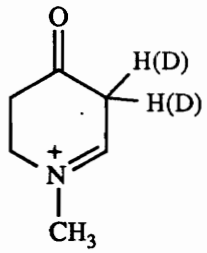

113a

4.3.2. Metabolism Studies

The 4-benzoyloxy-1-methyl-1,2,3,6-tetrahydropyridine (**114**) was incubated with MAO-B in a sodium phosphate buffer and the incubation mixture was placed in a spectrophotometer which was thermostated at 37 °C. The absorbance at 324 nm, which is the λ_{max} of the corresponding aminoenone **113**, was monitored since, based on our chemical considerations, 4-benzoyloxy-1-methyl-2,3-dihydropyridinium (**150**), which could be formed if **114** is a substrate of MAO-B, would be expected to hydrolyze to the corresponding aminoenone (Scheme 43). The absorbance at 324 increased slowly to an O.D. of 0.045 and after 45 minute leveled off (Fig. 69). MPTP (**98**) then was added to measure remaining enzyme activity. No $MPDP^+$ (**100**), however, was observed which indicated that the MAO-B was no longer active.

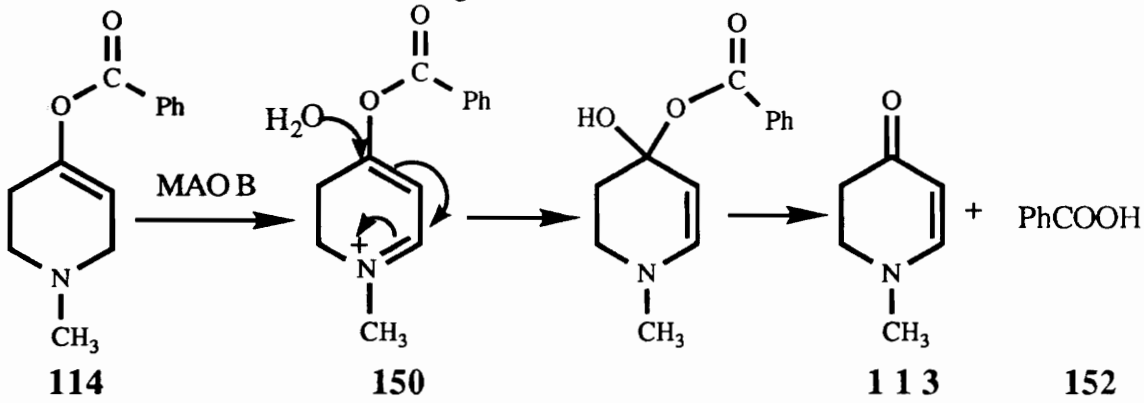

114 **150** **113** **152**

Scheme 43. Proposed metabolic pathway for BOMTP.

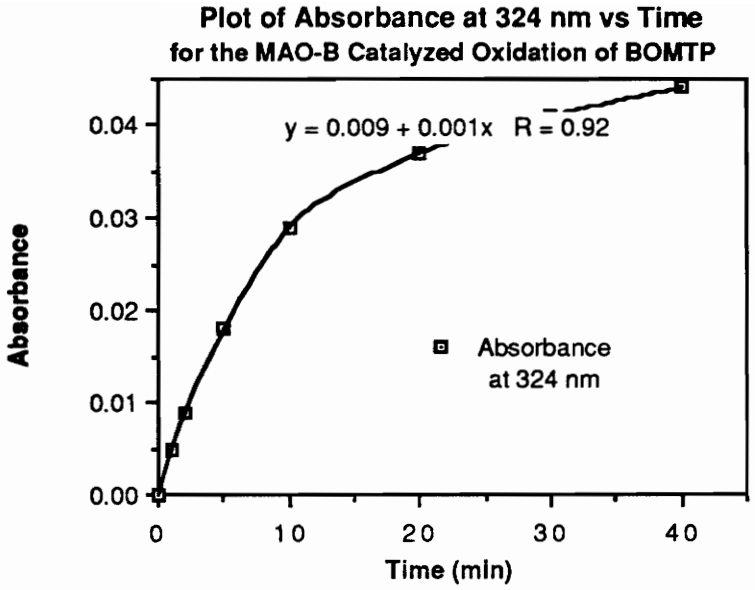

Fig. 69.

In order to monitor the changes of the λ_{max} during the incubation, a solution of **114** with MAO-B was scanned repeated from 450 nm to 210 nm against a background spectrum taken at 0 time. The results showed an absorbance at 292 nm (Fig. 70 and Fig. 71) which was attributed to the formation of either the dihydropyridinium analog **150** or pyridinium analog **134.** The absorbance disappeared after treatment with $NaBH_4$. The resulting tracing showed a negative absorbance due to loss of starting material.

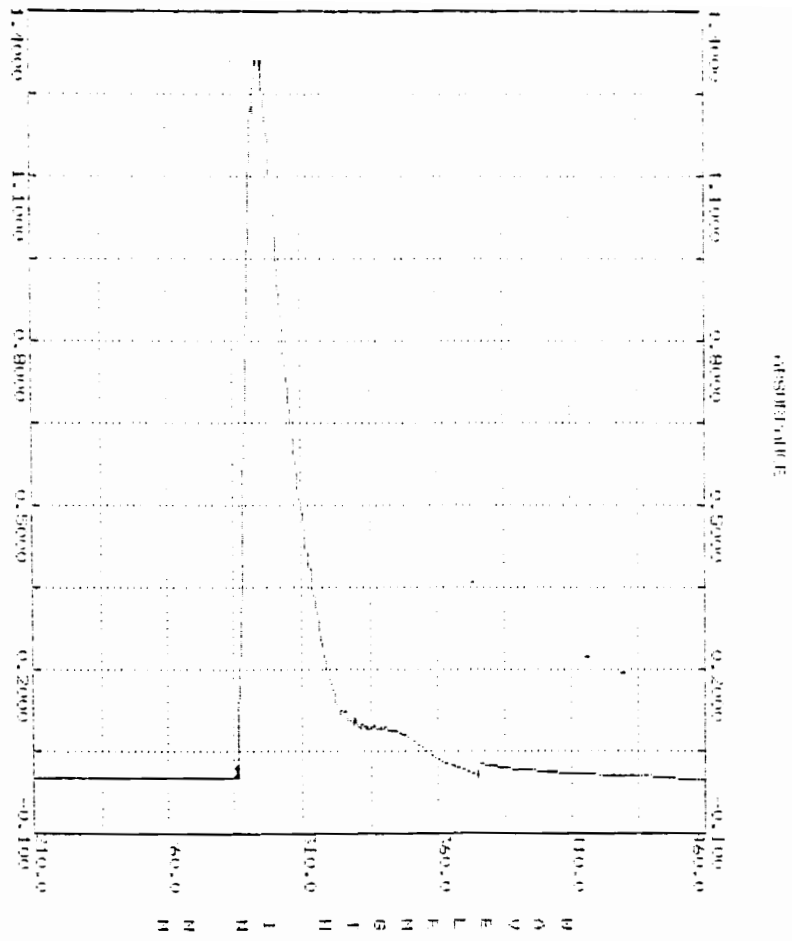

Figure. 70. UV Spectrum of the Metabolite Derived from BOMTP at Higher Concentration (5 mM).

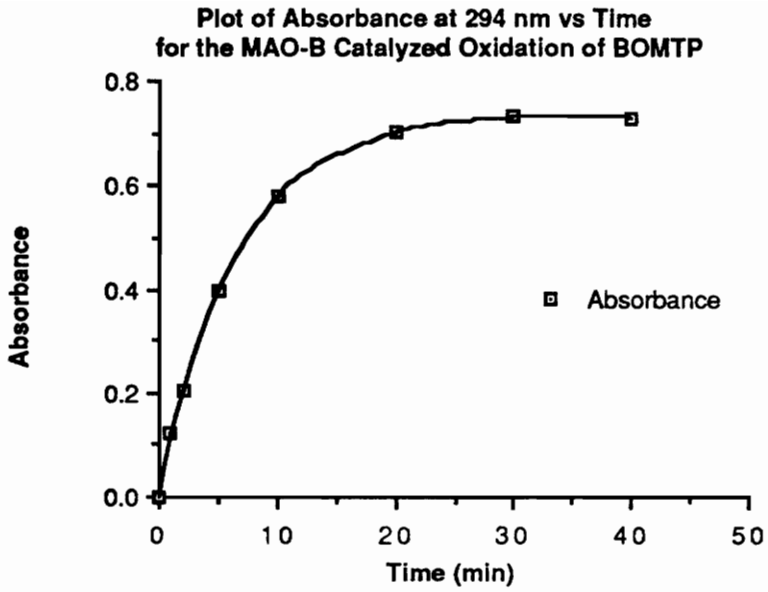

Fig. 71.

Although the absorbance at 294 nm disappeared at pH = 1 following the addition of HCl, the absorbance reappeared following basification to pH 12. The formation of the absorbance at 292 nm from the BOMTP incubation is, however, enzymatically mediated since no new chromophore was formed when BOMTP was incubated without MAO-B. In order to confirm the finding, the enzyme was preincubated with a known MAO-B inhibitor, deprenyl (**10**), at 37 °C for 10 minute and the inhibitor and enzyme mixture was then mixed with the BOMTP buffer solution. No chromophore was observed up to 100 minute at 37 °C. Based on these information, the conclusion is that the absorbance at about 292 nm observed in earlier experiments with BOMTP is mediated by MAO-B. In other words, the BOMTP is a substrate of MAO-B which catalyzed the formation of an metabolite absorbing at 292 nm.

There was about a 12 nm difference between the absorbance at 292 nm observed from the incubation mixture and the synthesized 4-benzoyloxy-1-methyl-2,3-dihydropyridinium species (**150**) which showed a absorbance at λ_{max} 280 nm. Based on these data we postulated that the metabolite with λmax at 292 nm, which was formed in the incubation with MAO-B, may not be the expected dihydropyridinium compound. An alternative structure, the dione **167** was considered (Scheme 44).

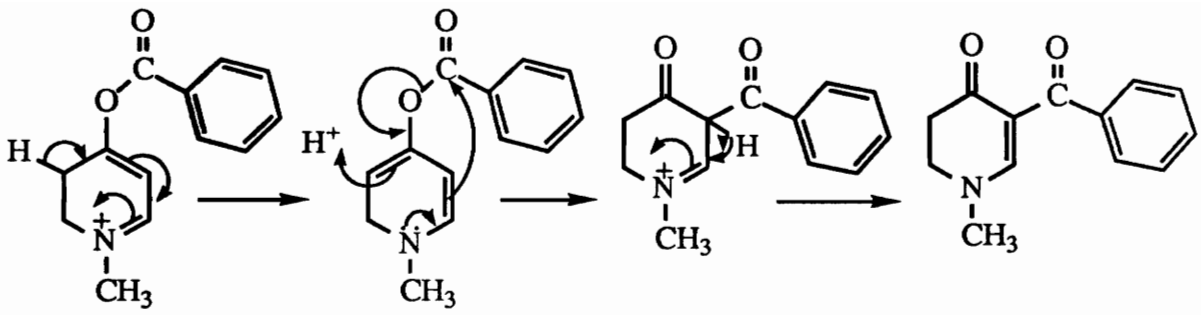

150 **165** **166** **167**

Scheme 44. Proposed mechanism for formation of **167**.

The methylene chloride extract from the incubation mixture did show the expected final products, the aminoenone **113** and benzoic acid **152**, but only in very small amounts. Although the benzoic acid **152** could form from simple chemical hydrolysis of the substrate, the DMPO **113** could only form from the metabolite BOMDP$^+$, which should be mediated by the enzyme. However, the compound(s) resulting in the absorbance at 292 nm remained in the aqueous solution in a high percent based on comparison of the abundance after the extraction with methylene chloride.

The source of the absorbance at 292 nm was clarified by the following experiment. When MAO-B was incubated with BOMTP **113** at a concentration of 100 μM and 500 μM, the incubation mixture showed an initial absorbance at 280 nm (Fig. 72), that is exactly the same as the absorbance observed for synthetic **150**. The explanation for the appearance of a λ_{max} at 292 nm at high concentrations (5 mM) of **114** is that, although the λ_{max} for **114** is at 240 nm (ε = 12,550), there is a shoulder at about 275 nm (ε = 310). When using the high concentration of the substrate in the incubation mixture, the background was overranged and the subtraction of the background resulted in an apparent λ_{max} at 292 nm.

To confirm further that the MAO-B catalyzed metabolite of the **114** is the dihydropyridinium species **150**, synthetic **150** and the metabolite derived from incubation were analyzed by HPLC with a diode array detector on a C18 column (Fig. 73). The results showed

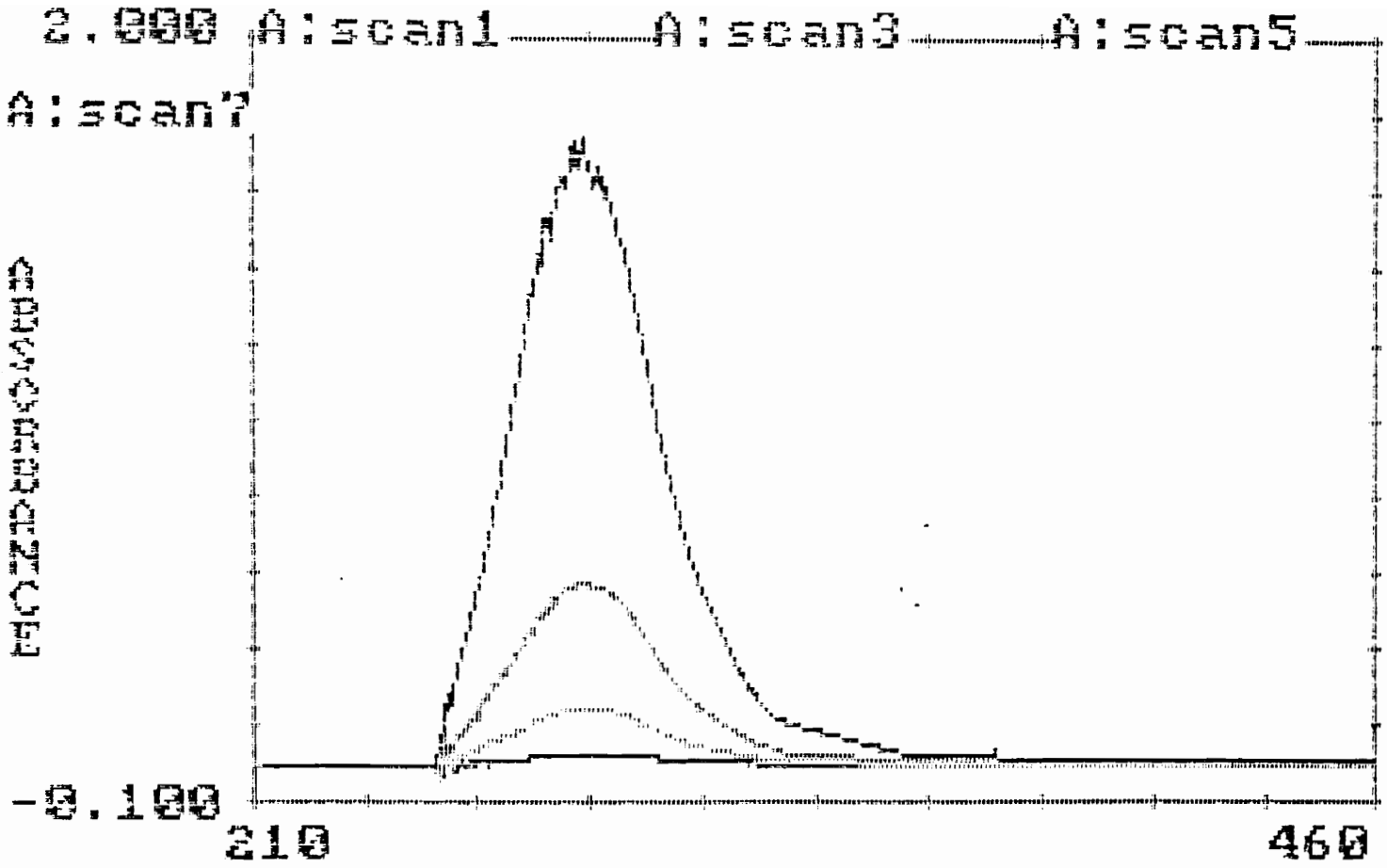

Figure. 72. UV Spectrum of the Metabolite Derived from BOMTP at Lower Concentration (0.5 mM).

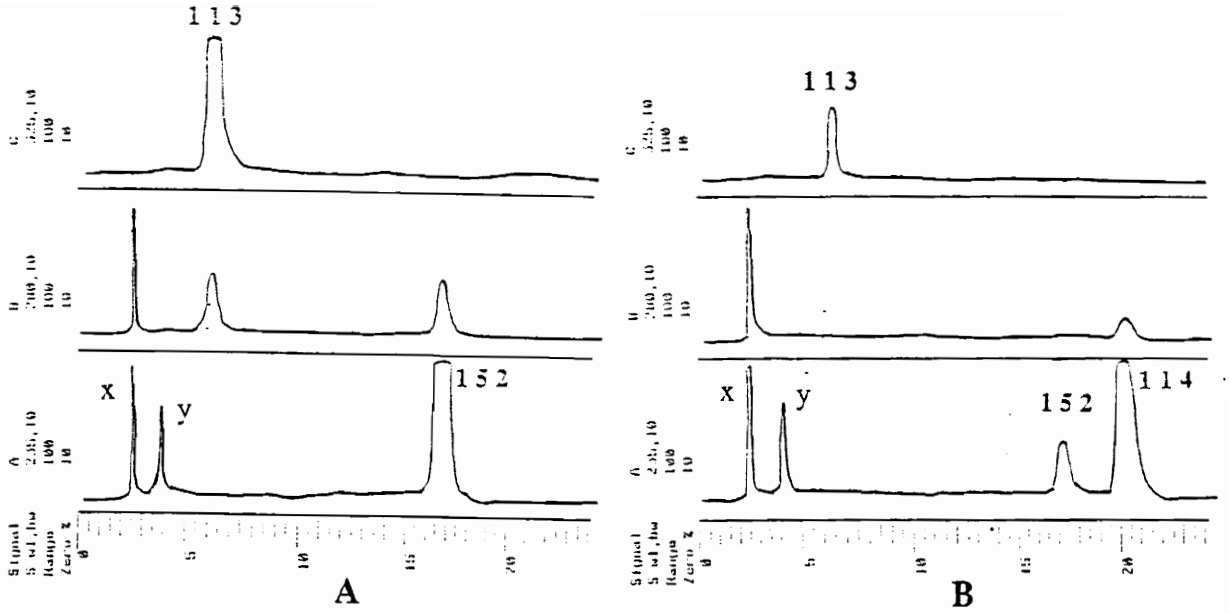

Figure. 73. HPLC Tracings of BOMTP Incubation Mixture with MAO-B (B) and Synthetic BOMDP+ (A).

the expected products aminoenone **113** and benzoic acid **152** and the tracings of the two samples are almost identical except that the incubation sample had the substrate **114** as an additional compound. However, the identity of the peaks **X** and **Y** is not clear at this time.

Although synthetic **150** appeared to hydrolyze rapidly in the acidic $CDCl_3$ solution, it is quite stable in buffer solution (pH = 7.4) as observed for the metabolite generated in the MAO-B incubation. Synthetic **150** also showed the same behavior as the the metabolite in terms of its absorbance at 280 nm disappearance at lower pH 2 followed by reappearance at higher pH 10. This behavior may be explained by assuming that under acidic conditions the equilibrium mixture between **150**, its conjugate base **165** and the 2,4-dihydropyridinium species **171** is composed predominantly of **171** (Scheme 45). The 2,5-isomer **171** would not be expected to have a chromophore above 240 nm, which would account for the loss of the 280 nm chromophore upon addition of HCl.

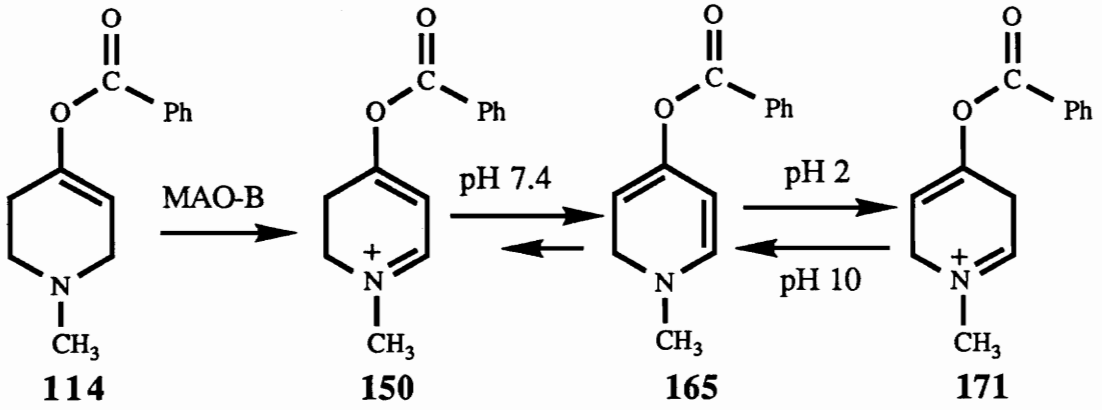

Scheme 45. Proposed equilibria of the the different dihydropyridine species.

In an attempt to evaluate these speculations, synthetic **150** was dissolved in D_2O buffer (pH 7.4) and analyzed by ^1H NMR spectroscopy at pH 7.4 and at pH 2 by addition of DCl. No clear ^1H NMR spectral feature was obtained, probably due to partial hydrolysis of the $BOMDP^+$. It is not clear at this point that whether the dihydropyridinium is simply convert to dihydropyridine and

partially hydrolyze to DMPO and benzoic acid or change to something else since the ^1H NMR spectrum was quite complicated.

Based on the above information, however, it is clear that the benzoyl moiety is well tolerated by the active site of MAO-B. The immediate metabolite is the expected dihydropyridinium compound **150**. All of the properties of the metabolite and synthetic **150** are identical. The reason why **150** is resistant to hydrolysis in buffer solution is still unclear. The ^1H NMR spectral results described above are particularly difficult to interpret. The tendency of the synthetic material to hydrolyze and/or undergo other reactions, even in pH 7.4 buffer, while the metabolically generated product is stable for days needs to be understood better. Unfortunately, this instability has prevented the isolation of **150** as a pure species.

The estimated value of the molar extinction coefficient (ε) for BOMDP$^+$ was determined as follows: Synthetic BOMDP$^+$ (**150**) was slowly hydrolyzed to the corresponding DMPO (**113**) as evidenced by the increase in the absorbance at 325 nm which correspond to the formation of DMPO and decrease the absorbance at 280 nm corresponding to the loss of **150** (Fig. 74). Since the extinction coefficient for DMPO is known[118] and assuming the conversion from the BOMDP$^+$ to DMPO is quantitative, the extinction coefficient for BOMDP$^+$ was preliminary estimated as ε = 10,000.

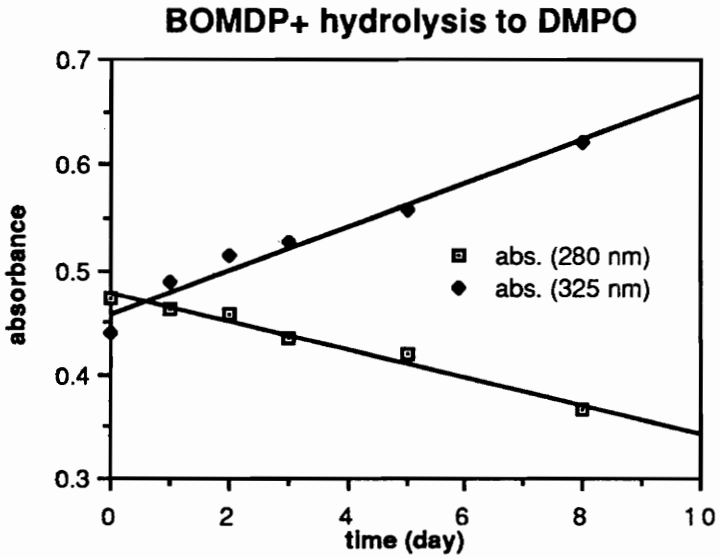

Fig. 74. Measurement of BOMDP$^+$ converting to DMPO.

Based on the ε = 10,000 of the BOMDP+, the K_m (385 μM) and V_{max} (50 nmole/min· U) was also estimated from the following curves (Fig. 75 and Fig. 76).

The MAO-B inhibitory properties of **114** also were examined using the conversion of MPTP to MPDP+ to monitor remaining enzyme activity. The results by comparing with the buffer solution control (Fig. 77) showed that **114** is an moderate inactivator of MAO-B.

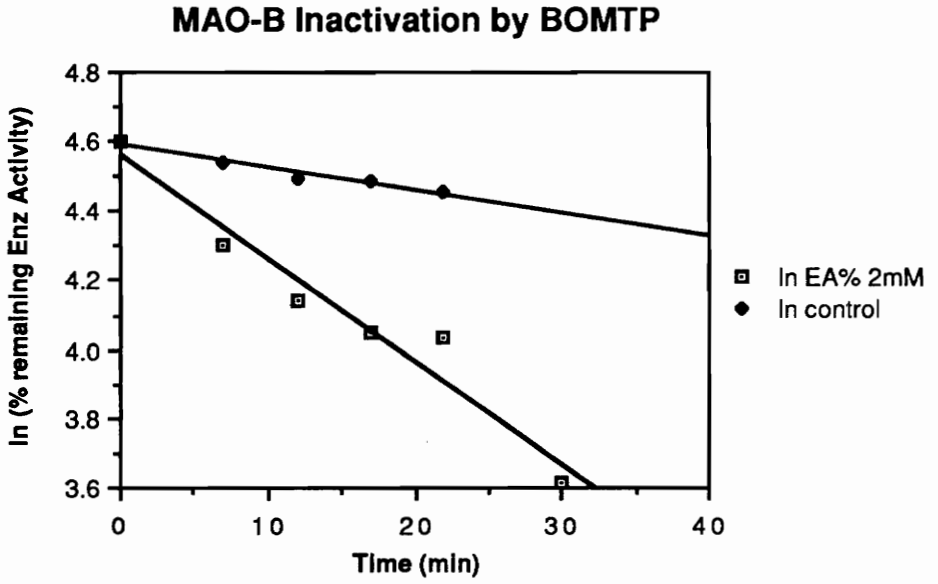

Fig. 77.

The 4-(2-acetylsalicyloyl)-1-methyl-1,2,3,6-tetrahydro-pyridine (ASMTP, **136**) was also incubated with MAO-B in sodium phosphate buffer and the incubation mixture was placed in the spectrophotometer which was thermostated at 37 °C. The UV absorbance was obtained by scanning from 450 nm to 210 nm at different time points with the zero time scan as the subtracted background. The abundance of the absorbance at 304 nm increased slowly up to an O.D. of 1.5 and then leveled off (Fig. 78). The absorbance then slowly shifted towards 330 nm. An aliquot of the incubation mixture was mixed with MPTP in order to measure the remaining activity of MAO-B. No absorbance at 345 nm (no MPDP+ formation) was observed and this result indicated inactivation of the

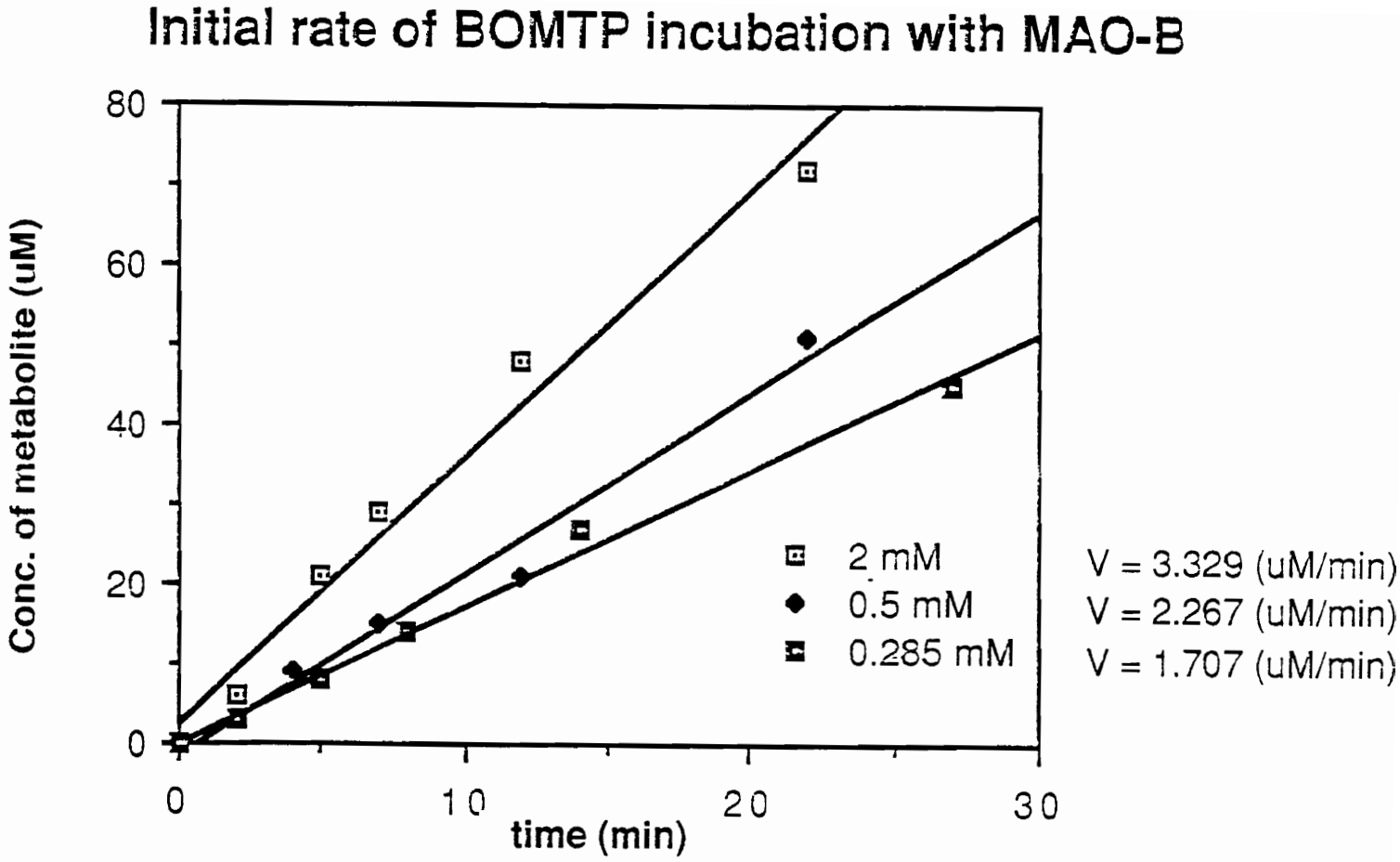
Initial rate of BOMTP incubation with MAO-B
Conc. of metabolite (uM)
80
60
40
20
0
0
10
20
30
time (min)
2 mM
0.5 mM
0.285 mM
V = 3.329 (uM/min)
V = 2.267 (uM/min)
V = 1.707 (uM/min)

Figure. 75.

Double reciprocal plot for the MAO-B catalyzed oxidation of BOMTP

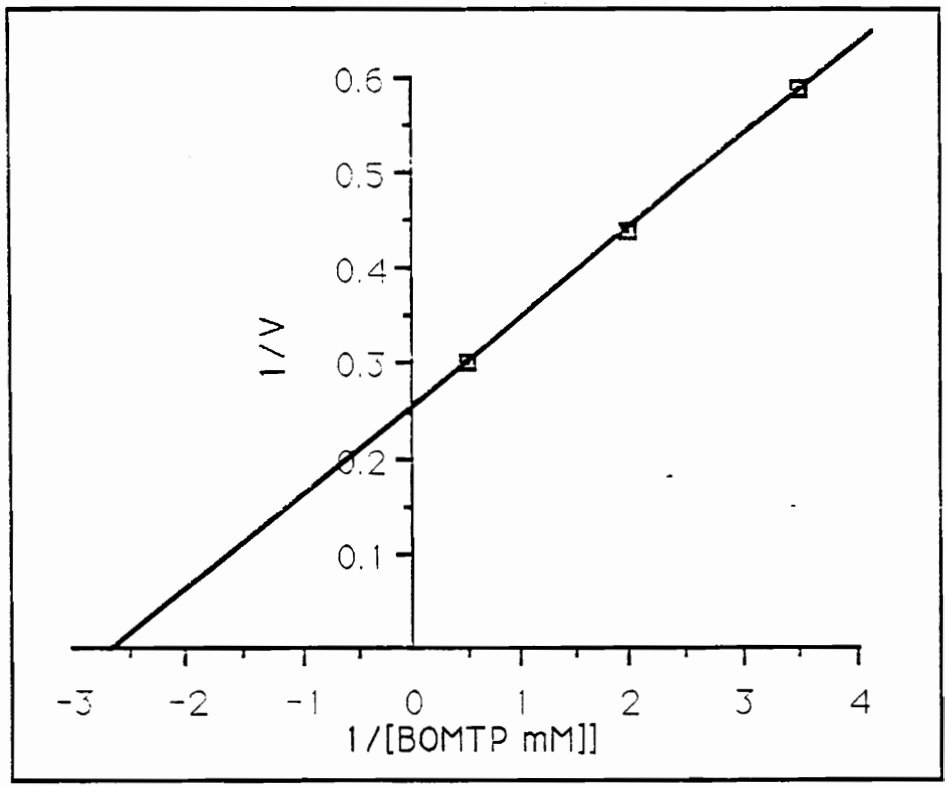

Figure. 76.

MAO-B. The aqueous incubation mixture then was extracted with methylene chloride and the organic layer was analyzed by GC/MS. The GC mass spectrum showed several peaks which corresponded to small amounts of expected products including the aminoenone **113**, acetylsalicylic acid **168**, salicylic acid **169** as well as the substrate **136**. But the absorbance in the buffer solution still remained about the same as before the extraction with methylene chloride suggesting that the compound absorbing at 330 nm is quite water soluble.

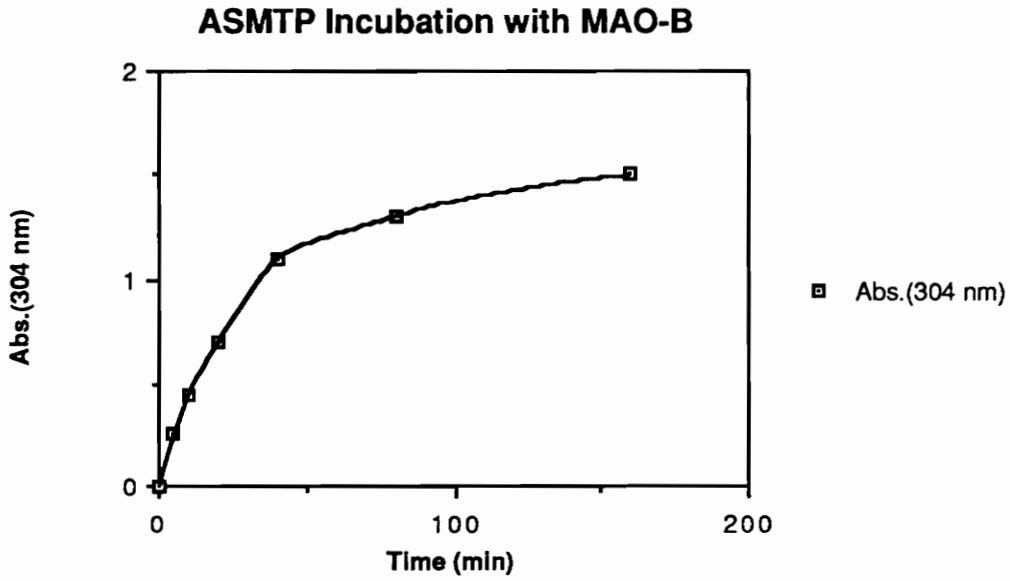

Fig. 78.

During the acetylsalicylic acid (ASA) incubation with MAO-B, a new peak formed at 296 nm (Fig. 79). Since acetylsalicylic acid is not likely to be a substrate of MAO-B, the absorbance at 296 nm was considered to be due to the formation of salicylic acid (λ_{max} = 300 nm),[120] which probably is a consequence of chemical hydrolysis. This assumption was confirmed by showing the conversion of acetylsalicylic acid to the salicylic acid under same conditions employed in the enzyme studies (Fig. 80).

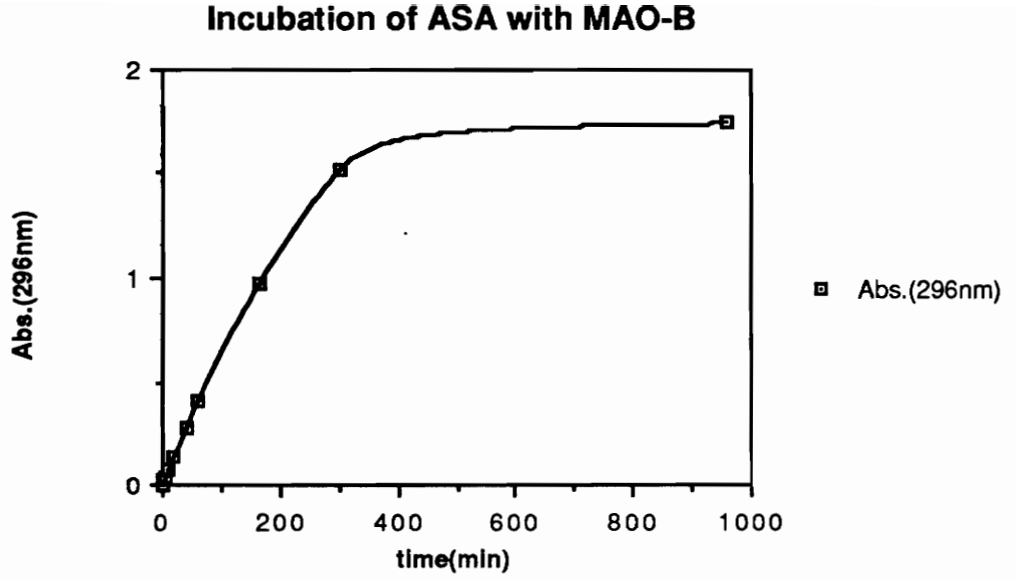

Fig. 79.

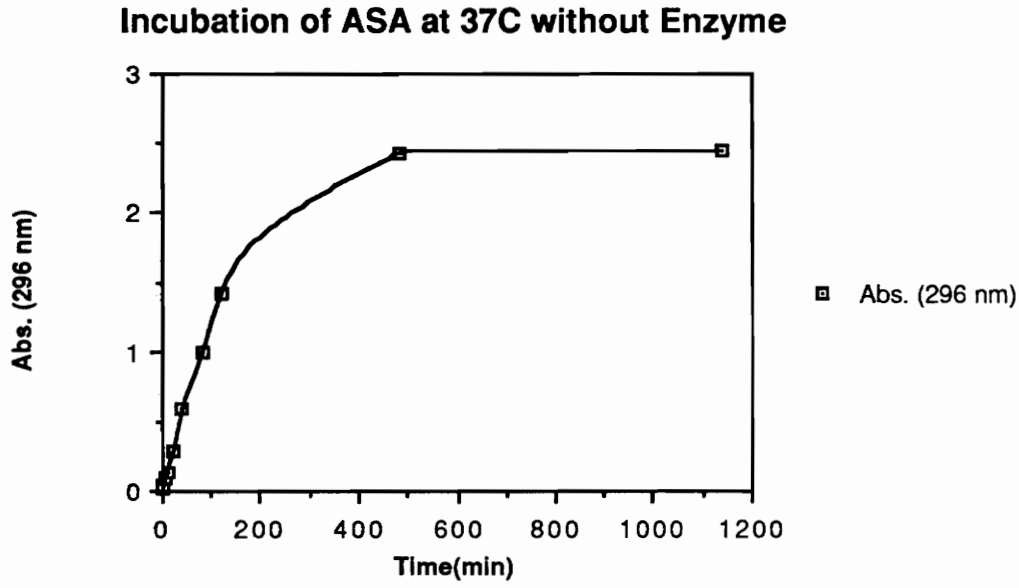

Fig. 80

The same result was obtained with 4-(2-acetylsalicyloyl)-1-methyl-1,2,3,6-tetrahydropyridine (**136**) under these conditions. Thus incubation of **136** in the absence of enzyme led to the formation of a new chromophore with λ_{max} 305 nm which is likely to be due to the formation of salicylic acid via hydrolysis of **136** (Fig. 81).

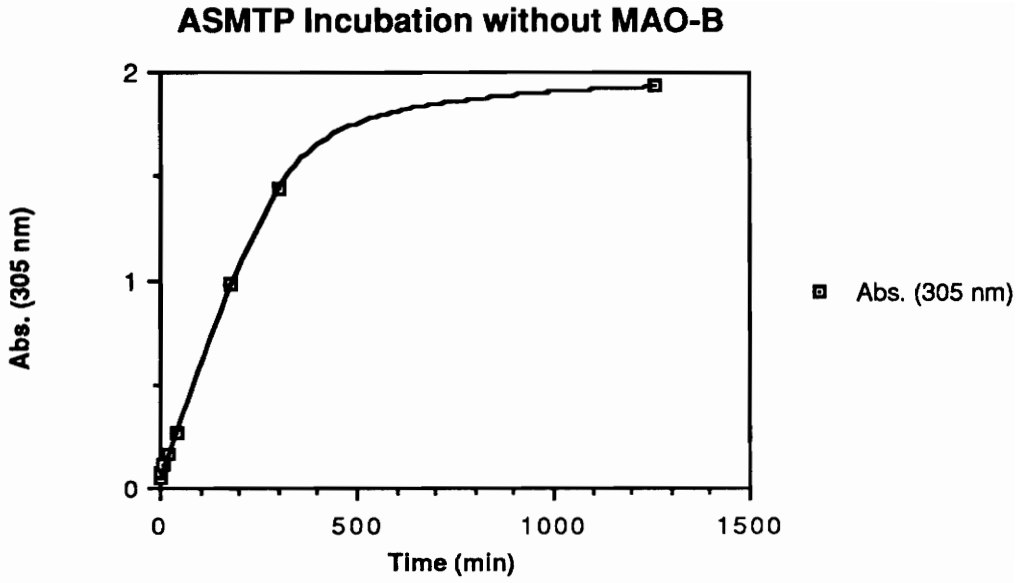

Fig. 81.

These results led us to consider the possibility that the acetylsalicylic acid, in other words the acetyloxy function group, is chemically unstable under the incubation conditions. Therefore it was not clear if the formation of the absorbance observed previously from the incubation of **136** with MAO-B is enzymatically mediated or due to simply chemical hydrolysis. Both pathways may contribute since compounds **114** and **136** have similar structural features, and therefore it is reasonable to expect that **136** would be a substrate of MAO-B. Although **136** is likely to be a substrate of MAO-B based on its structural similarity with **114** and the observed time dependent inactivation of the enzyme, its substrate properties could not be demonstrated unambiguously due to the chemical instability of the acetyloxy group and the possibility that the UV spectrum of the hydrolysis product probably overlaped with that of the expected dihydropyridinium species **170**.

In order to identify what compound(s) was responsible for the inactivation of the enzyme, substance likely to be formed in the incubation mixture including 1-methyl-4-piperidone (**115**), acetylsalicylic acid (**168**), benzoic acid (**152**), compounds which could be formed by simple hydrolysis of the substrate, and 1-

methyl-2,3-dihydro-4-pyridone (**113**), which only can be formed by enzymatic oxidation via the dihydropyridinium metabolite, were incubated with MAO-B followed by assessment of remaining enzyme activity with MPTP. The results showed none of these compounds is responsible for the inactivation of MAO-B. Therefore the corresponding dihydropyridinium species are probably the compounds responsible for the enzyme inactivation.

4.4. Experimental

1-Methyl-1,2,3,6-tetrahydro-4-(trimethylsilyloxy)-pyridine (116). A mixture of dry 1-methyl-4-piperidone (**115**, 30 mL, 0.24 mol, dried by distillation from P_2O_5 under vacuum at 190 °C), chlorotrimethylsilane (45 mL, 0.36 mol) and triethylamine (100 mL, 1.08 mol) in 300 mL of dry 1,4-dioxane was heated under reflux for 3 days. At the end of the reaction, the white solid (triethylamine hydrochloride) was removed by suction and washed with ethyl ether (40 mL). The combined organic filtrates were then washed with 5% $NaHCO_3$ and water, dried over $MgSO_4$ and evaporated under reduced pressure at 90 °C for 15 minutes, to yield 33 g (75%) of a light yellow oil: ^1H NMR ($CDCl_3$) 4.75 (t, 1H, olefinic proton), 2.85 (d, 2H H-6), 2.48 (t, 2H, 2-H), 2.26 (s, 3H, N-methyl), 2.12 (m, 2H, H-3), 0.1 (s, 9H, Si-methyls); GC/MS (m/z, %) [GC temperature program: 50 °C for 1 minute, then 25 °C/minute up to 275 °C (retention time 3.15 minute)] 185 ($M^{+\cdot}$, 50), 184 ($M^{+\cdot}$- H, 100), 170 (15), 142 (10), 127 (45), 96 (45), 73 (55).

3-Benzylaminothiocarbonyl-1-methyl-4-piperidone (123). The starting material, 1-methyl-1,2,3,6-tetrahydro-4-(trimethylsilyloxy)pyridine (**116**, 2 mL, 11.89 mmol) was mixed with methyllithium (8.49 mL, 11.89 mmol) under a nitrogen atmosphere and the resulting solution was allowed to stir at room temperature overnight. The solution then was diluted with 30 mL of dry THF and added to benzylisothiocyanate (1.57 mL, 11.89 mmol) in 25 mL dry THF dropwise. A yellow precipitate formed immediately. The yellow solid was obtained by suction (about 4 g, mp 134-139 °C dec.) and then dissolved in water. After filtering, the filtrate was adjusted to pH = 6-7 by adding 1N HCl and extracted with methylene chloride. The methylene chloride was dried over $MgSO_4$, filtered and evaporated to yield a yellow solid which, unfortunately, decomposed in the Dry-Pistal with toluene as solvent: GC/MS (m/z, %) [GC temperature program: 50 °C for 1 minute, then 25 °C/minute up to 275 °C (retention time 10.11 minute)] 262 ($M^{+\cdot}$, 10), 261 (30), 260 (80), 226 (20), 156 (30), 155 (100), 154 (70), 106 (25), 91 (70).

4-Benzoyloxy-1-methyl-1,2,3,6-tetrahydropyridine (BOMTP, 114). A mixture of the 1-methyl-4-trimethylsilyloxy-1,2,3,6,-tetrahydropyridine (1 mL, 6 mmol) and methyllithium (4.5 mL of 1.4 M ether solution, 6 mmol) was stirred at room temperature for 6 hours to form a clear yellow enolate solution. Hexamethyl-phosphoramide (HMPA, distilled from CaH_2, 5 mL, 18 mmol) was added to the enolate solution which caused color to darken to an orange-brown. Next, benzoic anhydride (1.4 g, 6 mmol) in 15 mL of dry THF was added rapidly color change to yellow. The mixture was stirred for another hour and poured into 50 mL of water (pH about 7-8) and extracted with hexane (30 mL x 2). After separation, the combined hexane layer was washed with 5% of sodium bicarbonate and the organic layer was dried over $MgSO_4$. After removing the solvent, the product (550 mg, 42%) as a light oil was obtained. The product was further purified by centrifugal chromatography with methylene chloride/ethyl acetate (1:1, 1:2 and 1:3) as the solvents to form a light yellow crystalline solid: mp 47-49 °C; UV λ_{max}(water) 233 nm (ε 12550); ^1H NMR ($CDCl_3$) 8.15-8.05 and 7.65-7.42 (m, 5H, aromatic protons), 5.52 (t, 1H, olefinic proton on C-5 of the tetrahydropyridine ring), 3.12 (d, 2H, H-6), 2.72 (t, 2H, H-2), 2.42 (s, 3H, N-methyl), 2.40 (m, 2H, H-3); GC/MS (m/z, %) [GC temperature program: 50 °C for 1 minute, then 25 °C/minute up to 275 °C (retention time of the product is 6.21 minute)] 217 ($M^{+\cdot}$, 10), 112 ($M^{+\cdot}$- PhCO, 40), 105 (benzoyl cation, 100), 96 ($M^{+\cdot}$ - benzoyloxy, 35), 77 (45) 70 (30). Anal. Calcd for $C_{13}H_{15}NO_2$: C 71.87, H 6.96, N 6.45. Found: C 71.74, H 6.98, N 6.45.

4-Benzoyloxy-1-methylpyridinium Iodide (134). The 4-hydroxypyridine (950 mg, 10 mmol) suspended in distilled chloroform (100 mL) was heated under reflux for 30 minute with benzoic anhydride (2.26 g, 10 mmol). After cooling, the solution was washed with potassium carbonate (30 mL) and distilled water (20 mL) and dried over magnesium sulfate and filtered. Evaporation of the solvent gave 4-benzoyloxypyridine (**133**) as a white solid: GC/MS (m/z, %) [GC temperature program: 50 °C for 1 minute, then

25 °C/minute up to 275 °C (retention time 5.94 minute)] 199 ($M^{+\cdot}$, 5), 105 (benzoyl cation, 100), 77 (45) 51 (20). The solid **133** then was redissolved in distilled acetone (30 mL) and excess iodomethane (3.2 mL, 50 mmol) was added. The resulting solution was stirred at room temperature for 3 hours. Meanwhile a yellow solid was formed and it was obtained by suction (2.56 g, 74% overall). The product was recrystallized from acetone to give a light yellow crystalline solid: mp 203-205 °C (dec); UV λ_{max} (water) 246 nm (ε = 20180 M^{-1}); ^1H NMR (CD_3OD) 9.02 (d, 2H, H-2 and H-6), 8.26 (m, 2H, H-2' and H-6'), 8.16 (d, 2H, H-3 and H-5), 4.48 (s, 3H, N-methyl). Anal. Calcd for $C_{13}H_{12}NO_2I$: C 45.77, H 3.55, N 4.11. Found: C 45.73, H 3.57, N 4.12.

4-Benzoyloxy-1-methyl-1,2,3,6-tetrahydropyridine (BOMTP, 114). The 4-Benzoyloxy-1-methylpyridinium iodide (**134**, 1 g, 2.94 mmol) was dissolved in methanol (30 mL) and the solution was cooled to 0 °C by an ice-bath. Sodium borohydride (224 mg, 5.88 mmol) was added to the solution at 0 °C and the reaction mixture was stirred for about 5 minute. The solution was reduced to a small volume by removing the solvent and distilled water (20 mL) and methylene chloride (30 mL) were added. The product was extracted with methylene chloride (30 mL x 2) and the organic layer was dried over magnesium sulfate and filtered. After evaporating the solvent, the product was obtained as an off-white solid (530 mg, 83%) and was recrystallized from hexane:methylene chloride (1:1) to give an off-white crystal: mp. 46-48 °C. The spectroscopic data of the compound are identical with that of the product synthesized by original method which was fully characterized.

4-Benzoyloxy-1-methyl-1,2,3,6-tetrahydropyridine N-oxide (151). To a solution of 4-Benzoyloxy-1-methyl-1,2,3,6-tetrahydropyridine (20 mg, 0.09 mmol) in methylene chloride was added with *m*-chloroperoxybenzoic acid (32 mg, 0.09 mmol) at 0 °C. The solution was stirred at 0 °C for 5 hours, and a white solid residue was obtained after removing the solvent under reduced pressure. The residue was filtered through a short alumina column with methylene chloride and methylene chloride/methanol (9:1) to form

the N-oxide free base as off-white crystalline solid: mp 88-90 °C; ^1H NMR ($CDCl_3$) 8.18 (d, 2H, H-2' and H-6'), 7.65 (t, 1H, H-4'), 7.55 (t, 2H, H-3' and H-5'), 5.55 (t, 1H, H-5), 4.1 (d, 2H, H-6), 3.65 (t, 2H, H-2), 3.4 (s, 3H, N-methyl group), 2.8 (m, 2H, H-3). Anal. Calcd for $C_{13}H_{15}NO_3 \cdot 1.2H_2O$: C 61.22, H 6.82, N 5.49. Found: C 61.22, H 6.88, N 5.78.

4-Benzoyloxy-1-methyl-2,3-dihydropyridine (BOMDP$^+$ 150). The N-oxide **151** was dissolved in 20 mL of dry methylene chloride (dried by through a column with activated alumina). To the methylene chloride solution was added with trifluoroacetic anhydride (TFAA, 0.5 mL, 3.5 mmol) and the resulting reaction mixture was stirred at 0 °C for 2 hours. After removing the solvent and excess TFAA, the product was characterized by ^1H NMR: ^1H NMR ($CDCl_3$) 8.52 (d, 2H, H-6), 8.08 (d, 2H, H-2' and H-6'), 7.68 (t, 1H, H-4'), 7.5 (t, 2H, H-3' and H-5'), 6.78 (d, 2H, H-5), 4.18 (t, 2H, H-2), 3.68 (s, 3H, N-methyl group), 3.18 (t, 2H, H-3).

4-(2-Acetylsalicyloyl)-1-methylpyridinium Iodide (140). The 4-hydroxypyridine (475 mg, 5 mmol) was suspended in distilled chloroform (100 mL) and the reaction mixture was heated under reflux with acetylsalicyloyl chloride (995 mg, 5 mmol) for 30 minute. After cooling, the solution was washed with potassium carbonate solution (20 mL) and distilled water (15 mL) and the organic layer was dried over magnesium sulfate and filtered. After removing the solvent, the 4-(2-acetylsalicyloyl)pyridine (**137**) was obtained as a light yellow crystalline solid (1.2 g, 93%): GC/MS (m/z, %) [GC temperature program: 50 °C for 1 minute, then 25 °C/minute up to 275 °C (retention time 7.03 minute)] 257 ($M^{+\cdot}$ 2), 215 (5), 163 (50), 121 (100), 92 (20), 65 (20); ^1H NMR ($CDCl_3$) 8.75 (d, 2H, H-2 and H-6), 8.22 (d, 1H, H-6'), 7.95 (d, 1H, H-3'), 7.68 (t, 1H, H-4'), 7.40 (t, 1H, H-5'), 7.22 (d, 2H, H-3 and H-5), 2.38 (s, 3H, $COCH_3$). The 4-(2-acetylsalicyloyl)pyridine **137** then was dissolved in distilled acetone (50 mL) and the iodomethane (1.6 mL, 25 mmol) was added to the solution. The reaction mixture was stirred overnight at room temperature and a yellow solid started to form at about 3 hours. The

solid (1.5 g, 81%) was collected by suction and further purified by recrystallization from acetone to yield yellow needles: mp 175-177 °C; UV λ_{max} (water) 229 nm (ε = 22180 M^{-1}); ^1H NMR ($CDCl_3$) 9.02 (d, 2H, H-2 and H-6), 8.30 (dd, H, H-6'), 8.08 (d, 2H, H-3 and H-5), 7.84 (m, 1H, H-4'), 7.52 (m, 1H, H-5'), 7.32 (dd, 1H, H-3'), 4.48 (s, 3H, N-methyl), 2.35 (s, 3H, $COCH_3$). Anal. Calcd for $C_{15}H_{14}NO_4I$: C 45.13, H 3.54, N 3.51. Found: C 45.06, H 3.54, N 3.50.

4-(2-Acetylsalicyloyl)-1-methyl-1,2,3,6-tetrahydropyridine Oxalate (136·HOOCCOOH). To a solution of 4-(2-acetylsalicyloyl)-1-methylpyridinium iodide (**140**, 713 mg, 2 mmol) in methanol (50 mL) cooled to 0 °C was added sodium borohydride (76 mg, 2.0 mmol). After stirring for about 5 minute at 0 °C, the reaction mixture was reduced to a small volume by removing the solvent under reduced pressure at room temperature. Distilled water (20 mL) was added to the solution and the product was extracted with methylene chloride (30 mL x 2). The organic layer was dried over magnesium sulfate and filtered. The crude solid product (400 mg, 73%) was obtained by evaporating the solvent. The free base form of the product was converted to an oxalate salt in chloroform by adding oxalic acid (131 mg, 1 eq.) in dry ethyl ether (15 mL). The solid obtained was recrystallized from methanol:ethyl ether (1:2) to yield the white crystalline **136**: mp 142-144 °C; UV λ_{max} (sodium phosphate buffer, pH = 7.4) 240 nm (ε = 18900 M^{-1}); GC/MS (m/z, %) [GC temperature program: 50 °C for 1 minute, then 25 °C/minute up to 275 °C (retention time of the free base is 7.10 minute)] 275 ($M^{+\cdot}$ 5), 163 (30), 121 (100), 112 (20), 96 (20), 70 (20), ^1H NMR (CD_3OD) 8.15 (d, 1H, H-6'), 7.75 (t, 1H, H-4'), 7.42 (t, 1H, H-5'), 7.25 (d, 1H, H-3'), 5.68 (bs, 1H, H-5), 3.92 (bs 2H, H-6), 3.58 (t, 2H, H-2), 3.02 (s, 3H, N-methyl), 2.75 (bs, 2H, H-3), 2.38 (s, 3H, $COCH_3$). Anal. Calcd for $C_{17}H_{19}NO_8$: C 55.89, H 5.24, N 3.83. Found: C 55.62, H 5.25, N 3.82.

2,3-Dihydro-1-methyl-4-pyridone (DMPO, 113). To a solution of 1-methyl-4-piperidone (**115**, 2 mL, 16.3 mmol, distilled) in 5% acetic acid (150 mL) was added mercury acetate (15.6 g, 48.8

mmol) and the reaction mixture was heated to about 90 °C for 18 hours with stirring. The colorless solution turned to a yellow color during the period of the reaction. The reaction mixture was cooled in an ice-water bath and saturated with hydrogen sulfide. The resulting black mercuric sulfide was filtered and washed with 5% acetic acid. The combined filtrates were stirred vigorously in a 1-liter Erlenmeyer flask with 200 mL of methylene chloride while an excess of 25% aqueous sodium hydroxide was added carefully in the cold. The methylene chloride was promptly separated, the aqueous solution was extracted with additional methylene chloride (200 mL x 3), and the combined extracts were dried over magnesium sulfate and filtered. The solvent was removed under reduced pressure to form 1.6 g (60%) of crude product, which was purified by a aluminum column (activated, basic, Brockmann 1, 150 mesh) with ethyl acetate as solvent. The product was eluted in the first fraction (25 mL) and was further purified by PTLC (silica gel, 1 mm) with ethyl acetate:methanol (4:1) as the eluent. The purified product was obtained as a yellow oil: GC/MS (m/z, %) [GC temperature program: 50 °C for 1 minute, then 25 °C/minute up to 275 °C (retention time 3.16 minute)] 111 ($M^{+\cdot}$ 100), 82 (70), 55 (80), ^1H NMR ($CDCl_3$) 6.98 (d, 1H, H-2), 4.98 (d, 1H, H-3), 3.44 (t, 2H, H-6), 3.04 (s, 3H, N-methyl), 2.52 (t, 2H, H-5).

Incubations of 4-benzoyloxy-1-methyl-1,2,3,6-tetra-hydropyridine (BOMTP) with MAO-B. Sodium phosphate buffer (0.1 M, pH 7.4) was used to prepare a 5 mM solution of BOMTP. BOMTP (10.85 mg) was dissolved in 0.1 mL of MeOH and transfered to a 10 mL volumetric flask, filled with 9.8 mL of phosphate buffer and vortexed. The BOMTP buffer solution (1 mL, 5 mM) and MAO-B purified following literature method[121] (50 μL, 0.1 U) was placed in the spectrometer which was thermostated at 37 °C. After 30 sec of equilibration, the absorbance at 324 nm was monitored every 10 sec up to 45 minute. The absorbance at 324 was increased slowly up to 0.045. After 45 minute, half of the incubation mixture with MAO-B (0.5 mL) was mixed with 0.5 mL of 5 mM MPTP and the resulting mixture was monitored at 345 nm every 10 sec for up to 2 minute.

No enzyme activity was observed. The control sample was run under the same conditions (0.5 mL of 5 mM MPTP solution with 0.2 μL, 0.04 U, of MAO-B monitored at 345 nm at every 10 sec for up to 2 minute). BOMTP solution (0.5 mL, 5 mM) with MAO-B (2 μL, 0.04 U) was scanned from 400 nm to 210 nm at 2 minute, 5 minute, 10 minute, 20 minute, 40 minute and the mixture at 0 time scanned as background. Tracing showed a absorbance at 292 nm. The absorbance disappeared after $NaBH_4$ was added. A negative peak was observed which may result from the 0 time background what was not a real 0 time since it which was taken 20 sec after the formation of the incubation mixture.

Incubation of BOMTP with MAO-B

#	time (minute)	abs. (324 nm)
1	0	0
2	1	0.005
3	2	0.009
4	5	0.018
5	10	0.029
6	20	0.037
7	30	0.041
8	40	0.044

Incubation of BOMTP with MAO-B

#	time (min)	abs. (292 nm)
1	0	0
2	1	0.120
3	2	0.204
4	5	0.399
5	10	0.580
6	20	0.702
7	30	0.732
8	40	0.731

The same incubation as above was repeated and the incubation mixture was extracted with methylene chloride (3 mL x 2). The

organic layer was dried over megnasium sulfate and filtered. The solvent of the filtrate was evaporated and the residue was redissolved in 200 μL of methanol to form a sample for GC/MS analysis. The GC/MS result showed peaks corresponding to the **113**, Benzoic acid and other unidentified components. The aqueous layer after extraction with methylene chloride was remeasured by UV and the absorbance at 292 nm was still there. The aqueous layer was then analyzed by HPLC with a C18 column and a diode array detector after removed the protein by adding cool methanol and centrifugaled for 2 minute at 14,000 rsp with A:B (90:10) as solvent system [A = (CH_3CN:H_2O:Et_3N:HOAc)(10:90:1:5), B = CH_3CN] and flow rate at 1 mL/minute.

BOMTP solution (0.8 mL, 5 mM) with MAO-B (50 μL, 0.05 U different bench of enzyme from the above bench) was scanned from 400 nm to 210 nm at 2 minute, 5 minute, 10 minute, 20 minute, 40 minute, 80 minute and the mixture as the background. At the end of the incubation, the HCl solution (1 M, several drops) was added until pH to about 1.5 and the acidic mixture was scanned again. No UV absorbance at 292 nm was observed and the mixture was readjusted to pH about 12.5. The absorbance at 292 nm was observed again although at lower intensity.

Incubation of BOMTP with inactivated MAO-B by deprenyl. Deprenyl sodium phosphate buffer solution (0.1 mL, 1 mM, pH = 7.4) was mixed with MAO-B (50 μL, 0.05 U) and 350 μL of phosphate buffer (0.1 M, pH = 7.4) at 37 °C and the resulted solution was thermostated for 10 minute. BOMTP buffer solution (50 μL, 5 mM) was added to form an incubation mixture with final BOMTP concentration at 0.5 mM. The incubation mixture at zero time was taken as background and the UV spectrum was scanned from 450 nm to 210 nm at 0, 2, 5, 10, 20, 60, 100, and 190 minute. No absorbance was observed.

Inhibition Assay of MAO-B by BOMTP.

Procedure of the enzyme inhibition studies:

1. Start the UV instrument and take it to Program 6 Kinetic data. Touch the R/S key, toggle with the enter key, have the total time of each run at 2 minute. Set the wavelength at 345 nm for the monitoring of $MPDP^+$ formation. Calibrate the UV spectrophotometer with 0.5 mL of 5 mM MPTP phosphate buffer solution in a 1 mL cuvette.

2. Homogenize the enzyme (MAO-B), two runs with a homogenizer.

3. Clean the cuvette thoroughly, and place 0.5 mL of 5 mM MPTP solution, place it in the UV spectrophotometer. Place 80 μL of 5 mM stock solution of BOMTP in a small vial with 20 μL of phosphate buffer, take 100 μL of MAO-B (0.1U), start the stopwatch and add the enzyme to the vial to form a enzyme-inhibitor mixture with a final 2 mM of BOMTP concentration. Shake it well and add 25 mL of this mixture to the cuvette containing 0.5 mL of 5 mM MPTP, shake the cuvette twice and place it in the UV instrument and push the R/S key to read the data. This first read is taken as time t=0. Place the vial containing the enzyme and BOMTP in the incubator which is at 37 °C and the temperature of the UV is also 37 °C.

4. Replace the tip on the 25 μL pipette, at the end of the run, quickly wash the UV cell and place 0.5 mL of 5 mM MPTP into the cell, place it back in the spectrophotometer. Take another 25 mL of enzyme-inhibitor mixture from the vial which was placed in the incubator, add it to the cuvette containing 0.5 mL of 5 mM MPTP. The cuvette then was shacked twice and placed back in the spectrophotometer and the kinetic data obtained as t=5 minute.

5. Repeat the same procedure for t=10 minute, 15 minute, 20 minute and 30 minute and plot the data on the Mac. Cricket Graph.

6. Once the enzyme inhibition studies are carried out, run a simple study without inhibitor, use only the MAO-B and MPTP as negative control.

The BOMTP sodium phosphate buffer solution (80 μL, 5 mM) was mixed with MAO-B (100 μL, 0.1 U) and 20 μL of buffer solution (pH = 7.4) to form a assay mixture with BOMTP concentration as 2 mM. A aliquot (25 μL) of the resulted mixture at 37 °C was

transfered at 5, 10, 15, 20, 30 minute to a cell incubated at 37 °C with MPTP buffer solution (0.5 mL, 5 mM). The initial rate of the formation of the $MPDP^+$ for each aliquot at different time point was obtained from the spectrophotometer as a slope of the kinetic data. The k_{obs} was obtained as the slope of the curve with ln (% of remaining enzyme activity) vs time. The mixture (35 µl) of MAO-B (100 µL, 0.1 U) and sodium phosphate buffer solution (100 µL, pH = 7.4) at 37 °C and then transfered at 5, 10, 15, 20, 30 minute to a cell incubated at 37 °C with MPTP buffer solution (0.5 mL, 5 mM) was taken as control.

Inhibition of MAO-B by BOMTP

#	time (min)	initial rate (r)	% (r)	ln (% EA, 2 mM)
1	0	0.0943	100.000	4.605
2	7	0.0695	73.700	4.300
3	12	0.0592	62.778	4.140
4	17	0.0540	57.264	4.048
5	22	0.0532	56.416	4.032
6	30	0.0356	37.116	3.614

Buffer solution as control

#	time (min)	initial rate (r)	% (r)	ln (control)
1	0	0.01719	100.000	4.605
2	5	0.01616	94.008	4.543
3	10	0.01533	89.180	4.494
4	15	0.01503	89.005	4.489
5	20	0.01480	86.097	4.455

Incubation of ASMTP with MAO-B. The ASMTP buffer solution (0.5 mL, 5 mM, 18.25 mg/10 mL of sodium phosphate buffer, pH = 7.4) was mixed with 50 µL of MAO-B (0.05 U) at 37 °C and followed same procedure as above. The UV spectrum was recorded at different time up to 160 minute.

Incubation of ASMTP with MAO-B

#	time (min)	abs. (304 nm)

1	0	0
2	5	0.25
3	10	0.45
4	20	0.70
5	40	1.10
6	80	1.30
7	160	1.50

The incubation mixture was then extracted with methylene chloride (2 mL x 2) and the aqueous layer was measured by UV spectrophotometer again after the trace amount of organic solvent was blowed off by N_2. The UV spectrum showed same absorbance as that of before the extraction with almost same intensity and the aqueous sample was also analyzed by HPLC followed same procedure as for BOMTP. The organic layer was dried over magnesium sulfate and filtered and the concentrated filtrate was checked by GC/MS with temperature program as 50 °C for 1 minute, then 25 °C/minute up to 275 °C. The GC/MS results indicated the existence of aminoenone (**113**), 1-methyl-4-piperidone (**115**), acetylsalicylic acid, salicylic acid, ASMTP and other unidentified compounds.

Incubation of 1-methyl-4-piperidone (MPD) with MAO-B The 1-methyl-4-piperidone buffer solution (0.5 mL, 3 mM, 3.7 µl of substrate/10 mL sodium phosphate buffer, pH = 7.4) mixed with MAO-B (50 µL, 0.05 U) and the resulted mixture was taken as the background. The mixture was incubated at 37 °C and scanned from 450 nm to 210 nm up to 40 minute. No peak formation was observed on UV spectrum. The MPTP buffer solution (0.3 mL, 5 mM) was then added to the above incubation mixture. The resulted mixture was measured at 345 nm which corresponding to the absorbance of $MPDP^+$ for 2 minute. The result showed the formation of $MPDP^+$, which indicated that the enzyme was still active.

Incubation of 2,3-dihydro-1-methyl-4-pyridone (DMPO) with MAO-B. DMPO buffer solution (0.5 mL, 3 mM, 3.33 mg/10 mL of sodium phosphate buffer solution, pH = 7.4) was incubated up to 40 minute with MAO-B followed above procedure.

No peak formation on UV spectrum was observed. MPTP buffer solution (0.2 mM, 5 mM) was added to the incubation mixture and the formation of $MPDP^+$ was observed on UV spectrum by scanning from 450 nm to 210 nm up to 55 minute, which indicating the enzyme activity. (Since aminoenone has a absorbance at 324 nm, the absorbance of $MPDP^+$ at 345 was partially automatically subtracted by the instrument, therefore the absorbance at 361 nm turned out to be an observed λ_{max}).

Formation of $MPDP^+$ with DMPO/MAO-B plus MPTP

#	time (min)	abs.(361 nm)
1	0	0.04
2	2	0.09
3	4	0.13
4	6	0.18
5	15	0.32
6	25	0.43
7	35	0.52
8	45	0.60
9	55	0.65

Incubation of Acetylsalicylic acid (ASA) with MAO-B. ASA buffer solution (0.5 mL, 3 mM, fresh made 5.4 mg of ASA/10 mL of sodium phosphate buffer, pH = 7.4) was incubated at 37 °C with MAO-B up to 20 hours following above method. A peak formation on UV spectrum was observed at 296 nm.

Incubation of ASA with MAO-B

#	time (min)	abs. (296 nm)
1	0	0
2	2	0.02
3	5	0.04
4	10	0.08
5	20	0.14
6	40	0.28
7	60	0.41

8	165	0.97
9	300	1.51
10	960	1.74

MPTP solution (0.2 mL, 5 mM) was added to the incubation mixture and the formation of $MPDP^+$ corresponding to the absorbance at 345 nm was recorded after taking the new resulted mixture as background.

Formation of MPDP with ASA/MAO-B plus MPTP

#	time (min)	abs. (345 nm)
1	0	0.056
2	2	0.230
3	5	0.365
4	10	0.610
5	20	0.990

Incubation of benzoic acid (BA) with MAO-B. BA buffer solution (fresh made solution, 1 mL, 5 mM, 2.17 mg of BA/2 mL of sodium phosphate buffer, pH = 7.4) was mixed with MAO-B (10 μL, 0.04 U) and measured by spectrophotometer as above up to 20 minute. No peak formation on UV spectrum was observed. MPTP buffer solution (0.2 mL, 5 mM) was added to above solution and absorbance at 345 nm corresponding to the formation of $MPDP^+$ was observed, which indicating the enzyme was still active.

Formation of $MPDP^+$ with BA/MAO-B mixture

#	time (min)	abs. (345 nm)
1	0	0.09
2	2	0.32
3	5	0.53
4	10	1.00

Stability test for ASA at 37 °C in sodium phosphate buffer. ASA sodium phosphate buffer solution (fresh made solution, 1 mL, 3 mM) was thermostated at 37 °C up to 19 hours and the UV

spectrum was scanned from 460 nm to 210 nm. A peak at 296 nm was formed probably due to the formation of salicylic acid.

Stability of ASA at 37 °C in sodium phosphate buffer

#	time (min)	abs. (296 nm)
1	0	0.02
2	2	0.04
3	5	0.09
4	10	0.14
5	20	0.28
6	40	0.59
7	80	0.99
8	120	1.42
9	480	2.43
10	1140	2.45

Stability test for ASMTP at 37 °C in sodium phosphate buffer. ASMTP sodium phosphate buffer (fresh made solution, 1 mL, 5 mM) was thermostated at 37 °C for 21 hours and the solution was scanned from 460 nm to 210 nm at different time point. The UV spectrum showed a peak formation at 305 nm, which might resulted from the formation of 1-methyl-4-salicyloyl-1,2,3,6-tetrahydro-pyridine.

Stability of ASMTP at 37 °C in phosphate buffer

#	time (min)	abs. (305 nm)
1	0	0.048
2	2	0.072
3	10	0.110
4	20	0.165
5	40	0.272
6	180	0.980
7	300	1.438
8	1260	1.932

REFERENCES

1. Mitchell, J. R., Horning, M. G. (1984) Drug Metabolism and Drug Toxicity. Raven Press. New York, p 1.
2. Gibson, G., Skett, P. (1986) Introduction to Drug Metabolism. Chapman and Hall, pp. 1-38.
3. Nogrady, T. (1985) Medicinal Chemistry: A biochemical approach. Oxford University Press, New York, p362.
4. Miller, E. C.; Miller, J. A. (1985) Some historical perspectives on the metabolism of xenobiotic chemicals to reactive electrophiles. in Bioactivation of Foreign Compounds. (Anders, M. W. ed.), Academic Press, Inc., Orlando, pp. 3-28.
5. Cummings, S., Prough, R. (1983) Metabolic formation of toxic metabolites. in Biological Basis of Detoxication. (Caldwell, J.; Jacoby, W. eds.) Academic Press, Inc. New York, pp. 2-30.
6. Holtzman, J. L. (1982) Role of reactive oxygen and metabolite binding in drug toxicity. *Life Sci.* **30,** 1-9.
7. Borm, P., Mingels, M., Hulshoff, A., Frankhuyzen-Sierevogel, A., Noordhoek, J. (1983) Rapid formation of N-hydroxymethylpentamethyl-melamine by mitochondria from rat small intestinal epithelium. *Life Sci.* **33,** 2113-2119.
8. Gooderham, N. J., Murray, S., Rice, J. C., Boobis, A. R., Davies, D. S. (1989) Dietary heterocyclic amines and human cancer. *Drug Metab. Rev.* **20,** 285-305.
9. Gooderham, N. J., Rice, J. C., Boobis, A. R., Davies, D. S. (1988) *Human Toxicol.*, **7,** 79.
10. Chen, S., Besman, M. J., Shively, J. E., Yanagibashi, K., Hall, P. F. (1989) Human aromatase. *Drug Metab. Rev.* **20,** 511-517.
11. Mukhtar, H., Khan, W. A. (1989) Cutaneous cytochrome P-450. *Drug Metab. Rev.* **20,** 657-673.
12. Marietta, M. P., Vessel, E. S., Hartman, R. D., Weisz, J., Dvorchik, H. (1979) Characterization of cytochrome P-450-dependent aminopyrine N-demethylase in rat brain: comparison with hepatic aminopyrine N-demethylation. *J. Pharmacol. Exp. Ther.* **208,** 271-279.

13. Vessey, D. (1982) Hepatic metabolism of drugs and toxins. in Hepatology (Zakim, D., Boyer, T. eds.) W. B. Saunders, Philadelphia, pp.197-230.
14. Benedetti, S., Dostert, P., Tipton, K. (1988) Contributions of monoamine oxidase to the metabolism of xenobiotics. in Progress in Drug Metabolism (Gibson, G. ed) Taylor and Francis Ltd. **Vol. 11,** pp. 149-174.
15. Cooper, D., Schleyer, H., Rosenthal, O. (1973) Chemistry of cytochrome P-450 purified from endocrine systems. *Drug Metab. Dispos.* **1,** 21-28.
16. Bend, J., Hook, G., Gram, T. (1973) Characterization of lung microsomes as related to drug metabolism. *Drug Metab. Dispos.* **1,** 358-367.
17. Orrenius, S., Ellin, A., Jakobsson, S, Thor, H., Cinti, D.; Schenkman, J. Estabrook, R. (1973) The cytochrome P-450 containing monooxygenase system of rat kidney cortex microsomes. *Drug Metab. Dispos.* **1,** 350-357.
18. Lehninger, A. (1975) Oxidation-reduction enzymes and electron transport. in Biochemistry. Worth Publishers, Inc., New York, pp. 477-508. 19. Haugen, D., van der Hoeven, T., Coon, M. (1975) Purified liver microsomal cytochrome P-450. *J. Biol. Chem.* **250,** 3567-3570.
20. Lu, A., West, S. (1980) Multiplicity of mammalian microsomal cytochromes P-450. *Pharmacol. Rev.* **31,** 277-295.
21. Mazel, P. (1971) Experiments illustrating drug metabolism *in vitro*. in Fundamentals of Drug Metabolism and Drug Disposition (LaDu, B., Mandel, H., Way, E. eds.), Williams and Wilkings, Baltimore, pp. 546-582.
22. White, R., Coon, M. J. (1980) *Ann. Rev. Biochem.*, **49,** 315-56.
23. Pocchiari, F., Pataccini, R., Castelnovo, P., Longo, A., Cassgrande, C. (1986) *Drug Res.* **36,** 334.
24. Tipton, K. F., McCrodden, J. M., Youdim, M. B. H. (1986) Oxidation and enzyme-activated irreversible inhibition of rat liver monoamine oxidase-B by 1-methyl-4-phenyl-1,2,3,6-tetrahydropyridine (MPTP). *Biochem. J.* **240,** 379-383.

25. Silverman, R. B., Hoffman, S. J., Catus, W. B. (1980) A mechanism for mitochondrial monoamine oxidase catalyzed amine oxidation. *J. Am. Chem. Soc.*, **102,** 7126-7128.
26. Glover, V., Gibb, C., Sandler, M. (1986) The role of MAO in MPTP toxicity-A review. *J. Neural Trans. Suppl.* **XX,** 65-76.
27. Unzeta, M., Castro, J., Gomer, N., Tipton, K. F. (1983) *Brit. J. Pharmacol.*, **80,** 622.
28. Downing, J. (1986) The psychological and physiological effects of MDMA on normal volunteers. *J. Psychoactive Drugs* **18**, 335-340.
29. Peroutka S. J. (1988) Incidence of recreational use of 3,4-methylenedioxymethamphetamine (MDMA, "Ecstasy") on an undergraduate campus. *n. Eng. j. Med.* **317**, 1542-1543.
30. McKenna, D. J.; Peroutka, S. J. (1990) Neurochemistry and Neurotoxicity of 3,4-Methylenedioxylmethamphetamine (MDMA, "Ecstasy"), *J. Neurochem.*, **54**, 14-22.
31. Schmidt, C. J.; Wu, L.; Lovenberg W. (1986) Methylenedioxy-methamphetamine: a potentially neurotoxic amphetamine analogue. *Eur. J. Pharmacol.* **124,** 175-178.
32. Ricaurte G.; Bryan, G., Strauss, L.; Seiden, L.; Schuster, C. (1985) Hallucinogenic amphetamine selectively destroys brain serotonin nerve terminals. *Science* **229**, 986-988.
33. Mokler, D. J.; Robinson, S. E.; Rosecrans, J. A. (1987) 3,4-Methylenedioxymethamphetamine (MDMA) produces long-term reductions in brain 5-hydroxytryptamine in rats. *Eur. J. Pharmacol.* **138**, 265-268.
34. Battaglia, G., Yeh, S. Y., O'Hearn, E., Molliver, M. E., Kuhar, M. J., De Souza, E. B. (1987) 3,4-Methylenedioxymethamphetamine and 3,4-methylenedioxyamphetamine destroy serotonin terminals in rat brain: quantification of neurodegeneration by measurement of [^{3}H]paroxetine-labeled serotonin uptake sites. *J. Pharmacol. Exp. Ther.* **242,** 911-916.
35. Schmidt, C. J. (1987) Acute administration of methylenedioxyamphetamine: comparison with the neurochemical effects of its N-demethyl and N-ethyl analogues. *Eur. J. Pharmacol.* **136**, 81-88.

36. Schmidt, C. J. (1987) Neurotoxicity of the psychedelic amphetamine, methylenedioxymethamphetamine. *J. Pharmacol. Exp. Ther.* **240**, 1-7.
37. Schmidt, C. J., Taylor, V. L. (1987) Depression of rat brain tryptophan hydroxylase activity following the acute administration of methylenedioxymethamphetamine. *Biochem. Pharmacol.* **36**, 4095-4102.
38. Wang, S. S., Ricaurte, G. A., Molliver, M. E. (1987) [^{3}H]-3,4-Methylenedioxymethamphetamine (MDMA) interactions with brain membranes and glass fiber filter paper. *Eur. J. Pharmacol.* **138**, 439-443.
39. Molliver, M. E., O'Hearn, E., Battaglia, G., De Souza, E. B. (1986) Direct intracerebral administration of MDA and MDMA does not produce serotonin neurotoxicity. *Soc. Neurosci. Abst.* **12**, 1234.
40. Schmidt, C. J., Gibb, J. W. (1985) Role of the dopamine uptake carrier in the neurochemical response to methamphetamine: effects of amfonelic acid. *Eur. J. Pharmacol.* **109**, 73-80.
41. Stone, D. M.; Johnson M.; Hanson, G. R.; Gibb, J. W. (1988) Role of endogenous dopamine in the central serotonergic deficits induced by 3,4-methylenedioxymethamphetamine. *J. Pharmacol. Exp. Ther.* **247**, 79-87.
42. Slikker, Jr., W., Gollamude, R., Ali, S. F., Kolta, M., Lipe, G., Webb, P., Lopez, M., Leakey, J. (1989) The effect of metabolic induction and inhibition on methylenedioxymethamphetamine (MDMA) induced neurochemical alterations. *FASAB Abstract* # 4706, 73rd Annual Meeting, New Orlerns, Louisiana, March 19-23.
43. Wang, S. S., Ricaurte, G. A., Peroutka, S. J. (1987) [^{3}H]-3,4-Methylenedioxymethamphetamine (MDMA) interactions with brain membranes and glass fiber filter paper. *Eur. J. Pharmacol.* **138**, 439-443.
44. Lim, H. K.;,Foltz, R. L. (1988) *In vivo* and *in vitro* metabolism of 3,4-methylenedioxymethamphetamine in the rat: Identification of metabolites using an ion trap detector. *Chem. Res. Tox.* **1**, 370-378.
45. Miramatsu, M., Kumagal, Y., Unger, S. E., Cho, A. K. (1990) Metabolism of methylenedioxymethamphetamine: Formation of

dihydroxymethamphetamine and a quinone identified as its glutathione adduct. *J. Pharmacol. Exp. Ther.* **254,** 521-526.
46. Kostrzewa, R. M. (1989) Neurotoxins that affect central and peripheral catecholamine neurons. in Neuromethods, Vol 12 Drugs as tools in neurotransmitter Research. (Boulton, A. A., Baaker, G. b., Juorio, A. V. eds), Humana Press, Clifton, New Jersey, pp.1-33.
47. Biel, J. H., Abood, L. G. (1971) Biogenic amines and physiological membranes in drug therapy. Marcel Dekker, Inc., New York, **Vol. 5,** Part B, pp. 390-391.
48. Dougan, D., Wade, D., Duffield, P. (1987) How metabolites may augment some psychostimulant actions of amphetamine. *Trends Pharmacol. Sci.* **8**, 277-280.
49. Paul, S., Axelrol, J., Diliberto, E. (1977) Cateachol estrogenforming enzyme of brain: Demonstration of a cytochrome P-450 monooxygenase. *Eucocrinol.* 101, 1604-1610.
50. Rotman, A., Daly, J. W., Creveling, C. R. (1976) Oxygen-dependent reaction of 6-hydroxydopamine, 5,6-dihydroxytrypatamine, and related compounds with protein in vitro: a model for cytotoxicity. *Mol. Pharmacol.* **12,** 887-899.
51. Butcher, L. L. (1975) Degenerative processes after punctate intracerbral administration of 6-hydroxydopamine. *J. Neural Trans.* **37,** 189-208.
52. Zweig, J. S.; Castagnoli, Jr., N. (1977) *In vitro* O-demethylation of the psychomimetic amine, 1-(2,5-dimethoxy-4-methylphenyl)-2-aminopropane. *J. Med. Chem.* **20**, 414.
53. Heathcock, C. H.; Ratcliffe, R. (1971) A stereoselective total synthesis of Guaiazulenic sesquiterpenoids a-Bulnesene and Bulnesol. *J. Am. Chem. Soc.* **93**, 1746-1757.
54. Silverstern, R. M.; Clayton Bassler, G.; Morrill, T. C. (1981) Spectrometric Identification of Organic Compounds. John Wiler and Sons, Inc., New York, 4th edition, pp. 1-212.
55. Cheng, A. C.; Castagnoli, Jr., N. (1984) Synthesis and physicochemical and neurotoxicity studies of 1-(4-substituted-2,5-dihydroxyphenyl)-2-aminoethane analogues of 6-hydroxydopamine. *J. Med. Chem.* **27**, 513.

56. Zhao, Z., Castagnoli, N., Ricaurte, G. A., Steele, T., Martello, M. Synthesis and neurotoxicological evaluation of putative metabolites of the serotonergic neurotoxin 2-methylamino-1-(3,4-methylenedioxyphenyl)propane (Methylenedioxymethamphetamine, MDMA). *Chem. Res. Toxicol.* In press.
57. Commins, D. L., Vosmer, G., Virus, R. M., Woolverton, W. L., Schuster, C. R., Seiden, L. S. (1987) Biochemical and histological evidence that methylenedioxymethamphetamine (MDMA) is toxic to neurons in the rat brain. *J. Pharmacol. Exp. Thur.* **241,** 338-345.
58. Greene, T.W., (1981) Protective groups in organic synthesis, John Wiley and Sons, Inc., p. 40.
59. Neeman, M., Hashimoto, Y., (1962) The structure of Estriol monoglucosiduronic acid from human pregnancy urine, *J. Am. Chem. SOc.* **84**, 2972.
60. Holsztynska, E. J., Domino, E. F. (1985) Biotransformation of phencyclidine. *Drug Metab. Rev.* **16,** 285-320.
61. Domino, E. (1964) Neurobiology of phencyclidine (Sernyl), a drug with an unusual spectrum of pharmacological activity. *Int. Rev. Neurobiol.* **6,** 303-347.
62. Lerner, S. E., Burns, R. S. (1978) Phencyclidine use among youth: history, epidemiology, and acute and chronic intoxication. *Natl. Inst. Drug Abuse. Res. Monogr. Ser.* **21**, 66.
63. Vincent, J., Kartalovski, B., Geneste, P., Kamenka, J., Lazdunski, M. (1979) Interaction of phencyclidine ("angel dust") with a specific receptor in rat brain membranes. *Proc. Nalt. Acad. Sci.* **76,** 4678-4682.
64. Quirion, R., Hammer, R., Herkenham, M., Pert, C. (1981) Phencyclidine (angel dust)/ σ "opiate" receptor: Visualization by tritium-sensitive film. *Proc. Nalt. Acad. Sci.* **78,** 5881-5885.
65. Baker, J. K., Wohlford, J. G., Bradbury, B. J., Wirth, P. N. (1981) Mammalian metabolism of phencyclidine. *J. Med. Chem.* **24,** 666-669.
66. Cho, A. K, Hallstrom, G., Matsumoto, R. M., Kammerer, R. C. (1983) in Phencyclidine and related arylcyclohexylamines: Present and future applications (Kamenka, J. M., Domino, E. F., Geneste, P., eds.) NPP Books, Ann Arbor, MI, pp. 205-214.

67. Cho, A., Kammerer, R., Abe, L. (1981) The identification of a new metabolite of phencyclidine. *Life Sci.*, **28**, 1075-1079.
68. Mitchell, J. R., Horning, M. G. eds. (1984) Drug metabolism and drug toxicity, Raven Press, New York, pp.1-436.
69. Newberne, P. M., Butler, W. H. eds. (1978) Rat hepatic neoplasia. MIT Press, Boston, pp. 100-113.
70. Coon, M. J., Conney, A. H., Estabrook, R. W., Gelboin, H. V., Gillette, J. R., O'Brien, P. J. eds. (1980) Microsomes, Drug Oxidations, and chemical carcinogenesis. Academic Press, New York, pp. 985-988.
71. Ward, D. P., Trevor, A. J., Kalir, A., Adams, J. D., Baillie, T. A., Castagnoli, N. (1982) Metabolism of phencyclidine. The role of iminium ion formation in covalent binding to rabbit microsomal protein. *Drug Metab. Dispos.*, **10**, 690.
72. Kalir, A., Trevor, A. J., Ward, D. P., Adams, J. D., Baillie, T. A., Castagnoli, N. (1983) in Phencyclidine and related arylcyclohexylamines: Present and future applications NPP Books, Ann Arbor, MI, pp. 267-278.
73. Hallstrom, G., Kammerer, R. C., Nguyen, C. H., Schmitz, D. C., DiStefano, E. W., Cho, A. K. (1983) Phencyclidine metabolism *in vitro*. The formation of a carbinolamine and its metabolites by rabbit liver preparations. *Drug Metab. Dispos.* **11**, 47-53.
74. Osawa, Y., Coon, M. (1989) Selective mechanism-based inactivation of the major phenobarbital-inducible P-450 cytochrome from rabbit liver by phencyclidine and its oxidation product, the iminium compound. *Drug Metab. Dispos.* **17**, 7-13.
75. Hoag, M.K.P., Trevor, A.J., Kalir, A., Castagnoli, Jr.,N. (1987) Phencyclidine iminium ion NADPH-dependent metabolism, covalent binding to macromolecules, and inactivation of cytochrome(s) P-450, *Drug Metab. Dispos.* **15**, 485.
76. Hoag, M.; Schmidt-Peetz, M.; Lampen, P.; Trevor, A.; Castagnoli, Jr., N. (1988) Metabolic studies on phencyclidine: Characterization of a phencyclidine iminium ion metabolite. *Chem. Res. Toxicol.* **1**, 128-131.
77. Holsztynska, E. J., Domino, E. F. (1983) in Phencyclidine and related arylcyclohexylamines: Present and future applications

(Kamenka, J. M., Domino, E. F., Geneste, P. eds.) NPP Books, Ann Arbor, MI, pp.215-248.

78. Zhao, Z., Leung, L., Trevor, A, Castagnoli, Jr, N. (1991) C-Formylation in the presence of rat brain mitochondria of the 2,3,4,5-tetrahydropyridinium metabolite derived from the psychotomimetic drug phencyclidine. *Chem. Res. Toxicol.* **4,** 426-429.

79. Lin, D., Feintiman, A., Foltz, R., Forney, R., Sunshine, I. (1975) Quantification of phencyclidine in body fluids by gas chromatography-chemical ionization mass spectrometry and identification of two metabolites. *Biomed. Mass Spectrm.* **2,** 206.

80. Staab, H. A., Polenski, B. (1962) Heterocyclische amide der ameisensaure, *Ann.*, **655**, 95.

81. Colman, N. Herbert, D. (1986) Folates and the nervous system. in Folates and Pterins, Vol. 3 (Blakley, R., Whitehead, V. Eds.) John Wiley and Sons, New York, pp 342-344.

82. Biorge, S.; Black, A.; Bockbrader, H.; Chang, T.; Greor, V.; Lobbestael, S.; Nuglel, D.; Pavia, M.; Radulovic, L.; Woolf, T. (1990) Stnthesis and metabolic profile of CI-966: A potent, orally-active inhibitor of GABA uptake. *Drug Develop. Res.*, **21**, 189-193

83. Olah, G. A., Narang, S. C., Balaram Gupta, B. G., Malhotra, R. (1979) Synthetic methods and Reactions. 62. Transformations with chlorotrimethylsilane/sodium iodide, a convenient in situ iodotrimethylsilane reagent. *J. Org. Chem.* **44,** 1247-1251.

84. Deziel, R. (1987) Mild Palladium (0)-catalyzed deprotection of allyl esters. A useful application in the synthesis of carbapenems and other β-lactam derivatives. *Tetrahedron Lett.* **28,** 4371-4372.

85. Kalir, A., Edery, H., Pehal, Z., Balderman, D., Porath, G. (1969) 1-Phenylcycloalkylamine derivative. II. Synthesis and pharmacological activity. *J. Med. Chem.* **12,** 473-477.

86. Lowry, O. H., Rosebrough, N. J., Farr, A. L., Randall, R. J. (1951) Protein measurement with the Folin phenol reagent. *Biol. Chem.* **193,** 265-275.

87. Bundgaard, H., (1985) Design of prodrugs. Elsevier, Amsterdam, p31.

88. Bodor, N., Farag, H. H., Brewster, M. E. (1981) Site-specific, sustained release of drugs to the brain. *Science* **214** 1370-1372.

89. Langston, J., Ballard, P., Tetrud, J., Irwin, I. (1983) Chronic parkinsonism in human due to a product of meperiding-analog synthesis. *Science* **219,** 979-980.
90. Langston, J., Irwin, I., Langston, E., Forno, L. (1984) 1-Methyl-4-phenylpyridinium ion (MPP^+): identification of a metabolite of MPTP, a toxin selective to the substantia nigra. *Neurosci. Lett.* **48,** 87-92.
91. Sanchez-Ramos, J., Barrett, J., Goldstein, M., Weiner, W., Hefti, F. (1986) 1-Methyl-4-phenylpyridinium (MPP^+) but not 1-Methyl-4-phenyl-1,2,3,6-tetrahydropyridine (MPTP) selectively destroys dopaminergic neurons in cultures of dissociated rat mesencephalic neurons. *Neurosci. Lett.* **72,** 215-220.
92. Trevor, A. J., Castagnoli, N., Caldera, P., Ramsay, R. R., Singer, T. P. (1987) Bioactivation of MPTP: Reactive metabolites and possible biochemical sequelae. *Life Sci.* 40, 713-719.
93. Peterson, L., Caldera, P., Trevor, A., Chiba, K., Castagnoli, N.,Jr. (1985) Studies on the 1-methyl-4-phenyl-2,3,-dihydropyridinium species 2,3-$MPDP^+$, the monoamine oxidase catalyzed oxidation product of the nigrostriatal toxin 1-Methyl-4-phenyl-1,2,3,6-tetrahydropyridine (MPTP). *J. Med. Chem.* **28,** 1432-1436.
94. Ottoboni, S.; Caelson, T. J.; Trager, W. F.; Castagnoli, K.; Castagnoli, N. Jr. (1990) Studies on the cytochrome P-450 catalyxed ring α-carbon oxidation of the nigrostriatal toxin 1-methyl-4-phenyl-1,2,3,6-tetrahydropyridine (MPTP). *Chem. Res. Toxicol.,* **3,** 423-427.
95. Chiba, K., Peterson, L. A., Castagnoli, K. P., Trevor, A. J., Castagnoli, N. (1985) Studies on the molecular mechanism of bioactivation of the selective nigrostriatal toxin 1-methyl-4-phenyl-1,2,3,6-tetrahydro-pyridine. *Drug metab. Dispos.* **13,** 342-347.
96. Tipton, K., McCrodden, J., Youdim, M. (1986) Oxidation and enzyme-activated irreversible inhibition of rat liver monoamine oxidase-B by 1-methyl-4-phenyl-1,2,3,6-tetrahydropyridine (MPTP). *Biochem. J.* **240,** 379-383.
97. Heikkila, R., Hess, A., Duvoisin, R. (1984) Dopaminergic neurotoxicity of 1-methyl-4-phenyl-1,2,5,6-tetrahydropyridine in mice. *Science* **224,** 1451-1453.

98. Heikkila, R., Manzino, L., Cabbat, F., Duvoisin, R. (1984) Protection against the dopaminergic neurotoxicity of 1-methyl-4-phenyl-1,2,5,6-tetrahydropyridine by monoamine oxidase inhibitors. *Nature* **311,** 467-469.
99. Singer, T., Salach, J., Crabtree, D. (1985) Reversible inhibition and mechnism-based irreversible inactivation of monoamine oxidases by 1-methyl-4-phenyl-1,2,3,6-tetrahydropyridine (MPTP). *Biochem. Biophys. Res. Commun.* **127,** 707-712.
100. Singer, T., Salach, J., Castagnoli, N., Treavor, A. (1986) Interactions of the neurotoxic amine 1-methyl-4-phenyl-1,2,3,6-tetrahydropyridine with monoamine oxidase. *Biochem. J.* **235,** 785-789.
101. Javitch, J. A., D'Amato, R. J., Strittmatter, S. M, Snyder, S. H. (1985) Parkinsonism-inducing neurotoxin, N-methyl-4-phenylpyridine by dopamine neurons explains selective toxicity. *Proc. Natl. Acad. Sci. U.S.A.* **82,** 2173-2177.
102. Ramsay, R. R., Dadgar, J., Trevor, A., Singer, T. P. (1986) Energy-driven uptake of N-methyl-4-phenylpyridine by brain mitochondria mediates the neurotoxicity of MPTP. *Life Sci.* **39,** 581-588.
103. Nicklas, W. J., Youngster, S. K., (1987) Toxicity. MPTP, MPP^+ and mitochondrial function." *Life Sci.* **40,** 721-729.
104. Youngster, S. K., Sonsalla, P. K., and Heikkila, R. E.(1987) Evaluation of the biological activity of several analogs of the dopaminergic neurotoxin MPTP. *J. Neurochem.* **48,** 929-934.
105. Maret, G., Testa, B., Jenner, P., Tayar, N. E., Carrupt, P. (1990) The MPTP story: MAO activates tetrahydropyridine derivatives to toxins causing Parkinsonism. *Drug Metab. Rev.* **22,** 291-332.
106. Langston, J.; Irwin, I.; Langston, E.; Forno, L. (1984) The importance of the 4'-5' double bond for neurotoxicity in primates of the pyridine derivative MPTP. *Neurosci. Lett.*, **50,** 289-294.
107. Brossi, A. (1985) Further explorations of unnatural alkaloids, *J. Natural Products,* **48,** 878-893.
108. Youngster, S.; Sonsalla, P.; Sieber, B.; Heikkila, R. (1989) Structure-activity study of the mechanism of 1-methyl-4-phenyl-1,2,3,6-tetrahydropyridine (MPTP)-induced neurotoxicity. I.

Evaluation of the biological activity of MPTP analogs, *J. Pharmacol. Exp. Ther.*, **249,** 820-828.

109. Riachi, N.; Arora, P.; Sayre, L. Harik, S. (1988) Potent neurotoxic fluorinated 1-methyl-4-phenyl-1,2,3,6-tetrahydropyridine analogs as potential probes in models of Parkinson's disease, *J. Neurochem.*, **50,** 1319-1321.

110. Youngster, S. K., Sonsalla, P. K., Sieber, B. A., and Heikkila, R. E. (1989) Structure-activity study of the mechanism of 1-methyl-4-phenyl-1,2,3,6-tetrahydropyridine (MPTP)-induced neurotoxicity. 1. Evaluation of the biological activity of MPTP analogs. *J. Pharmacol. Exp. Ther.* **249,** 820-828.

111. Hoppel, C., Greenblatt, D., Kwok, H., Arora, P., Singh, M., Sayre, L. (1987) Inhibition of mitochondrial respiration by analogs of 4-phenylpyridine and 1-methyl-4-phenylpyridinium cation (MPP^+), the neurotoxic metabolite of MPTP. *Biochem Biophys. Res. Comm.* **148,** 684-686.

112. Rollema, H., DeVires, J., Damsma, G., Westerink, B., Kranenborg, G., Kuhr, W., Horn, A. (1988) The use of in vivo brain dialysis of dopamine, acetycholine, aminoacids, and lactic acid in studies on the neurotoxin 1-methyl-4-phenyl-1,2,3,6-tetrahydropyridine (MPTP). *Toxicol.* **49,** 503-511.

113. Naiman, N., Rollema, H., Johnson, E., Castagnoli, N. (1990) Studies on the 4-benzyl-1-methyl-1,2,3,6-tetrahydropyridine, a nonneurotoxic analogue of the parkinsoniam inducing agent 1-methyl-4-phenyl-1,2,3,6-tetrahydropyridine. *Chem. Res. Tox.* **3,** 133-138.

114. Zhao, Z., Naiman, N., Castagnoli, K., Castagnoli, N. (1991) Design, synthesis, and biological evaluation of novel 1-methyl-4-substituted-1,2,3,6-tetrahydropyridine analogs of MPTP. *J. Med. Chem.* Manuscript in preparation.

115. Wanner, K., Eiden, F. (1984) Benzothiazole durch C-C spaltung von α-[(2-nitrophenyl)thio]ketonen, *Liebigs Ann. Chem.* 1100-1108.

115a. House, H. O., Czuba, L. J., Gall, M., Olmstead, H. D. (1968) The chemistry of carbanions. XVIII. Preparation of trimethylsilyl enol ethers. *J. Org. Chem.*, **34,** 2324-2336.

116. March, J. Advanced Organic Chemistry, 3rd ed. John Wiley and Sons, New York, p325.
117. Olofson, R., Cuomo, J., Bauman, B., (1978) An efficient synthesis of enol carbonates. *J. Org. Chem.* **43,** 2073-2075.
118. Cadogan, J. I. G. (1959) Reactions of pyridyl benzoates with some perbenzoic acids. *J. Chem. Soc.* 2844.
119. Guerry, P., Neier, R. (1984) Reduction von 4-pyrinonen. *Synthesis,* 485-488.
120. Lang, L. (1966) Absorption spectra in the ultraviolet and visible region. Academic Press Inc. New York, Vol. 1 pp. 93-94.
121. Salach, J.; Weyler, W.; (1987) Preparation of the flavin-containing aromatic amine oxidases oh human placenta and beef liver. In "Methods in Enzymology" Vol. 142, pp. 627-677.

VITA

Zhiyang Zhao was born on June 28, 1957 in Shanghai, China. He received a Bachelor of Science in Pharmacy from Shanghai College of Traditional Chinese Medicine in Shanghai, China in 1982. He then worked in the Department of Pharmacy, Shanghai College of Traditional Chinese Medicine for about four years. In August of 1988, he was awarded a Master of Science in Chemistry from the Department of Chemistry, Virginia Polytechnic Institute & State University, Virginia, USA under the direction of Professor David G. I. Kingston. He then studied Drug Metabolism under direction of Peters' Professor Neal Castagnoli, Jr. in the Department of Chemistry, VPI & SU, and his research work was sponsored by the Harvey W. Peters Research Center for Parkinson's Disease and Disorders of the Central Nervous System. He was awarded a Doctor of Philosophy in Chemistry from Virginia Polytechnic Institute & State University in the Fall of 1991.

Zhiyang Zhao